PONTIFICIA UNIVERSIDAD CATOLICA DE CHILE

SCHOOL OF ENGINEERING

OVERLOOKED TOPICS IN BUILDING CODES: FLOOR ACCELERATIONS AND ACCIDENTAL TORSION

FRANCISCO XAVIER FLORES SOLANO

Thesis submitted to the Office of Graduate Studies in partial fulfillment of the requirements for the Degree of Doctor in Engineering Sciences

Advisor:

DIEGO LOPEZ-GARCIA

Santiago de Chile, January 2017

PONTIFICIA UNIVERSIDAD CATOLICA DE CHILE
SCHOOL OF ENGINEERING

OVERLOOKED TOPICS IN BUILDING CODES: FLOOR ACCELERATIONS AND ACCIDENTAL TORSION

FRANCISCO XAVIER FLORES SOLANO

Members of the Committee:

DIEGO LOPEZ-GARCIA

FINLEY A. CHARNEY

JOSE LUIS ALMAZAN

MATIAS HUBE

JUSTIN MARSHALL

CRISTIAN VIAL

Thesis submitted to the Office of Graduate Studies in partial fulfillment of the requirements for the Degree of Doctor in Engineering Sciences

Santiago de Chile, January 2017

ACKNOWLEDGMENTS

First, I would like to thank God for so many blessings and opportunities throughout my life. I would especially like to thank my advisors and special friends, Dr. Diego López-García and Dr. Finley Charney for all their guidance. I will be eternally grateful to them for giving me the opportunity to work with them, for the trust that they put in me and believing that I was going to be able to finish this dual degree. I am grateful for their encouragement, patience and for always looking out for my wellbeing as student throughout my Ph.D. Many thanks to the University of Cuenca for the support given to finish my Ph.D while I was teaching. A special thanks to Pablo Vanegas and Esteban Pacheco for being understanding and supporting this investigation from the beginning. I want to thank my committee, Dr. Matias Hube, Dr. Cristian Vial, Dr. José Luis Almazán and Dr. Justin Marshall for being part of this investigation and for serving on my committee.

I want to thank my father and my mother, Francisco Flores Crespo and Ana Lucia Solano for encouraging me to complete this objective. For listening to me during difficult times, for giving me strength when I needed it, and for showing so much interest in my research even though it was sometimes impossible to understand. I would have never achieved my goals without their example of hard work and life lessons. I want to especially thank my wife, Alexandra Shourds, for her infinite support. Without the internal peace that I found since I met her it would have been very difficult to work on this degree. I am so grateful to my brother and sister for their support and for believing in me while pursuing my Ph.D.

I want to take this opportunity to thank a special friend, Juan Fernando Durán who helped me the whole year while I was in Chile. I also would like to thank all the friends that I made in Chile, especially to Jose Colombo, Wilson Torres and David Ugalde for helping making my time in Chile a memorable experience.

TABLE OF CONTENTS

Page

ACKNOWLEDGMENTS III

LIST OF TABLES VII

LIST OF FIGURES VIII

ABSTRACT XII

RESUMEN XIV

1. INTRODUCTION
   - 1.1 Overview and Motivation of Work 1
   - 1.2 Dissertation Organization 5
   - 1.3 Objectives 6
   - 1.4 Methodology 8
   - 1.5 Results and Scientific Contribution 10
     - 1.5.1 Acceleration Demands on NSCs 11
     - 1.5.2 Influence of Accidental Torsion in nonlinear analysis. 17
   - 1.6 Summary and Conclusions 25
   - 1.7 References 29

2. ASSESSMENT OF FLOOR ACCELERATIONS IN SPECIAL STEEL MOMENT FRAMES
   - 2.1 Introduction 33
   - 2.2 Methodology 36
   - 2.3 Overview of Buildings Analyzed 37
   - 2.4 Modeling approach 39
   - 2.5 Validation of the Models 42
   - 2.6 Earthquake Ground Motions 43

2.7 Ground Motion Scaling 43
2.8 Nonlinear Static Pushover Analysis 45
2.9 Peak Floor Accelerations 47
2.10 Floor Response Spectra 50
2.10.1 Floor Response Spectrum Ratio 55
2.11 Conclusions 58
2.12 Acknowledgements 61
2.13 References 61

3. FLOOR ACCELERATIONS IN BUILDINGS HAVING DIFFERENT STRUCTURAL SYSTEMS
3.1 Introduction 64
3.2 Methodology 66
3.3 Overview of Buildings Analyzed 67
3.4 Modeling SMFs 68
3.5 Modeling BRBs 69
3.6 Peak Floor Accelerations 70
3.7 Floor Response Spectra 73
3.8 Conclusions 76
3.9 Acknowledgements 77
3.10 References 78

4. THE INFLUENCE OF ACCIDENTAL TORSION ON THE INELASTIC DYNAMIC RESPONSE OF BUILDINGS DURING EARTHQUAKES
4.1 Introduction 80
4.2 Modeling of Second Order Effects in 3-D Structural Analysis 86
4.3 Description of System Analyzed 87
4.4 Mathematical Model 90
4.5 Torsional Properties of Systems 91
4.6 Nonlinear Static Analysis 94
4.7 Nonlinear Dynamic Analysis 105

4.8 Influence of Gravity Columns on Modeling P-Theta Effects 120
4.9 Summary, Conclusions and Recommendations 125
4.10 Acknowledgements 128
4.11 References 128

APPENDIX A: ACCELERATION DEMANDS ON NONSTRUCTURAL COMPONENTS IN STEEL SPECIAL MOMENT FRAME 131

APPENDIX B: THE INFLUENCE OF ACCIDENTAL TORSION ON THE INELASTIC DYNAMIC RESPONSE OF BUILDINGS DURING EARTHQUAKES 144

APPENDIX C: P-DELTA EFFECTS IN THE TORSIONAL RESPONSE OF STRUCTURES 158

APPENDIX D: ADDITIONAL RESULTS. “ASSESSMENT OF FLOOR ACCELERATIONS IN SPECIAL STEEL MOMENT FRAMES” 171

APPENDIX E: ADDITIONAL RESULTS. “FLOOR ACCELERATIONS IN BUILDINGS HAVING DIFFERENT STRUCTURAL SYSTEMS” 177

APPENDIX F: ADDITIONAL RESULTS. “THE INFLUENCE OF ACCIDENTAL TORSION ON THE INELASTIC DYNAMIC RESPONSE OF BUILDINGS DURING EARTHQUAKES” 182

LIST OF TABLES

Page

4. THE INFLUENCE OF ACCIDENTAL TORSION ON THE INELASTIC DYNAMIC RESPONSE OF BUILDINGS DURING EARTHQUAKES

Table 1: Member Sections for all Models 89

Table 2: Stability and Amplification Factors 92

Table 3: Torsional Irregularity Factors 93

Table 4: Summary of Fundamental Periods of Vibration (sec) 95

Table 5: Collapses Among 11 Ground Motions under Dynamic Loading: 111

Table 6: Collapses among 11 Ground Motions under Dynamic Loading: Model B and Model B-2 114

Table 7: Collapses Among 11 Ground Motions under Dynamic Loading: Model C and Model C-2 120

Table 8: Collapses under Dynamic Loading Comparison 125

LIST OF FIGURES

Page

1. INTRODUCTION

Figure 1: Normalized Peak Floor Acceleration (PFA/PGA): 2-Story Model 12

Figure 2: FRS at the 2nd (roof) level of the 2-Story Model.....13

Figure 3: Normalized Peak Floor Acceleration (PFA/PGA): 2-Story Model 16

Figure 4: FRS at the 2nd (roof) and 1st level of the 2-Story Models 17

Figure 5: Nonlinear static response of Models A (left) and A-2 (right) 22

Figure 6: Response histories of roof drift for Models A (left) and A-2 (right) under the Duzce-Bolu ground motion 24

2. ASSESSMENT OF FLOOR ACCELERATIONS IN SPECIAL STEEL MOMENT FRAMES

Figure 1: Typical Building Plan View 38

Figure 2: Elements of the models that do not include the gravity system 39

Figure 3: Elements of the models that include the gravity system 41

Figure 4: Far-Field Ground Motions Spectra a) Before Normalization b) After Normalization 44

Figure 5: Scaling Ground Motions a) 2-Story Model b) 8-Story Model 45

Figure 6: Pushover Curves and Dynamic Analyses: 2-Story Models 46

Figure 7: Pushover Curves and Dynamic Analyses: 4- and 8-Story Models 46

Figure 8: Normalized Peak Floor Acceleration (PFA/PGA): 2-Story Model 48

Figure 9: Normalized Peak Floor Acceleration (PFA/PGA): 4-Story Model 49

Figure 10: Normalized Peak Floor Acceleration (PFA/PGA): 8-Story Model 49

Figure 11: FRS at the 2nd (roof) level of the 2 Story Models 51

Figure 12: FRS at the 4th (roof) level of the 4-Story Models.....52

Figure 13: FRS at the 8th (roof) level of the 8-Story Models.....53

Figure 14: FRS at all floor levels of the 4-Story Model 55

Figure 15: FRSR values (2-Story Model).....56

Figure 16: FRSR values (4-Story Model).....57

Figure 17: FRSR values (selected floors of the 8-Story Model) 58

3. FLOOR ACCELERATIONS IN BUILDINGS HAVING DIFFERENT STRUCTURAL SYSTEMS

Figure 1: Building Overview a) SMF b) BRBF 68

Figure 2: Normalized Peak Floor Acceleration (PFA/PGA): 2-Story Model 71

Figure 3: Normalized Peak Floor Acceleration (PFA/PGA): 4-Story Model 72

Figure 4: Normalized Peak Floor Acceleration (PFA/PGA): 8, 9-Story Model 72

Figure 5: FRS at the 2nd (roof) and 1st level of the 2-Story Models 74

Figure 6: FRS at the 4th (roof) and 1st level of the 4-Story Models.....75

Figure 7: FRS at the Roof and 1st level of the 8,9-Story Models 76

4. THE INFLUENCE OF ACCIDENTAL TORSION ON THE INELASTIC DYNAMIC RESPONSE OF BUILDINGS DURING EARTHQUAKE

Figure 1: Structural System Analyzed (Model A) 89

Figure 2: Nonlinear static responses for Model A 97

Figure 3: Nonlinear static response curves for Model A-2 99

Figure 4: Nonlinear static response curves for Model B 100

Figure 5: Nonlinear static response curves for Model B-2 102

Figure 6: Nonlinear static response curves for System C 103

Figure 7: Sequence of yielding in nonlinear static analysis (Model A-2) 104

Figure 8: Response histories of roof drift for Model A (Duzce-Bolu) 107

Figure 9: Response histories of roof drift for Model A-2 (Duzce-Bolu) 109

Figure 10: Response histories of roof drift Model A and Model A-2 (Landers-Yermo) 110

Figure 11: Response histories of roof drift for Model B (Kocaeli-Duzce) 112

Figure 12: Response histories of roof drift for Model B-2 (Kocaeli-Duzce) 113

Figure 13: Response histories of roof drift for Model B (Cape Mendocino-Rio) ... 116

Figure 14: Response histories of roof drift for Model B-2 (Cape Mendocino-Rio) 117

Figure 15: Response Histories and Inter-Story Drifts Model C (San Fernando-LA) 119

Figure 16: Influence of P-Theta effects on nonlinear static response 122

Figure 17: Nonlinear Dynamic Analyses Comparison 124

PONTIFICIA UNIVERSIDAD CATOLICA DE CHILE
ESCUELA DE INGENIERIA

OVERLOOKED TOPICS IN BUILDING CODES: FLOOR ACCELERATIONS AND ACCIDENTAL TORSION

Thesis submitted to the Office of Research and Graduate Studies in partial fulfillment of the requirements for the Degree of Doctor in Engineering Sciences by

FRANCISCO X. FLORES

ABSTRACT

This investigation studies two different topics that are considered somewhat overlooked in building codes: acceleration demands on Nonstructural Components (NSCs) and accidental torsion in nonlinear dynamic response history analysis (NRHA). Despite the vast research that has been performed to establish minimum requirements in building codes, the procedures given specifically by ASCE 7-10 to evaluate acceleration demands and accidental torsion effects are still too simplified or nonexistent.

Acceleration demands on NSCs are investigated in two sections: the first section examines the level of detail required in a structural model to realistically assess acceleration demands, and the second section analyzes the differences in acceleration demands on NSCs supported by two different structural systems. In the first section, it was found that acceleration demands are generally smaller when the structure behaves inelastically, especially when the period of the NSC is similar to one of the modal periods of the supporting structure. In addition, it was found that the gravity system does not significantly influence the acceleration demands. In the second section it was found that ASCE 7-10 significantly overestimates the acceleration demands at the upper stories of multistory buildings. Moreover, acceleration demands in the two lateral resisting systems considered in this study turned out to be qualitatively similar to each other, and quantitative differences are significant when the structures behave inelastically.

The second part of the dissertation studies the influence of accidental torsion in NRHA by subjecting different structures to different nonlinear static and dynamic analyses. The relevance of several issues such the level of torsional irregularity, inclusion of accidental torsion at the design stage, the actual bidirectional nature of the seismic input, and modeling of P-Delta were examined. It was found that accidental torsion has a significant effect on the inelastic response of structures, and that accurate assessment of its effects require both correct modeling of P-Delta effects and simultaneous application of both horizontal components of the seismic ground motions.

Keywords: acceleration demands, accidental torsion, nonlinear analysis.

Members of the Doctoral Thesis Committee:

DR. DIEGO LOPEZ-GARCIA

DR. FINLEY CHARNEY

DR. JOSE LUIS ALMAZAN

DR. MATIAS HUBE

DR. JUSTIN MARSHALL

DR. CRISTIAN VIAL

Santiago, January 2017

PONTIFICIA UNIVERSIDAD CATOLICA DE CHILE
ESCUELA DE INGENIERIA

OVERLOOKED TOPICS IN BUILDING CODES: FLOOR ACCELERATIONS AND ACCIDENTAL TORSION

Tesis enviada a la Dirección de Investigación y Postgrado en cumplimiento parcial de los requisitos para el grado de Doctor en Ciencias de la Ingeniería.

FRANCISCO XAVIER FLORES SOLANO

RESUMEN

En esta investigación se analizan dos temas relacionados con la respuesta sísmica de estructuras que aún no han sido analizados con suficiente detalle: la demanda de aceleración en Componentes No Estructurales (CNEs) y la torsión accidental en Análisis Tiempo Historia No-Lineal (ATHNL). A pesar de que estos temas han sido objeto de investigaciones de otros autores su inclusión en los códigos de diseño sísmico modernos, en particular en ASCE 7-10, es demasiado simplificada.

Las aceleraciones en CNEs se estudian en dos secciones. En la primera sección se examina el nivel de detalle requerido en la modelación estructural para evaluar correctamente las aceleraciones en CNEs, y en la segunda sección se examinan las diferencias entre aceleraciones en dos sistemas estructurales distintos. En la primera sección se encontró que las aceleraciones en CNEs son generalmente menores cuando se considera el comportamiento inelástico de la estructura, sobre todo cuando el período del CNE es igual a uno de los períodos modales de la estructura. También se encontró que la parte de la estructura que sólo soporta cargas de gravedad no influye significativamente en las aceleraciones en CNEs. En la segunda sección se encontró que las especificaciones de ASCE 7-10 son muy conservadoras para CNEs situados en los pisos superiores de estructuras de múltiples pisos. También se encontró que distintos sistemas estructurales resultan en aceleraciones en CNEs cualitativamente similares entre sí, y cuantitativamente distintas en grado significativo sólo cuando la respuesta estructural es inelástica.

En la segunda parte de esta disertación se estudia la influencia de la torsión accidental en ATHNL. Se examina la influencia de factores tales como el nivel de irregularidad torsional, la naturaleza bidireccional de la excitación sísmica, y los efectos de segundo orden (P-Delta). Se encontró que la torsión accidental influye significativamente en la respuesta sísmica no lineal de estructuras, y que la evaluación realista de su influencia requiere modelar correctamente los efectos de segundo orden y la acción simultánea de ambas componentes horizontales de registros sísmicos.

Palabras clave: aceleraciones, componentes no estructurales, torsión accidental.

Members of the Doctoral Thesis Committee:

DR. DIEGO LOPEZ-GARCIA

DR. FINLEY CHARNEY

DR. JOSE LUIS ALMAZAN

DR. MATIAS HUBE

DR. JUSTIN MARSHALL

DR. CRISTIAN VIAL

Santiago, Enero de 2017

1. INTRODUCTION

1.1 Overview and Motivation of Work

The importance of building codes in structural design is nowadays unanimously acknowledged. Buildings codes provide practicing engineers with methodologies and minimum requirements that facilitate the design of buildings and other structures. The majority of these minimum requirements are based on a large amount of analytical and experimental research performed over time, lessons learned from the behavior of real structures subjected to actual loads and engineering judgement or intuition. A clear example of change in structural design over time is the so-called performance based seismic design. This approach takes into consideration different limit states (not just collapse prevention, as implicit in conventional design) and different levels of seismic hazards. One of the new interests created in the research community by this new design philosophy is the safety of nonstructural components. Despite this interest, seismic demand on nonstructural components is one of the areas in building codes that has been somewhat overlooked for different reasons (such as insufficient research) and has not been given the required importance. Another topic that has been somewhat overlooked in building codes and standards is the inclusion of accidental torsion in nonlinear analysis. Even though these two topics having nothing in common they are related to each other by the fact that they both have been somehow underestimated and might need to be addressed in a more accurate manner in future revisions of building codes. Thus the purpose of the investigations presented herein is to contribute to the understanding of seismic demands on nonstructural components and the effects of accidental torsion in buildings subjected to earthquakes.

Recent events like the 1994 Northridge (USA), 1995 Kobe (Japan) and 2010 Maule (Chile) earthquakes have shown that the majority of buildings performed as expected against collapse. However, there were cases where the building system did not suffer any structural damage but the extent of nonstructural damage inside the building was such that the facility completely lost its functionality after the event [1, 2]. In hospitals such situation is a major risk against life; moreover the direct and indirect economic losses due to damage in nonstructural components can be greater than the cost of the structure [3].

Nonstructural Components (NSCs) in buildings are divided into two main categories: those that are sensitive to interstory deformations and those that are sensitive to accelerations [4]. Acceleration-sensitive NSCs, which are one of the topics of this investigation, include parapets, suspended ceilings, ducts, boilers, chiller tanks, etc. [5]. NSCs can also be classified as "rigid" or "flexible" depending on their natural period of vibration. Acceleration-sensitive NSCs are not subjected to the ground accelerations, but rather to the total (ground plus relative) accelerations at the floor level to which they are anchored or attached. Such accelerations are usually referred to as floor accelerations.

The current U.S. seismic design code, ASCE 7-10 [6], provides a procedure to determine seismic demands on acceleration-sensitive NSCs. The procedure is for the most part based on experience, engineering judgment and intuition rather than on experimental and analytical results [7]. Even though it is a very practical approach it is perhaps oversimplified since it is intended to be applicable to NSCs located in any type of structure, regardless of whether the structure behaves elastically or inelastically, regardless of the fundamental period of the structure, and, perhaps more importantly, regardless of the type of structural system.

In most studies on seismic demands on acceleration-sensitive NSCs the supporting structure was assumed to behave elastically [3, 8, 9]. A few authors, however, have studied the effect of the building inelastic behavior on the accelerations imposed on NSCs, and have found that acceleration demands are generally smaller than those assessed assuming elastic response of the supporting structure, although in some cases, particularly for short-period NSCs, demands based on inelastic structural response might actually be greater. Some of these studies were performed considering simple SDOF structures [4, 10], and others studied the effect of plasticity in MDOF structures [11-17]. In these latter studies, however, the level of modeling refinement was not as high as that typical of other types of studies such as assessment of collapse performance using the FEMA P-695 methodology [18].

One of the main purposes of this study is to contribute to a more detailed and more realistic understanding of seismically induced floor accelerations. Unlike past studies, the models used in this research have the amount of detail required to evaluate the collapse performance using the FEMA P-695 methodology. These models are Special Steel Moment Frames (SMFs) investigated by Zareian et al. [19] for the ATC 76-1 project [20] and the Buckling Restrained Braced Frames (BRBFs) studied by Atlayan [21] and taken from the ATC 76-1 project as well.

The first part of this investigation focuses on the acceleration demands on NSCs, and is divided into two sections: the first section examines the level of modeling detail required to accurately assess floor accelerations, and the second section examines acceleration demands on NSCs in buildings that have different structural systems. The first section evaluates the acceleration demands on NSCs located in 2-, 4- and 8-story SMFs, and the possible influence of the gravity system is also considered. The second section compares

acceleration demands on NSCs in buildings that have two different structural systems: Special Steel Moment Frames (SMFs) and Buckling Restrained Braced Frames (BRBFs). The main purpose is to evaluate whether floor accelerations depend on the type of structural system, an issue currently not considered in ASCE 7-10.

The second part of this investigation examines whether accidental torsion needs to be included or not when performing nonlinear analysis. As it is known at the present time, nonlinear dynamic response history analysis (NRHA) is becoming an accepted procedure to assess the performance of building structures during earthquakes. In support of this trend, several documents [22-26] have emerged to provide guidance in terms of mathematical modeling, ground motion selection and scaling, and specification/evaluation of acceptance criteria. Additionally, several standards or prestandards [6, 27-30] provide specific requirements for performing such analysis.

A review of these documents has indicated various areas of agreement and disagreement. One of the most striking areas of disagreement is related to methodologies required to capture accurate three-dimensional response, and more specifically, whether or not accidental torsion is required. In regards to accidental torsion, there are two issues. First, there is the question as to whether accidental torsion is needed in the (generally linear elastic) analysis used to design the structure that will be later analyzed using the NRHA procedure. Second, there is the issue of whether or not accidental torsion must be included in the nonlinear response history analysis itself. Related to the second issue is the specific manner in which the decision to omit or include accidental torsion in the NRHA is made, and how the accidental torsion is included in the analysis if it has been determined that it is necessary to include it.

Whether or not accidental torsion should be included in NRHA was extensively debated by members of the task committee charged with developing a fully revised set of requirements for NRHA for Chapter 16 of the 2015 NEHRP Provisions [31]. The main supporting idea of not including accidental torsion in the NRHA is based primarily on practical considerations, as it is thought that requiring as many as four additional analyses (for four different mass offset locations per ground motion, with a minimum of 11 ground motions required) is onerous.

In the second part of this investigation, the need to include accidental torsion in NRHA analysis is further investigated through the evaluation of the response of a 9-story steel building with Buckling Restrained Braces (BRB) to resist lateral loads. Three versions of the building are considered, wherein the only difference is the plan location of individual braced frames. The variation in plan location produces different levels of torsional irregularity, from moderate to extreme. Additionally, these buildings were designed with and without Chapter 12 accidental torsion requirements provided by ASCE7-10. The evaluation is performed by means of nonlinear static and dynamic analyses and the influence of accidental torsion is quantified by the location of the center of mass.

1.2 Dissertation Organization

This dissertation is organized using the paper format, where the traditional chapters in a dissertation are replaced by papers that have been submitted to peer-reviewed journals and conferences. In this dissertation, two journal papers and one conference paper are presented. Additionally three more conference papers that show similar results to the ones shown in the journal papers but from a somewhat different perspective are also included as appendices.

The dissertation begins with this introductory chapter where the complete study is summarized. This chapter includes an overview and motivation for the work, objectives, methodology, results and scientific contribution and overall conclusions. Chapter 2 is a paper published in the Journal of Constructional Steel Research entitled "Assessment of floor accelerations in special steel moment frames". Chapter 3 is a conference paper presented at the 2015 Structures Congress entitled "Floor accelerations in buildings having different structural systems". Chapter 4 is a manuscript submitted to Earthquake Spectra entitled "The influence of accidental torsion on the inelastic dynamic response of buildings during earthquakes". Finally, four appendices are provided. Appendix A is a conference paper presented at the XI Chilean Conference on Seismology and Earthquake Engineering entitled "Acceleration demands on nonstructural components in special steel moment frames". Appendix B is a conference paper also presented at the XI Chilean Conference on Seismology and Earthquake Engineering entitled "The influence of accidental torsion on the inelastic dynamic response of buildings during earthquakes". Appendix C is a conference paper presented at the 16th World Conference on Earthquake Engineering entitled "P-Delta effects in the torsional response of structures". Finally Appendix D presents results that due to page limit constraints were not included in the journal papers nor in the conference papers.

1.3 Objectives

This investigation was carried out with the main objective of evaluating the importance of acceleration demands on nonstructural components and the importance of accidental torsion in nonlinear dynamic analyses. Specific issues to be investigated within each topic are:

Acceleration Demands on NSCs:

- Evaluate the influence of the inelastic response of the structure.
- Quantify the importance of model refinement and establish the influence of the gravity system.
- Compare the computed accelerations on flexible and rigid NSCs with the accelerations computed using the equations given by ASCE7-10.
- Compare the acceleration demands on NSCs supported by two different lateral force resisting systems.

Accidental Torsion when performing Nonlinear Analysis

- Evaluate the influence of Accidental Torsion when structures are subjected to earthquakes that represent a hazard with a 2-percent probability of being exceeded in 50 years.
- Quantify the influence of torsional P-Delta effects.
- Compute the influence of bidirectional loading on the dynamic response of the structure.
- Evaluate the influence of accidental torsion at the design stage.
- Evaluate the influence of accidental torsion in buildings with different levels of torsional irregularity.

1.4 Methodology

This dissertation is comprised of two topics that are related to each other by; (a) the fact that they have not been conclusively examined in previous research; and (b) the possible need to revise their inclusion in future building codes. The first part explores the influence of inelastic behavior and the effects of the lateral force resisting system on the acceleration demands on nonstructural components. The second part of the investigation focuses on the influence of accidental torsion in nonlinear dynamic analysis. In both cases the study was performed using steel buildings and the analyses were performed using OpenSees [32]. However, the study that focused on acceleration demands was performed using 2D models while the study that examined the effects of accidental torsion was performed using 3D models.

To evaluate the acceleration demands on NSCs, two different types of structural systems were considered: Special Steel Moment Resisting Frames (SMFs) and Buckling Restrained Braced Frames (BRBFs). In the paper "Assessment of Floor Accelerations in Special Steel Moment Frames", the first step was to validate the accuracy of the SMF models. Because the building models were taken from a previous study performed by Zareian et al. in the ATC 76-1 project, a new FEMA P-695 analysis was performed using the models created for this investigation in order to compare results with the ones reported by Zareian et al. As specified by the FEMA P-695 methodology, the strength and stiffness of the gravity system was not included in the analysis performed by Zareian et al. In this study, however, once the models without the gravity system were validated, the gravity system was explicitly modeled in order to evaluate its possible influence on floor accelerations. The gravity system was modeled using partially-restrained (PR) connections

that have different strength levels, and the gravity columns were modeled using fiber sections with a bilinear material with 10% kinematic hardening. The flexural capacity of the PR connections was another parameter that was investigated and it was taken as a percentage (0%, 35%, 50% and 70%) of the full plastic moment capacity of the beam (M_p).

Once the models were validated and the gravity system incorporated, the structures were subjected to the two horizontal components from 22 sites, giving 44 Far-Field ground motions specified in FEMA P-695. The level of intensity to which the ground motions are scaled is the Design Earthquake (DE). This criterion was adopted because the acceleration demands on NSCs indicated in ASCE 7-05 and in ASCE 7-10 [6, 33] are consistent with the DE. The total acceleration response is obtained at each floor, and is then used as input to compute the floor response spectrum that indicates the demands on flexible NSCs. On the other hand the demand on rigid NSCs is equal to the Peak Floor Accelerations (PFA), which is the maximum total acceleration measured at a given floor. In order to compute the influence of structural inelastic deformations, the floor accelerations were also computed using the same models behaving elastically.

The paper "Floor Accelerations in Buildings having different Structural Systems" followed the same methodology described in the former paragraph. However, the acceleration demands in SMF models were compared with those in BRBF models. The floor accelerations in the SMF models were computed with and without the gravity system, and those in the BRBFs were computed without the gravity system but using two different types of beam-column-brace connections: pinned and continuous (fixed).

Accidental torsion was investigated following a different methodology. The analyses were performed in three dimensions in order to adequately capture the torsional response of the building models. The lateral resisting system of the models are Buckling Restrained Braced Frames (BRBFs), and different models having different levels of torsional irregularity were considered. The building models were subjected to nonlinear static pushover and nonlinear dynamic analyses. In order to evaluate the influence of torsional P-Delta effects, two different sets of buildings were studied: one with all the gravity columns explicitly modeled and another with one leaning column at the building centroid. In the first case both lateral and torsional P-Delta effects are included, while in the second case only the lateral P-Delta effects are included. Other issues that were studied are the relevance of bidirectional ground motion input and the relevance of accidental torsion at the design stage.

In order to evaluate the sensitivity of the buildings to torsional response, nonlinear static pushover analyses were performed by applying the loads at different levels of eccentricity. On the other hand the dynamic analyses were performed using 11 ground motions scaled at the Maximum Considered Earthquake (MCE) and were applied using different levels of eccentricity, which were induced by moving the center of mass.

1.5 Results and Scientific Contribution

This section summarizes the most important results obtained in the investigations described in this dissertation. This section is comprised of two subsections, one for each of the main topics of this investigation (acceleration demands in NSCs and influence of accidental torsion in nonlinear analysis).

1.5.1 Acceleration Demands on NSCs

One of the objectives of this investigation is to compute acceleration demands on NSCs using very detailed inelastic models. Thus the models used in this study comply with the requirements necessary to perform a FEMA P-695 analysis where the collapse performance of structures is evaluated. In addition, the influence of the gravity system is examined. The first paper "Assessment of floor accelerations in special steel moment frames" (Chapter 2) focused only on the acceleration demands on Steel Special Moment Frames (SMFs). The acceleration demands were computed on rigid and flexible NSCs supported by 2-, 4- and 8-story elastic and inelastic SMFs. Moreover, the gravity system was incorporated using partially restrained (PR) gravity connections, which in turn have different strength levels. The adopted nomenclature in the study is nStory + sGS, where n is the number of stories and s is the percentage of full strength assigned to the PR connections (if sGS is not included, the model does not include the gravity system and instead includes a leaning column to account for P-Delta effects). The methods to evaluate the demands on rigid and flexible NSCs were the Peak Floor Acceleration (PFA) and the Floor Response Spectrum (FRS), respectively. The demands obtained using these methods were then compared with the ones specified by ASCE7-10.

Representative examples of acceleration demands on rigid NSCs are shown in Figure 1 (a) and (b). The figure displays median PFAs (normalized by the PGA) in the elastic and inelastic 2-Story models, respectively. From these figures it can be concluded that inelastic behavior reduces PFAs considerably and the influence of the gravity system on floor accelerations in the inelastic models is not very significant, regardless of the strength level of the PR connections. It can also be concluded that the acceleration demands on rigid NSCs

computed using the ASCE 7 approach are very conservative, at least for the scenario considered in this study (the supporting structure is a SMF, and is located in an area of high seismic activity).

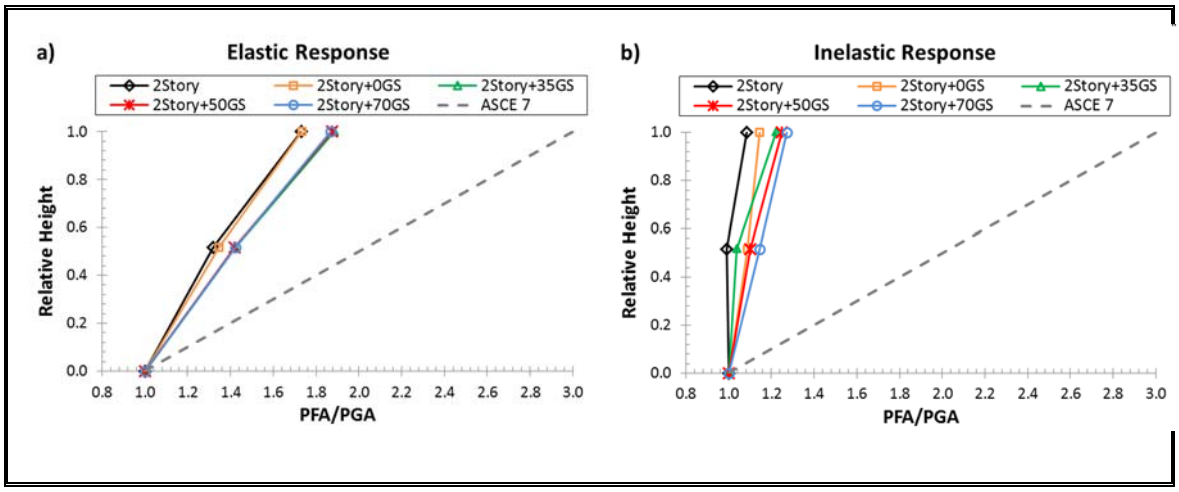

Figure 1. Normalized Peak Floor Acceleration (PFA/PGA): 2-Story Model

Representative examples of acceleration demands on flexible NSCs are shown in Figure 2 (a) and (b). This figure shows the FRS corresponding to the second (roof) level of the 2-Story model. It can be observed that FRS are characterized by large spectral ordinates at the modal periods of the structure. In order to better appreciate this observation, the modal periods of the model that does not include the gravity system are indicated by vertical dashed lines. However, the amplitude of the spectral ordinates in the vicinity of the first modal period are much smaller when the structure behaves inelastically than when the structure behaves in a linearly elastic manner. It can also be observed that the presence of the gravity system is relevant only when the strength of the PR connections is not negligible, but such relevance is not considerable. Regarding the accelerations computed using the ASCE 7-10 approach, it can be seen that they are conservative except at first mode resonance, in which case they underestimate the expected demand.

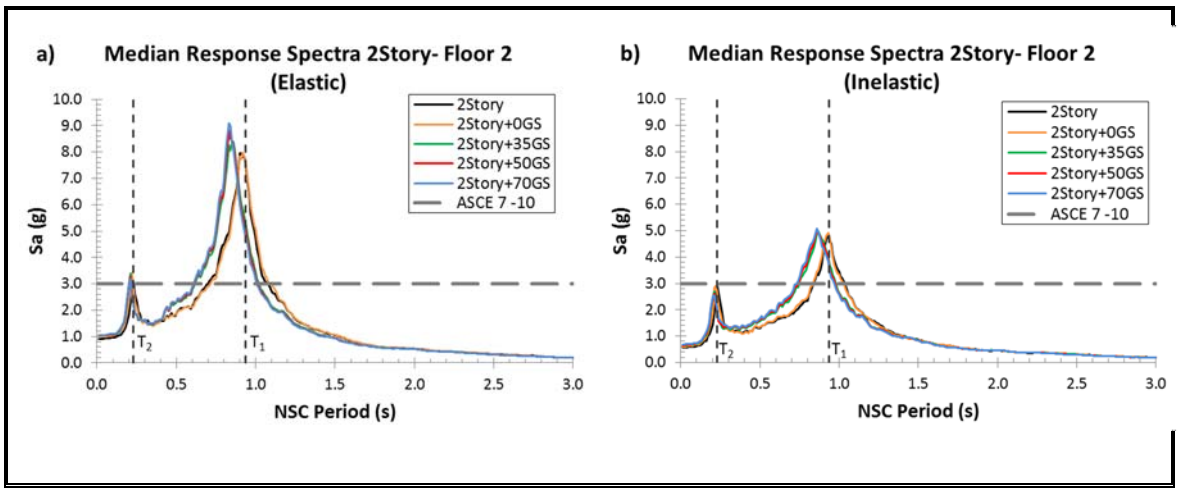

Figure 2. FRS at the 2nd (roof) level of the 2-Story Model

These results illustrate the most important trends shown in the paper "Assessment of floor accelerations in special steel moment frames". Other important outcomes include:

- Even though nonlinear time history analysis is computationally expensive and challenging, it should nevertheless be preferred whenever possible because it gives results that are very different (generally much smaller) from those given by the much simpler linear elastic analysis.
- The influence of the gravity columns on floor accelerations is much less relevant than on other structural response issues such as, for instance, collapse performance.
- The strength of the gravity connections has some influence on floor accelerations. Such influence is most significant on Floor Response Spectra (FRS) at first mode resonance, diminishes at higher mode resonance, and becomes essentially negligible on PFAs.
- As reported in the literature, spectral ordinates of FRS in inelastic building models are in some particular cases indeed greater than those of elastic building models, but

such observation turned out to be true only at higher mode resonance, and only marginally so.

- It was found that in the 0.0 s – 0.5 s range (the period range of most nonstructural components, NSCs), spectral ordinates of FRS in linearly elastic building models range from accurate to conservative by up to 150%. The degree of accuracy, however, is very sensitive to the period of the NSC, which makes accurate assessments difficult in actual case scenarios and in code provisions.

- The acceleration demands on rigid NSCs (inelastic building models) are roughly equal to the PGA, regardless of the floor level at which the NSC is attached. Thus, such accelerations are not expected to be as large as those indicated by the ASCE 7 approach, especially at the topmost floor levels.

- In contrast, the acceleration demands on flexible NSCs are very high. Considering again the realistic 0.0 s – 0.5 s NSC period range, acceleration demands are in the range of 3.0 g - 4.5 g in the extreme case of higher mode resonance. These demands are reasonably well predicted by the ASCE 7 approach for NSCs located at the roof level, but not for those located at other floors.

The second paper that is part of the study on acceleration demands ("Floor accelerations in buildings having different structural systems", presented at the Structures Congress 2015) examines differences between acceleration demands on NSCs supported by two different structural systems: SMFs and BRBFs (Chapter 3).

As already mentioned the SMFs and BRBFs analyzed in this study were taken from the ATC 76-1 project. These structural systems are comparable to each other since their

seismic performance factors are the same. The response modification coefficient (R) is equal to 8, the overstrength factor (Ω_o) is equal to 3 and the deflection amplification factor (C_d) is equal to 5.5. The SMFs and BRBFs were designed using Modal Response Spectrum Analysis (RSA) for a design category D_{max} (S_s=1.5g, S_1=0.6g), for a typical gravity load, and considering Site Class D.

The mathematical models of the BRBs and SMFs were developed using OpenSees [32]. Two different models are used for the SMFs: one that does not incorporate the gravity system and one model that it does. The gravity system is modeled using partially-restrained (PR) connections that have a flexural capacity equal to 35% the full plastic moment of the beam (M_p). As shown in the first paper already described, the exact strength level of the gravity connections is not really relevant on acceleration demands, hence only one level was considered in the second paper. On the other hand, the BRBFs are analyzed using two different types of beam-column-brace connections: pinned and continuous (fixed).

Three different analyses where used to compute the acceleration demands on rigid and flexible NSCs: the one specified in the current US code (ASCE 7-10), linear elastic analysis, and nonlinear time history analysis. In the case of the time history analyses the methods used to evaluate the demands on rigid and flexible NSCs were the Peak Floor Accelerations (PFA) and the Floor Response Spectrum (FRS) accelerations, respectively.

Representative examples are shown in Figure 3 (a) and (b), which display median PFA values for SMFs and BRBFs, respectively, and are compared with the PFA values given by the ASCE 7-10 approach. Demands on NSCs in the BRBFs are larger than those on NSCs in the SMFs and are very close to the ones computed using ASCE 7-10. On the other hand,

the demands on NSCs in inelastic models are similar in both SMFs and BRBFs, and close to the PFA along the height of the structure. In the more flexible structures (BRBs with pinned connections and SMF without the gravity system) demands on NSCs are somewhat smaller than those in the stiffer structures.

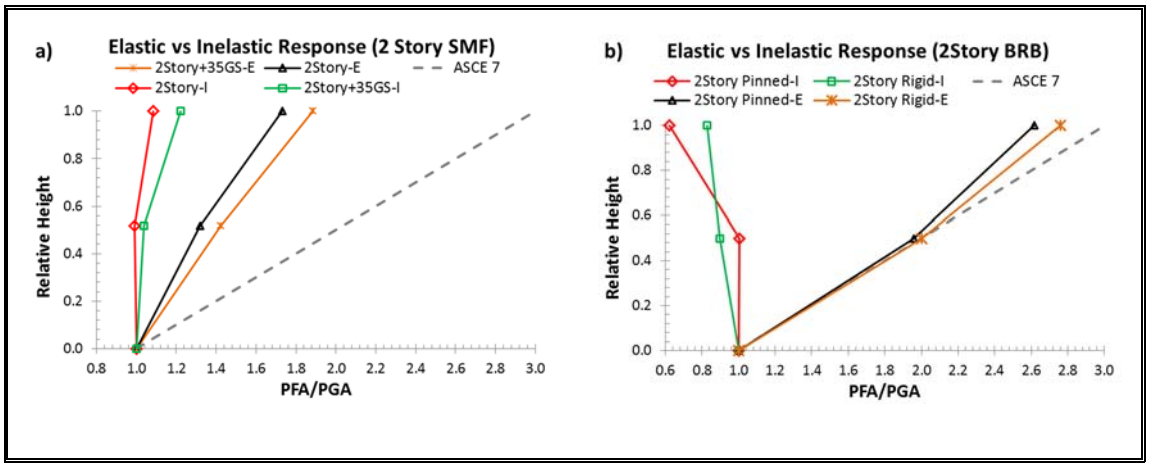

Figure 3 Normalized Peak Floor Acceleration (PFA/PGA): 2-Story Model

Representative examples of demands on flexible NSCs are shown in Figure 4 (a-b) and (c-d). As before, demands are greatly amplified when the period of the NSC is in resonance with one of the modal periods of the supporting structure. Elastic demands at the roof level are much higher in the BRBF, especially at modal resonance. Elastic demands at the first floor level and at second mode resonance is also much higher in the BRBF. However, inelastic behavior dramatically reduces demands in the BRBF. It can also be concluded that stiffer structures (BRBF with rigid connections and SMF with the gravity system) yield larger floor accelerations.

In summary, it was concluded that while acceleration demands on NSCs turned out to be qualitatively similar in both structural systems, some significant quantitative differences were observed. Such differences might be large enough to justify further research from

which the influence of the structural system could be more comprehensively characterized and eventually included in code provisions.

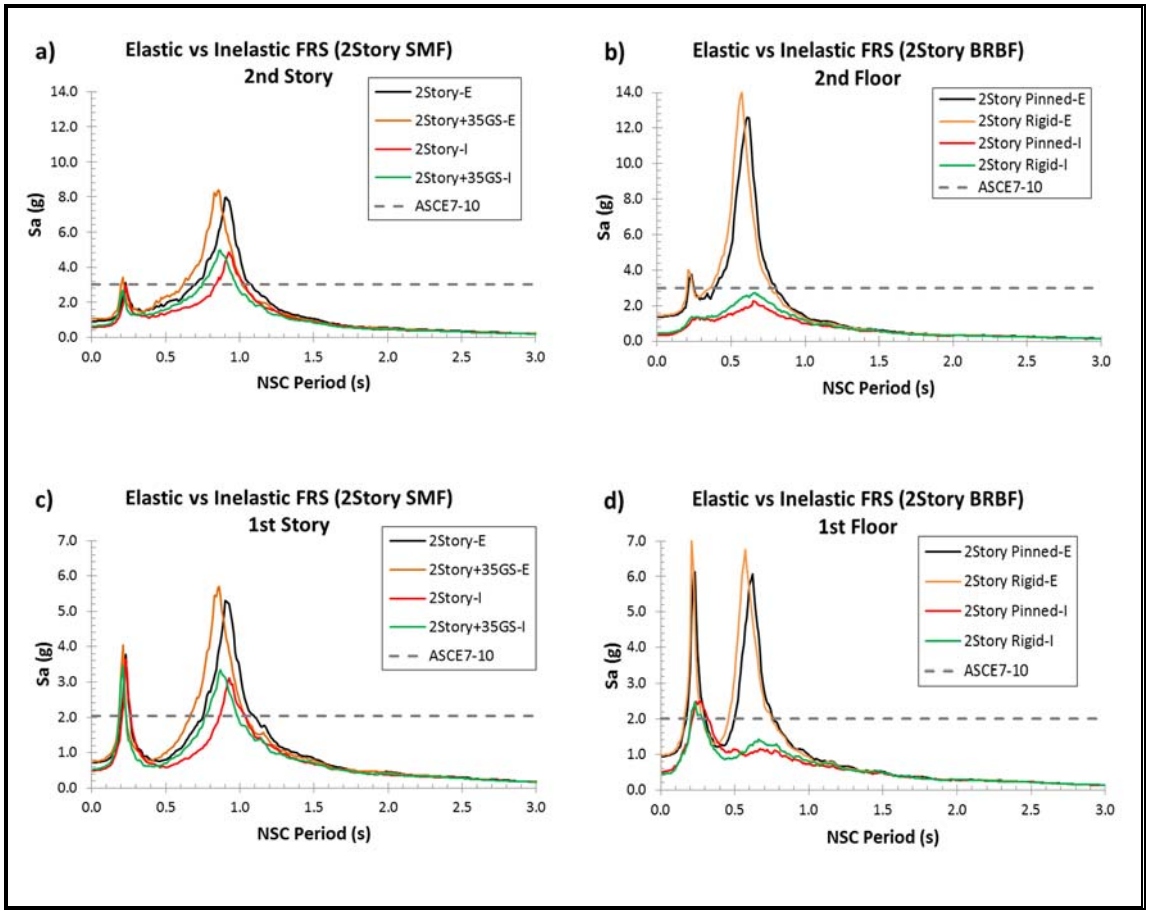

Figure 4 FRS at the 2nd (roof) and 1st level of the 2-Story Models

1.5.2 Influence of Accidental Torsion in nonlinear analysis.

The second main objective of this dissertation is to evaluate the influence of accidental torsion in nonlinear analysis. This issue is evaluated in detail in the paper "The Influence of Accidental Torsion on the Inelastic Dynamic Response of Buildings during Earthquakes" submitted to Earthquake Spectra (Chapter 4). Possible need to include accidental torsion in Nonlinear Response History Analysis (NRHA) is investigated through the evaluation of the seismic response of a 9-story steel building with Buckling Restrained Braces (BRB) to resist

lateral loads. Three versions of the building are considered, wherein the only difference is the plan location of individual braced frames resulting in different levels of torsional irregularity, from none to extreme. In the analysis the issues to be investigated are the influence of accidental eccentricity, the influence of bi-directional loading, and the influence of different criteria to model 3-dimensional second order effects.

A total of six models were studied which were divided into two groups: Models A, B and C were designed without accidental torsion and Models A-2, B-2 and C-2 were designed considering accidental torsion. The difference between Models A, B and C is the torsional irregularity which was obtained by moving the lateral resisting system (BRBs) from bays located near the center of the building to bays located near the edges. System A has a Type-1b (extreme) torsional irregularity, System B has a Type 1a torsional irregularity, and system C is not torsionally irregular. The same irregularities apply to Models A-2, B-2 and C-2. The six buildings were created with the purpose of evaluating the influence of accidental torsion on structures having different levels of torsional irregularities, and the influence of accidental torsion at the design stage.

Another important issue studied in this investigation is second-order effect, which was included following two different criteria. In the first approach the models include a "leaning column" at the center of the building, wherein the P load on the column is the entire gravity load (1.0D + 0.25L). Here, P-Delta effects (i.e., lateral second-order effects) are fully captured but torsional P-Theta effects (i.e., rotational, or torsional, second-order effects) are not accounted for. In the second approach, which captures both P-Delta and P-Theta effects, all the gravity columns are explicitly included in the models, and the P load on each column is the load determined by the corresponding tributary area. Results given by the models that

have a single leaning column are identified with the symbol P-Δ, and results given by the models that explicitly account for all the gravity columns are identified with the symbol P-Δθ. The symbol θ in the second case indicates that torsional P-Theta effects are included in addition to P-Δ effects.

In the following summary of results, only the ones given by Models A and A-2 are presented. The remaining results can be found in the aforementioned paper (Chapter 4). The evaluation of the topics of interest in this investigation was pursued by performing nonlinear static pushover and nonlinear time history analyses. Nonlinear static analysis was performed in two different manners: unidirectional and bidirectional. Both analyses were performed using displacement control with a first-mode lateral load distribution. Gravity load (1.05D +0.25L) was applied prior to lateral loading. In the unidirectional pushover analysis the lateral load was applied in the N-S direction at some eccentricity towards the East from the center of mass, and no load was applied in the E-W direction. In the bidirectional pushover analysis 100% of the lateral load in the N-S direction was applied in the same manner, along with (i.e., simultaneously) some percentage of the lateral load in the E-W direction applied without eccentricity.

Representative results given by pushover analysis are shown in Figure 5, where the roof drift ratio is measured at the center of mass. Here, for clarity, mass eccentricities lower than 5% are not shown because they had a minimal impact on performance. However, increasing the eccentricity from 5% to 6% in Model A (Figure 5a) and from 3 to 4% in Model A-2 (Figure 5d) had a tremendous influence on the shape of the pushover curve. As shown in Figure 5b and 5e, the sudden change in pushover response does not occur when P-Theta effects are ignored.

Figure 5c and Figure 5f illustrate the influence of bidirectional loading on extremely irregular systems when the N-S loading eccentricity is 5% and 3% of the building width for Models A and A-2, respectively. P-Theta effects are included, and orthogonal (E-W) loading is applied at the center of mass at some percentage of the full load. This percentage of the load is referred to herein as the Orthogonal Load Factor (OLF). It can be seen that a "bifurcation" in behavior (i.e., a sudden loss of strength) occurs when the orthogonal load reaches just 4% of the full value for Model A and 23% of the full value for Model A-2. This percentage varies depending on the amount of accidental torsion in the building. As it will be shown later in Chapter 4, the bifurcation in the nonlinear static response curve occurs as a result of the orthogonal frames (i.e., frames along the E-W direction) entering into a yielding stage, which creates a mechanism that causes the collapse of the structure.

One of the omissions in ASCE 7 is that it does not specify what approach should be taken to design the structure and satisfy accidental torsion requirements in the design (inter-story drift limit at the edges). This is especially needed when the building has a torsional irregularity (TIF>1.2) in just one of the principal directions. A common procedure is to make the frames stiffer (and stronger) in the direction where there is a torsional irregularity and leave unchanged the frames in the orthogonal direction. However, results described in the former paragraph indicate that it might be necessary to increase the frame sections in both orthogonal directions in order to prevent the "bifurcation" behavior.

Nonlinear Dynamic Response History analysis was carried out for each model using 11 ground acceleration recordings, representing actual earthquake events. These motions were selected from Table A-4A of the FEMA P-695 far-field record set list. Among the

eleven motions, according to ASCE 7-16 [34], no more than one "unacceptable response" (interpreted herein as a collapse) is allowed.

As it was done in pushover analysis, two types of nonlinear dynamic response history analyses were performed: unidirectional and bidirectional. The unidirectional analysis was performed without the orthogonal ground motion component while the bidirectional analysis included the two horizontal components. The parameters varied in the analyses included the amount of accidental eccentricity and inclusion or non-inclusion of P-Theta effects. Accidental torsion, where included, was generated by shifting the center of mass laterally (to the East) some percentage of the 240-ft width of the building. The horizontal component with the largest peak ground acceleration was selected for use in the N-S direction, and each component was amplitude scaled in such a way that the scaled component is consistent with the risk-based Maximum Considered Earthquake (MCE_R) level shaking at the lateral period of vibration in the N-S and E-W direction. For each analysis the system was first subjected to gravity load, followed by ground shaking. The roof drifts shown in the response history plots are the largest measured at the edge of the building.

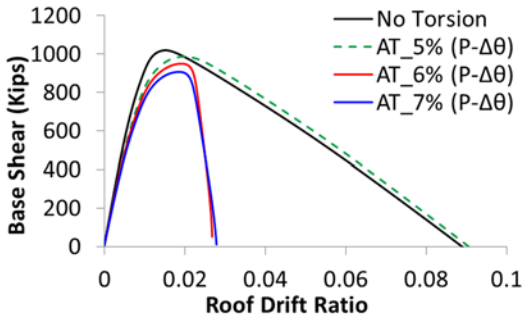

a) Unidirectional loading with Various Eccentricity (with P-Theta)

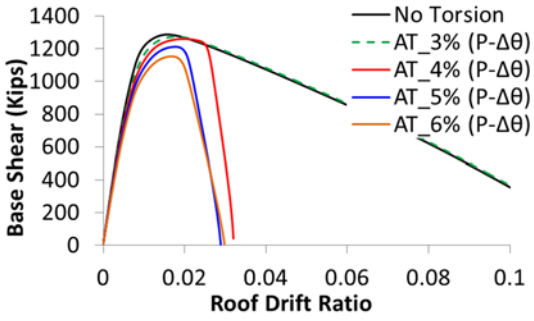

d) Unidirectional loading with Various Eccentricity (with P-Theta)

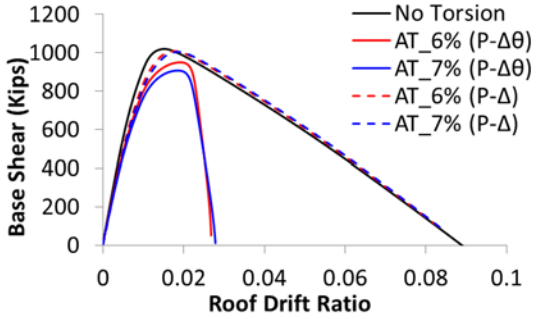

b) Unidirectional loading (with and without P-Theta)

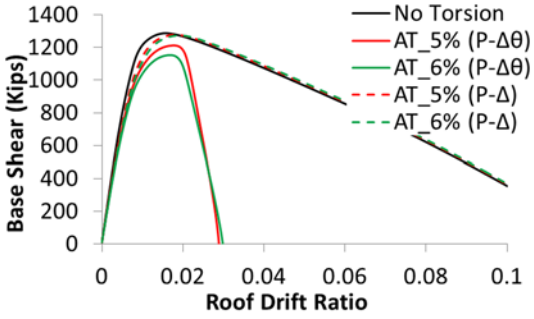

e) Unidirectional loading (with and without P-Theta)

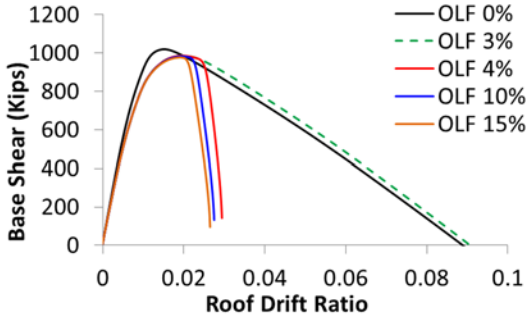

c) Bidirectional loading with 5% Eccentricity (With P-Theta)

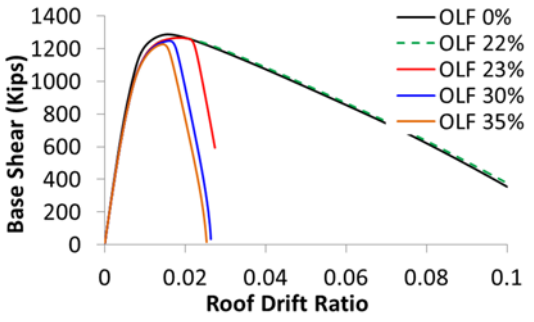

f) Bidirectional loading with 5% Eccentricity (With P-Theta)

Figure 5 Nonlinear static response of Models A (left) and A-2 (right)

Representative results given by nonlinear response time history analysis are shown in Figure 6. Results for Model A-2 are presented to show that inclusion of accidental torsion requirements at the design stage does not necessarily improve the performance. Figure 6a and Figure 6d show the response history of the roof drift ratio under unidirectional shaking (Duzce-Bolu ground motion) including P-Theta effects. As may be observed, in both models the roof drift response increases only slightly when the accidental torsion eccentricity varies from 0% to 5%. Under bidirectional loading, however, dynamic instability occurs when P-Theta effects are accounted for, and again the response of Model A-2 is only marginally better than the response of Model A. Figure 6c and Figure 6f illustrate once more the importance of P-Theta effects: when they are not included the bidirectional response shows no dynamic instability whatsoever.

It is clear from the analyses reported that accidental torsion has an important influence on the computed seismic response of structures predicted by nonlinear static analysis and nonlinear dynamic analysis. Additionally, the detrimental effect of accidental torsion is severely impacted by bidirectional loading, and by the P-Theta effect. The influence of accidental torsion increases with the degree of initial torsional irregularity.

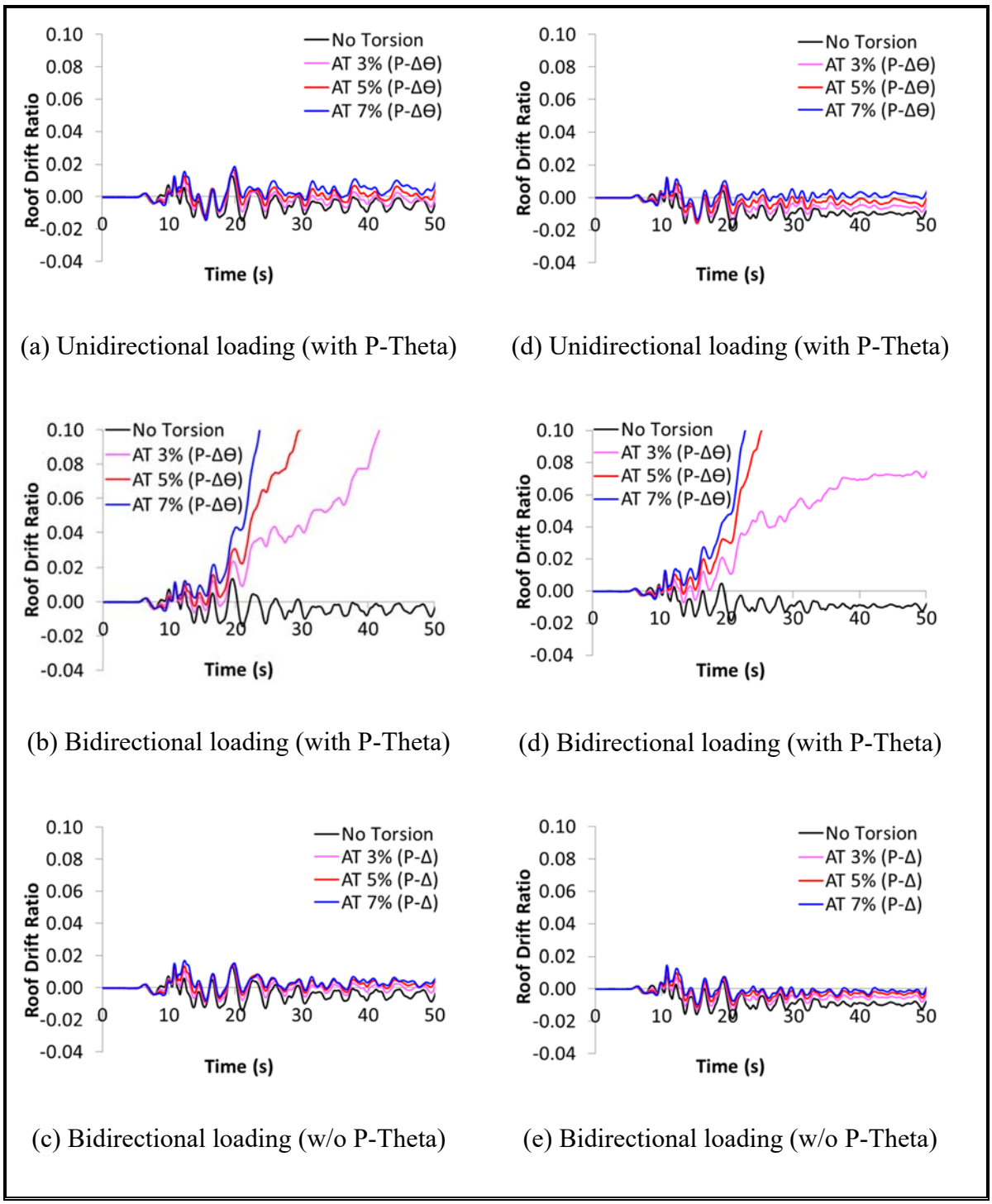

Figure 6 Response histories of roof drift for Models A (left) and A-2 (right) under the Duzce-Bolu ground motion

1.6 Summary and Conclusions

This final section of this chapter provides a summary of this dissertation. The first part of this investigation focused on evaluating the acceleration demands on Nonstructural Components (NSCs). The influence of detailed nonlinear models of Special Steel Moment Frames (SMFs) that incorporate the gravity system was studied and the results are described in the journal paper "Assessment of floor accelerations in special steel moment frames" (Chapter 2). The next investigation on this topic consists of a comparison between the acceleration demands on NSCs supported by two different structural systems: Special Steel Moment Frames and Buckling Restrained Braced Frames. Both demands were then compared with those provided by ASCE7-10. The study was published in the conference paper "Floor accelerations in buildings having different structural systems" (Chapter 3). Finally a different investigation on what is deemed as another overlooked topic in building codes, i.e., the influence of accidental torsion in nonlinear analyses, was performed. This last study focused on different parameters related to accidental torsion. The response of six building models that have different levels of torsional irregularity and were designed under different conditions was evaluated. As a result, the paper entitled "The influence of accidental torsion on the inelastic dynamic response of buildings during earthquakes" was submitted to Earthquake Spectra (Chapter 4).

The investigation on the two main topics of this dissertation provided significant insight into the acceleration demands on Nonstructural Components and into the influence of accidental torsion in nonlinear analyses. In what follows, the overall conclusions drawn from the research described in this dissertation are summarized.

Acceleration Demands on NSCs:

The following conclusions were drawn from the study where floor accelerations were computed using detailed models of Special Steel Moment Frames:

- The most relevant modeling issue is the inelastic behavior of the structure. This observation is evident even when the median seismic demand is barely larger than the elastic limit.
- The influence of the gravity columns on floor accelerations is negligible when it is assumed that the strength of the Partially Restrained (PR) connections in the gravity system is zero. This observation contrasts starkly with what was observed in [35], where it was found that the gravity columns have a significant influence on the collapse performance of SMFs.
- The gravity system does have some influence on floor accelerations when the strength of the PR connections is not zero. Such influence is most significant on Floor Response Spectra (FRS) at first mode resonance, diminishes at higher mode resonance, and becomes essentially negligible on PFAs. In all cases, the exact level of the strength of the PR connections is not relevant.
- As reported in the literature, spectral ordinates of FRS of inelastic building models are in some particular cases indeed greater than those of elastic building models, but such observation turned out to be true only at higher mode resonance, and only marginally so (by at most 15%, usually even less in the most realistic scenario where the gravity system is included considering some strength level of the PR connections).

- Floor accelerations obtained assuming linear behavior of the structure are then essentially conservative. However, it was found that in the 0.0 s – 0.5 s range, spectral ordinates of FRS of linearly elastic building models range from accurate to conservative by up to 150%. The degree of accuracy, however, is very sensitive to the period of the NSC, which makes accurate assessments difficult in actual case scenarios and in code provisions.

- The acceleration demands on rigid NSCs (inelastic building models) are roughly equal to the PGA, regardless of the floor level at which the NSC is attached. The acceleration demands on rigid NSCs are not expected to be as large as those indicated by the ASCE 7 approach, especially at the topmost floor levels.

- The acceleration demands on flexible NSCs (again, inelastic building models) were very high. Considering again the realistic 0.0 s – 0.5 s NSC period range, acceleration demands are in the range of 3.0 g - 4.5 g in the extreme case of higher mode resonance. These demands are reasonably well predicted by the ASCE 7 approach for NSCs located at the roof level, but not for those located at other floors.

The following conclusions were obtained from the study where floor accelerations in SMFs were compared with those in BRBFs:

- Qualitatively, acceleration demands are essentially similar in both structural systems.

- Quantitatively, however, some differences were found. Accelerations demands in BRBFs are generally smaller (sometimes, but not always, by a significant margin) than those in SMFs.

- The influence of inelastic behavior on acceleration demands is more pronounced in BRBFs than in SMFs.
- The observed differences possibly justify both further research and eventual inclusion of the influence of the structural system in future code provisions related to acceleration demands.

Accidental Torsion in Nonlinear Analysis

- Accidental torsion has an important influence on the computed seismic response of structures given by nonlinear static analysis and nonlinear dynamic analysis.
- Such influence increases with the degree of torsional irregularity. However, it is important to note that even moderately irregular building models were severely impacted by accidental torsion in both nonlinear static and nonlinear dynamic analysis. In the case of regular building models, collapse performance might not be significantly affected by accidental torsion, but the interstory drift response at the building corners might increase up to 60% due to accidental torsion.
- Based on these results it appears that the exclusion of accidental torsion induced by mass eccentricities as low as 3% of the building width is possibly unconservative for building systems with torsional irregularity factors (TIFs) lower than about 1.2, is likely unconservative for buildings with TIFs greater than about 1.2, and can be regarded as potentially unsafe for systems with TIFs greater than about 1.4.
- Analysis under unidirectional loading often failed to capture potential dynamic instability, even when P-Theta effects were included.

- It was found in all cases that dynamic instability is not correctly captured if P-Theta effects are excluded.
- It was found that the models designed considering accidental torsion requirements did not perform as well as expected despite the fact that their performance is somewhat better than that of the models designed without accidental torsion. It is believed that the provisions given by ASCE 7 should be more precise about how to increase the strength of the building to fulfill drift and strength requirements when accidental torsion is included.
- In all cases, nonlinear response history analysis must be carried out considering: (1) full bidirectional loading; (2) accidental torsion; and (3) both P-Delta and P-Theta effects
- If the structure is geometrically regular, P-Theta effects can be correctly accounted for by placing leaning columns at a distance from the center of mass equal to the radius of gyration.

1.7 References

[1] B. Reitherman, T. Sabol, R. Bachman, D. Bellet, R. Bogen, D. Cheu, P. Coleman, J. Denney, M. Durkin, C. Fitch, Nonstructural damage, Earthquake Spectra 11(S2) (1995) 453-514.

[2] E. Miranda, G. Mosqueda, R. Retamales, G. Pekcan, Performance of nonstructural components during the 27 February 2010 Chile earthquake, Earthquake Spectra 28(S1) (2012) S453-S471.

[3] E. Miranda, S. Taghavi, Approximate floor acceleration demands in multistory buildings. I: Formulation, Journal of structural engineering 131(2) (2005) 203-211.

[4] J. Lin, S.A. Mahin, Seismic response of light subsystems on inelastic structures, Journal of Structural Engineering 111(2) (1985) 400-417.

[5] S. Taghavi, E. Miranda, Response assessment of nonstructural building elements, Pacific Earthquake Engineering Research Center2003.

[6] ASCE, ASCE 7-10: Minimum Design Loads for Buildings and Other Structures, American Society of Civil Engineers, American Society of Civil Engineers/Structural Engineering Institute, Reston, VA, 2011.

[7] A. Aref, M. Bruneau, M. Constantinou, A. Filiatrault, G.C. Lee, A.M. Reinhorn, A.S. Whittaker, Seismic Response Modification of Structural and Nonstructural Systems and Components in Acute Care Facilities, Research Progress and (2004) 95.

[8] B. Kehoe, M. Hachem, Procedures for estimating floor accelerations, Proc., ATC-29-2 Seminar on Seismic Design, Performance, and Retrofit of Nonstructural Components in Critical Facilities, Applied Technology Council, Redwood City, Calif, 2003.

[9] M. Singh, L. Moreschi, L. Suárez, E. Matheu, Seismic design forces. I: Rigid nonstructural components, Journal of structural engineering 132(10) (2006) 1524-1532.

[10] I. Politopoulos, C. Feau, Some aspects of floor spectra of 1DOF nonlinear primary structures, Earthquake engineering & structural dynamics 36(8) (2007) 975-993.

[11] R.A. Medina, R. Sankaranarayanan, K.M. Kingston, Floor response spectra for light components mounted on regular moment-resisting frame structures, Engineering structures 28(14) (2006) 1927-1940.

[12] R. Sewell, C. Cornell, G. Toro, R. McGuire, R. Kassawara, A. Singh, J. Stepp, Factors influencing equipment response in linear and nonlinear structures, Transactions of the 9th international conference on structural mechanics in reactor technology. Vol. K2, 1987.

[13] R. Sankaranarayanan, R.A. Medina, Acceleration response modification factors for nonstructural components attached to inelastic moment-resisting frame structures, Earthquake Engineering & Structural Dynamics 36(14) (2007) 2189-2210.

[14] I. Politopoulos, Floor spectra of MDOF nonlinear structures, Journal of Earthquake Engineering 14(5) (2010) 726-742.

[15] M. Rodriguez, J. Restrepo, A. Carr, Earthquake-induced floor horizontal accelerations in buildings, Earthquake engineering & structural dynamics 31(3) (2002) 693-718.

[16] S.R. Chaudhuri, R. Villaverde, Effect of building nonlinearity on seismic response of nonstructural components: a parametric study, Journal of structural engineering 134(4) (2008) 661-670.

[17] J. Wieser, G. Pekcan, A.E. Zaghi, A. Itani, M. Maragakis, Floor accelerations in yielding special moment resisting frame structures, Earthquake Spectra 29(3) (2013) 987-1002.

[18] FEMA, Quantification of Building Seismic Performance Factors (FEMA P-695), Federal Emergency Management Agency, Washington, D.C, 2009.

[19] F. Zareian, D. Lignos, H. Krawinkler, Evaluation of seismic collapse performance of steel special moment resisting frames using FEMA P695 (ATC-63) methodology, Proceedings of Structures Congress ASCE, New York, 2010.

[20] NIST, Evaluation of the FEMA P-695 Methodology for Quantification of Building Seismic Performance Factors (NIST GCR 10-917-8), National Institute of Standards and Technology, Gaithersburg, MD, 2010.

[21] O. Atlayan, F.A. Charney, Hybrid buckling-restrained braced frames, Journal of Constructional Steel Research 96 (2014) 95-105.

[22] NIST, Nonlinear Structural Analysis for Seismic Design (NIST GCR 10-917-5), National Institute of Standards and Technology, Gaithersburg, MD, 2010.

[23] NIST, Applicability of Nonlinear Multiple-Degree-of-Freedom Modeling for Design (NIST GCR 10-917-9), National Institute of Science and Technology, Gaithersburg, MD, 2010.

[24] PEER, Guidelines for Performance Based Design of Tall Buildings, Pacific Earthquake Engineering Research Center, University of California, Berkeley, CA, 2010.

[25] PEER, Modeling and Acceptance Criteria for Seismic Design and Analysis of Tall Buildings (PEER/ATC 72-1). Pacific Earthquake Engineering Research Center, Richmond, CA, 2010.

[26] NIST, Selecting and Scaling Earthquake Ground Motions for Performing Response-History Analysis (NIST GCR 11-917-5), National Institute of Science and Technology, Gaithersburg, MD, 2011.

[27] FEMA, NEHRP recommended seismic provisions for new buildings and other structures (FEMA P-750), Federal Emergency Management Agency, Washington, DC (2009).

[28] ASCE, Seismic Rehabilitation of Existing Buildings (ASCE/SEI 41-13), American Society of Civil Engineers Reston, Virginia, 2013.

[29] SFBC, Requirements and Guidelines for the Seismic Design of New Tall Buildings Using Non-Prescriptive Design Procedures, 2013 San Francisco Building Code Administrative Bulletin 083, San Francisco, CA, 2013.

[30] LATBSDC, An Alternative Procedure for Seismic Analysis and Design of Tall Buildings Located in The Los Angeles Region, Los Angeles Tall Building Structural Design Council, Los Angeles, CA, 2014.

[31] FEMA, 2015 NEHRP Recommended Provisions for New Buildings and Other Structures (FEMA P-1050), Federal Emergency Management Agency, Washington, D.C, 2015.

[32] S. Mazzoni, F. McKenna, M.H. Scott, G.L. Fenves, OpenSees command language manual, Pacific Earthquake Engineering Research (PEER) Center (2006).

[33] ASCE, ASCE 7-05: Minimum Design Loads for Buildings and Other Structures, American Society of Civil Engineers, American Society of Civil Engineers/Structural Engineering Institute, Reston, VA, 2006.

[34] ASCE, ASCE 7-16: Minimum Design Loads for Buildings and Other Structures, American Society of Civil Engineers, American Society of Civil Engineers/Structural Engineering Institute, Reston, VA, 2017.

[35] F. Flores, F. Charney, D. Lopez-Garcia, The influence of gravity column continuity on the seismic performance of special steel moment frame structures, Journal of Constructional Steel Research 118 (2016) 217-230.

2. ASSESSMENT OF FLOOR ACCELERATIONS IN SPECIAL STEEL MOMENT FRAMES

2.1 Introduction

Structural design of buildings against seismic loads has changed over the last several years. The reasons for the changes are advances in research and experiences of real events that have occurred. Current building codes provide design rules that have, as the main goal, to limit the probability of collapse of the building during an earthquake. Recent events like the 1994 Northridge (USA), 1995 Kobe (Japan) and 2010 El Maule (Chile) earthquakes have shown that the majority of buildings performed as expected against collapse. However, there were cases where the building system did not suffer any structural damage but the nonstructural damage inside the building made it impossible to occupy the facility after the event [1, 2]. In hospitals this represents a major risk against life; moreover the direct and indirect economic losses can be greater than the cost of the structure [3].

Nonstructural Components (NSCs) in buildings are divided into two main categories: those that are sensitive to story drifts and those that are sensitive to accelerations [4]. Examples of NSCs sensitive to story drifts are: masonry walls, windows, interior doors, partitions, etc. Acceleration sensitive NSCs include parapets, suspended ceilings, ducts, boilers, chiller tanks, etc. [5]. The acceleration-sensitive NSCs receive the forces that arise from the motion of the structure to which they are anchored or attached, from now on denoted as the "supporting structure". The method usually used to estimate the accelerations that affect the NSCs is the Floor Response Spectrum (FRS) method. This approach computes the elastic response spectrum of a selected floor using as input the total acceleration response of the same floor. It can be applied when the interaction

between the NSC and the supporting structure is not significant, i.e., when the response of the structure is essentially the same regardless of whether the NSC is present or not. In general, the interaction between the NSC and the supporting structure is not significant when the mass of the NSC is less than approximately 1.0 percent the mass of the supporting structure [6]. If the NSC mass is larger, dynamic interaction will occur between NSCs and the supporting structure, and the FRS method might in some cases produce overly conservative results [7].

Research has been performed to understand the acceleration demands on NSCs. Most of the investigations were executed considering the supporting structure to behave elastically [3, 8, 9]. However, several authors have studied the effect of the building inelastic behavior on the accelerations that are imposed on NSCs. The general trend is that inelastic deformations in the supporting structure reduce the acceleration demands with respect to the demands based on the elastic response of the supporting structure. However, in some cases, particularly for short-period NSCs (say, NSC period less than 0.5 sec), demands based on inelastic structural response might actually be greater. Some of these studies were performed using simple SDOF structures [4, 10], and others studied the effect of plasticity in MDOF structures [11-17].

Currently, nonlinear dynamic analysis is performed using models that present different levels of detail depending on the required outcome. For example, the FEMA P-695 methodology [18] requires very detailed nonlinear models that are able to capture collapse of structures when they are subjected to ground motions scaled to different levels of intensity. In the case of acceleration demands on NSCs, the mathematical models that have been studied so far usually do not have the level of detail as required by other analyses such as the FEMA P-695. For instance, Sewell et al. [12] studied a 5-story lumped-mass shear beam structure, therefore inelastic deformations occurred only at the springs representing the story force-deformation relationship.

Rodriguez et al. [15] investigated the floor accelerations of 3-, 6- and 12-story buildings with cantilever walls. The inelastic deformations in the walls occurred only at the bottom of the first story. Medina et al. [11] studied the floor accelerations of stiff and flexible one-bay frames of 3, 6, 9 and 18 stories. The one-bay frames used in the study were designed to satisfy the strong-column weak-beam requirement. Therefore, inelastic deformations were allowed to occur only at the beam ends and at the bottom of the first story columns. Chaudhuri and Villaverde [16] studied the effect of inelastic structure response on the seismic demands on NSCs. In the investigation 4-, 8-, 12- and 16-story flexible and stiff moment steel frames were analyzed. The frames were modeled using fiber sections with a bilinear material with post-yield stiffness equal to 3% of the initial stiffness. More recently, Wieser et al. [17] studied the floor accelerations using three dimensional models. A total of four buildings were analyzed. The numerical models of the buildings used elastic beam-column elements for the gravity system and fiber sections for the lateral force resisting system. The material assigned to the fiber sections is a nonlinear steel material with 2% post-yield stiffness ratio.

These studies demonstrate the analytical sophistication of research that has been performed to characterize the floor accelerations when MDOF structures are subjected to ground motions and behave inelastically. However, it can be seen that the models that have been used did not have all the details that a complete nonlinear mathematical model could include. Fiber models can capture plastification well but since strength degradation was not included, the buildings cannot collapse under larger ground motion intensities. Additionally, models with the capability of plastification only at the beam ends and at the bottom of the first story columns cannot present story mechanisms because plastic hinges in the columns are not allowed to occur.

The main purpose of this study is to contribute to a more detailed and more realistic understanding of floor accelerations by quantifying the level of detail required in a structural model when floor accelerations are computed. This is why the structures chosen to be investigated are the Special Steel Moment Frames (SMFs) analyzed by Zareian et al. [19] for the ATC 76-1 project [20]. These models have the amount of detail required to evaluate their collapse performance using the FEMA P-695 methodology. At the moment, this methodology can be considered the most stringent in terms of requirements of nonlinear mathematical models. In order to define even further the importance of the level of detail of the model, the gravity system is also considered in this investigation. In a recent study [21], it was found that the gravity system has a significant influence on the collapse performance of the same SMFs considered in this investigation. Finally, this study also intends to obtain an accurate quantitative assessment of the level of acceleration demands that can be realistically expected in NSCs anchored to multi-story SMFs located in areas where the level of seismic activity is high, such as the western United States, Japan, and Chile.

The method FRS method is used in this study to characterize the seismic demands on NSCs anchored at different floor levels in multi-story SMFs. Therefore, the interaction between the NSCs and the primary structure is neglected due to the (assumed) small mass of the NSCs (most generally the actual scenario in office and residential multi-story buildings).

2.2 Methodology

The numerical models of the SMFs to be analyzed were created using OpenSees [22]. The first step was to verify the accuracy of the models by performing a FEMA P-695 analysis and by comparing the results with the ones presented by Zareian et al. in the ATC 76-1 project. As specified by the FEMA P-695 methodology, the strength and stiffness of the gravity system was not included in the analysis performed by Zareian et al. In this study, however, once the models

without the gravity system were verified, the gravity system was explicitly modeled in order to evaluate its possible influence on floor accelerations. The gravity system is modeled using partially-restrained (PR) connections that have different strength levels, and the gravity columns were modeled using fiber sections with a bilinear material with 10% kinematic hardening.

Once the models were validated and the gravity system incorporated, the structures were subjected to the 44 Far-Field ground motions as specified by the FEMA P-695 methodology. The level of intensity to which the ground motions are scaled is the Design Earthquake (from now on denoted simply as DE). This criterion was adopted because the acceleration demands on NSCs indicated in ASCE 7-05 [23, 24] and in ASCE 7-10 [23, 24] are consistent with the DE. The total acceleration response is obtained for each floor, and is then used as input to compute the floor response spectrum. In order to compute the influence of inelastic deformations in the models, the floor accelerations were also computed but with the models behaving elastically.

2.3 Overview of Buildings Analyzed

As already mentioned, the buildings analyzed were taken from the ATC 76-1 project. Complete information about the design and the nonlinear models can be found in the referenced document [20]. However, a summary of the main information is provided herein. The study performed by Zareian et al. considered buildings of 1, 2, 4, 8, 12 and 20 stories. They were designed following the ASCE 7-05 [23] requirements with the exception that the deflection amplification factor C_d was taken equal to the response modification factor, R, as specified in FEMA P-695. The gravity system was not included in the analysis as the P-695 procedure specifies.

Two different analysis methods were used to design the buildings: the Equivalent Lateral Force (ELF) method and the Modal Response Spectrum Analysis (RSA) method. All the SMFs

were designed using reduced beam section connections (RBS) for a seismic design category D_{max} (S_s=1.5g, S_1=0.6g), for a typical gravity load, and considering Site Class D.

This investigation analyzes a subset of the buildings from the ATC 76-1 project. These are the 2-, 4- and 8-story models designed using the RSA method. The base of the columns of the buildings were fixed for the 4- and 8-story models, and pinned for the 2-story model. The nomenclature that identifies these structures in ATC 76-1 is 2RSA (2 story), 3RSA (4 story) and 4RSA (8 story). Figure 1 shows the plan view for all the buildings. The bay width (center line dimensions) between columns of each SMF is 20 ft. The height of the first story is 4.6 m. (15 ft) (to top of steel beam), and the height of all other stories is 4 m (13 ft). According to ATC 76-1, this configuration is representative of multistory SMF buildings. The design dead load (D) is 4.31 kN/m^2 (90 psf) uniformly distributed over each floor, and the cladding load is applied as a perimeter load of 1.2 kN/m^2 (25 psf). The unreduced design live load (L) is 2.4 kN/m^2 (50 psf) on all floors and 0.96 kN/m^2 (20 psf) on the roof. These loads were considered in the analysis in a combination of 1.0 D + 0.25 L.

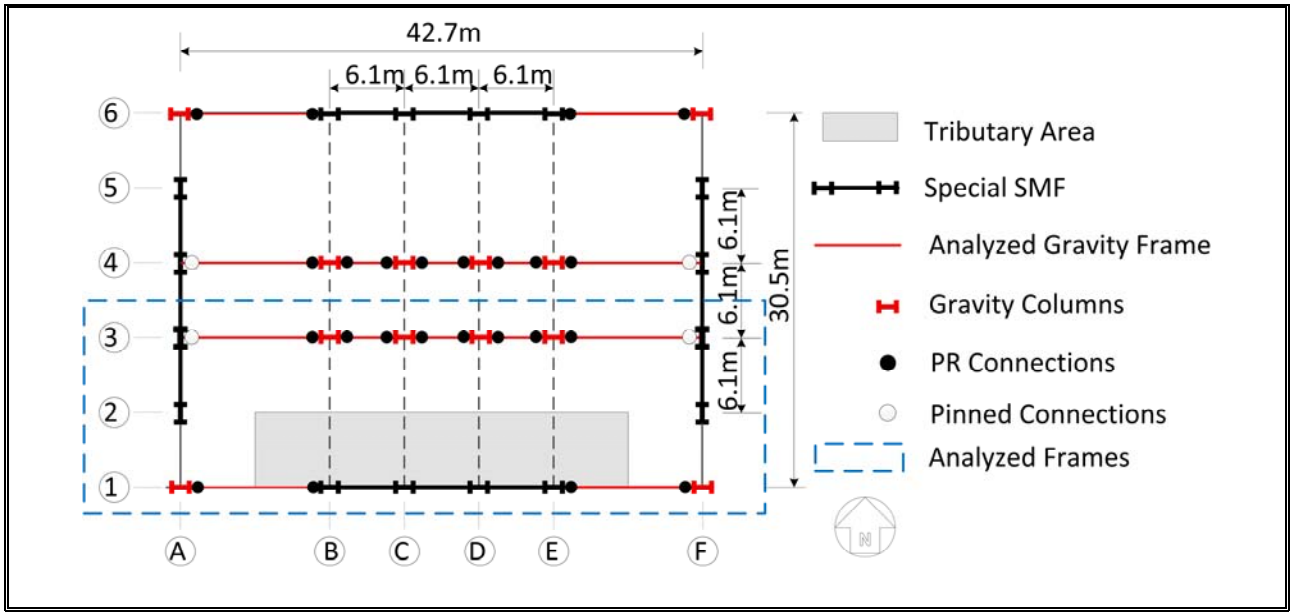

Figure 1 Typical Building Plan View

Figure 1 illustrates the configuration of the gravity system only in the direction to be analyzed (East-West). As already mentioned, gravity connections are considered to be PR connections. The lateral strength of the SMF columns oriented on the weak axis (A3, F3) is not considered because the sole influence of the gravity columns is intended to be evaluated. However, future research is required to evaluate the influence of columns oriented on the weak axis if they are included in the analysis.

2.4 Modeling approach

The numerical two-dimensional models idealized to perform the nonlinear analysis were created using OpenSees. Material and geometric nonlinearities were included in every model. In the case where the gravity system was not included, P-Delta effects were considered using a leaning column with no flexural stiffness placed parallel to the SMF. The load applied to this column represents half of the total load from the gravity system that was not tributary to the SMF columns. For the cases where the gravity system was included, a leaning column was not required.

The approach applied to model the frames was using elastic elements and the nonlinear behavior was lumped into plastic hinges located at the ends of the members. The components of the SMF with nonlinear behavior are shown in Figure 2 and they are: panel zones, plastic hinges located at the RBSs of the beam and plastic hinges at the column ends.

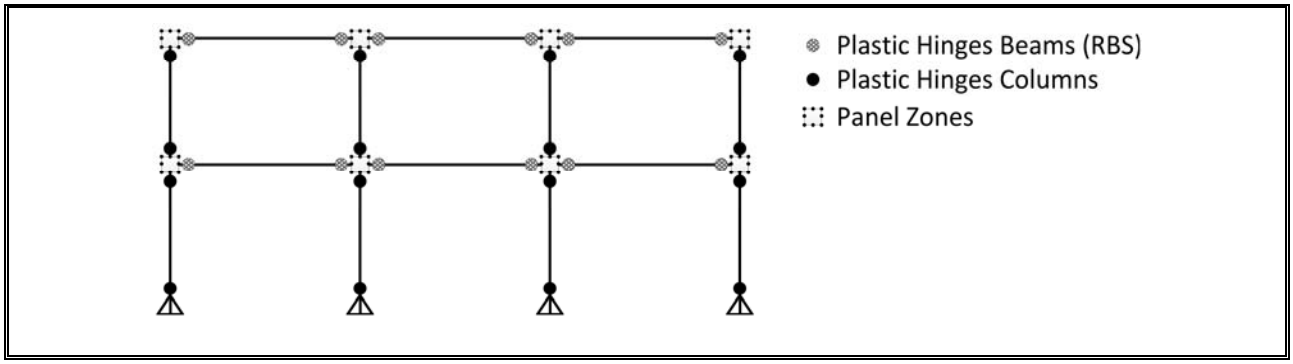

Figure 2 Elements of the models that do not include the gravity system

A complete description of the inelastic behavior of each component can be found in the ATC 76-1 report. However, a brief overview is provided herein. The hysteretic behavior of the RBSs in the beams is modeled using a rotational spring. Using OpenSees, the behavior was characterized by the material called "Bilin". The constitutive law of this material is based on the modified Ibarra-Krawlinkler deterioration model [25], and the parameters to define it are described by Lignos and Krawinkler [26].

Panel zones are modeled using a rectangular region composed of eight very stiff elastic beam-column elements and one nonlinear rotational spring to represent shear distortions in the panel zone [27]. These deformations are due to shear yielding and column flange flexure yielding and are represented by a tri-linear backbone curve assigned to the rotational spring.

The phenomenological component used to characterize the nonlinear behavior of the SMF columns is the same as the one used for the beams. This approach was taken because at the time the analysis was perfromed OpenSees did not have a component with a hysteretic behavior that includes the axial force – bending moment (P-M) interaction. To account for the reduced bending strength of the columns due to the axial force, a representative axial force was computed. Even though the axial force changes during a dynamic analysis, this representative axial force is computed before the analysis and the bending strength is reduced accordingly. It was obtained by performing a nonlinear static pushover analysis and it was considered to be equal to $P_{grav} + 0.5\ P_{E,max}$, where P_{grav} is the gravity load that the column is subjected to and $P_{E,max}$ is the maximum load that the column receives during the pushover analysis. The pushover analysis is performed until a reduction of 20% in the base shear, V_{max}, is reached. With the axial load determined, the reduced bending strength is computed using the AISC P-M interaction equation [28] and subsequently used in the models.

The additional components modeled in the case where the gravity system was included are: PR connections and gravity columns modeled using fiber sections. The complete frame with the gravity system placed in parallel is shown in Figure 3.

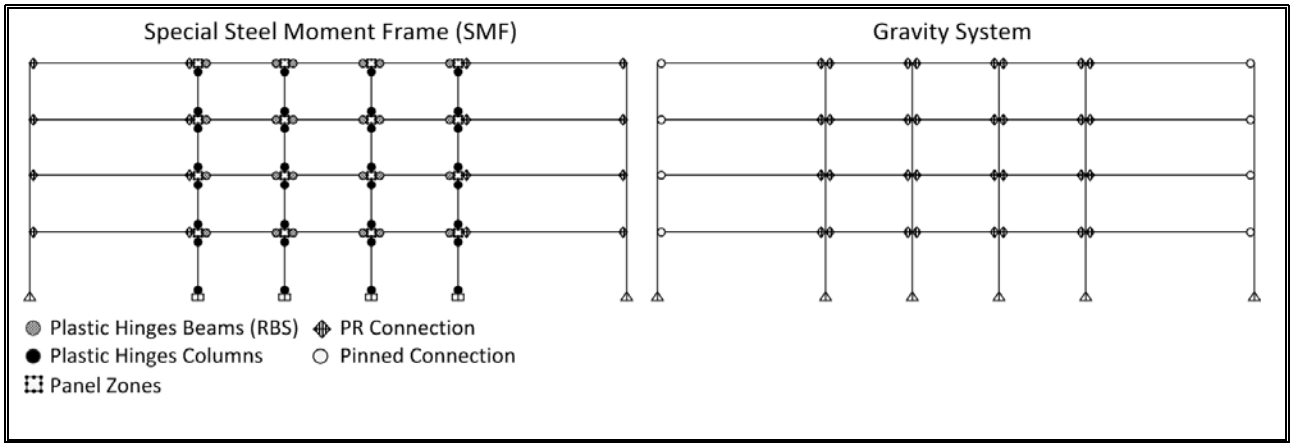

Figure 3 Elements of the models that include the gravity system

In order to account for any inelastic deformation that could occur in the gravity columns, they were modeled using force-based fiber elements with a bilinear material with strain hardening equal to 10% of the initial stiffness. The benefit of using fiber sections is that the axial-moment interaction is taken into account. However, because strength degradation is not included, the capability of the model to represent collapse is limited. This is why plastic hinges at columns of the SMFs were modeled using a phenomenological approach.

The flexural strength of the gravity connections was considered to be a percentage of the plastic moment strength (M_p) of the beam. Different strength levels were studied with the purpose of establishing possible influence on floor accelerations. Liu and Astaneh [29] performed cyclic tests on different simple connections and the range of flexural strength depend on the type of connection. For instance, shear tab connections with and without the contribution of the concrete slab were able to develop a moment equal to 36%M_p and 18%M_p respectively. On the other hand, stronger connections developed moments up to 72%M_p. Based on these results, the percentages

assigned to the PR connections were 0%, 35%, 50%, and 70%. The 0% represents the influence purely of the gravity columns, and the 35% is the minimum strength required by the connections to avoid yielding under gravity loads. Although probably too large, the 50% and 70% are considered in order to acquire an extended possible range of behavior.

Even though the cyclic behavior of the PR connections is complicated to characterize, it was considered that a simple model, such as the one given by ASCE 41-13 [30], would be accurate enough to the purpose of this study. One of the parameters given by this model is the rotation at which the PR connections yield (0.005 radians). Therefore, the stiffness of the PR connections is different for each strength level. More information regarding the modeling of the PR connections can be found in Flores et. al [21].

For the nonlinear dynamic response history analysis, a Rayleigh damping of 2.5% is assigned to the first modal period T_1 and to period $T = 0.2\ T_1$ in all cases. As proposed by Zareian and Medina [31], stiffness proportional damping is assigned to elements that remain elastic, and mass proportional damping is assigned to nodes or elements where mass is lumped.

2.5 Validation of the Models

As already mentioned, the SMFs investigated in this study were studied by Zareian et al. [20] and the results were presented in the ATC 76-1 project . Therefore, to validate the models that do not include the gravity system, a complete collapse evaluation of the 2-, 4- and 8-story models was performed and compared with the already published results. The difference between the results reported by Zareian et al. and the ones found in this study was marginal. A more detailed description of the validation process can be found in [21].

2.6 Earthquake Ground Motions

The ground motions used in this study were taken from the FEMA P-695 methodology and they belong to the group of Far-Field ground motions. The Far-Field record set consists of twenty-two horizontal component pairs of records from sites located at a distance equal to or greater than 10 km from the fault rupture. Some of the criteria used by the FEMA P-695 methodology to choose the ground motions are: earthquakes with magnitude larger than or equal to 6.5, the source mechanism of the earthquakes is either strike-slip or reverse, the site conditions are either soft rock (Site Class C) or stiff soils (Site Class D). More information regarding the record selection criteria can be found in [18].

2.7 Ground Motion Scaling

The ground motions are scaled to represent a specific intensity which in this study is the Design Earthquake (DE). Under this level of intensity, the immediate occupancy of the structures after the earthquake is expected. Thus, the design of NSCs have to be considered in order to prevent damage or movement. On the other hand, under higher level intensities such as the Maximum Considered Earthquake (MCE) the limit state to be controlled is “life safety”, so the structure will suffer considerable damage but the collapse has to be prevented. Therefore at MCE level of intensity, NSCs are not a major concern.The method used to scale the records is the one proposed by the FEMA P-695 methodology, and is briefly explained herein. The scaling process involves two steps: normalization and scaling. The first step normalizes individually each record with respect to the value of peak ground velocity computed in the PEER NGA database (PGV_{PEER}). Figure 4 displays the spectra of the Far-Field components before and after normalization.

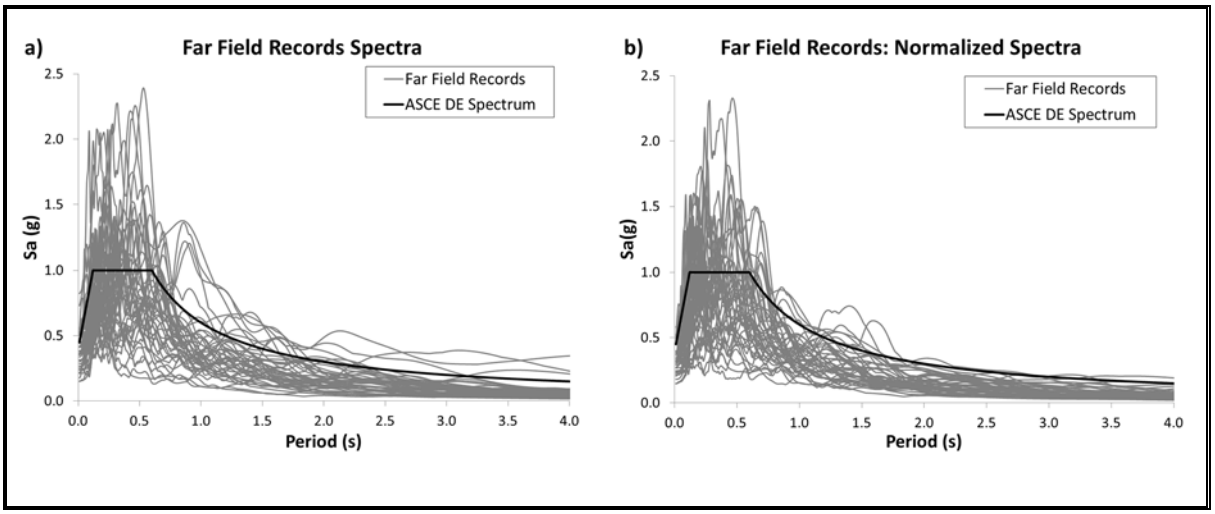

Figure 4 Far-Field Ground Motions Spectra a) Before Normalization b) After Normalization

The second step is to scale the set of records to the DE spectral acceleration. The FEMA P-695 procedure establishes that the records are to be scaled to the MCE spectral acceleration, but, for the reasons described before, in this study the records were scaled to the DE spectral acceleration. The approach to scale the records requires that the median spectral acceleration of the set of records matches the DE demand at the fundamental period (T). It has to be mentioned that the fundamental period of vibration used for scaling is not the true computed period (from eigenvalue analysis). Instead, as specified in FEMA P-695, the design period from ASCE 7, i.e., $T = C_u T_a$ was used, where C_u is a coefficient that represents an upper limit on the calculated period and T_a is an empirical approximation of the fundamental period [24]. However, floor accelerations were also computed using records scaled to the true computed period of the structure and the results of both analyses were virtually the same. Figure 5 shows the records scaled to the DE for the 2- and 8- story buildings.

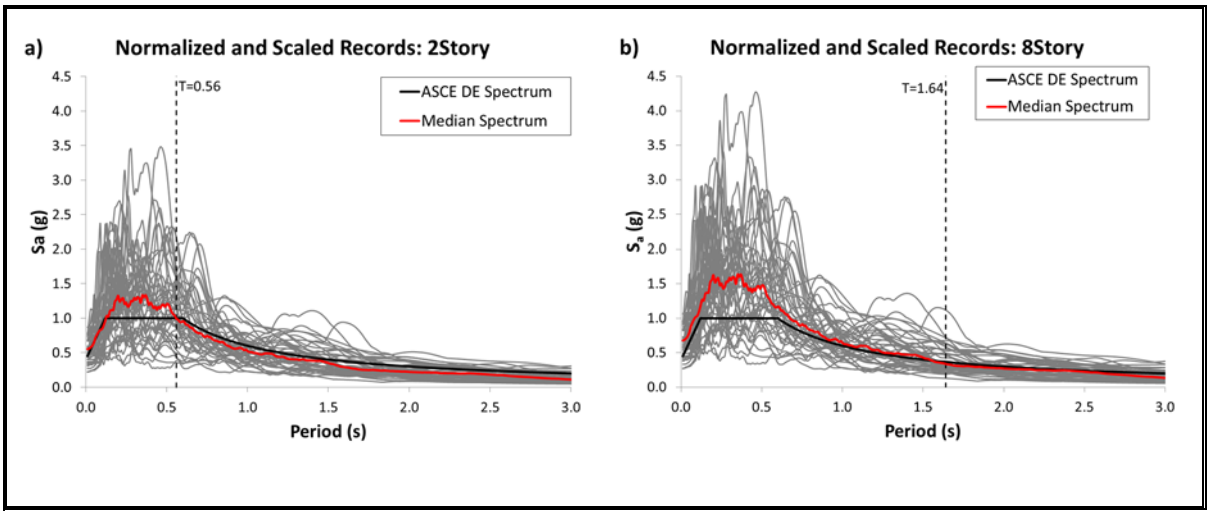

Figure 5. Scaling Ground Motions a) 2-Story Model b) 8-Story Model

Naturally, the Design Response Spectrum considered in the scaling procedure is the same Design Response Spectrum considered in the design process of the building models. The corresponding PGA is equal to 0.4 g, a typical value in areas where the level of seismic activity is significant.

2.8 Nonlinear Static Pushover Analysis

In the FEMA P-695 methodology, nonlinear static pushover analysis is to be performed to compute the overstrength and the period-based ductility of a given building model. In this study, the pushover analysis is instead used to estimate the level of inelastic demand on the buildings. For this purpose, the median roof displacement response obtained from the nonlinear dynamic analyses is shown with a vertical dashed line on the pushover plots. From now on, the following nomenclature is adopted: nStory + sGS, where n is the number of stories and s is the percentage of full strength assigned to the PR connections (if sGS is not included, the model does not include the gravity system, and instead includes a leaning column to account for P-Delta effects). Figure 6 presents the pushover curves obtained for the 2-Story models. The roof drift response indicated by the nonlinear dynamic analyses is also represented in this figure: the gray area indicates the

range of roof drift values, and the vertical dashed line represents the median value. It can be seen that the 2-Story model remains basically elastic at the estimated DE demand (median value). Therefore, the difference between the accelerations given by the elastic models and those given by the inelastic models might not be of practical significance. This observation is the main motivation to evaluate acceleration estimates given by simple elastic models.

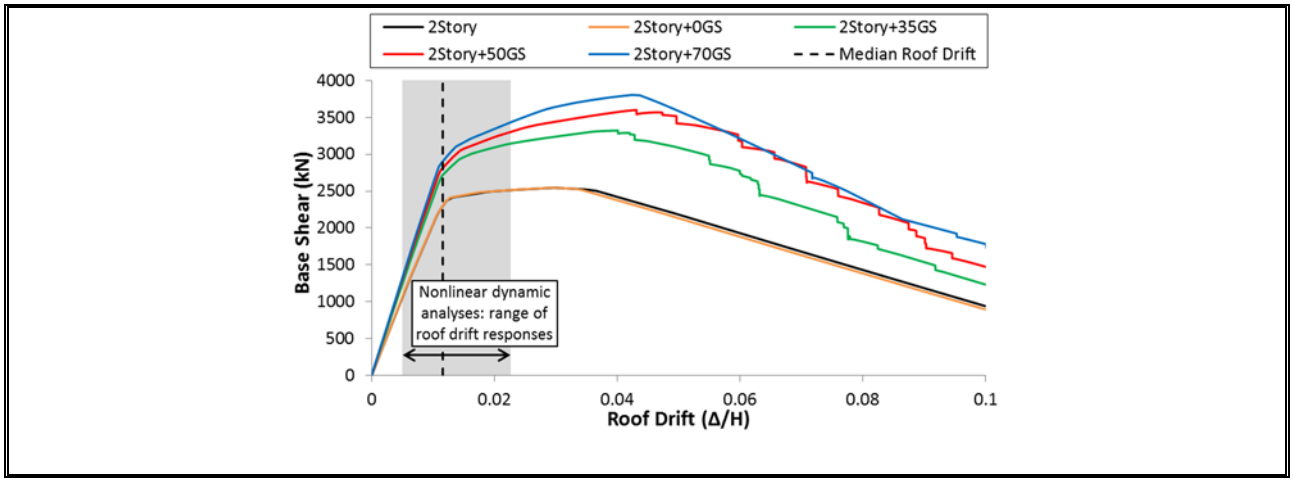

Figure 6. Pushover Curves and Dynamic Analyses: 2-Story Models

Figure 7 displays the pushover curves for the 4- and 8-Story models along with the roof drift response indicated by the nonlinear dynamic analyses. While there is now some level of inelastic deformations at the DE demand, the yielding is not too extensive, hence estimates given by simple elastic models might in principle still be somewhat representative.

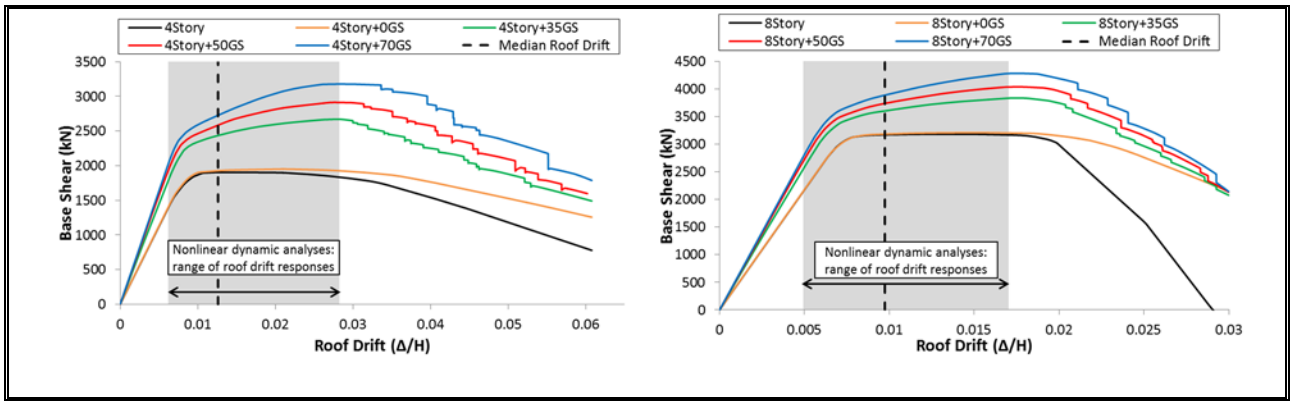

Figure 7 Pushover Curves and Dynamic Analyses: 4- and 8-Story Models

2.9 Peak Floor Accelerations

The Peak Floor Acceleration (PFA) is the maximum total acceleration measured at a given floor, and is equal to the acceleration demand on a rigid NSC located at that floor. The PFA at a given floor is also the "anchor" acceleration value of the FRS of the same floor.

The horizontal seismic design force F_p indicated in both ASCE 7-05 [24] and ASCE 7-10 [24] for acceleration-sensitive NSCs is given by:

$$F_p = \frac{0.4 a_p S_{DS} W_p}{\frac{R_p}{I_p}} \left(1 + 2\frac{z}{H}\right) \leq 1.6 S_{DS} I_p W_p \qquad F_p \geq 0.3 S_{DS} I_p W_p \qquad (1)$$

where a_p is the component amplification factor, R_p and I_p are the component response modification and importance factor, respectively, W_p is the weight of the component, S_{DS} is the DE short period spectral acceleration and z/H is the relative height of the floor at which component is anchored. One of the topics of interest in this study is the variation of the PFA along the height of the building. Implicit in equation 1 (a_p = 1 for rigid NSCs) is a linear height-wise variation of the PFA from a value equal to the PGA (= 0.4 S_{DS}) at the ground level (i.e., z/H = 0) to a value equal to 3 times the PGA at the roof level (i.e., z/H = 1). It can be seen that ASCE 7 does not consider if the supporting structure behaves elastically or inelastically, does not differentiate among the different types of lateral resisting systems, and does not take into the account the number of stories or floor levels.

Figure 8 (a) and (b) display median PFAs (normalized by the PGA) of the elastic and inelastic 2-Story models, respectively. Contrary to what was expected, PFAs computed using the inelastic models turned out to be significantly lower than those computed using the elastic models. The explanation, however, is related to the fact that the estimated DE demand is the *median* value of the individual demands imposed by each record. Therefore, recalling Figure 6, approximately

half of the records imposed inelastic demands, and the gray area representing the range of roof drift values clearly indicate that the inelastic response due to the more demanding records is indeed significant. Hence, while the median roof displacement is slighly larger than the elastic limit, results indicate that the median inelastic PFAs are significantly different from the media elastic PFAs. Therefore, the influence of inelastic behavior on PFAs appears to be much more significant than that indicated by the median roof displacement demand (which in this case indicates essentially elastic behavior). On the other hand, it can also be seen from Figure 8 that the influence of the gravity system on floor accelerations in the inelastic models is not very significant, regardless of the strength level of the PR connections.

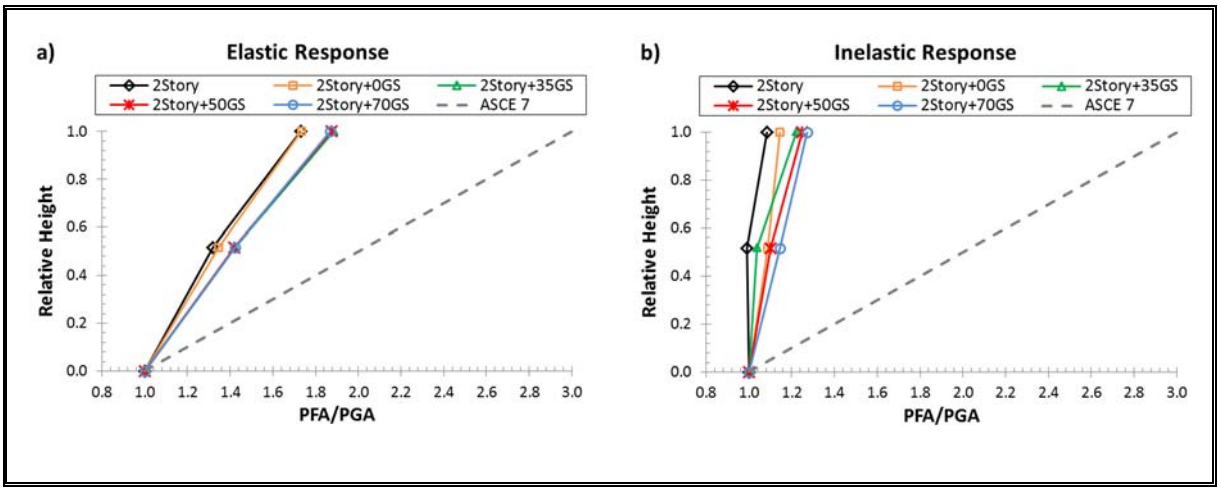

Figure 8. Normalized Peak Floor Acceleration (PFA/PGA): 2-Story Model

Figure 9 (a) and (b) present PFAs of the 4-Story models. Consistent with what was observed in Figure 7 (i.e., DE inelastic demand greater than that of the 2-Story model), the differences between accelerations in the elastic and inelastic models are now even more important than those observed in the previous case (the 2-Story model). Again, the influence of the gravity system in the inelastic models is not very significant. The exception is the roof level, where the presence of

the gravity system increases the PFA, particularly when the strength of the PR connections is not zero. The influence of the exact strength level, however, is virtually irrelevant.

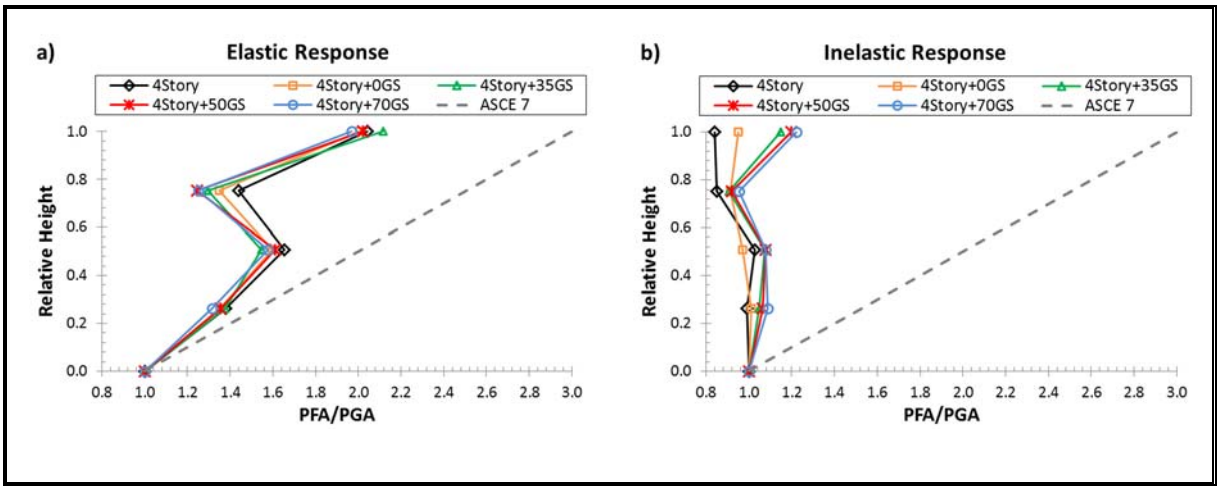

Figure 9 Normalized Peak Floor Acceleration (PFA/PGA): 4-Story Model

Figure 10 a) and b) display the PFAs of the 8-Story models. Again, the inelastic acceleration demands are significantly lower than the elastic demands, and the influence of the gravity system is even less than that observed in the 2-Story model.

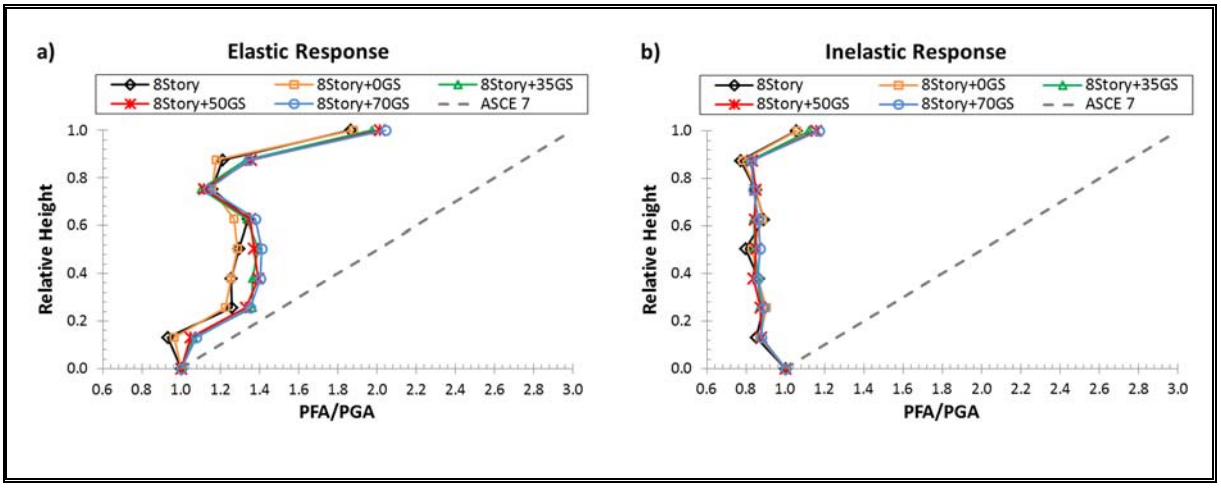

Figure 10 Normalized Peak Floor Acceleration (PFA/PGA): 8-Story Model

Interestingly, it is found that in the inelastic models the PFAs are roughly equal (usually less, occasionally greater) to the PGA at almost all floor levels of the three buildings. Therefore, DE

acceleration demands on rigid NSCs can in general be expected to be roughly equal to the PGA, which in turn means that the design accelerations indicated in ASCE 7 for *rigid* NSCs are very conservative, at least for the scenario considered in this study (the supporting structure is a SMF, and is located in an area of high seismic activity).

2.10 Floor Response Spectra

The FRS indicate the acceleration demands on flexible NSCs. As mentioned before, FRS are obtained by computing the absolute acceleration response spectrum of the total acceleration response history at the floor of interest. Since the response spectrum is computed in the usual, "standard" way, FRS indicate the acceleration demand on NSCs that behave elastically. Recalling equation 1, the ASCE 7 approach indicates that the horizontal seismic design force F_p for NSCs is obtained considering that the demand is reduced by the component response modification factor R_p, implying that NSCs are allowed to develop inelastic deformations. However, factor R_p is in general different for each type of NSC, and is not considered in this study (in other words, this study evaluates floor accelerations, not the design seismic force F_p). All FRS shown in this paper are median spectra of the set of FRS corresponding to each ground motion, and were obtained considering a damping ratio equal to 2%, typical of most NSCs. As noticed, this value is lower than what a structure could have because this is a characteristic known about NSC [7]. Furthermore, this is a typical value that is believed most NSCs have and it has been commonly used in research [6, 8, 10, 13, 14, 16].

Figures 11 (a) and (b) show the FRS corresponding to the second (roof) level of the 2-Story model. It can be observed that the spectral shape is essentially the same regardless of whether the supporting structure behaves elastically or inelastically: FRS are characterized by large spectral ordinates at the modal periods of the structure. In order to help appreciate this observation, the

modal periods of the model that does not include the gravity system are indicated by dashed lines. However, the amplitude of the spectral ordinates in the vicinity of the first modal period are much less when the structure behaves inelastically than when the structure behaves in a linearly elastic manner. In the extreme case, the spectral ordinate of the elastic model is roughly equal to 8.0 g (no gravity system) and 9.0 g (gravity system with non-zero strength of the PR connections) at first mode resonance, but the spectral ordinate of the inelastic models is not greater than 5.0 g. It can also be observed that the presence of the gravity system is relevant only when the PR connections have some strength. In such a case, the first modal period decreases (the structure becomes stiffer when the PR connections do have some strength), and spectral ordinates are somewhat different in the vicinity of the first modal period. Finally, the exact strength level of the PR connections does not have an influence on the FRS.

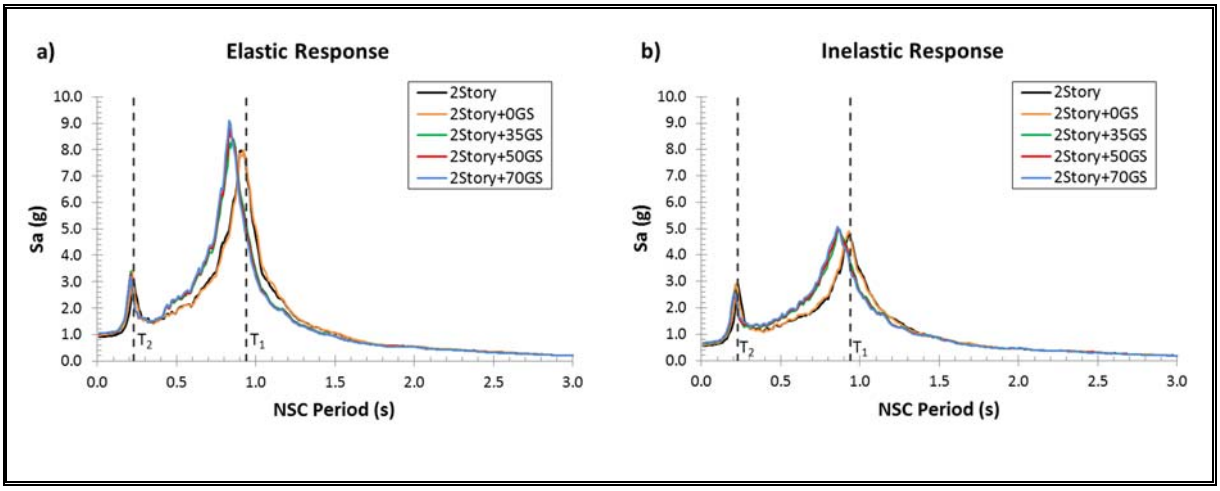

Figure 11. FRS at the 2nd (roof) level of the 2 Story Models

Figure 12 (a) and (b) show the FRS corresponding to the fourth (roof) level of the 4-Story model. Again, the spectral shape is essentially the same regardless of whether the supporting structure behaves elastically or inelastically. In this case, however, the amplitude of the spectral ordinates are much less when the structure behaves inelastically not only in the vicinity of the first

modal period but also in the vicinity of the second modal period. Once more, it can also be observed that the presence of the gravity system is relevant only when the PR connections have some strength. In this case, however, spectral ordinates are somewhat different not only in the vicinity of the first modal period but also in the vicinity of the second modal period. Again, the exact strength level of the PR connections does not have an influence on the FRS.

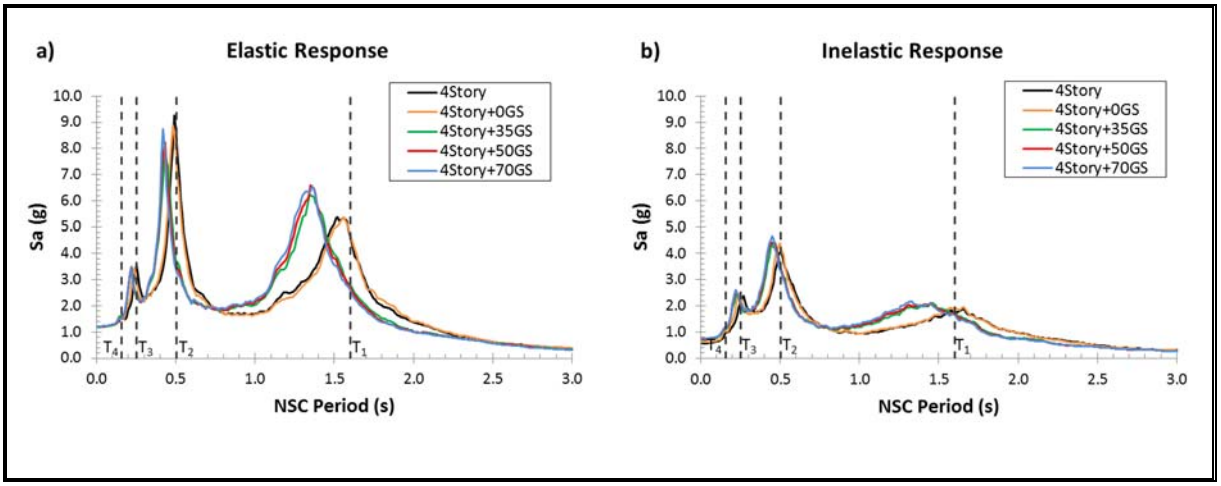

Figure 12. FRS at the 4th (roof) level of the 4-Story Models

Figure 13 (a) and (b) show the FRS corresponding to the eighth (roof) level of the 8-Story model. As before, the spectral shape is essentially the same regardless of whether the supporting structure behaves elastically or inelastically. In this case, however, the amplitude of the spectral ordinates are much less when the structure behaves inelastically in the vicinity of the third modal period as well. Again, it can also be observed that the presence of the gravity system is relevant only when the PR connections have some strength. In this case, however, spectral ordinates are not different in the vicinity of the first modal period (inelastic models) but they are somewhat different in the vicinity of the second and third modal periods. Again, the exact strength level of the PR connections does not have an influence on the FRS.

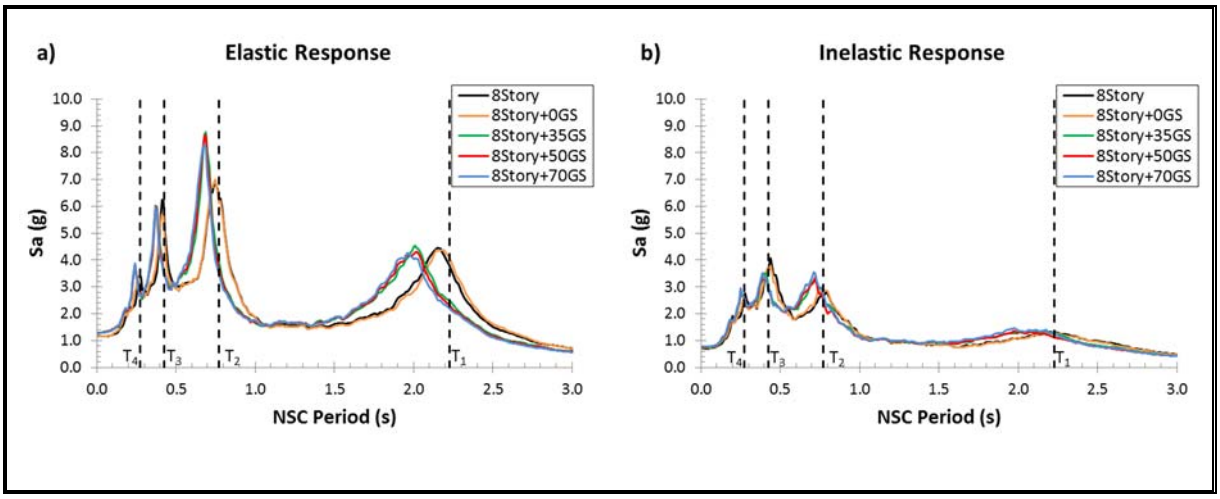

Figure 13. FRS at the 8th (roof) level of the 8-Story Models

It was already mentioned that the design acceleration demand on *rigid* NSCs indicated in ASCE 7 depends neither on the type of lateral resisting system nor on the number of stories or floor levels. Notably, equation 1 also indicates that the ASCE 7 design acceleration demands on *flexible* NSCs located at a given relative height of the supporting structure are also independent of the characteristics of the supporting structure. For instance, equation 1 indicates that the acceleration demand on flexible NSCs that behave elastically (i.e., R_p = 1) and are located at the roof level (i.e., relative height z/H = 1) is equal to 3.0 x 2.5 = 7.5 times the PGA (a_p = 2.5 for flexible NSCs), regardless of the characteristics of the supporting structure. Recalling that the building models considered in this study were designed for a PGA = 0.4 g (DE level), ASCE 7 indicates that the design acceleration demand on elastic, flexible NSCs located at the roof level is equal to 0.4 g x 7.5 = 3.0 g, regardless of the number of stories (i.e., same value for the 2-, 4- and 8-Story models). Keeping in mind that the period of flexible NSCs is in most cases less than 0.5 s, Figures 11(b), 12(b) and 13(b) (structure behaving inelastically, the realistic scenario) indicate that the ASCE 7 design demand is exceeded in the 4- and 8-Story models in the extreme case of higher mode resonance, and is conservative otherwise. Of course, such extreme demands (up to 4.5 g) are

very high, which is why protective measures such as floor isolation systems are a topic of current research.

Figure 14 shows FRS of all floor levels of the 4-Story Model considering different modeling criteria: elastic (left) and inelastic (right), without the gravity system (top) and with the gravity system having a strength level of the PR connections equal to 50% (bottom). Qualitatively, the height-wise variation of the FRS is essentially independent of the modeling criterion. Quantitatively, however, FRS depend mainly on whether the structure behaves elastically or inelastically, and the influence of the gravity system is of lesser relevance. Interestingly, Figure 14 indicates that maximum demands on flexible NSCs occur at higher mode resonance rather than at first mode resonance, which is relevant because, as mentioned before, the natural period of most NSCs is less than 0.5 s, precisely the period range of higher mode resonance. Further, the ASCE 7 approach indicates that the larger the relative height z/H of a given floor, the larger the acceleration demand on flexible NSCs located at that floor (implicit in equation 1), but Figure 14 clearly indicates that such trend is true only at first mode resonance (it is visibly not true at higher mode resonance). Again, this observation is relevant because the characteristics of flexible NSCs are such that first mode resonance is unlikely in relatively flexible structures such as the SMFs considered in this study, whereas higher mode resonance is much more probable. It is emphasized that these last observations are qualitatively valid regardless of the modeling criteria. Finally, FRS at all floor levels of the 2- and 8-Story models were also computed, and it was found that the observations made for the FRS of the 4-Story model are also valid for the 2- and 8-Story models, and are not shown for the sake of brevity.

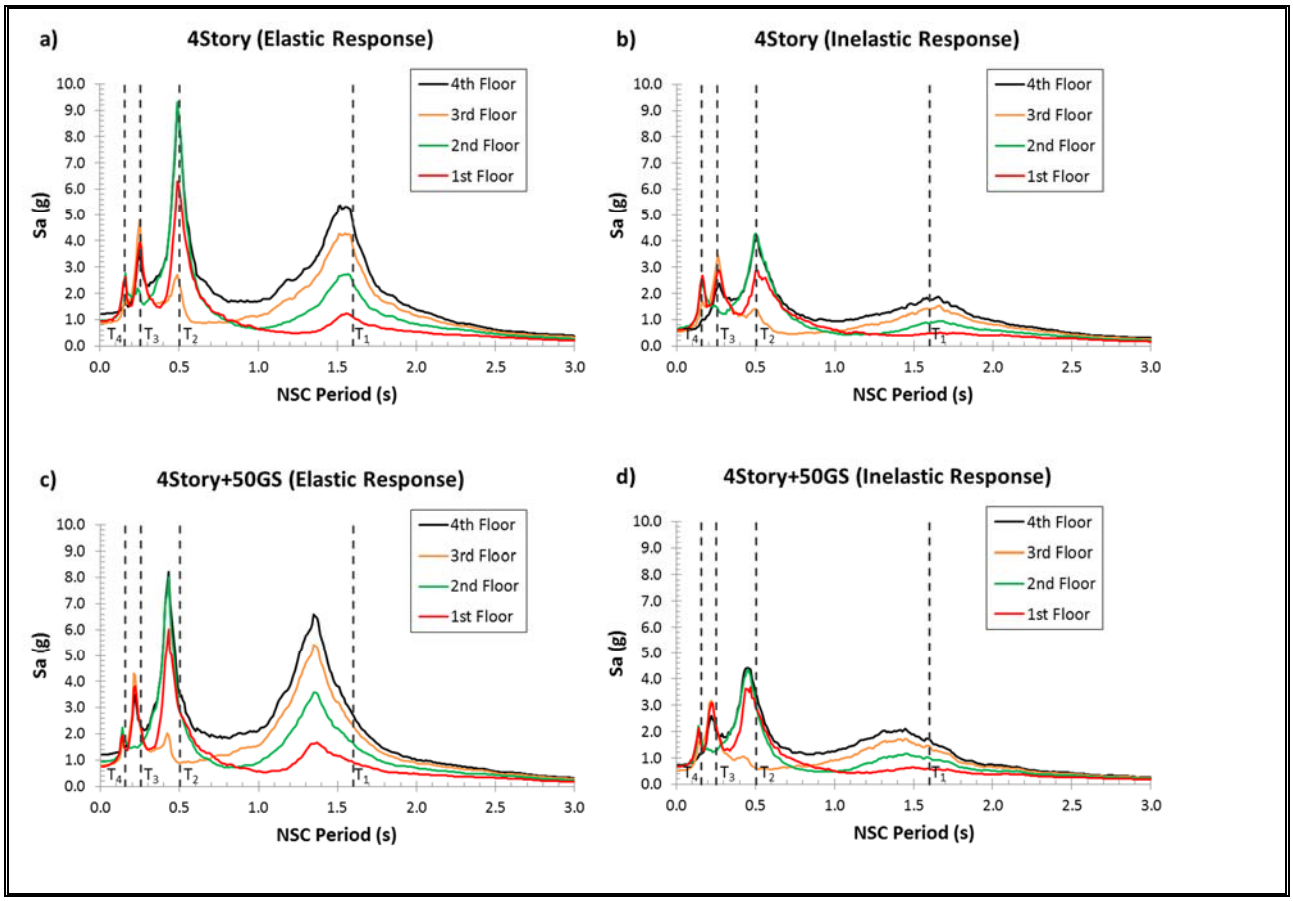

Figure 14. FRS at all floor levels of the 4-Story Model

2.10.1 Floor Response Spectrum Ratio

It was observed in the previous section that spectral ordinates of FRS are of lower amplitudes when the building behaves inelastically. However, it has been reported in the literature that in some cases in fact the opposite is true [12-16]. In order to thoroughly investigate this issue, the ratio of the spectral acceleration for the inelastic building models to that of the corresponding elastic building models was computed. This ratio is called the Floor Response Spectrum Ratio (FRSR), and it takes a value larger than unity when inelastic behavior in the supporting structure leads to a higher spectral ordinate than that corresponding to the case where the building behaves elastically.

Values of the FRSR corresponding to the first and roof levels of the 2-Story models are shown in Figure 15. While these results generally confirm what was already reported (spectral ordinates of the inelastic models much less than that of the elastic models at first mode resonance), the results also indicate that in fact the opposite is observed at second mode resonance, most noticeable at the first story level. However, the value of the corresponding FRSR is not large (≈ 1.1), and is virtually equal to unity in the most realistic case where the gravity system is considered and the PR connections have some strength.

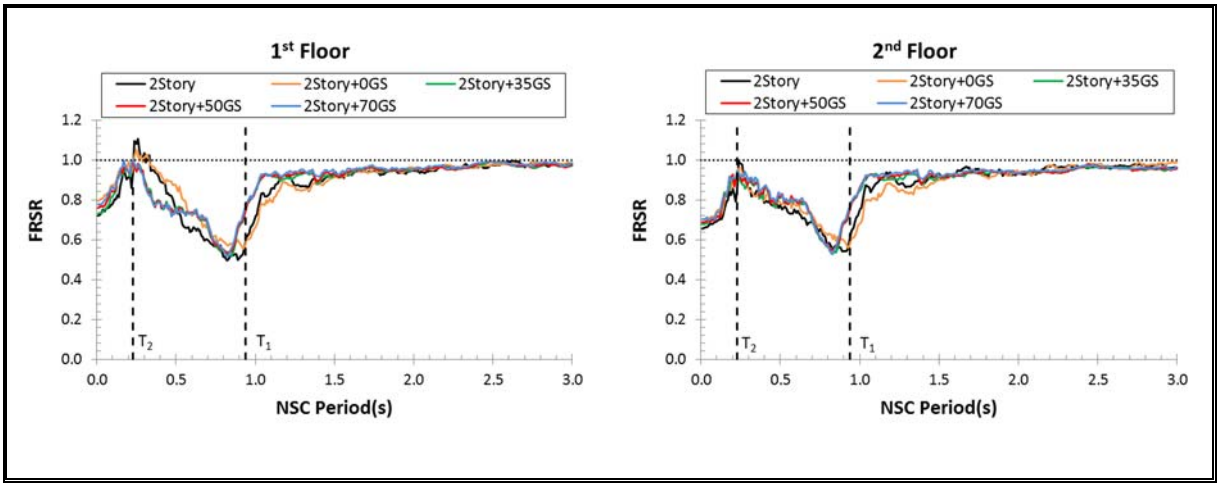

Figure 15. FRSR values (2-Story Model)

Values of the FRSR corresponding to all floor levels of the 4-Story models are shown in Figure 16. In this case, FRSR values greater than unity are observed at the first floor (third and fourth mode resonance), at the second floor (fourth mode resonance), and at the third floor (third mode resonance). However, the value of the FRSR is never large (at most 1.15), and in the most realistic case where the gravity system is considered and the PR connections have some strength, the FRSR takes values that are less than or at most equal to those corresponding to the case where the gravity system is not considered.

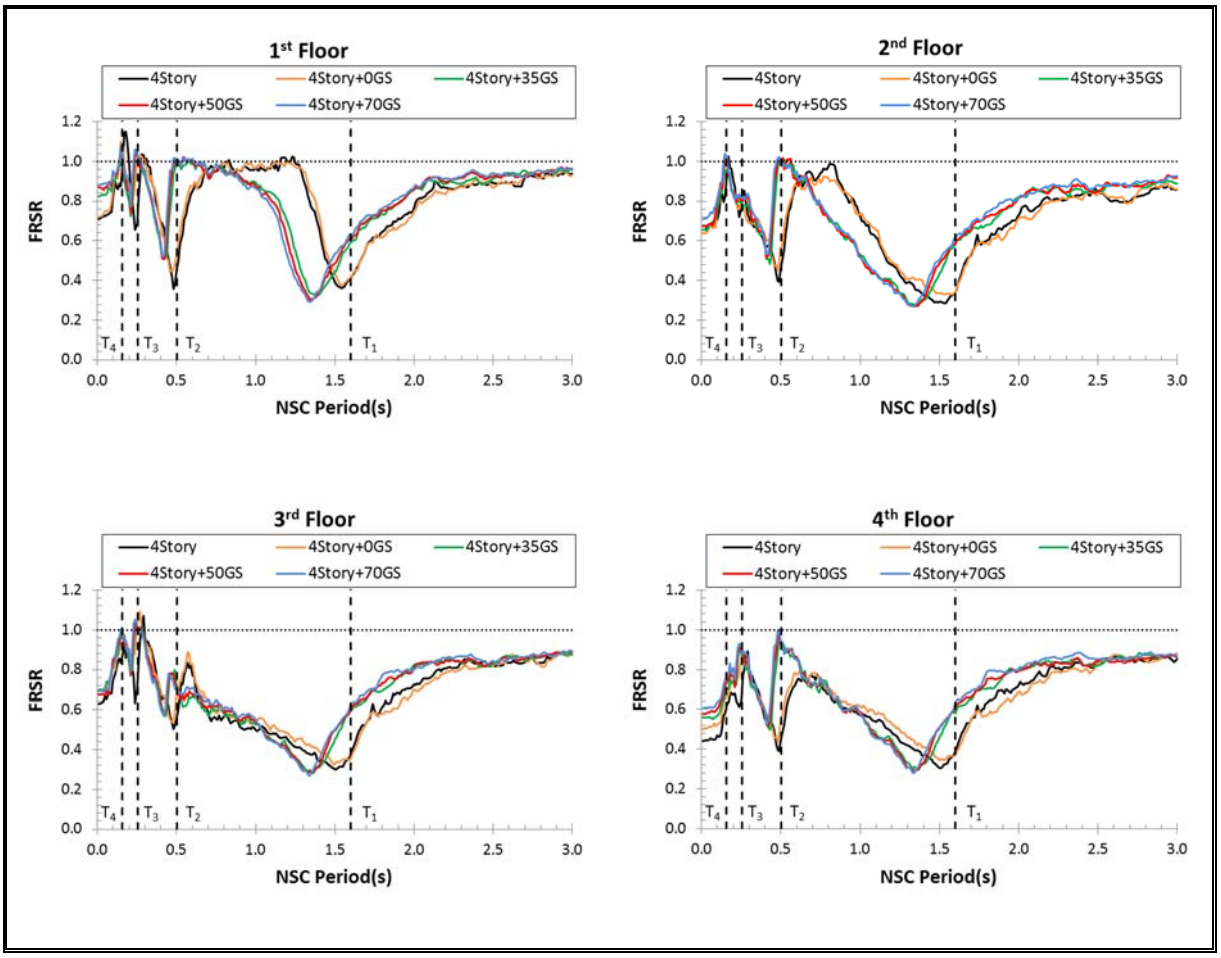

Figure 16. FRSR values (4-Story Model)

Values of the FRSR corresponding to the first, second, sixth, and seventh floors of the 8-Story models, which are the floors at which greater values of FRSR were observed, are shown in Figure 17. In this case, FRSR values greater than unity are observed at all the selected floors, and at higher mode resonance (third mode or higher). But again, the value of the FRSR is never large (at most 1.15), and in the most realistic case where the gravity system is considered and the PR connections have some strength, the FRSR takes values that are less than or at most equal to those corresponding to the case where the gravity system is not considered.

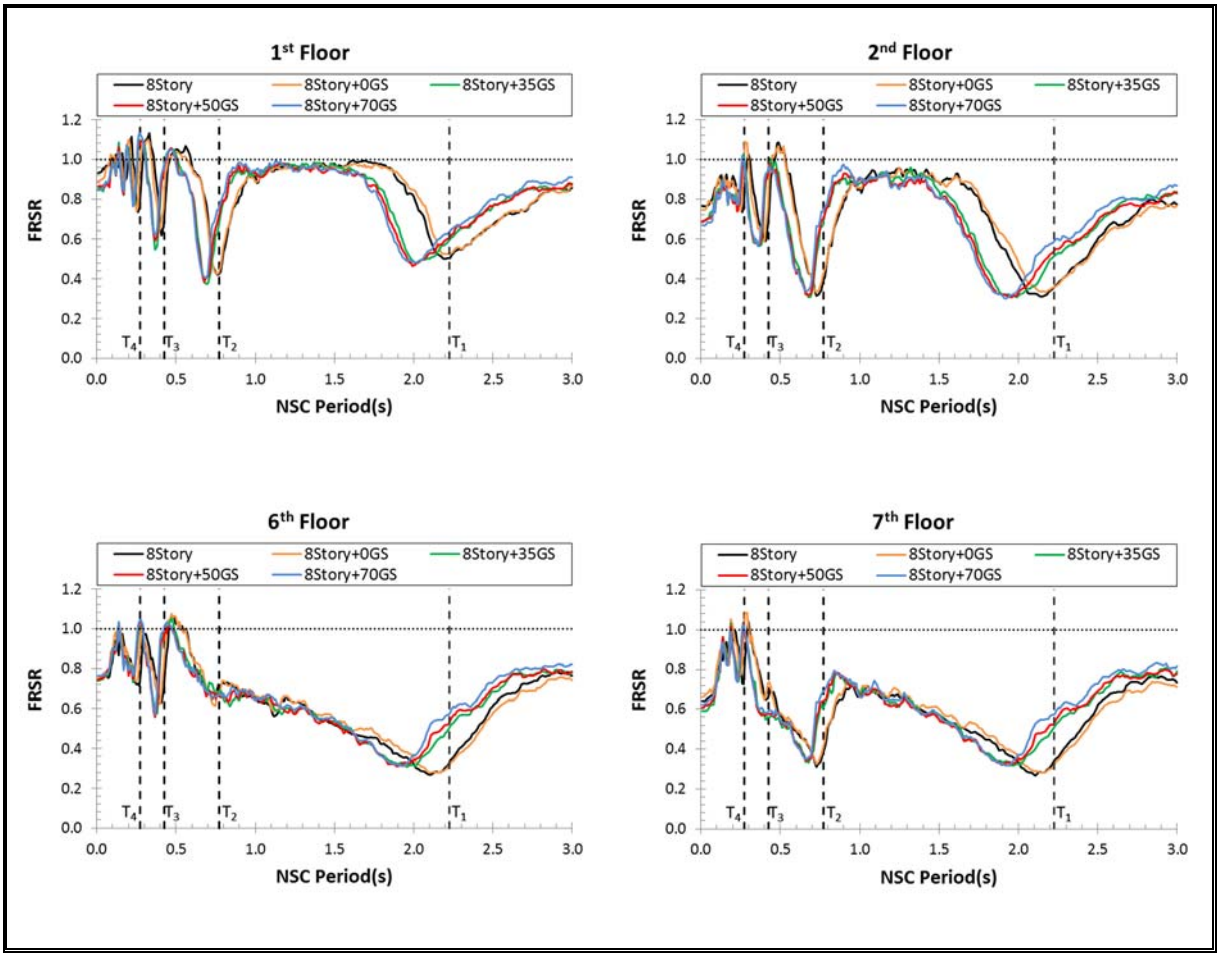

Figure 17. FRSR values (selected floors of the 8-Story Model)

2.11 Conclusions

In this study, floor accelerations in Special Steel Moment Frames (SMFs) were investigated considering different modeling options, from a simple linear elastic model of the lateral force resisting system to a sophisticated nonlinear model complying with the requirements of FEMA P-695. Particular attention was paid to the gravity system, which has been shown to significantly influence the collapse performance of SMFs [21]. The building models were subjected to the FEMA P-695 set of far-field ground motions scaled to the DE response spectrum the buildings were designed for, which is representative of seismic demands in areas of high seismic activity in

the western United States and in countries such as Japan and Chile. From the analysis of results obtained by time history analysis, the conclusions of this investigation are:

- The most relevant modeling issue is the inelastic behavior of the structure. This observation is evident even when the median seismic demand is barely larger than the elastic limit. Although nonlinear time history analysis is still challenging, it leads to levels of accuracy that more than compensate for its drawbacks.
- The influence of the gravity system on floor accelerations is negligible when it is assumed that the strength of the Partially Restrained (PR) connections in the gravity system is zero. This observation contrasts starkly with what was observed in [21], where it was found that the gravity system has a significant influence on the collapse performance of SMFs, even when the strength of the PR connections is zero.
- The gravity system does have some influence on floor accelerations when the strength of the PR connections is not zero. Such influence is most significant on Floor Response Spectra (FRS) at first mode resonance, diminishes at higher mode resonance, and becomes essentially negligible on PFAs. In all cases, the exact level of the strength of the PR connections is not relevant. Hence, given the complexities of realistically modeling the nonlinear behavior of the gravity system, it is concluded that its inclusion in models intended to assess floor accelerations is probably not justified. Again, this observation is very different from observations reported in [21], where both the presence of the gravity system and the strength of the PR connections were found to strongly influence the collapse performance of SMFs.

- As reported in the literature, spectral ordinates of FRS of inelastic building models are in some particular cases indeed greater than those of elastic building models, but such observation turned out to be true only at higher mode resonance, and only marginally so (by at most 15%, usually even less in the most realistic scenario where the gravity system is included considering some strength level of the PR connections).

- As a corollary of the former conclusion, floor accelerations obtained assuming linear behavior of the structure are then essentially conservative. Setting apart what was mentioned in the former conclusion, it was found that in the 0.0 s – 0.5 s range (the period range of most nonstructural components, NSCs), spectral ordinates of FRS of linearly elastic building models range from accurate to conservative by up to 150%. The degree of accuracy, however, is very sensitive to the period of the NSC, which makes accurate assessments difficult in actual case scenarios and in code provisions.

- The acceleration demands on rigid NSCs (inelastic building models) are roughly equal to the PGA, regardless of the floor level at which the NSC is attached. Therefore, in areas of high seismic activity, where DE PGA values are roughly equal to 0.4 g – 0.6 g, the acceleration demands on rigid NSCs are not expected to be as large as those indicated by the ASCE 7 approach, especially at the topmost floor levels.

- In contrast, the acceleration demands on flexible NSCs (again, inelastic building models) turned out to be very high. Considering again the realistic 0.0 s – 0.5 s NSC period range, acceleration demands are in the range of 3.0 g - 4.5 g in the extreme case of higher mode resonance. These demands are reasonably well predicted by the ASCE 7 approach for NSCs located at the roof level, but not for those located at other floors. Indeed, while ASCE 7 implicitly indicates that acceleration demands on flexible NSCs increase monotonically

with the height of the location of the NSC, such trend was not observed in this study (in the 0.0 s – 0.5 s period range), and acceleration demands on flexible NSCs located at mid-height floor levels are in some cases as large as those on NSCs located at the roof level.

It is emphasized that these conclusions are valid only for the particular structural system considered in this study, i.e., SMFs. The validity of such conclusions for floor accelerations in building structures having other structural systems is the topic of an ongoing research project.

2.12 Acknowledgements

Financial support was provided by the Pontificia Universidad Catolica de Chile and by the Virginia Tech Department of Civil and Environmental Engineering. This support is gratefully acknowledged.

2.13 References

[1] B. Reitherman, T. Sabol, R. Bachman, D. Bellet, R. Bogen, D. Cheu, P. Coleman, J. Denney, M. Durkin, C. Fitch, Nonstructural damage, Earthquake Spectra, 11 (1995) 453-514.

[2] E. Miranda, G. Mosqueda, R. Retamales, G. Pekcan, Performance of nonstructural components during the 27 February 2010 Chile earthquake, Earthquake Spectra, 28 (2012) S453-S471.

[3] E. Miranda, S. Taghavi, Approximate floor acceleration demands in multistory buildings. I: Formulation, Journal of structural engineering, 131 (2005) 203-211.

[4] J. Lin, S.A. Mahin, Seismic response of light subsystems on inelastic structures, Journal of Structural Engineering, 111 (1985) 400-417.

[5] S. Taghavi, E. Miranda, Response assessment of nonstructural building elements, Report No. PEER 2003/05. Dept. of Civil and Environmental Engineering, Stanford University, Stanford, CA. Pacific Earthquake Engineering Research Center, Richmond, CA, 2003.

[6] A. Singh, A.H.S. Ang, Stochastic prediction of maximum seismic response of light secondary systems, Nuclear Engineering and Design, 29 (1974) 218-230.

[7] R. Villaverde, Seismic design of secondary structures: state of the art, Journal of structural engineering, 123 (1997) 1011-1019.

[8] B. Kehoe, M. Hachem, Procedures for estimating floor accelerations, in: Proc., ATC-29-2 Seminar on Seismic Design, Performance, and Retrofit of Nonstructural Components in Critical Facilities, Applied Technology Council, Redwood City, Calif, 2003.

[9] M. Singh, L. Moreschi, L. Suarez, E. Matheu, Seismic design forces. I: Rigid nonstructural components, Journal of structural engineering, 132 (2006) 1524-1532.

[10] I. Politopoulos, C. Feau, Some aspects of floor spectra of 1DOF nonlinear primary structures, Earthquake engineering & structural dynamics, 36 (2007) 975-993.

[11] R.A. Medina, R. Sankaranarayanan, K.M. Kingston, Floor response spectra for light components mounted on regular moment-resisting frame structures, Engineering structures, 28 (2006) 1927-1940.

[12] R. Sewell, C. Cornell, G. Toro, R. McGuire, R. Kassawara, A. Singh, J. Stepp, Factors influencing equipment response in linear and nonlinear structures, in: Transactions of the 9th international conference on structural mechanics in reactor technology. Vol. K2, 1987.

[13] R. Sankaranarayanan, R.A. Medina, Acceleration response modification factors for nonstructural components attached to inelastic moment-resisting frame structures, Earthquake Engineering & Structural Dynamics, 36 (2007) 2189-2210.

[14] I. Politopoulos, Floor spectra of MDOF nonlinear structures, Journal of Earthquake Engineering, 14 (2010) 726-742.

[15] M. Rodriguez, J. Restrepo, A. Carr, Earthquake-induced floor horizontal accelerations in buildings, Earthquake engineering & structural dynamics, 31 (2002) 693-718.

[16] S.R. Chaudhuri, R. Villaverde, Effect of building nonlinearity on seismic response of nonstructural components: a parametric study, Journal of structural engineering, 134 (2008) 661-670.

[17] J. Wieser, G. Pekcan, A.E. Zaghi, A. Itani, M. Maragakis, Floor accelerations in yielding special moment resisting frame structures, Earthquake Spectra, 29 (2013) 987-1002.

[18] FEMA, Quantification of Building Seismic Performance Factors, FEMA P-695, Washington, D.C., 2009.

[19] F. Zareian, D. Lignos, H. Krawinkler, Evaluation of seismic collapse performance of steel special moment resisting frames using FEMA P695 (ATC-63) methodology, in: Proceedings of Structures Congress ASCE, Orlando, FL, 2010, pp. 12-14.

[20] NIST, Evaluation of the FEMA P-695 Methodology for Quantification of Building Seismic Performance Factors, GCR 10-917-8, (2010).

[21] F.X. Flores, F.A. Charney, D. Lopez-Garcia, Influence of the Gravity Framing System on the Collapse Performance of Special Steel Moment Frames (Accepted for publication), Journal of Constructional Steel Research, (2014).

[22] S. Mazzoni, F. McKenna, M.H. Scott, G.L. Fenves, OpenSees command language manual, Pacific Earthquake Engineering Research (PEER) Center, (2006).

[23] ASCE, Minimum Design Loads for Buildings and Other Structures, ASCE Standard ASCE/SEI 7-05, in, American Society of Civil Engineers, Reston, VA, 2005.

[24] ASCE, Minimum Design Loads for Buildings and Other Structures, ASCE Standard ASCE/SEI 7-10, in, American Society of Civil Engineers, Reston, VA, 2010.

[25] L.F. Ibarra, R.A. Medina, H. Krawinkler, Hysteretic models that incorporate strength and stiffness deterioration, Earthquake engineering & structural dynamics, 34 (2005) 1489-1511.

[26] D.G. Lignos, H. Krawinkler, Deterioration modeling of steel components in support of collapse prediction of steel moment frames under earthquake loading, Journal of Structural Engineering, 137 (2010) 1291-1302.

[27] F.A. Charney, J. Marshall, A Comparison of the Krawinkler and Scissors Models for Including Beam-Column Joint Deformations in the Analysis of Moment-Resisting Steel Frames, Engineering journal., 43 (2006) 31.

[28] AISC, Specification for Structural Steel Buildings, ANSI/AISC 360-05, American Institute of Steel Construction., Chicago, IL, (2005).

[29] J. Liu, A. Astaneh-Asl, Cyclic testing of simple connections including effects of slab, Journal of Structural Engineering, 126 (2000) 32-39.

[30] ASCE, Seismic Rehabilitation of Existing Buildings, ASCE Standard ASCE/SEI 41-13, American Society of Civil Engineers, Reston, Va., 2013.

[31] F. Zareian, R.A. Medina, A practical method for proper modeling of structural damping in inelastic plane structural systems, Computers & structures, 88 (2010) 45-53.

3. FLOOR ACCELERATIONS IN BUILDINGS HAVING DIFFERENT STRUCTURAL SYSTEMS

3.1 Introduction

Seismic demands on Nonstructural Components (NCs) attached to buildings is a topic that often times is overlooked by building codes and the research community. In the present, structural design of buildings is moving towards a design where the only limit state is not just the collapse prevention. The so-called Performance Based Earthquake Engineering Design (PBEE) evaluates the performance of the structure at different levels of intensity using different limit sates. One of these is the "immediate occupancy" limit state which requires the structure to be fully operational after an earthquake. Recent events like the 1994 Northridge (USA), 1995 Kobe (Japan) and 2010 El Maule (Chile) earthquakes have shown that the majority of buildings performed as expected against collapse. However, the nonstructural damage inside the building made impossible to occupy the facility after the event [1, 2]. Besides the safety hazard that this could represent, the direct and indirect economic losses can be greater than the cost of the structure [3]. As a result more and more facilities are being designed considering the performance of the NSCs attached to the supporting structure.

NCs in buildings are divided into two main categories: sensitive to story drifts and sensitive to accelerations [4]. Acceleration sensitive NCs, the topic of this investigation, include parapets, suspended ceilings, ducts, boilers, chiller tanks, etc. [5]. Depending on their natural period of vibration they can also be classified as "rigid" or "flexible". These NCs are exposed to the accelerations that arise from the motion of the structure to which they are anchored or attached.

The current specification in U.S., ASCE7-10 [6], provides a procedure to evaluate the accelerations and seismic forces at which NCs are subjected to during an earthquake. The

procedure has been based most part on experiences, engineering judgment and intuition rather than on experimental and analytical results [7]. Even though it is a practical approach it is perhaps oversimplified since it is intended to be applicable to NCs located in any type of structure, regardless of whether the structure behaves elastically or inelastically, regardless of the fundamental period of the structure, and, perhaps more importantly, regardless of the kind of structural system.

The commonly used methods by researchers to estimate the accelerations that affect rigid and flexible NSCs are the Peak Floor Acceleration (PFA) method and the Floor Response Spectrum (FRS) method respectively [8]. The PFA method quantifies the maximum total acceleration at each floor during an earthquake. The FRS computes the elastic response spectrum of a selected floor using as input the total acceleration response of that floor. The later approach can be applied when there is no interaction between the NC and the supporting structure, i.e. the seismic response of the structure is not affected by the presence of the NC. The interaction between the structure and NC can be neglected with the mass of the NC is less than approximately 1.0 percent the mass of the supporting structure [9]. If the NSC mass is larger, dynamic interaction will occur between NSCs and the supporting structure, and the FRS method might in some cases produce overly conservative results [8].

The purpose of this study is to compare the acceleration demands on NCs when they are attached in two different structural systems. Several studies have been performed to evaluate the NCs accelerations. Much of these studies were carried out using elastic models [3, 10, 11], while other researchers have focused on the effect of the structure's inelastic behavior on the NCs accelerations [12-18]. Generally the accelerations decrease when the supporting structure behaves inelastically. However, there are instances when the accelerations are larger.

The level of accuracy required to perform nonlinear dynamic analysis differs depending on the type of analysis to be executed. For instance, in order to evaluate the collapse performance of structures using the FEMA P-695 methodology [19], the mathematical models have to be able to characterize collapse. Thus the level of detail required is very high making this one of the most stringent analysis to perform. In the case where the accelerations of NCs are evaluated, the common procedure that has been taken is to use either elastic models or inelastic models but not with the level of accuracy as required by other methodologies i.e. the P-695. In this study, very detailed mathematical models are used to evaluate the demands on NCs. Special Steel Moment Frames (SMFs) and Buckling Restrained Brace Frames (BRBFs) taken from the ATC76-1 project [20] are analyzed to compare the accelerations on NCs. The main purpose of this study is to evaluate and verify what is stated by ASCE7-10 where the accelerations are the same regardless the type of system where the NC is attached.

Taghavi and Miranda [21] already showed in their study that the acceleration response of the floors change depending on the type of lateral resisting system due to the difference in mode shapes and modal participation factors. However, the model used in the study was a simplified model that depends on a single parameter to emulate the type of structural system. Therefore, the study presented herein will contribute to a more detailed and more realistic understanding of floor accelerations.

3.2 Methodology

The mathematical models of the BRBs and SMFs were developed using OpenSees [22]. Two different models are used for the SMFs: one that does not incorporate the gravity system and one that it does. The gravity system is modeled using partially-restrained (PR) connections that have a flexural capacity equal to 35% the plastic moment of the beam (Mp). As shown in the study

performed by Flores et al.[23] the strength of the gravity connections has a minimum influence on the NCs demands. On the other hand, the BRBFs are analyzed using two different types of beam-column-brace connections: pinned and continuous (fixed).

The structures were subjected to the 44 Far-Field ground motions as specified by the FEMA P-695 methodology. The level of intensity to which the ground motions are scaled is the Design Earthquake (from now on denoted simply as DE). The procedure used to scale the ground motions is the one given by P-695. The accelerations demands on the NCs are then computed using the Floor Response Spectrum (FRS) method. In this method, the spectrum is computed using as input the response of the total accelerations measured at each floor. In this study the influence of the inelastic behavior of the buildings on the NCs response is also quantified. Therefore the floor accelerations for the mathematical models behaving elastically are also computed.

3.3 Overview of Buildings Analyzed

The SMFs and BRBFs analyzed in this study were taken as already stated from the ATC 76-1 project. More information regarding the buildings used in this study can be found in the referenced document [20]. As known, these structural systems are comparable since their seismic performance factors are the same. The response modification coefficient (R) is equal to 8, the overstrength factor (Ω) is 3 and the deflection amplification factor (Cd) is equal to 5.5. The SMFs and BRBFs were designed using Modal Response Spectrum Analysis (RSA) for a design category Dmax (Ss=1.5g, S1=0.6g), for a typical gravity load, and considering Site Class D.

The SMFs analyzed are the 2-, 4- and 8-story models identified in ATC76-1 as 2RSA (2 story), 3RSA (4 story) and 4RSA (8 story). The base of the columns of the buildings were fixed for the 4- and 8-story models, and pinned for the 2-story model. The typical plan view of these structures is shown in Figure 1 (a). The BRBFs are the 2-, 4- and 9-story models identified as 2S-

LB-25BDmax (2 story), 4S-LB-15BDmax (4 story) and 8S-LB-15BDmax (8Story). The notation utilized in ATC76-1 stands for BRBF with diagonal (Lighting Bolt) brace configuration with 15ft Bay widths designed at seismic design category Dmax. In the case of the 2-story model it can be seen the bay width is 25ft. Unlike the SMFs the base of the columns were fixed for all the BRBs. The building layout for the 4- and 8- story is shown in Figure 1 (b). The building layout for the 2-story model is similar but with five 25ft bays.

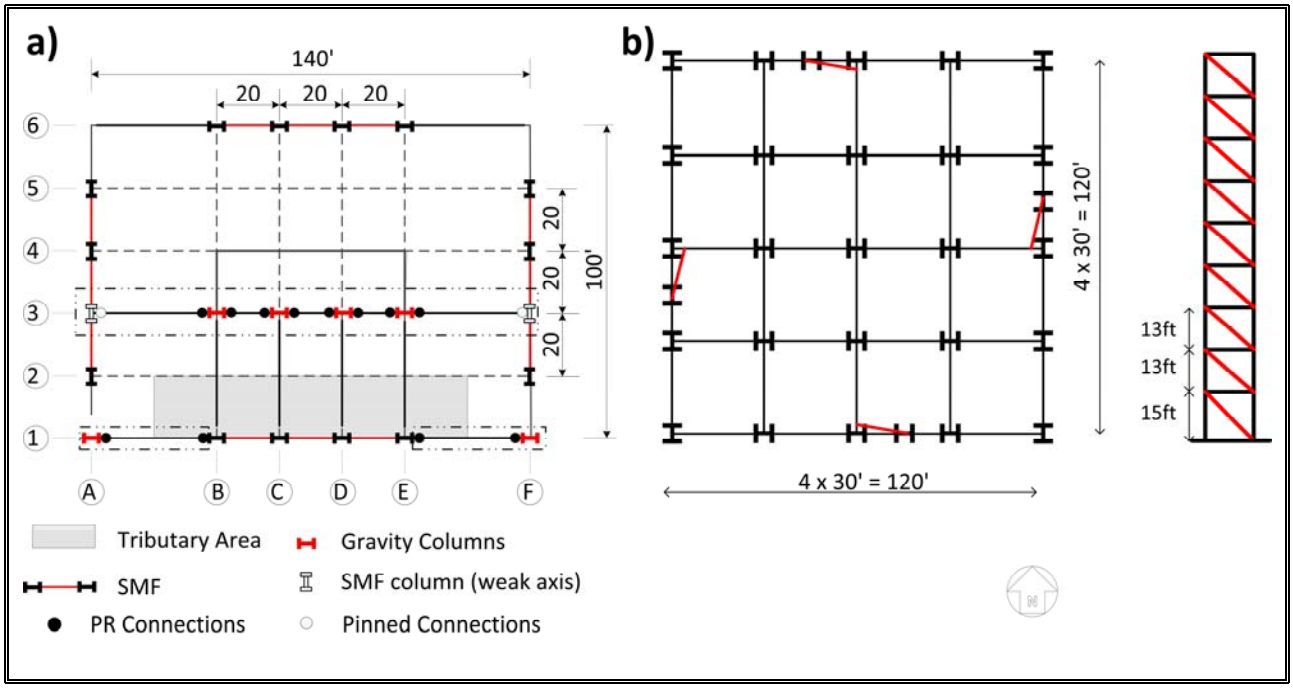

Figure 1 Building Overview a) SMF b) BRBF

3.4 Modeling SMFs

Two-dimensional models were idealized to perform the nonlinear analysis. Material and geometric nonlinearities were included in every model. In the case where the gravity system was not included, P-Delta effects were considered using a leaning column with no flexural stiffness placed parallel to the SMF. The SMF was modeled using elastic elements and lumping the inelastic behavior into plastic hinges at the end of the members. The components of the SMF with nonlinear behavior are: panel zones, plastic hinges located at the RBSs of the beam and plastic hinges at the

column ends. The additional components modeled when the gravity system was included are: PR connections and gravity columns modeled using fiber sections. Inherent Rayleigh damping of 2.5% is assigned to the first modal period T1 and to period T = 0.2 T1 in all cases. As proposed by Zareian and Medina [24], stiffness proportional damping is assigned to elements that remain elastic, and mass proportional damping is assigned to nodes or elements where mass is lumped.

Due to space limitations no more details regarding modeling are described. More information regarding modeling the SMFs can be found in the ATC76-1 project or in the studies by Flores et al. [23]

3.5 Modeling BRBs

The BRBFs were also modeled using OpenSees. Unlike the SMFs where the nonlinear behavior was modeled using phenomenological models, the beams and columns of the BRBFs were modeled using elements with fiber sections. Additionally rigid offsets were used at the beam column connections and brace to frame connections to model the gusset plates. BRBs were modeled with a corotational truss element with yielding steel core area. Since a single truss element was used for the whole brace, equivalent elastic modulus was used to model the yielding and the non-yielding core (tapered ends) of the brace. Consistent with the design, the total brace stiffness was calibrated to be 1.5 times the single truss element stiffness (with yielding core area) that would extend from work-point to work-point. Both moment resisting (MR) and non-moment resisting (NMR) beam-column connections were used for the braced bay connections. Inherent damping was modeled as Rayleigh damping by setting the critical damping ratio to 2.5% at the fundamental and third modes of the structure. A leaning column was used to model second order effects. The effect of the gravity framing system was neglected in the models. More information regarding modeling the BRBFs can be found in study by Atlayan and Charney [25].

3.6 Peak Floor Accelerations

In this section of the study, the accelerations rigid NSCs are subjected to are computed for the SMFs and BRBFs. The three methods used to compute the accelerations are: using the specifications given by the current US code (ASCE 7-10), performing linear and nonlinear time history analysis.

ASCE7-10 provides the design accelerations on rigid NCs implicitly in the general formula to compute the horizontal seismic design force for NCs. The horizontal seismic design force F_p is given by:

$$F_p = \frac{0.4 a_p S_{DS} W_p}{\frac{R_p}{I_p}} \left(1 + 2\frac{z}{H}\right) \leq 1.6 S_{DS} I_p W_p \qquad F_p \geq 0.3 S_{DS} I_p W_p \qquad (1)$$

where a_p is the component amplification factor (a_p equal to 1.0 and 2.5 for rigid and flexible NSCs respectively), R_p and I_p are the component response modification and importance factor, respectively, W_p is the weight of the component, S_{DS} is the DE short period spectral acceleration and z/H is the relative height ratio of the floor at which component is anchored. Implicit in Eq. (1) (a_p = 1 for rigid NSCs) is a linear height-wise variation of the PFA from a value equal to the PGA (= 0.4 S_{DS}) at the ground level (i.e., z/H = 0) to a value equal to 3 times the PGA at the roof level (i.e., z/H = 1.0). It can be seen that ASCE 7 does not consider whether the supporting structure behaves elastically or inelastically, does not differentiate among the different types of lateral resisting systems, and does not take into the account the number of stories or floor levels.

The Peak Floor Acceleration (PFA) is the maximum total acceleration measured at a given floor, and is equal to the acceleration demand on a rigid NSC located at that floor. This method is used for the linear and nonlinear time history analyses and the results are shown next. Figure 2 (a) and (b) displays the median PFA for the SMF and BRBF respectively. Additionally, the PFA

computed using the ASCE7-10 is shown in the figures. The accelerations on the NCs on the BRBF are larger than the ones on the SMF and they are very close to the ones computed using the code. The reason why the accelerations on the BRBF are larger is believed to be the difference on the base of the columns conditions. On the other hand, the accelerations on the NCs when the models behave inelastically are similar and the PFA is similar to PGA along the height. The less rigid structures, BRBs with pinned connections and SMF without the gravity system subjected the NCs to lower accelerations than rigid structures. The lateral resisting system that decreased the demands the most was the BRB with pinned connections.

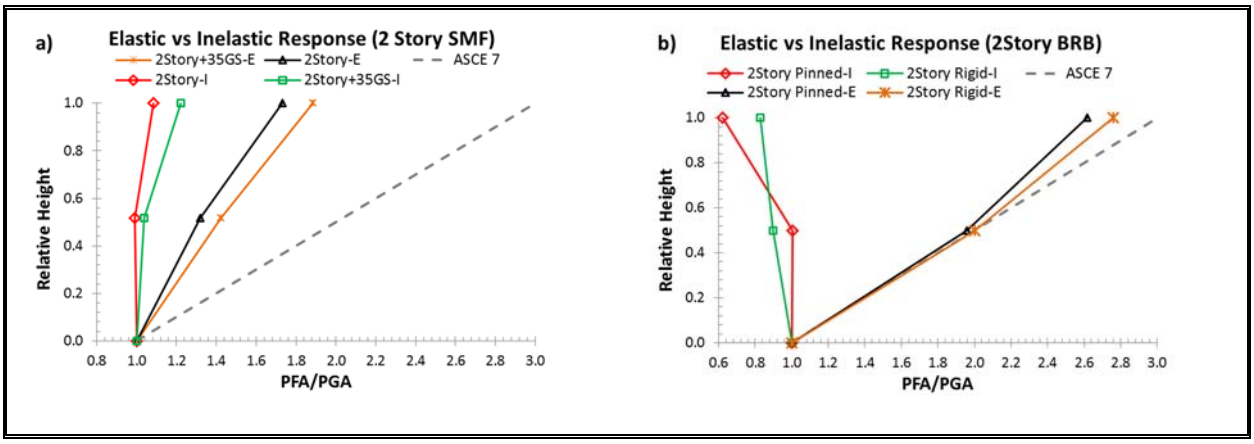

Figure 2 Normalized Peak Floor Acceleration (PFA/PGA): 2-Story Model

Figure 3 shows the median PFA results for the 4-story model. The same trends on the accelerations are seen for both lateral resisting sytems. However, the accelerations on NCs when the BRBs behave elastically are larger than the SMFs. On the other hand, accelerations are reduced more on the BRBs when the structures behave inelastically. In general, more rigid structure yielded larger demands on NCs and the configuration that decreased the PFA the most was the BRBF with pinned connections.

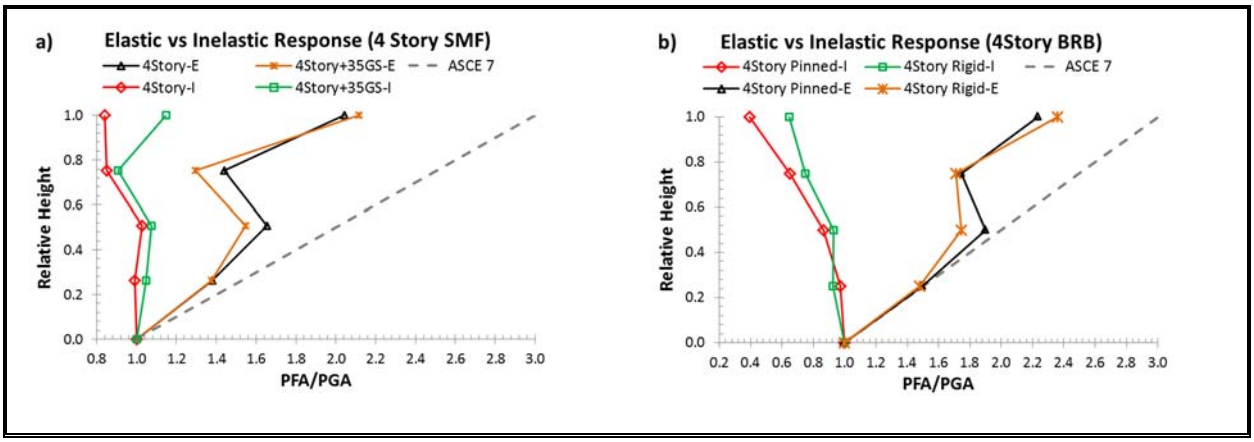

Figure 3 Normalized Peak Floor Acceleration (PFA/PGA): 4-Story Model

Figure 4 illustrates the comparison of the median responses obtained for an 8-story SMF and a 9-story BRBF. This was done because an 8-story BRB was not analyzed as part of the ATC76-1 project. However, the difference on the number of stories between the two buildings is minimal and the periods of vibration are very close. The shape of the PFA are very similar but the elastic BRBs present larger acceleration on the bottom stories. In some cases the elastic PFA are even larger than the ones computed using the ASCE7-10. The consequence of the inelastic behavior on the accelerations attached on the BRBFs is more pronounced than on the SMFs. The accelerations are decreased up to 0.6 the PGA when the BRB frame has pinned connections. The incorporation of the gravity system does not change the response significantly on the SMF.

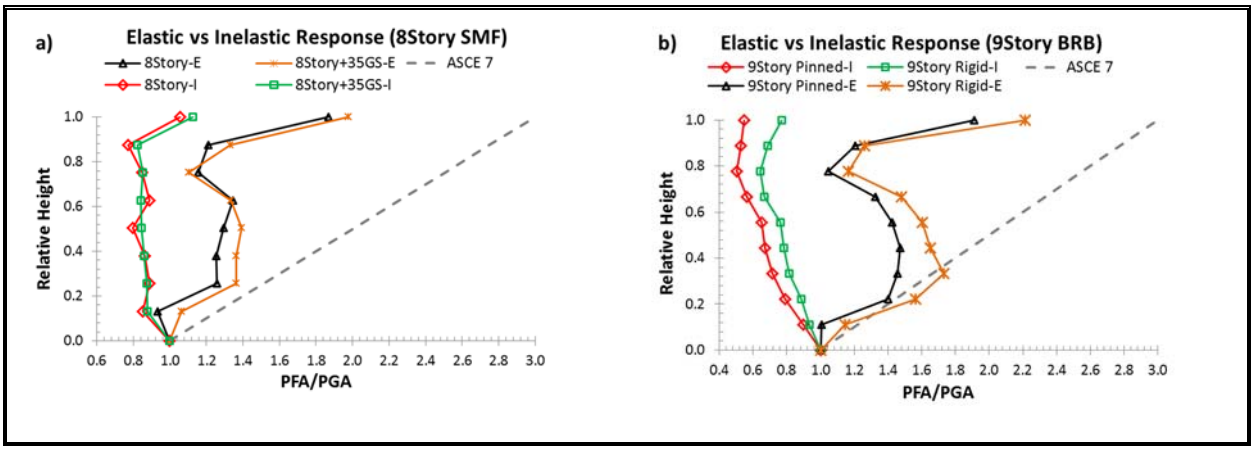

Figure 4 Normalized Peak Floor Acceleration (PFA/PGA): 8, 9-Story Model

From the results presented above, it can be concluded that ASCE7-10 overestimates the accelerations regardless the type of lateral resisting system. Moreover, when the inelastic behavior of the supporting structure is taken into consideration, the accelerations computed by the code are much larger. By comparing the BRBFs and SMFs accelerations it can be seen that the inelastic behavior on BRBFs decreased more the NCs accelerations than SMFs did. An ongoing investigation is being developed to determine why this is occurring.

3.7 Floor Response Spectra

In this section of the study, the accelerations for flexible NCs are computed. These accelerations are computed using the specifications given in the current US code (ASCE 7-10), performing linear time history analysis, and performing nonlinear time history analysis. The method used to evaluate the accelerations when linear and nonlinear analyses are performed is the Floor Response Spectrum method specified before. Due to space limitations the accelerations are compared at the first and roof level of the structures.

The difference on the design acceleration between rigid and flexible NCs according to to ASCE 7-10 depends on the component amplification factor (a_p = 2.5 for flexible NCs). For instance, Eq. (1) indicates that the acceleration demand on flexible NCs that behave elastically (i.e., R_p = 1) and are located at the roof level (i.e., relative height z/H = 1) is equal to 3.0 x 2.5 = 7.5 times the PGA, regardless of the characteristics of the supporting structure. Recalling that the building models considered in this study were designed for a PGA = 0.4 g (DE level) the accelerations at the roof level for all the structures is equal to 0.4 g x 7.5 = 3.0 g. On the other hand the acceleration in the first floor depends on the number of stories that the building has because the relative height (z/H) changes.

Figure 5 (a-b) and (c-d) shows the FRS at the roof and first floor of the 2-story model for the SMF and BRBF respectively. In both floors the accelerations are amplified when the NC period is in resonance with one of the fundamental periods of the supporting structure. The accelerations computed on the BRBF behaving elastically are much larger on the roof than the ones obtained for the SMF, especially on the fundamental periods. Another difference between the accelerations on the SMF and BRBF when they behave in an elastic manner is that the influence of the second mode in the first floor is not as important in the SMF as is on the BRBF. However, the inelastic behavior on BRBF reduces dramatically the accelerations on NSCs. From the results it can also be concluded that more rigid structures (BRBF with rigid connections and SMF with the gravity system) yield larger floor accelerations.

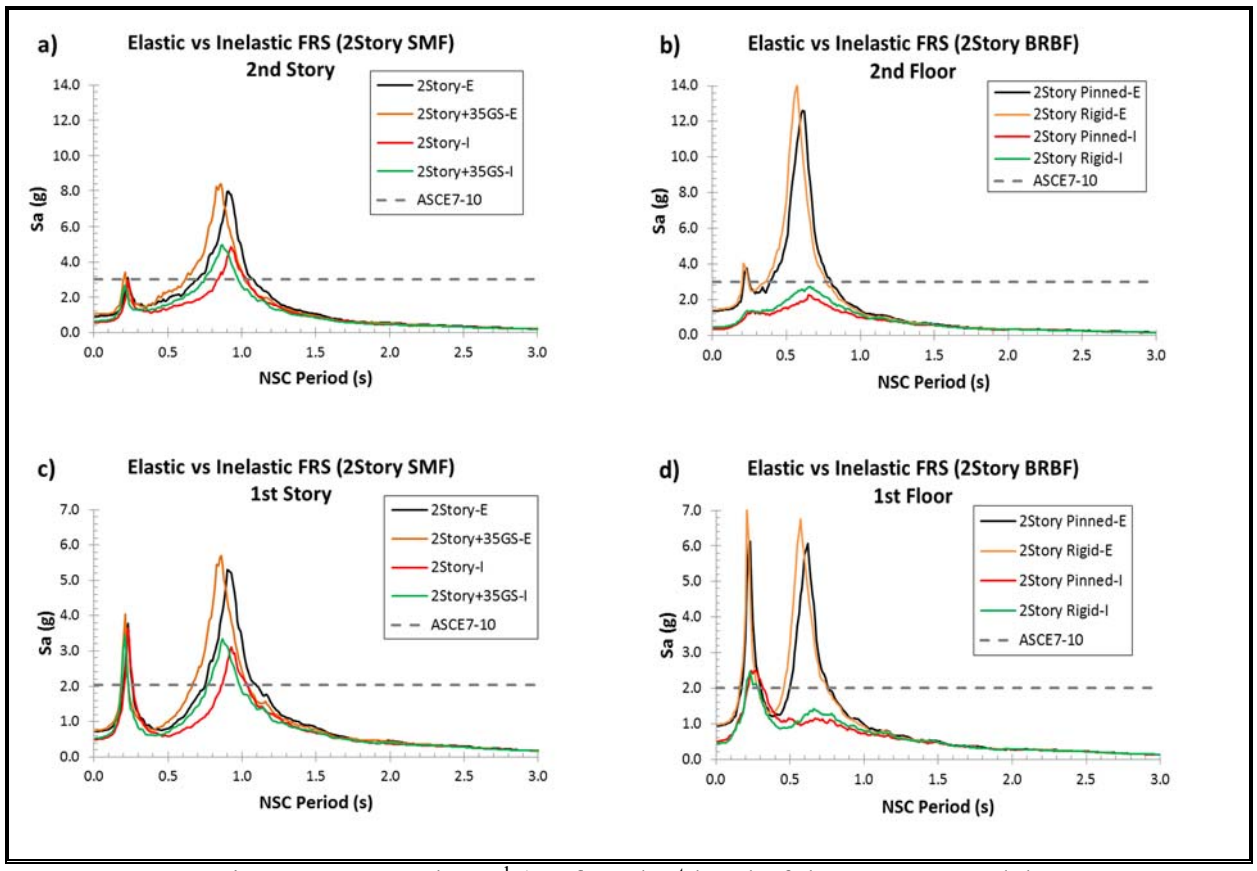

Figure 5 FRS at the 2nd (roof) and 1st level of the 2-Story Models

Figure 6 (a-b) and (c-d) shows the median FRS at the roof and first floor of the 4-story model for the SMF and BRBF respectively. Qualitatively and even quantitatively the FRS for both lateral systems when they behave elastically are very similar. The only exception is the acceleration in the first mode of the roof where the BRBF display a significantly larger quantity than the SMF. The reduction on the demands that the NCs are subjected to decreased drastically when the BRBF behaves in an inelastic manner. These reductions are larger than the ones experimented by the SMF, especially the first three fundamental modes. Similar to the 2-story models, floor accelerations in the more rigid structures are larger.

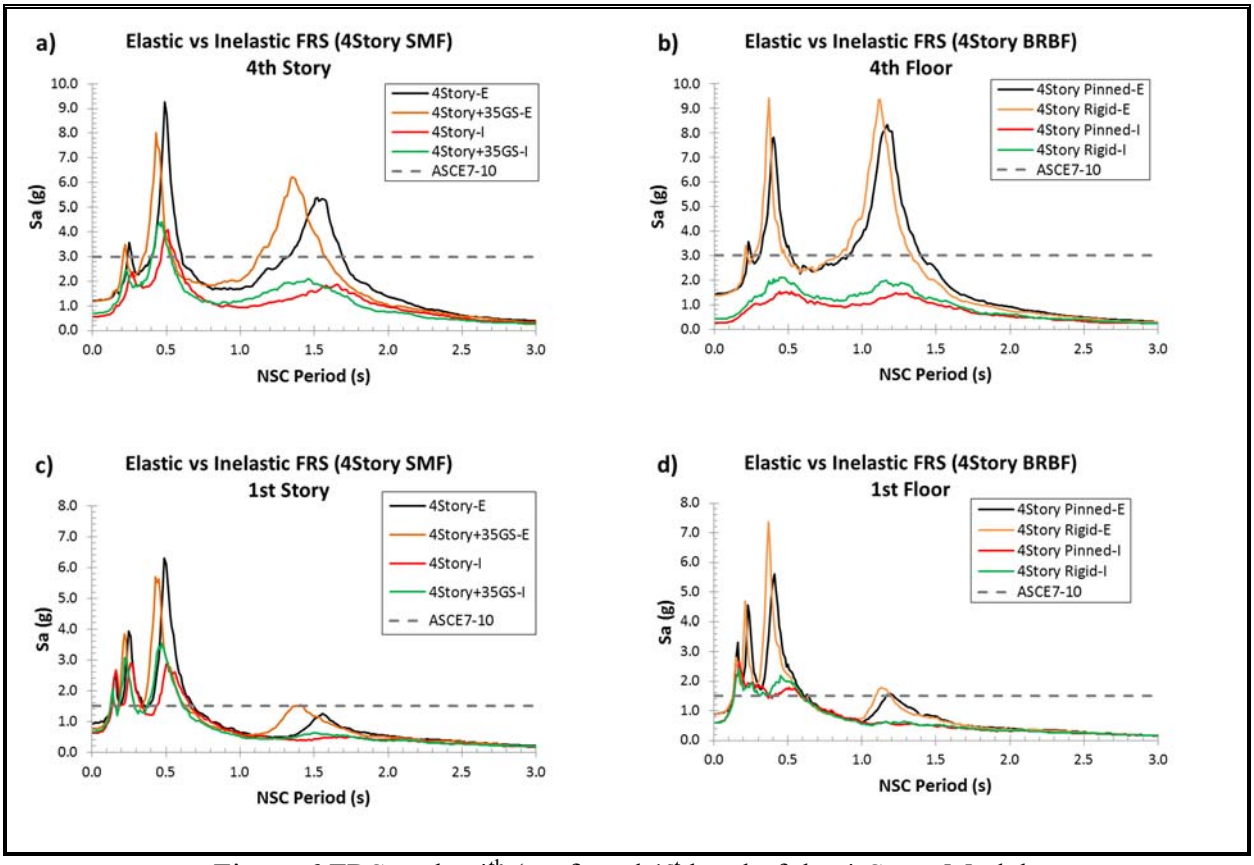

Figure 6 FRS at the 4th (roof) and 1st level of the 4-Story Models

Figure 7 (a-b) and (c-d) shows the median FRS at the roof and first floor of the 8- and 9-story model for the SMF and BRBF respectively. The results obtained when both lateral resisting

systems respond elastically are very similar quantitatively and qualitatively. The difference in the results between the SMF and BRBF arise when the inelastic behavior is incorporated in the analysis. The reductions on the accelerations at the fundamental modes are much larger in the BRBF than in the SMF.

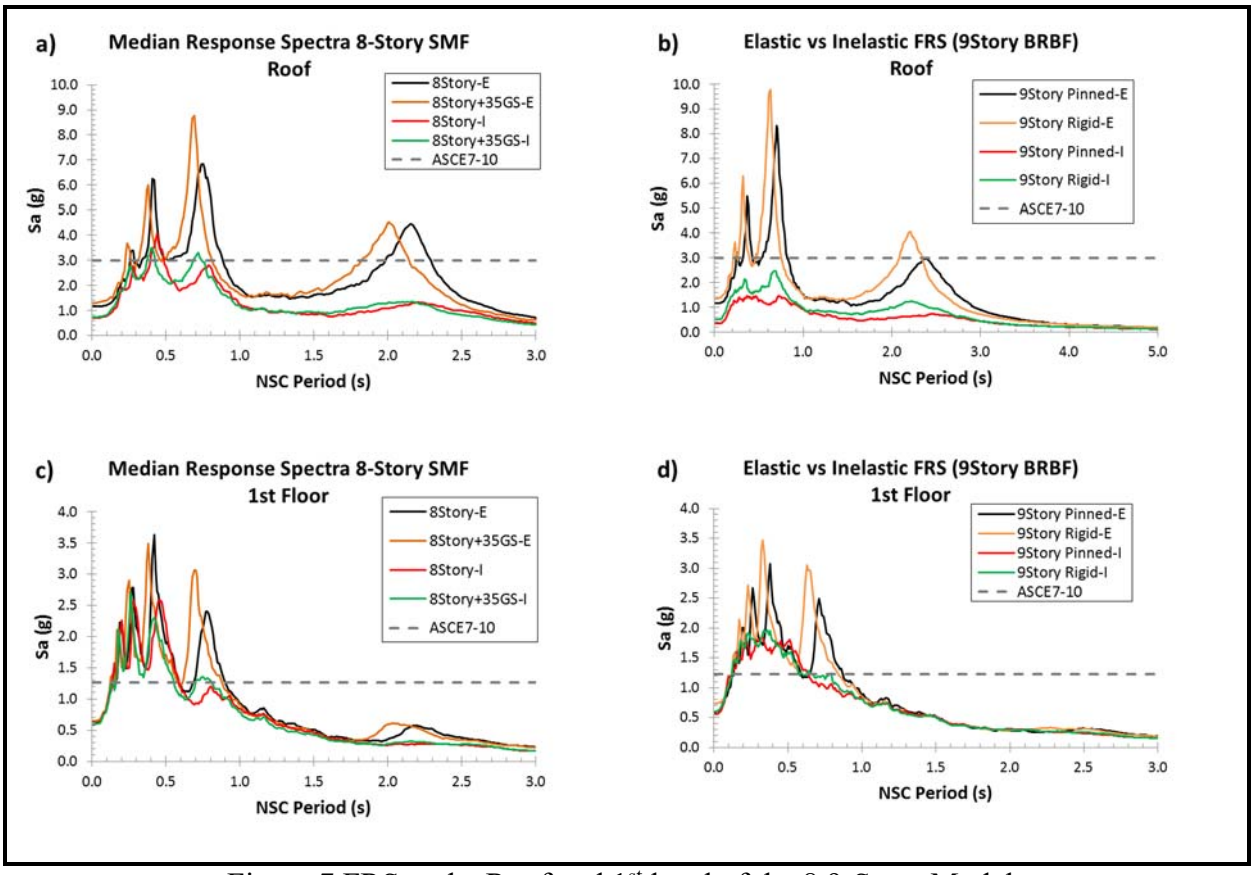

Figure 7 FRS at the Roof and 1st level of the 8,9-Story Models

3.8 Conclusions

In this study, floor accelerations in Special Steel Moment Frames (SMFs) and Buckling Restrained Brace Frames (BRBFs) were investigated considering different modeling options, from a simple linear elastic model of the lateral force resisting system to a sophisticated nonlinear model complying with the requirements of FEMA P-695. Particular attention was paid to the gravity system in the case of the SMFs and to the type of beam-colum-brace connections in the case of the

BRBFs. The building models were subjected to the FEMA P-695 set of far-field ground motions scaled to the DE response spectrum the buildings were designed for. From the analysis of results obtained by time history analysis, the conclusions of this investigation are:

- Both lateral resisting systems present similar trends on the accelerations for rigid NCs when they behave in an elastic manner. However, when the inelastic behavior was considered, BRBFs reduced more the accelerations than SMFs.
- It was found that ASCE7-10 overestimates the accelerations significantly in the upper stories of the building.
- The demands are similar to PGA in all the floors for the SMFs when the inelastic behavior is considered. On the other hand for the BRBFs this value ranged between 0.6-0.8PGA.
- Floor Response Spectra for all the structures show similar trends between SMFs and BRBFs when they behaved elastically. It was found however, that higher modes have more influence on BRBFs.
- The reduction in the accelerations at the fundamental modes, when the BRBFs behaved inelastically is larger than the SMFs. An ongoing investigation is trying to determine the reason.

3.9 Acknowledgements

Financial support was provided by the Pontificia Universidad Catolica de Chile and by the Virginia Tech Department of Civil and Environmental Engineering. This support is gratefully acknowledged.

3.10 References

[1] B. Reitherman, T. Sabol, R. Bachman, D. Bellet, R. Bogen, D. Cheu, P. Coleman, J. Denney, M. Durkin, C. Fitch, Nonstructural damage, Earthquake Spectra, 11 (1995) 453-514.

[2] E. Miranda, G. Mosqueda, R. Retamales, G. Pekcan, Performance of nonstructural components during the 27 February 2010 Chile earthquake, Earthquake Spectra, 28 (2012) S453-S471.

[3] E. Miranda, S. Taghavi, Approximate floor acceleration demands in multistory buildings. I: Formulation, Journal of structural engineering, 131 (2005) 203-211.

[4] J. Lin, S.A. Mahin, Seismic response of light subsystems on inelastic structures, Journal of Structural Engineering, 111 (1985) 400-417.

[5] S. Taghavi, E. Miranda, Response assessment of nonstructural building elements, Report No. PEER 2003/05. Dept. of Civil and Environmental Engineering, Stanford University, Stanford, CA. Pacific Earthquake Engineering Research Center, Richmond, CA, 2003.

[6] ASCE, Minimum Design Loads for Buildings and Other Structures, ASCE Standard ASCE/SEI 7-10, in, American Society of Civil Engineers, Reston, VA, 2010.

[7] A. Aref, M. Bruneau, M. Constantinou, A. Filiatrault, G.C. Lee, A.M. Reinhorn, A.S. Whittaker, Seismic Response Modification of Structural and Nonstructural Systems and Components in Acute Care Facilities, Research Progress and Accomplishments 2003-2004, (2004) 111-112.

[8] R. Villaverde, Seismic design of secondary structures: state of the art, Journal of structural engineering, 123 (1997) 1011-1019.

[9] A. Singh, A.H.S. Ang, Stochastic prediction of maximum seismic response of light secondary systems, Nuclear Engineering and Design, 29 (1974) 218-230.

[10] B. Kehoe, M. Hachem, Procedures for estimating floor accelerations, in: Proc., ATC-29-2 Seminar on Seismic Design, Performance, and Retrofit of Nonstructural Components in Critical Facilities, Applied Technology Council, Redwood City, Calif, 2003.

[11] M. Singh, L. Moreschi, L. Suarez, E. Matheu, Seismic design forces. I: Rigid nonstructural components, Journal of structural engineering, 132 (2006) 1524-1532.

[12] R.A. Medina, R. Sankaranarayanan, K.M. Kingston, Floor response spectra for light components mounted on regular moment-resisting frame structures, Engineering structures, 28 (2006) 1927-1940.

[13] R. Sewell, C. Cornell, G. Toro, R. McGuire, R. Kassawara, A. Singh, J. Stepp, Factors influencing equipment response in linear and nonlinear structures, in: Transactions of the 9th international conference on structural mechanics in reactor technology. Vol. K2, 1987.

[14] R. Sankaranarayanan, R.A. Medina, Acceleration response modification factors for nonstructural components attached to inelastic moment-resisting frame structures, Earthquake Engineering & Structural Dynamics, 36 (2007) 2189-2210.

[15] I. Politopoulos, Floor spectra of MDOF nonlinear structures, Journal of Earthquake Engineering, 14 (2010) 726-742.

[16] M. Rodriguez, J. Restrepo, A. Carr, Earthquake-induced floor horizontal accelerations in buildings, Earthquake engineering & structural dynamics, 31 (2002) 693-718.

[17] S.R. Chaudhuri, R. Villaverde, Effect of building nonlinearity on seismic response of nonstructural components: a parametric study, Journal of structural engineering, 134 (2008) 661-670.

[18] J. Wieser, G. Pekcan, A.E. Zaghi, A. Itani, M. Maragakis, Floor accelerations in yielding special moment resisting frame structures, Earthquake Spectra, 29 (2013) 987-1002.

[19] FEMA, Quantification of Building Seismic Performance Factors, FEMA P-695, Washington, D.C., 2009.

[20] NIST, Evaluation of the FEMA P-695 Methodology for Quantification of Building Seismic Performance Factors, GCR 10-917-8, (2010).

[21] S. Taghavi-Ardakan, Probabilistic seismic assessment of floor acceleration demands in multi-story buildings, in, 2006.

[22] S. Mazzoni, F. McKenna, M.H. Scott, G.L. Fenves, OpenSees command language manual, Pacific Earthquake Engineering Research (PEER) Center, (2006).

[23] F.X. Flores, D. Lopez-Garcia, F.A. Charney, Assessment of floor accelerations in special steel moment frames, Journal of Constructional Steel Research, 106 (2015) 154-165.

[24] F. Zareian, R.A. Medina, A practical method for proper modeling of structural damping in inelastic plane structural systems, Computers & structures, 88 (2010) 45-53.

[25] O. Atlayan, F.A. Charney, Hybrid buckling-restrained braced frames, Journal of Constructional Steel Research, 96 (2014) 95-105.

4. THE INFLUENCE OF ACCIDENTAL TORSION ON THE INELASTIC DYNAMIC RESPONSE OF BUILDINGS DURING EARTHQUAKES

4.1 Introduction

Nonlinear dynamic response history analysis (NRHA) is becoming an accepted procedure to assess the performance of building structures during earthquakes. In support of this trend, several documents [1-5] have emerged to provide guidance in terms of mathematical modeling, ground motion selection and scaling, and specification/evaluation of acceptance criteria. Additionally, several standards or prestandards [6-11] provide specific requirements for performing such analysis.

A review of these documents has indicated various areas of agreement and disagreement. One of the most striking areas of disagreement is related to methodologies required to capture accurate three-dimensional response, and more specifically, whether or not accidental torsion is required. In regards to accidental torsion, there are two issues. First, there is the question as to whether accidental torsion is needed in the (generally linear elastic) analysis used to design the structure that will be later analyzed using the NRHA procedure. Second, there is the issue of whether or not accidental torsion must be included in the nonlinear response history analysis itself. Related to the second issue is the specific manner in which the decision to omit or include accidental torsion in the NRHA is made, and how the accidental torsion is included in the analysis if it has been determined that it is necessary to include it.

A more fundamental issue is what constitutes accidental torsion. Usually, three sources are cited: (1) uncertainty in determination of center of mass, (2) uncertainty in location of center of

rigidity, and (3) the possible influence of torsional ground motion input. Items (1) and (2) are system dependent, and item (3) is site dependent. An additional complication that is particularly relevant to NRHA is that the instantaneous location of the center of rigidity will migrate as the main lateral load resisting components soften during yielding and stiffen during unloading. While it might be argued that the global torsional response that results from this migration is inherent in NRHA, significant uncertainties exist in characterizing the inelastic behavior and in this sense the induced torsion is in part accidental. Additionally, unless something is done to initiate it, a perfectly symmetric system (modeled as perfectly symmetric) will never experience a torsional response.

The traditional approach to initiate accidental torsion in dynamic analysis is to physically offset the center of mass, usually 5% of the building dimension perpendicular to the direction of loading. Numerous studies have questioned whether a 5% eccentricity is appropriate, and conclusions vary. Newmark [12], De la Llera and Chopra [13, 14], Ghayamghamian et al. [15], Stathopoulos and Anagnostopoulos [16], Basu and Giri [17] state that 5% is excessive. Pekau and Guimond [18] insists that 5% is insufficient. Additionally, some authors [15, 19] have suggested that imposing an artificial eccentricity is not the best approach for inducing accidental torsion, and that use of a torsional ground motion is preferred. The advantage of inducing a torsional ground motion is that the torsional effect can be developed in one analysis, whereas movement of the center of mass requires multiple analyses. The main drawback of using torsional ground motion input is that torsional ground motions are not recorded, and must instead be generated from available horizontal components. While a variety of procedures for determining the appropriate torsional ground motion exist [14, 20, 21], they are not yet general enough for use in practice due

to the wide variation in site conditions and building geometries. This issue is not explored further in this paper, and instead, accidental torsion is initiated by use of a mass offset.

The issue of accidental torsion in seismic design and analysis was, until recently, a resolved issue. Where linear elastic analysis procedures are used, most building codes require accidental torsion to be included, either by applying equivalent lateral forces at some eccentricity in static analysis, or by shifting the center of mass in dynamic analysis. However, a debate has arisen as to whether accidental torsion is in-fact needed in the design of all buildings. In this regard, DeBock et al. [22] have shown, using the FEMA P-695 Methodology [23], that accidental torsion is not warranted in the design of torsionally regular structures in low to moderate seismic hazard areas, but is needed for irregular structures in high seismic hazard areas. This observation, which is based on collapse criteria alone, was instrumental in the decision to relax the accidental torsion requirements in the 2015 NEHRP Provisions [6] and in ASCE 7-16 [11]. Specifically, in Chapter 12 of ASCE 7-16 the inclusion of accidental torsion in analysis and design is required only for systems in Seismic Design Categories B with a Type 1b Horizontal Irregularity (torsion), and in Seismic Design Categories C, D, E, and F with a Type 1a or 1b (torsion or extreme torsion) irregularity.

Whether or not accidental torsion should be included in NRHA was extensively debated by members of the task committee charged with developing a fully revised set of requirements for NRHA for Chapter 16 of the 2015 NEHRP Provisions [6]. Ultimately, the guidelines that were approved for the Provisions require the inclusion of accidental torsion in the elastic analysis-based design phase, but not in the subsequent NRHA that is used to evaluate the computed response. The decision not to include accidental torsion in the NRHA was based primarily on practical considerations, as it was thought that requiring as many as four additional analyses (for four

different mass offset locations per ground motion, with a minimum of 11 ground motions required) was onerous. It is noted, however, that the commentary for the 2015 Provisions suggests that the influence of uncertainties in the location of center of mass and/or in the strength and stiffness of structural components be evaluated for torsionally sensitive systems.

The development of new provisions for Chapter 16 of ASCE 7-16 began with the 2015 NEHRP provisions [6], but among the changes that were made was the requirement to include accidental torsion in the NRHA if it is required in the design of the structure. Accidental torsion is implemented by shifting the center of mass plus and minus 5% of the width of the building perpendicular to the main direction of shaking. This requirement was motivated in part by research performed by Flores, et al. [24] that showed that even for torsionally regular buildings, the computed drift at the edge of the building could be considerably greater than the drift at the center of mass. This is of particular importance because the ASCE 7-16 global acceptance criteria require that the global drift be evaluated at the edge of the building. Additionally, it was shown in Flores et al. that for torsionally irregular buildings, collapses may occur under MCE analysis when accidental torsion is included, and may not be captured if accidental torsion is not included in the analysis. This point is also very pertinent to ASCE 7-16 as the global acceptance criteria allows not more than one "unacceptable response" among the 11 ground motions analyzed.

It is noted that the ASCE 7-16 requirement to include accidental torsion in NRHA is a significant departure from prior practice. Among the tall building provisions [3, 4, 9, 10] only LATBSDC [10] requires that accidental torsion be considered, but only when the ASCE 7 torsional amplification factor A_x, computed from elastic analysis, is greater than 1.5. An A_x of 1.5 is slightly beyond the limit at which a system would have an extreme torsional irregularity. The PEER Guidelines [3, 4] justify the neglect of accidental torsion in the serviceability analysis of tall

building by stating that "the torsional eccentricity associated with random variability in loading and material properties will tend towards a mean of zero when considered over many stories and floor levels". While this is arguable for tall buildings, building code requirements need to address buildings of all height. The PEER guidelines are silent on requirements for including accidental torsion in NRHA. Among codes and standards prior to ASCE 7-16, ASCE 7-10 did not require accidental torsion in NRHA, and actually allowed 2-dimensional analysis in some cases (as did the 2009 NEHRP Provisions). ASCE 41-06 [25] and ASCE 41-13 [8] require that accidental torsion be included in NRHA, but only when separate linear analysis indicates that the system response is likely to be sensitive to accidental torsion. In is noted, however, that both ASCE 41-06 and ASCE 41-13 require accidental torsion to be included in NRHA where the building has no inherent torsion (e.g. perfectly symmetric systems).

The decision to include accidental torsion in the ASCE 7-16 NRHA procedures is in general agreement with recommendations made in analyses by Mansuri [26], Jarrett et al. [27], and Flores, et al. [24]. Even though the building systems analyzed by Mansuri were not particularly torsionally sensitive, it was noted that increases in response due to accidental torsion were significant, and were more significant for taller systems relative to shorter systems. Mansuri also noted that inelastic torsional response was generally greater than elastic torsional response, and that P-Delta effects had a very significant influence on behavior. In Jarrett et al. [27] it was found that shifting the location of center of mass had a more significant effect on torsional response of buildings than imposing random uncertainty in stiffness and strength of structural components. Based on this finding it was recommended, via proposed code language, that accidental torsion be included in NRHA, but that exceptions could be developed on the basis of preliminary nonlinear static pushover analysis. In Flores et al. [24], analysis of a doubly symmetric 9-story buckling restrained

braced system indicated that accidental torsion strongly influenced the computed response of systems that were, according to ASCE 7, torsionally regular, irregular, and extremely irregular. In addition, Flores et al. found that accurate modeling of three-dimensional P-Delta effects is essential in capturing nonlinear global response and stability. In Flores et al. the system designs that were evaluated did not include accidental torsion, and that the design assumed that the displacement magnification factor C_d is equal to the reduction factor R. These features were incorporated into the designs because the analytical models used were based on a design space (NIST 2010c) that was developed for evaluation of the FEMA P-695 Methodology, and this methodology ignores accidental torsion in design (analysis is generally 2-Dimensional) and it is specified that C_d=R.

In the new work presented in this paper, the need to include accidental torsion in NRHA is further investigated through the evaluation of the response of a 9-story steel building with Buckling Restrained Braces (BRB) used to resist lateral loads. However, designs were developed that do and do not incorporate accidental torsion, and the C_d value was taken as that required for BRB systems in ASCE 7. Three versions of the building are considered, wherein the only difference is the plan location of individual braced frames. The variation in plan location produces different levels of torsional irregularity, from moderate to extreme. In the analysis the amount of the accidental eccentricity used was varied, the influence of bi-directional loading was investigated, and methodologies for incorporating 3-dimensional second order effects were evaluated. The results of the new analysis agree in principle with Mansuri [26], Jarrett et al. [27], and Flores et al. [24] in the basic finding that accidental torsion is an important consideration in NRHA. Supplementary to this finding is that bi-directional loading should always be included, and that global second order effects are best represented by explicitly modeling all of the columns in the system.

4.2. Modeling of Second Order Effects in 3-D Structural Analysis

Most analysts recognize the importance of including second-order effects in NRHA. These effects cause amplification of lateral displacements (the P-Delta effect) as well as amplification of system torsional rotation (referred to herein as the *P-Theta effect*, where Theta is the global rotation about the vertical axis). Wilson and Habibullah [28] provide a thorough discussion of such effects, and present approximate methods for incorporating them in linear dynamic analysis of building systems with diaphragms that are idealized as rigid.

If both the gravity system and the lateral system are physically modeled in 3-D analysis, both the P-Delta and the P-Theta effects are automatically captured when element stiffness formulations include geometric stiffness. Such models with spatially distributed columns may be used for both rigid and semi-rigid diaphragm idealizations. If the gravity columns are not included in the model, the destabilizing gravity loads tributary to these columns must be accounted for, and this is often done using "leaner columns" which, in essence, lump some or all of the P-Delta effects into one or more elements with zero elastic stiffness and negative geometric stiffness.

Where geometric stiffness is not included in the elements of the lateral system, the leaner column can be used to represent the destabilizing gravity load for the full system. It is very important to note, however, that leaner columns, if improperly used, may not capture P-Theta effects entirely, and this omission can lead to significant underestimates of global displacements and failure to predict dynamic instability [24].

This paper specifically investigates the role that P-Theta effects play in assessing the torsional response of buildings. This is done by performing analysis with and without P-Theta effects, and comparing the computed response. Additionally, both the lateral and torsional stability coefficient are computed and presented for each system. The lateral stability coefficients, Q_Δ, are

determined by performing a static linear-material analysis for the structure under unidirectional lateral loads, without accidental torsion, with and without P-Delta effects, and computing the following quantity at each story level:

$$Q_\Delta = 1 - \frac{\Delta_o}{\Delta_f} \tag{1}$$

where Δ_o is the center of mass story drift computed without P-Delta and Δ_f is the story drift including P-Delta. The torsional stability coefficients, Q_θ , are determined by running a static linear-material analysis for the structure loaded with accidental torsion only, with and without P-Theta effects, and computing the following quantity at each story level:

$$Q_\theta = 1 - \frac{\theta_o}{\theta_f} \tag{2}$$

where θ_o is the difference in torsional rotations at the top and bottom of the story without P-Theta and θ_f is the same quantity computed for analysis that includes P-Theta. Lateral deflection and torsional rotation amplifiers, λ_Δ and, λ_θ respectively, are determined as follows:

$$\lambda_\Delta = \frac{1}{1 - Q_\Delta} \tag{3}$$

$$\lambda_\theta = \frac{1}{1 - Q_\theta} \tag{4}$$

4.3. Description of System Analyzed

The system analyzed, illustrated in Figure 1, is nine stories tall, with a rectangular plan consisting of two 30-ft bays in one direction, and eight 30-ft bays in the other direction. The system was adapted from a similar square-plan (four 30-ft bays in each direction) building described in

the ATC 76 project [29], and analyzed in two dimensions in detail by Atlayan and Charney [30]. The archetype taken from ATC 76 from which this study was based on was the 9S-LB-15B-Dmax. An important difference between the ATC 76 design and the systems analyzed herein is that in the ATC 76 design the displacement amplification factor (C_d) was taken equal to the response modification factor (R=8), as recommended by FEMA P-695. For the systems analyzed herein, the BRBs were re-designed with C_d taken equal to 5, which is the value specified by ASCE 7-10 and ASCE 7-16. This difference had an important influence in the design of the BRB frames because the redesigned system was controlled by strength in the case where no accidental torsion was included, whereas the original system was controlled by drift. When accidental torsion was incorporated drift controlled the design of some of the braces.

The lateral load resisting system consists of four bays BRB frames, with two bays in each direction (Figure 1). The yielding cores in the BRBs use ASTM A992 steel with a nominal yield strength of 50 ksi. Three variations of this system are investigated, wherein the only difference between the systems is the placement of the BRBs that resist load in the N-S direction. All systems have BRBs on gridlines A and C to resist loads in the E-W direction. For System A, BRBs for N-S loads are positioned only along gridlines 4 and 6 as shown in Figure 1. System B has N-S BRBs only on gridlines 3 and 7, and system C has N-S BRBs only on gridlines 2 and 8. Based on ASCE 7-10 definitions, System A has a Type-1b (extreme) torsional irregularity, System B has a Type 1a torsional irregularity, and system C is not torsionally irregular. It is important to note that accidental torsion was not included in the design of models A, B, and C. A separate set of models was developed that include accidental torsion in the design, and these are designated as models A-2, B-2, and C-2. For these systems, the design was done using Modal Response Spectrum Analysis (MRS) and accidental torsion was included in accordance with the requirements of ASCE 7-10.

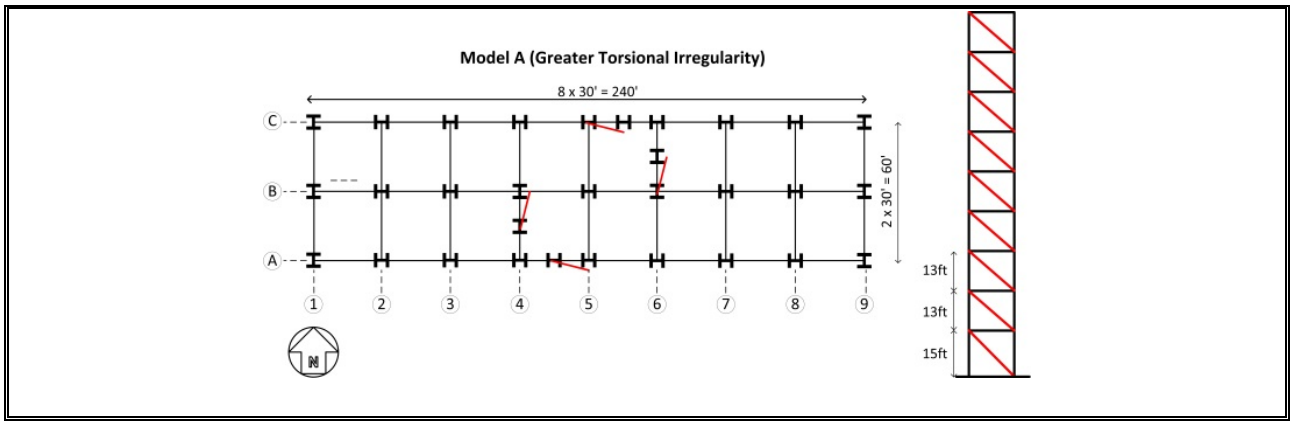

Figure 1. Structural System Analyzed (Model A)

The section sizes for each of the models are shown in Table 1. It can be seen from the table that the sections for Models A, B and C are the same because accidental torsion requirements were not considered in the design.

Table 1 Member Sections for all Models

	Model A,B,C			Model A-2			Model B-2			Model C-2		
Level	**Column**	**Beam**	**BRB (in^2)**	**Column**	**Beam**	**BRB (in^2)**	**Column**	**Beam**	**BRB (in^2)**	**Column**	**Beam**	**BRB (in^2)**
Roof	W14x120	W21x62	7	W14x370	W21x62	9	W14x311	W21x62	8	W14x193	W21x62	7
Level 8	W14x120	W24x76	7	W14x370	W24x76	9	W14x311	W24x76	8	W14x193	W24x76	7
Level 7	W14x120	W24x76	8	W14x370	W24x76	10	W14x311	W24x76	9	W14x193	W24x76	8
Level 6	W14x193	W24x76	8	W14x398	W24x76	10	W14x370	W24x76	9	W14x233	W24x76	8
Level 5	W14x193	W24x84	10	W14x398	W27x94	11	W14x370	W27x94	10	W14x233	W24x84	10
Level 4	W14x283	W24x84	10	W14x455	W27x94	11	W14x398	W27x94	10	W14x311	W24x84	10
Level 3	W14x283	W24x84	10	W14x455	W27x94	11	W14x398	W27x94	10	W14x311	W24x84	10
Level 2	W14x370	W24x84	11	W14x500	W27x94	12	W14x426	W27x94	11	W14x370	W24x84	11
Level 1	W14x370	W24x84	11	W14x500	W27x94	12	W14x426	W27x94	11	W14x370	W24x84	11

The increase in member sizes shown in Table 1 for systems A-2, B-2, and C-2 is indicative of the influence accidental torsion had on the design. Accidental torsion was incorporated by relocating the mass to induce a 5% eccentricity as required by ASCE 7-10. If the building has a torsional irregularity, the requirements to be applied are to check drifts at the edges (on grid lines 1 and 9) applying static forces with an eccentricity (5%) or moving the mass an eccentricity equal

to 5% the longest side of the building. Although Model C does not present a torsional irregularity, drifts were checked at the edge and Model C-2 was developed. The sections shown in this table represent the frames resisting lateral forces applied in the N-S direction. The sections resisting forces in the E-W direction are the same as the ones for Models A, B and C because in this direction the building did not present any torsional irregularity and the drifts at the edges were controlled by just increasing the sections in the N-S direction.

The gravity system consists of a metal deck and concrete floor slab supported by an assembly of steel beams and columns. The total seismic weight of the system, *W*, is 14490 kips, which represents a weight density of 8.6 pounds per cubic foot. The design floor load was 100 psf dead and 50 psf live. Seismic design was based on ASCE 7-10 [7] and the 2010 AISC Seismic Specification [31]. Design level spectral accelerations S_{DS} and S_{D1} are 1.0g and 0.6g, respectively.

4.4. Mathematical Model

Each system was analyzed in three dimensions using OpenSees [32]. Floor diaphragms were assumed rigid in-plane and flexible out of plane. The gravity system was included in the analysis, but did not contribute to the lateral strength and stiffness. P-Delta effects were included using two different approaches, each incorporating the P-Delta transformation within OpenSees. The first of these used a "leaning column" at the center of the building, wherein the *P* load on the column represented the entire gravity load (1.0D + 0.25L) of the system. Here, P-Delta effects are fully captured but P-Theta effects are not included. In the second approach, which captures both P-Delta and P-Theta effects, the story *P* loads were distributed by tributary area to each of the individual columns. The influence of the different P-Delta modeling approaches on the computed response (including a separate study that utilizes four leaning columns) is discussed in detail later in this paper. In the remainder of this paper results produced by the model that uses a single leaning

column are identified with the symbol P-Δ, and the results from the model that explicitly models all the columns are identified with the symbol P-Δθ. The symbol θ in the second case indicates that torsional P-delta effects are included *in addition* to P-Δ.

Material nonlinearities were included in the beams, columns, and braces of the BRB systems. Beams and columns were modeled using displacement control fiber elements and the BRBs were modeled using a phenomenological model. The analytical approach used to model the BRB system is discussed in detail in Atlayan and Charney [30]. In the dynamic analyses the effect of accidental torsion was introduced by modifying the diaphragm mass distribution such that the desired mass eccentricity was achieved. Inherent damping was modeled as Rayleigh damping by setting the critical damping ratio to 2% at the fundamental and fifth modes of the structure. The average damping over the first 12 modes (sufficient to capture 95 percent of the effective mass) was less than 3% critical for all models analyzed.

4.5. Torsional Properties of Systems

The lateral and rotational stability coefficients were computed for each story of the building (Eqs. 1 and 2), and the maximum values along the height computed for Systems A, B, C and A-2, B-2 and C-2 are reported in Table 2. Also provided are the corresponding amplification factors (Eqs. 3 and 4).

The lateral stability coefficients for all systems A, B and C are the same (0.088) because they all have the same lateral stiffness. Note that ASCE 7-10 and ASCE 7-16 require that P-Delta analysis be included in the design only where the maximum lateral stability coefficient is greater than 0.10, and that no requirements are provided at all for torsional stability. Thus, in this case none of the buildings would require P-Delta effects to be considered for design. As noted from

Table 2, however, the torsional stability coefficient for System A is very significant at 0.275, indicating an increase in static plan-wise torsional rotations by a factor of 1.379 due to P-Theta effects alone. The torsional stability coefficient and amplification factor for Systems B and C are somewhat less, but still significant for System B.

Table 2 Stability and Amplification Factors

Model	$\mathbf{Q_\Delta}$	$\boldsymbol{\lambda_\Delta}$	$\mathbf{Q_\theta}$	$\boldsymbol{\lambda_\theta}$
A	0.088	1.096	0.275	1.379
A-2	0.032	1.033	0.258	1.347
B	0.088	1.097	0.107	1.119
B-2	0.074	1.080	0.092	1.101
C	0.088	1.097	0.049	1.051
C-2	0.085	1.093	0.047	1.049

Another indicator of the likelihood of torsional response is the torsional irregularity factor (TIF) which is equal to the maximum ratio, over all stories, of the building edge story drift to the building center story drift when an equivalent lateral load is applied at a 5% eccentricity. In ASCE 7 this factor is used to determine if a torsional irregularity occurs. If the TIF is greater than 1.2 and less than 1.4 the building is torsionally irregular, and if the ratio is greater than or equal to 1.4 the system is extremely irregular. The TIFs computed for Systems A, B, C and A-2, B-2 and C-2 with different approaches for including geometric nonlinearity are shown in Table 3. It is interesting to note that the P-Δ model reports slightly lower TIFs than those obtained when no geometric nonlinearity is used. For the system with torsional irregularities, TIFs obtained using the P-Δθ model increase, particularly so for Model A and Model A-2 with the extreme torsional irregularity. It is also worthwhile to point out that even though the models that include accidental torsion

comply with drift requirements at the edge of the buildings, the TIFs are not necessarily reduced (e.g the TIF for model A2 is greater than that for model A). It is believed that the factor would reduce if the orthogonal resisting frames (E-W direction) were increased in size to control drifts during the design stage. However, because the torsional irregularity is in the N-S direction, only the N-S frames were increased in size to control drifts.

Table 3. Torsional Irregularity Factors

Model	**No P-Δ or P-θ**	**P-Δ**	**P-Δθ**	**Irregularity?**
A	1.86	1.81	2.05	Extreme
A-2	1.93	1.90	2.12	Extreme
B	1.32	1.30	1.33	Irregular
B-2	1.33	1.31	1.34	Irregular
C	1.16	1.15	1.15	None
C-2	1.16	1.15	1.16	None

As a final check of the torsional sensitivity of the buildings, the first three periods of vibration were computed with and without an accidental eccentricity, and using both the P-Δ and the P-Δθ methods. The results of the analysis using a 5% accidental eccentricity are presented in Table 4. For System A without a mass offset, it may be seen that the first mode is torsional, with a period of 4.940 s when geometric nonlinearity is not included. The first mode period slightly increases when the P-Δ model is used, but increases significantly to 5.800 s when the P-Δθ model is used. For the same system the P-Δ model influences the lateral modes, but not the torsional mode. It is noted that the torsion period for System A is significantly larger than the lateral periods, an indicator of extreme torsional flexibility. The periods of vibration for the systems that include a mass eccentricity towards the East of 12 ft. (5% of the long direction of the building) are also

given in Table 4. As it may be seen there is a slight increase in the torsional period for each of the geometric nonlinearity assumptions when accidental torsion is incorporated. However, in some cases like for Models B-2 and Model C there is a change in the order of the modes making for example torsional the first mode for B-2. The model that considers accidental torsion (A-2), presents the same trends but the structure is stiffer than System A. The trends of the results for Model B and B-2, shown in Table 4, are similar to that for System A and A-2, except that considering accidental torsion in the design made the first mode of vibration to be lateral instead of torsional. Thus Mode B-2 is less torsionally flexible in comparison with Model B. For System C and C-2, it is seen in Table 4 that the first two modes are lateral, and torsion dominates the third mode response. For these models the influence of geometric nonlinearity is similar to that for the other systems for the lateral modes of vibration, but the variation is not substantial in the torsional mode.

4.6. Nonlinear Static Analysis

Prior to performing NRHA on the systems, a series of nonlinear static analyses were performed. All analyses were performed using displacement control with a first-mode lateral load distribution. Gravity load (1.05D +0.25L) was applied prior to lateral loading. In these analyses 100 percent of the lateral load is always applied in the N-S direction at a variable eccentricity that effectively offsets the mass towards the East. Some percentage of the E-W direction load is simultaneously applied without eccentricity. Three basic parameters were varied: 1) the magnitude of accidental eccentricity as a percentage of the length perpendicular to the N-S load 2) whether or not P-Theta effects were included and 3) the percentage of full load that is applied on the E-W direction.

Table 4. Summary of Fundamental Periods of Vibration (sec)

Model	Mode	No Accidental Torsion				5% Accidental Torsion (mass eccentricity)			
		No P-Δ or P-Δθ	P-Δ	P-Δθ	Mode Type	No P-Δ or P-Δθ	P-Δ	P-Δθ	Mode Type
Model A	1	4.940	4.966	5.800	Torsion	5.038	5.005	5.905	Torsion
	2	2.920	3.060	3.060	Lat (E-W)	2.920	3.060	3.060	Lat (E-W)
	3	2.915	3.054	3.054	Lat (N-S)	2.860	2.991	3.001	Lat (N-S)
Model A-2	1	4.538	4.559	5.177	Torsion	4.623	4.586	5.267	Torsion
	2	2.928	3.068	3.068	Lat (E-W)	2.928	3.068	3.068	Lat (E-W)
	3	2.501	2.586	2.586	Lat (N-S)	2.456	2.537	2.543	Lat (N-S)
Model B	1	3.146	3.164	3.340	Torsion	3.321	3.356	3.514	Torsion
	2	2.920	3.060	3.060	Lat (E-W)	2.920	3.060	3.060	Lat (E-W)
	3	2.915	3.054	3.054	Lat (N-S)	2.762	2.841	2.904	Lat (N-S)
Model B-2	1	2.926	3.066	3.066	Lat (E-W)	3.058	3.073	3.207	Torsion
	2	2.908	2.923	3.059	Torsion	2.926	3.066	3.066	Lat (E-W)
	3	2.651	2.754	2.754	Lat (N-S)	2.523	2.585	2.628	Lat (N-S)
Model C	1	2.920	3.060	3.060	Lat (E-W)	2.966	3.098	3.103	Lat (N-S)
	2	2.915	3.054	3.054	Lat (N-S)	2.920	3.060	3.060	Lat (E-W)
	3	2.233	2.247	2.301	Torsion	2.196	2.215	2.265	Torsion
Model C-2	1	2.923	3.063	3.062	Lat (E-W)	2.923	3.063	3.062	Lat (E-W)
	2	2.859	2.974	2.990	Lat (N-S)	2.910	3.018	3.038	Lat (N-S)
	3	2.196	2.198	2.260	Torsion	2.158	2.167	2.224	Torsion

Prior to performing NRHA on the systems, a series of nonlinear static analyses were performed. All analyses were performed using displacement control with a first-mode lateral load distribution. Gravity load (1.05D +0.25L) was applied prior to lateral loading. In these analyses

100 percent of the lateral load is always applied in the N-S direction at a variable eccentricity that effectively offsets the mass towards the East. Some percentage of the E-W direction load is simultaneously applied without eccentricity. Three basic parameters were varied: 1) the magnitude of accidental eccentricity as a percentage of the length perpendicular to the N-S load 2) whether or not P-Theta effects were included and 3) the percentage of full load that is applied on the E-W direction.

In the first series of analyses the lateral load was applied in the N-S direction at some eccentricity towards the East from the center of mass, and the E-W direction load was not applied. This is referred to as Unidirectional Loading. Both P-Delta and P-Theta effects were included. The results are shown for System A in Figure 2a, where the roof drift ratio is measured at the center of mass. Here, for clarity, mass eccentricities lower than 5% are not shown because they had a minimal impact on performance. However, increasing the eccentricity from 5% to 6% had a tremendous influence on the shape of the pushover curve. As shown in Figure 2b, the sudden change in pushover response does not occur when P-Theta effects are ignored.

Figure 2c illustrates the influence of bidirectional loading on the extremely irregular System A, when the N-S loading eccentricity is 5% of the building width, P-Theta effects are included, and orthogonal (E-W) loading is applied at the center of mass at some percentage of the full load. This percentage of the load is referred to herein as the Orthogonal Load Factor (OLF). As may be seen, a bifurcation in behavior occurs when the orthogonal load reaches just 4% of the full value. This percentage varies depending on the amount of accidental torsion in the building. For instance, for a 3% mass eccentricity the orthogonal load that causes the bifurcation is equal to 39% of the full value.

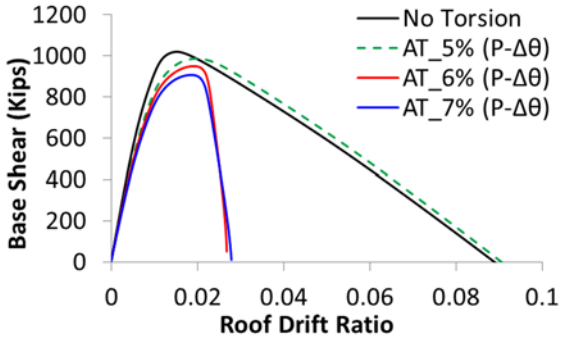

a) Unidirectional loading with Various Eccentricity (with P-Theta)

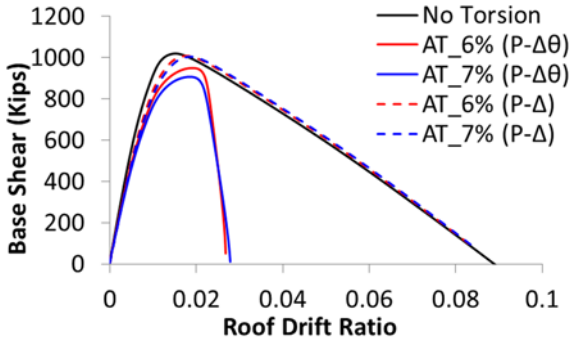

b) Unidirectional loading (with and without P-Theta)

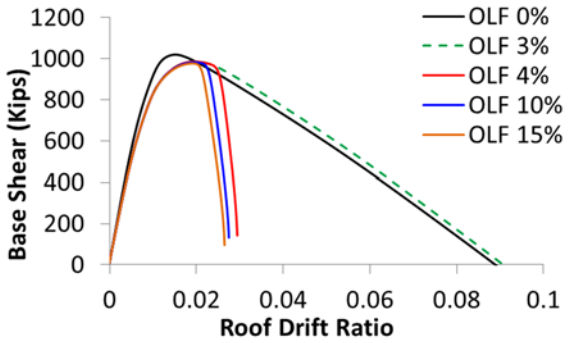

c) Bidirectional loading with 5% Eccentricity (With P-Theta)

Figure 2. Nonlinear static responses for Model A

To investigate if the bifurcation seen in Model A could be prevented by designing the structure including accidental torsion, Model A-2 was subjected to the same type of nonlinear static analyses described previously. The results are shown in Figure 3a where it can be seen that

the bifurcation occurs again and it actually happens at a value of accidental torsion lower than for Model A (4%). Again, the bifurcation is not seen when P-Delta is included and P-Theta effects are not included (Figure 3b). The influence of bidirectional loading is displayed in Figure 3c where the N-S loading eccentricity is 3% of the building width. In this case, the bifurcation in the pushover curve occurs when the OLF reaches a value of 23%. Although the amount of accidental torsion that causes the bifurcation in Model A-2 is lower than Model A, the strength of the building is larger in the N-S direction, which could result in a better dynamic performance of the system. As it will be shown later in this paper, the bifurcation in the nonlinear static response curve occurs as a result of the orthogonal frame entering into a yielding stage creating a mechanism that causes the collapse of the structure.

One of the omissions of ASCE 7 is that it does not specify what approach should be taken to design the structure and satisfy accidental torsion requirements in the design (control inter-story drifts at the edges). This is especially needed when the building has a torsional irregularity (TIF>1.2) in just one of the directions. A common procedure is to make the frames stiffer (and stronger) in the direction where there is a torsional irregularity and leave unchanged the frames in the orthogonal direction. However, it might be necessary to increase the frame sections in both orthogonal directions in order to prevent the bifurcation.

The behavior of Model B, which is moderately torsionally irregular, is similar to that of Model A. Figure 4a shows the response with unidirectional loading at various levels of eccentricity, with P-Theta effects included. The bifurcation in response does not occur until the eccentricity reaches 8%. Again, the sudden change in pushover response does not occur when P-Theta effects are ignored (Figure 4b). On the other hand, when orthogonal load effects are included for a system with 5% accidental eccentricity (Figure 4c), the system's behavior changes suddenly

when the OLF is 35%. At the limit of the bifurcation (accidental eccentricity equal to 7%) the OLF producing the bifurcation reduces to 13%.

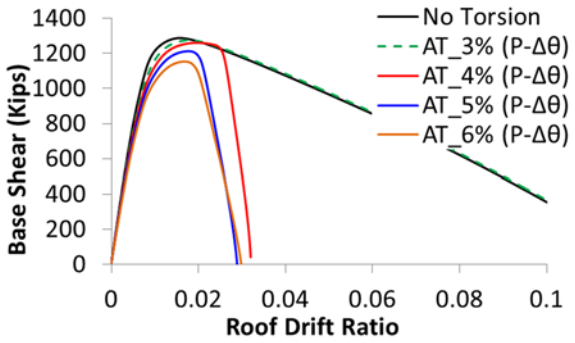

a) Unidirectional loading with Various Eccentricity (with P-Theta)

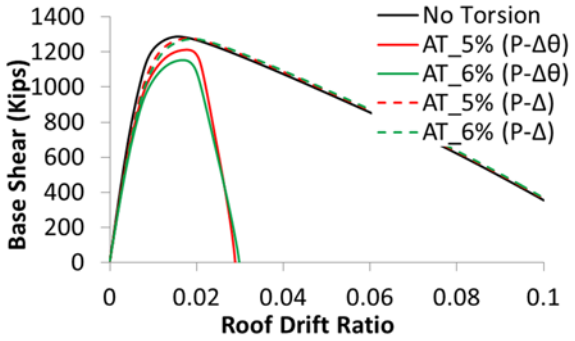

b) Unidirectional loading (with and without P-Theta)

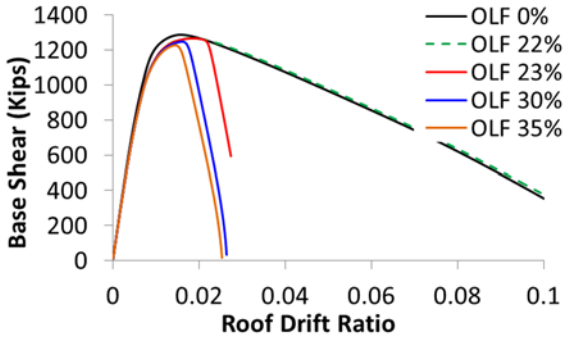

c) Bidirectional loading with 5% Eccentricity (With P-Theta)

Figure 3. Nonlinear static response curves for Model A-2

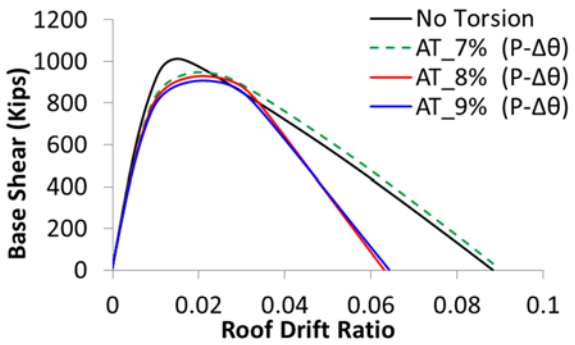

a) Unidirectional loading with Various Eccentricity (with P-Theta)

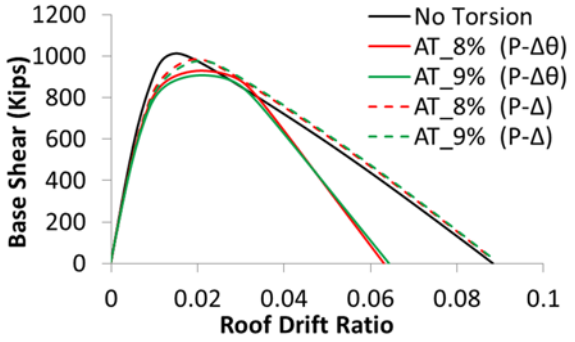

b) Unidirectional loading (with and without P-Theta)

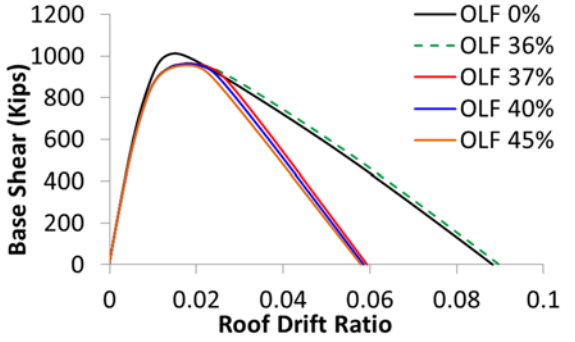

c) Bidirectional loading with 5% Eccentricity (With P-Theta)

Figure 4. Nonlinear static response curves for Model B

The results of Model B-2 are shown in Figure 5 where it can be seen when uniderctional loading is applied the bifurcation in the response curve still occured and the accidental eccentricity

causing bifurcation decreased from 8% to 7%. The bifurcation eccentricity decreased because collapse occurs when the orthogonal frame yields and this part of the building was not modified to satisfy drift requirements due to accidental torsion in the design stage. The importance of the P-Theta effects are displayed in Figure 5b where it can be seen that when they are not included the bifurcation in the pushover curve dissapears even for large accidental eccentricities. The vulnerability of the structure to bidirectional loading is shown in Figure 5c where for an accidental eccentricity of 5% an OLF of 23% is required to cause the bifurcation. On the basis of the pushover responses alone it seems that P-Theta effects are essential, and that evaluation of system behavior should include orthogonal loading effects. This is the case even for System B and B-2 for which is only moderately irregular (TIF=1.32 and 1.33 respectively).

Figure 6 illustrates the nonlinear static response curves for System C. For this torsionally regular system, N-S lateral loading at a 5% eccentricity has only a marginal influence on behavior when the system is loaded in one direction only (Figure 6a). There is a change in behavior when the OLF is 59%. However, the bifurcation for this system is not as distinctive, or did not occur at all, unlike the more torsional susceptible systems. Figure 6b shows the influence of including P-Theta effects, which is the same as already seen for the other systems, the sudden change in the pushover curves does not occur, even for large eccentricities. The results obtained for Model C-2 are virtually the same at observed for Model C and they are not shown in this section of the paper due to space constraints.

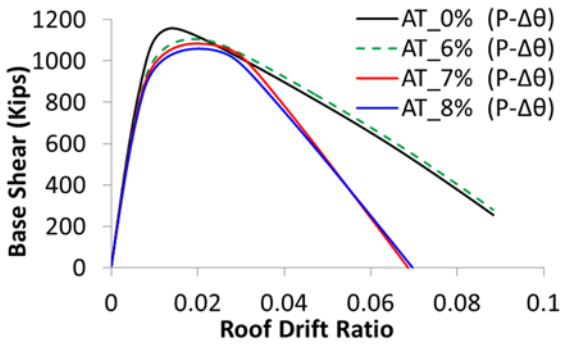

a) Unidirectional loading with Various Eccentricity (with P-Theta)

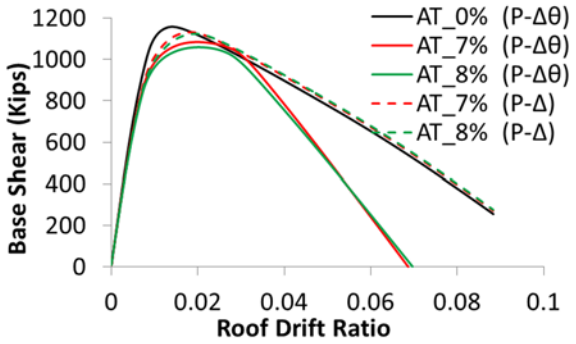

b) Unidirectional loading (with and without P-Theta)

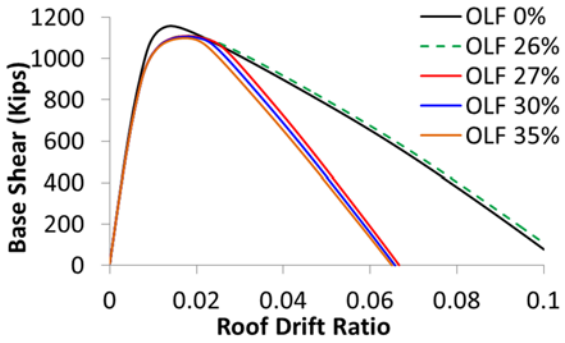

c) Bidirectional loading with 5% Eccentricity (With P-Theta)

Figure 5. Nonlinear static response curves for Model B-2

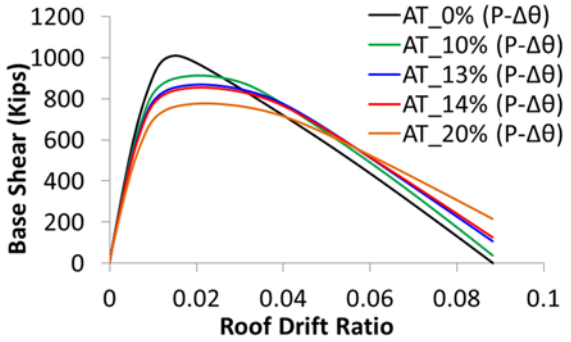

a) Unidirectional loading with Various Eccentricity (with P-Theta)

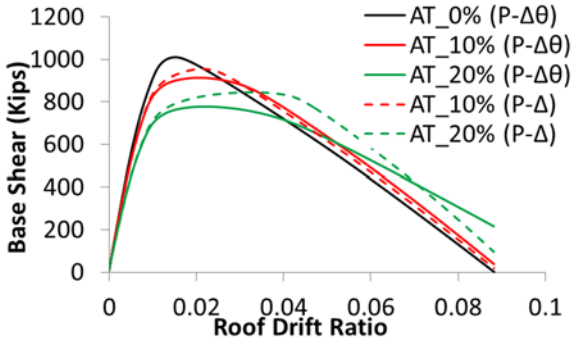

b) Unidirectional loading (with and without P-Theta)

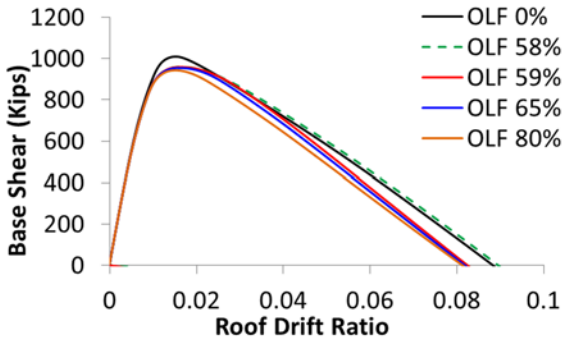

c) Bidirectional loading with 5% Eccentricity (With P-Theta)

Figure 6. Nonlinear static response curves for System C

Even though these buildings (Model C and C-2) did not show the bifurcation in the pushover curve, displacement and drift responses will be evaluated to quantify the importance of accidental

torsion in nonlinear dynamic analysis. The important findings related to nonlinear static analysis are that (1) including P-Theta effects is essential, (2) the response can change suddenly when accidental eccentricities are marginally increased, and (3) orthogonal loading has a strong influence on response. While it is not expected that a nonlinear static analysis will be used in lieu of NRHA to evaluate the system response, the findings above are important because nonlinear static analysis may be effective as a predictor to evaluate where accidental torsion should be considered. Clearly both P-Delta and P-Theta effects must be included in the analysis, and loading should be applied in a bidirectional manner. What is not known is the correct OLF to be used.

The bifurcation in the nonlinear static response is explained by use of Figure 7 which displays the sequence of yielding system A-2 with an eccentricity equal to 3% and 4%. The colored lines drawn next to the BRB frames on the right side of the figure are correlated directly to the points drawn in the response curves and they represent the different states of the structure. The number (N) placed next to the colored lines indicates the number of BRBs that are yielding at that specific point in the nonlinear static analysis.

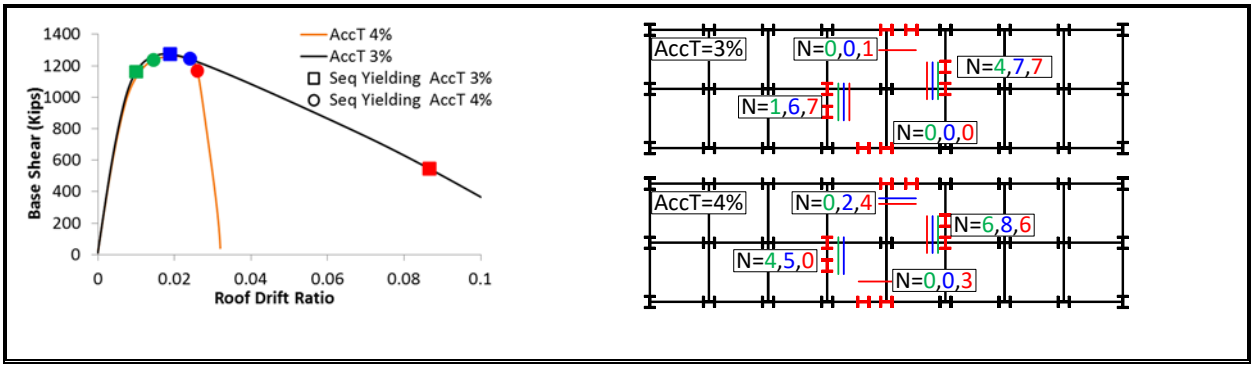

Figure 7. Sequence of yielding in nonlinear static analysis (Model A-2)

By comparing the state of the system at the red dot and square in Figure 7, the bifurcation occurrence is explained. It can be seen that for a 3% eccentricity just one of the orthogonal BRB frames is yielding while for 4% eccentricity both orthogonal BRB frames are yielding. Therefore,

the sudden degradation of the system capacity is due to yielding of the frames in the orthogonal direction. This outcome was also seen by de la Llera and Chopra (1996) in their investigation. It is important to note that the difference in the sequence of yielding between the models designed with (model A) and without accidental torsion (model A-2) was virtually the same.

4.7. Nonlinear Dynamic Analysis

Nonlinear Dynamic Response History analysis was carried out for each model using 11 ground acceleration recordings, representing actual earthquake events. These motions were selected from Table A-4A of FEMA P-695 far-field record set list. The selected records from the referenced table are the number: 1, 2, 3, 4, 7, 9, 11, 15, 17, 18, 21. Eleven records are used, as this is the minimum number required by Chapter 16 of ASCE7-16 when NRHA is to be performed. It is also noted that the global acceptance criteria from ASCE 7-16 limits the mean drift, recorded at the edge of the building, to 4% of the story height. Additionally, among the eleven motions, not more than one "unacceptable response" (interpreted herein as a collapse) is allowed. These requirements are applicable to Risk Category II buildings.

The horizontal component with the largest peak ground acceleration was selected for use for N-S direction shaking, and each component was amplitude scaled for consistency with the risk-based Maximum Considered Earthquake (MCE_R) level shaking at the lateral period of vibration in the N-S and E-W direction. For each analysis the system was first subjected to gravity load, followed by ground shaking. The roof drifts shown in the response history plots are the largest measured at the edge of the building for the ground motion analyzed. As with the nonlinear static analysis the parameters varied included the amount of accidental eccentricity, inclusion or non-inclusion of P-Theta effects, and presence of orthogonal load. Where the orthogonal component is not applied the loading is represented as "undirectional", and where the orthogonal loading is

applied it is at full value, and is “bidirectional”. Accidental torsion, where included, was generated by shifting the center of mass laterally (to the East) some percentage of the 240 ft. width of the building.

Figure 8a shows the response history of the roof drift ratio for System A under unidirectional shaking under the Duzce-Bolu ground motion including P-Theta effects. As may be observed, drifts at the edge of the roof were slightly increased when the accidental torsion eccentricity went from 0% to 5%. In Figure 8b the response under bidirectional loading is shown. It is important to emphasize again that for bidirectional loading, accidental eccentricity was included for loading only in the N-S direction, and that P-Theta effects are considered. The edge deflections increased to the point that the response is trending towards dynamic instability and this is occurring for eccentricities larger than 3%. Figure 8c shows the response history of roof drift of System A with 5% accidental eccentricity and full orthogonal loading but without P-Theta effects. The response for the system with no accidental eccentricity is shown for reference. As may be seen, the influence of P-Theta is dramatic. Clearly, analysis without P-Theta effects included may significantly underestimate response, and may indicate stable response where dynamic instability or collapses would occur if P-Theta is included.

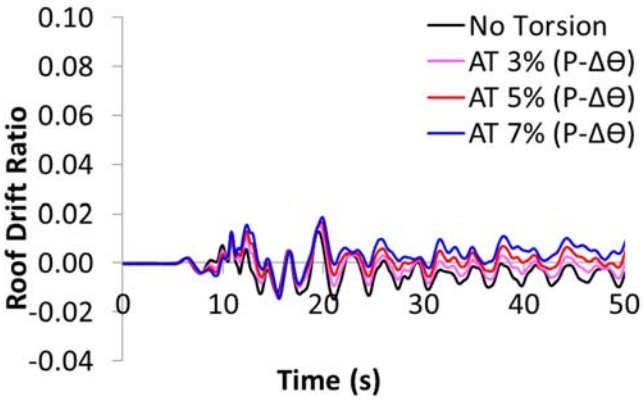

(a) Unidirectional loading (with P-Theta)

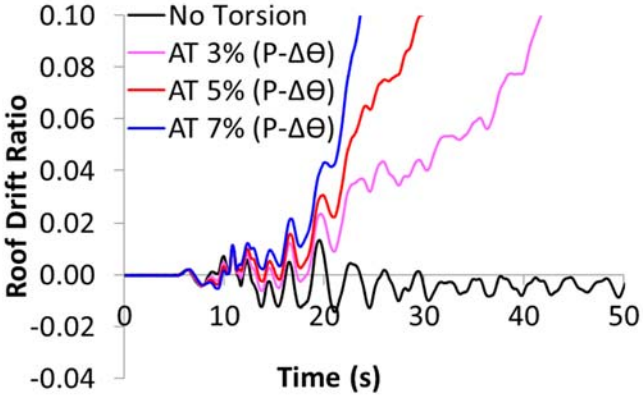

(b) Bidirectional loading (with P-Theta)

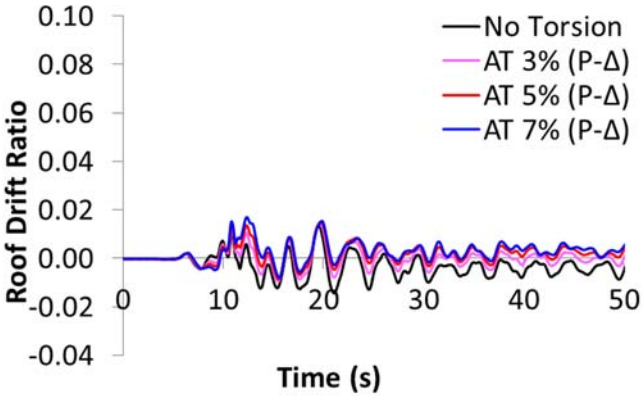

(c) Bidirectional loading (w/o P-Theta)

Figure 8. Response histories of roof drift for Model A (Duzce-Bolu)

Figure 9 displays the results for Model A-2. This case is presented to show that including the accidental torsion requirements during the design stage does not necessarily improve the system's performance. Figure 9a shows the response history of roof edge drift ratio under unidirectional ground motion including P-Theta effects. By comparing the responses between Model A (Figure 8) and A-2 (Figure 9) it can be seen that the latter has somewhat improved but not by a large margin. Figure 9b and Figure 9c display the results when the building was subjected to bidirectional loading with and without P-Theta effects respectively. It can be seen from Figure 9b that, when compared with that of model A, drift response improves for an accidental eccentricity equal to 3%, but dynamic instability still occurs for larger eccentricities. Figure 9c illustrates once more the importance of P-Theta effects where the response for all the analyzed eccentricities shows no dynamic instability whatsoever.

Figure 10 presents a comparison between Model A and Model A-2 and it is one of the cases where the performance of the building was improved by including accidental torsion requirements in the design stage. The ground motion analyzed in this case was Landers-Yermo. From Figure 10 (a) and (c) it can be seen that the improvement is significant in the unidirectional case. On the other hand when the system is subject to both ground motion components (Figure 10 (b) and (d)), Model A presents dynamic instability in all cases while for Model A-2 instability occurs when the accidental eccentricity is larger than 3%. Thus Model A-2 performed better than Model A if the structure is subjected to unidirectional ground motion or if there is no accidental eccentricity.

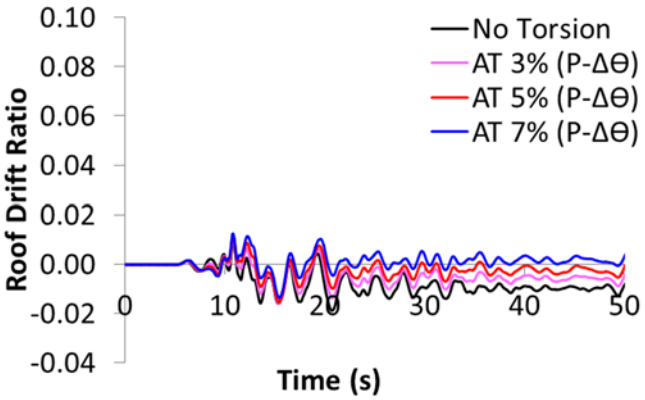

(a) Unidirectional loading (with P-Theta)

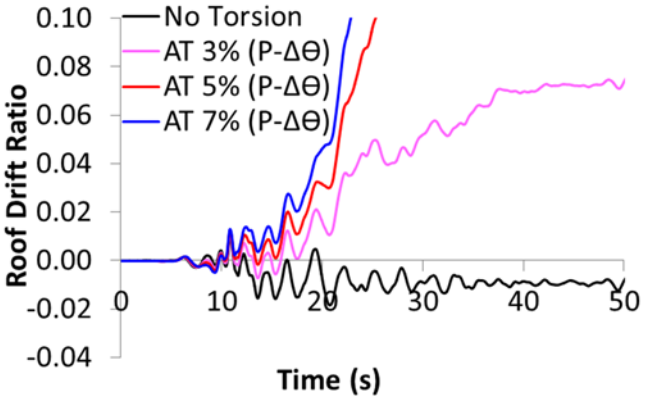

(b) Bidirectional loading (with P-Theta)

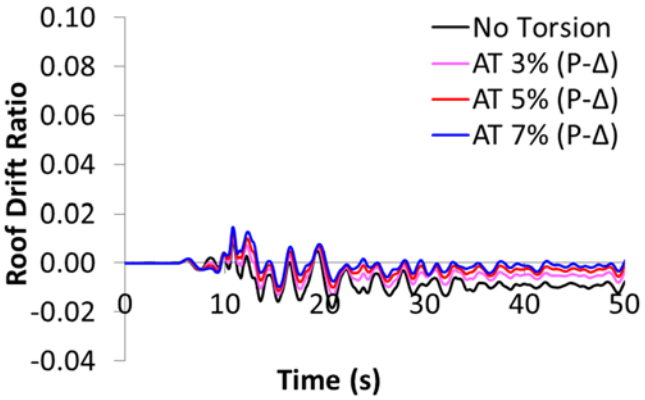

(c) Bidirectional loading (w/o P-Theta)

Figure 9. Response histories of roof drift for Model A-2 (Duzce-Bolu)

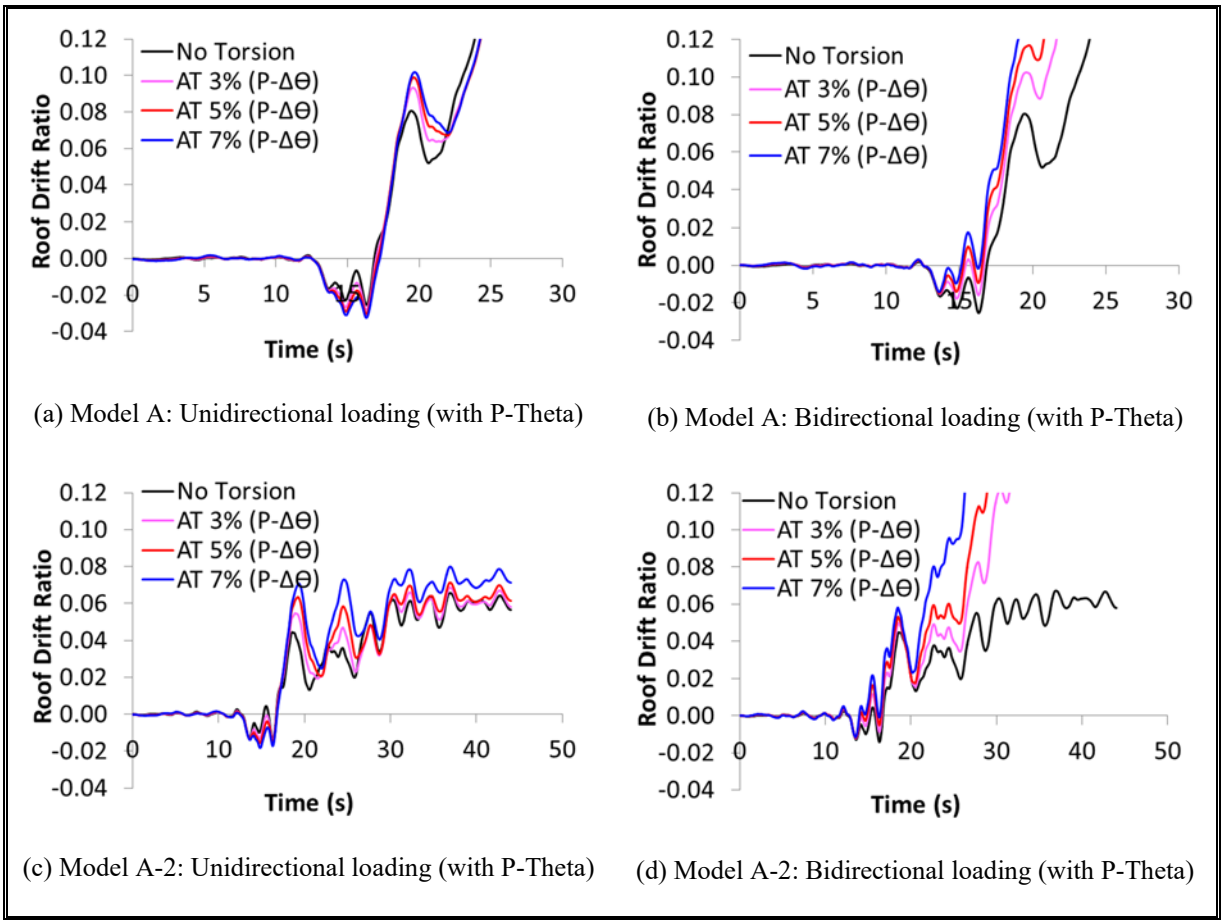

(a) Model A: Unidirectional loading (with P-Theta)

(b) Model A: Bidirectional loading (with P-Theta)

(c) Model A-2: Unidirectional loading (with P-Theta)

(d) Model A-2: Bidirectional loading (with P-Theta)

Figure 10. Response histories of roof drift Model A and Model A-2 (Landers-Yermo)

In this investigation the collapse of the system was considered when an inter-story drift of 10% was reached or when dynamic instability occurs. A summary of the number of collapses that occurred among the 11 analyzed earthquakes is shown in Table 5 for Models A and A-2. There are different conclusions that can be made by observing the information in the table. It can be seen the important influence that including accidental torsion in the design stage has when the structure is subjected to ground motions in one direction. However, the influence reduces considerably when the two components are used. The number of collapses for Model A-2 when it is subjected to bidirectional loading (P-Theta effects included) is larger or equal than 6 for an accidental eccentricity larger than 3%. It is also worthwhile to emphasize that there are no collapses when no accidental torsion is included. The most important information recovered from this table is the

influence of the P-Theta effects, where no collapses were recorded for Model A-2 when they were not included and 2 collapses occurred for Model A. Another important outcome is the influence of bidirectional loading in both models which increased the number of collapses considerably.

Table 5. Collapses Among 11 Ground Motions under Dynamic Loading:

Model A and Model A-2

	Model A				**Model A-2**			
Accidental Torsion	**0%**	**3%**	**5%**	**7%**	**0%**	**3%**	**5%**	**7%**
Unidirectional (P-Δθ)	2	2	2	2	0	0	0	0
Bidirectional (P-Δθ)	3	5	8	10	0	5	6	7
Bidirectional (P-Δ)	2	2	2	2	0	0	0	0

Response History traces for System B under the Kocaeli-Duzce earthquake are presented in Figure 11. In part (a) of the figure the response under unidirectional loading is shown with various mass eccentricities, and it is seen that the influence of accidental torsion can be significant for this torsionally irregular building. When bidirectional loading is applied the increase in the response initiates collapse for some of the eccentricities (Figure 11b). An interesting result to point out from Figure 11c is that for this ground motion P-Theta effects, while significant, are not quite as detrimental as they were for the previous cases.

The results for the case where accidental torsion requirements were considered in the design are presented in Figure 12. Model B-2 presents a considerable improvement for the cases where the system was subjected to unidirectional and bidirectional ground motions (Figure 12a and Figure 12b respectively). The P-Theta effects for this ground motion did not initiate collapse but did have a strong influence on computed drift (Figure 12c).

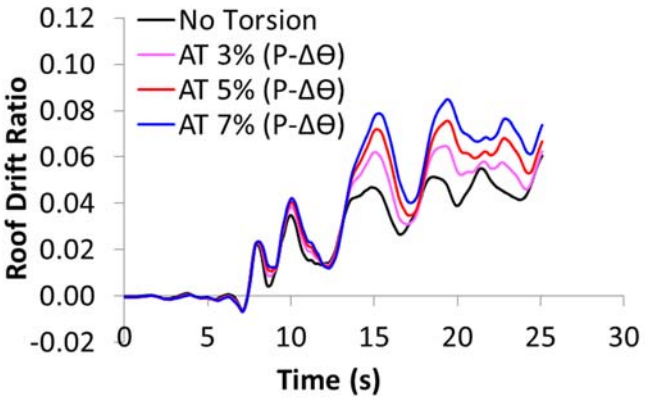

(a) Unidirectional loading (with P-Theta)

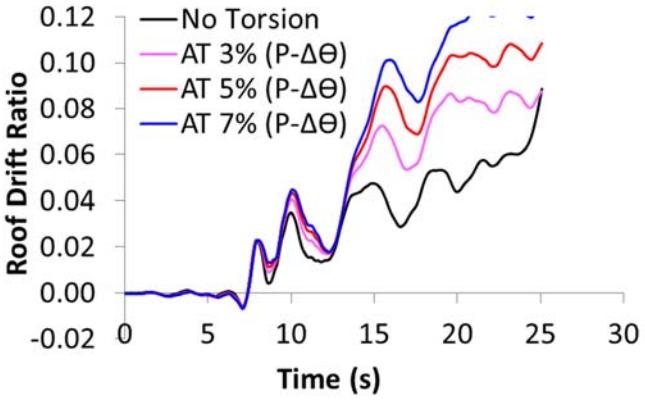

(b) Bidirectional loading (with P-Theta)

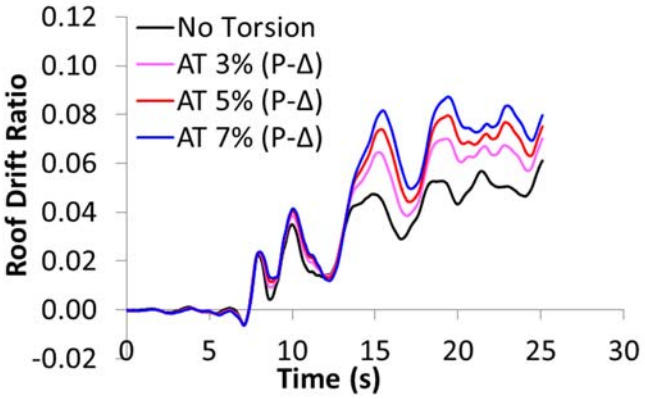

(c) Bidirectional loading (w/o P-Theta)

Figure 11. Response histories of roof drift for Model B (Kocaeli-Duzce)

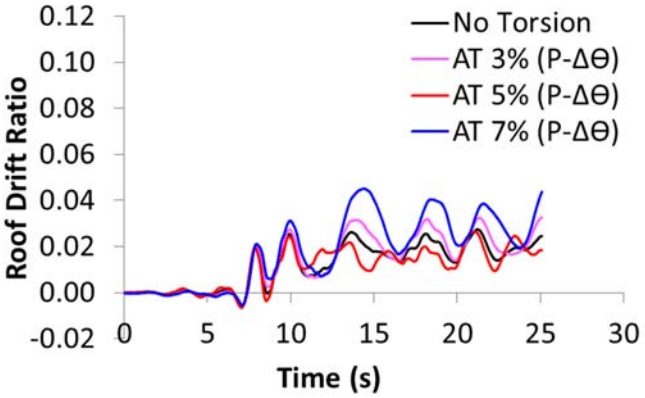

(a) Unidirectional loading (with P-Theta)

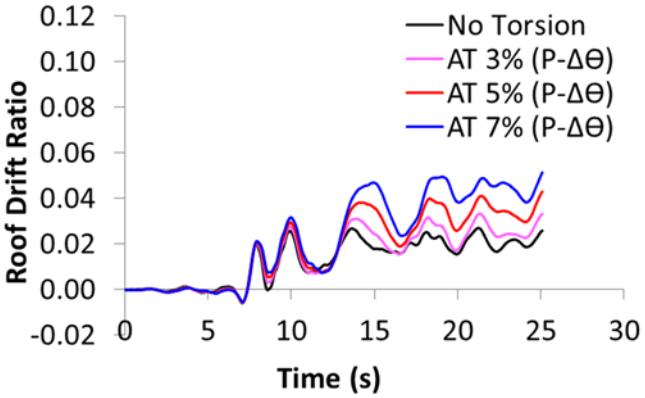

(b) Bidirectional loading (with P-Theta)

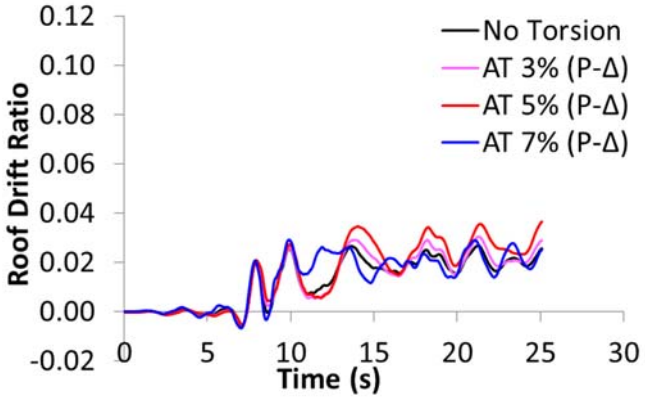

(c) Bidirectional loading (w/o P-Theta)

Figure 12. Response histories of roof drift for Model B-2 (Kocaeli-Duzce)

Even though including accidental torsion in the design of Model B-2 improved the performance of the original structure for some of the ground motions, it is not necessarily a trend seen in all the results. Table 6 shows a summary of the collapses occurred to Models B and B-2 under the different analyzed cases. Model B-2 improves the performance mostly when the structure is subjected to unidirectional loading and when no accidental torsion is considered. However, this improvement is not seen when both of the ground motion components are applied simultaneously and an accidental eccentricity is included because the number of collapses is similar in both models. By looking at the collapses when P-Theta effects are not included it can be said that Model B-2 improves the performance, but as it has been mentioned analyses without accidental torsion would be incorrect.

Table 6. Collapses among 11 Ground Motions under Dynamic Loading: Model B and Model B-2

	Model B				**Model B-2**			
Accidental Torsion	**0%**	**3%**	**5%**	**7%**	**0%**	**3%**	**5%**	**7%**
Unidirectional (P-Δθ)	2	3	3	3	1	1	1	1
Bidirectional (P-Δθ)	5	3	3	3	2	3	3	3
Bidirectional (P-Δ)	4	3	3	3	1	1	1	1

Based only on the number of collapses, it can be seen that accidental eccentricity when included in the analysis does not have as significant an influence on a torsional irregular building in comparison with the buildings with an extreme torsion irregularity. However, as it will be shown in the following case, drifts at the building edge can increase significantly when accidental torsion is included. Figure 13 presents the results for model B under the Cape Mendocino-Rio earthquake applied in both directions. Figure 13a illustrates the roof drift ratio time history where it can be seen that the maximum value without eccentricity is around 1.5% but it increases considerably

when accidental torsion is considered (up to 3%). Figure 13b and Figure 13c display the maximum story drift and the increments in the story drift in percentage, respectively. The latter is the increment in response with respect to the case with no accidental torsion in the analysis. Figure 13c shows that the maximum increment can be as high as 60 % and 40% for an accidental eccentricity equal to 5% and 3% respectively. Thus, despite the fact that accidental torsion might not cause as many collapses as it was seen for the building with an extreme torsional irregularity, it can increase the responses significantly.

In order to compare the performance of Model B when accidental torsion is considered in the design, Figure 14 presents the results under the Cape Mendocino-Rio earthquake for Model B-2. Figure 14a, b and c display a clear reduction in the response in comparison to Model B. However, the inter-story drift increment reaches a value of 25% and 40% for eccentricities of 5% and 7% respectively.

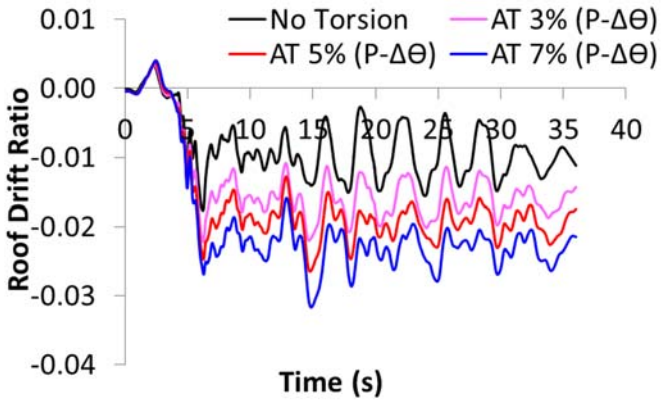

(a) Bidirectional loading (with P-Theta)

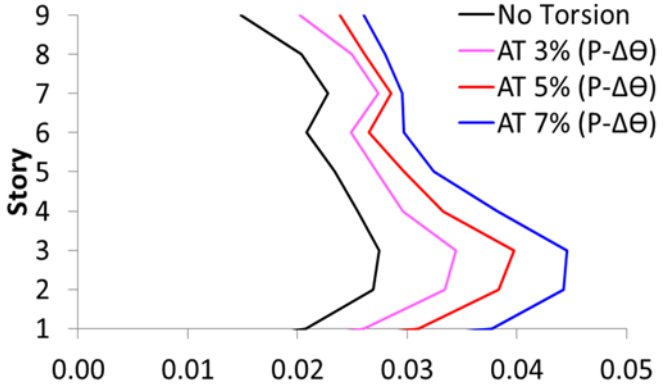

(b) Maximum Story Drifts

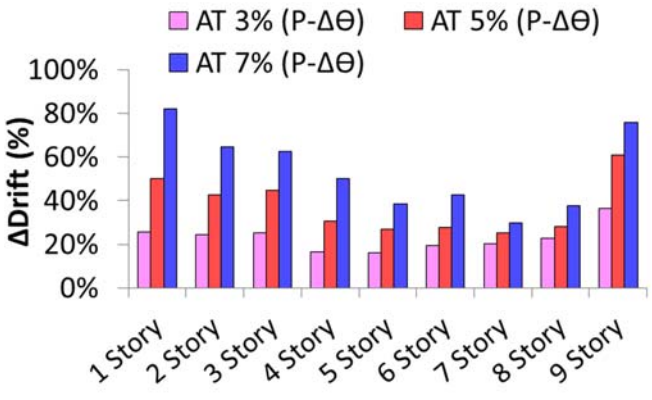

(c) Story Drift Increment Percentage

Figure 13. Response histories of roof drift for Model B (Cape Mendocino-Rio)

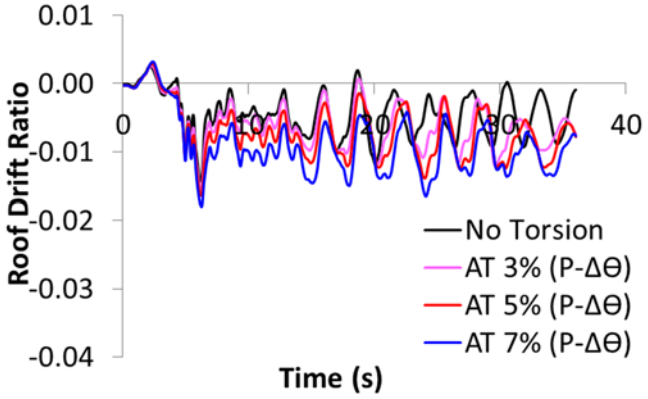

(a) Bidirectional loading (with P-Theta)

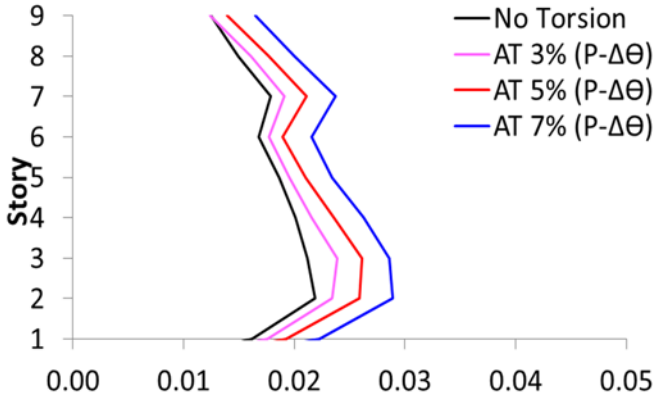

(b) Maximum Story Drifts

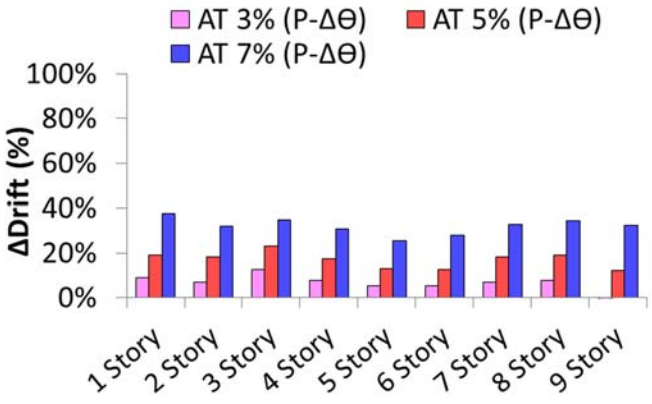

(c) Story Drift Increment Percentage

Figure 14. Response histories of roof drift for Model B-2 (Cape Mendocino-Rio)

According to ASCE 7-16, during the design stage (Chapter 12), buildings with no torsional irregularity do not have to fulfill accidental torsion requirements meaning mainly that inter-story drifts have to be checked just at the center of mass of the building. In this investigation, a Model C-2 was created where inter-story drifts were checked at edges of the building (results for Model C and Model C-2 were close to each other, and that is why Figure 15 shows the story drifts only for Model C.) The case shown in Figure 15a, b and c is Model C subjected to San Fernando-LA. Since it was already demonstrated the importance of subjecting the building to both components of ground motions and including P-Theta effects, the following results consider bidirectional loading and include P-Theta effects. Story drifts are shown in Figure 15. These drifts are less than the 4% limit given by Chapter 16 of ASCE7-16 when no accidental torsion is included, but they increased up to 60% for an accidental torsion of 5%. This is an important observation because it is commonly believed that buildings with no torsional irregularities should not be analyzed considering accidental torsion.

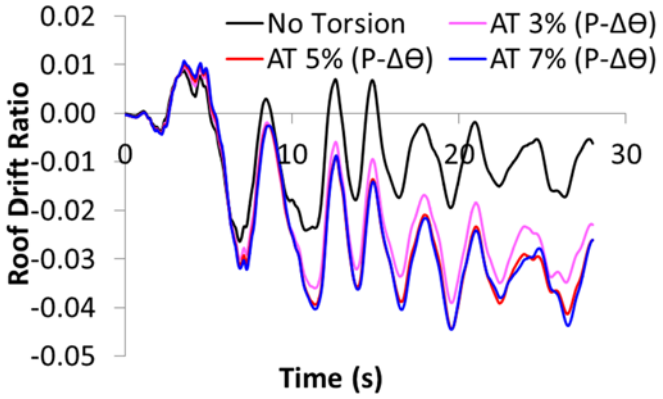

(a) Bidirectional loading (with P-Theta)

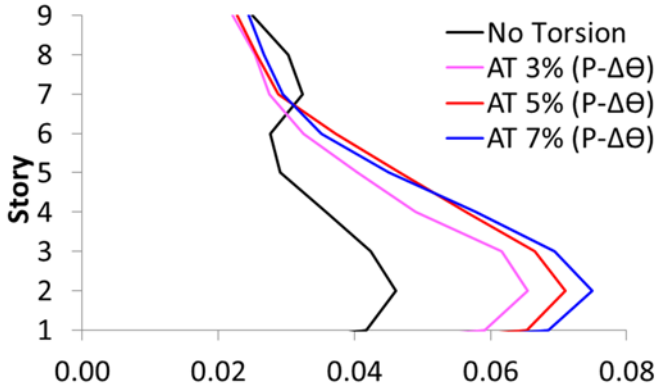

(b) Maximum Story Drifts

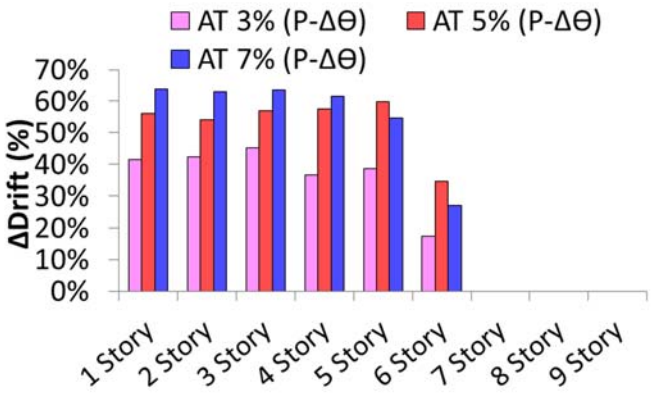

(c) Story Drift Increment Percentage

Figure 15. Response Histories and Inter-Story Drifts Model C (San Fernando-LA)

In spite of the fact that large story drift increments is the most important outcome of analyzing a regular building including accidental torsion, Table 7 summarizes the number of collapses that occurred in Model C and Model C-2 under bidirectional loading including P-Theta effects. For both models C and C2 the number of collapses is excessive (greater than the single unacceptable response allowed by ASCE 7-16). There is a significant reduction in the number of collapses where the design includes accidental torsion.

Table 7. Collapses Among 11 Ground Motions under Dynamic Loading:

Model C and Model C-2

	Model C				**Model C-2**			
Accidental Torsion	**0%**	**3%**	**5%**	**7%**	**0%**	**3%**	**5%**	**7%**
Bidirectional (P-Δθ)	2	4	3	4	2	2	3	3

From the results shown in this section, the importance of including both components of ground motion and to include P-theta effects is clear. In fact, all the collapses occurred because of yielding in the orthogonal frames. A sequence of yielding analysis was performed to corroborate this statement.

4.8. Influence of Gravity Columns on Modeling P-Theta Effects

Recent investigations carried out by DeBock et al. (2014) used the FEMA P-695 Methodology to investigate the influence that accidental torsion has on the collapse performance of buildings. The principal recommendation of the study was that accidental torsion need not be included in the design of buildings that are classified as torsionally regular, and need be included only in the higher seismic design categories if the structure is torsionally irregular. The study was the basis for relaxing the accidental torsion requirements in Chapter 12 of ASCE 7-16.

P-Theta effects were included in the DeBock study. However, instead of modeling the gravity columns explicitly, four leaning columns were used, with the leaning columns located at the center of each quadrant of the building. In order to evaluate the influence of using four leaning columns in lieu of modeling the columns explicitly, Model A-2 was re-analyzed with four leaning columns, as shown in Figure 16 a. The results from this model were compared to those obtained with the gravity columns modeled explicitly.

Figure 16b displays the nonlinear static response curves obtained using four leaning columns to incorporate P-Delta and P-Theta effects. Figure 16c shows the Model A-2 response curves with the columns modeled explicitly. From these figures it was found that the bifurcation point changed from an accidental torsion of 8% when four leaning columns were used, to 4% when the all columns were modeled explicitly. Moreover, the slope of the pushover curve, once the bifurcation occurred, is much steeper when the P-Theta effects are included using all the gravity columns. The secondary slope of the pushover curve has a great influence or is an indicator of the expected collapse performance of the building (Flores et al. 2016). From these results it appears that four leaning columns do not capture the P-Theta effects entirely. Therefore the approach recommended by Habibullah and Wilson (1987), where leaning columns are placed at the floor plate's radius of gyration is also studied for the nonlinear dynamic analysis. For this method only two leaning columns are placed to capture P-Delta and P-Theta effects. The location of these leaning columns is shown in Figure 16a and it was computed as follows:

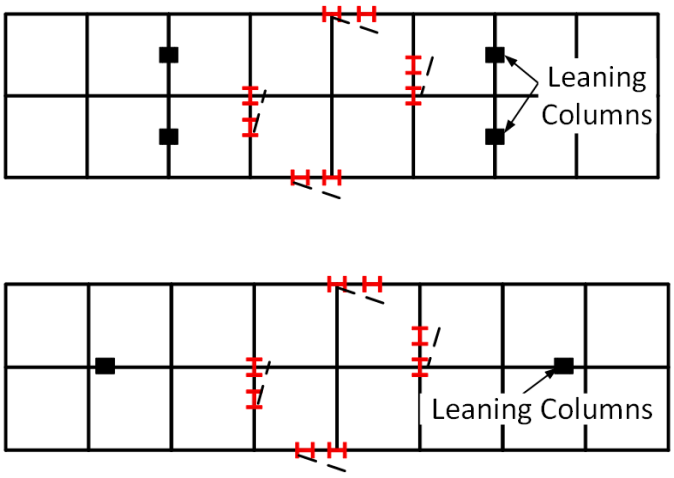

a) Model A-2 with 4 and 2 Leaning Columns

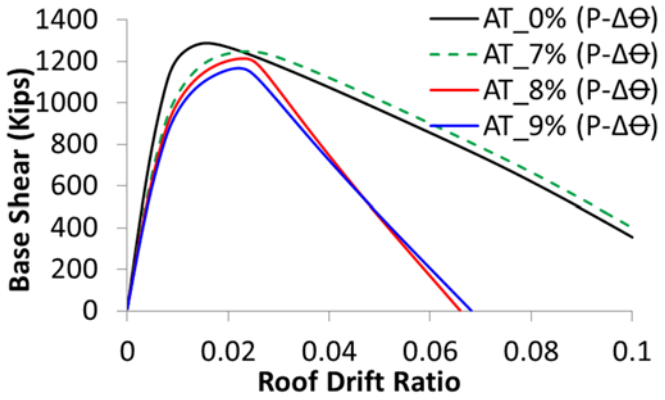

b) Unidirectional loading (Model A-2 with 4 Leaning Columns)

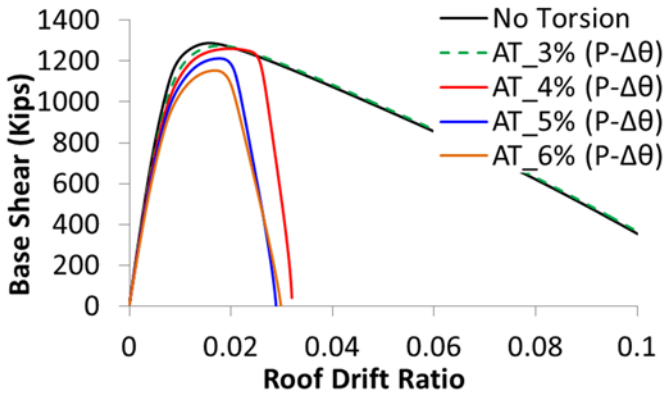

c) Unidirectional loading (Model A-2)

Figure 16. Influence of P-Theta effects on nonlinear static response

$$R_{LC} = \sqrt{\frac{\sum_{i=1}^{ncols} P_j r_j^2}{2P_{LC}}} \quad (5)$$

where P_j is the axial force in each column, r_j is the radial distance from the center of mass and P_{LC} is the half of the total gravity load.

Figure 17 presents roof drift histories for two out of the eleven ground motions considered. For each ground motion the results obtained using four leaning columns are shown on the left (Figure 17a, d), the results with columns modeled explicitly are shown in the middle (Figure 17b, e) and the results using two leaning columns at the radius of gyration are shown on the right (Figure 17c, f). As may be observed, the difference in results is striking but the two leaning columns model was able to represent correctly the P-Delta and P-Theta effects.

The influence of P-Theta modeling on predicting collapse is summarized in Table 8. It can be seen, for example, that for a 5% accidental eccentricity the number of collapses among 11 ground motions is 2 when four leaning columns are used, but this increases to 7 when the columns are modeled explicitly. It is interesting to note that the model with two leaning columns had virtually the same number of collapses than the model that has the gravity columns modeled explicitly with one exception when accidental torsion was not included.

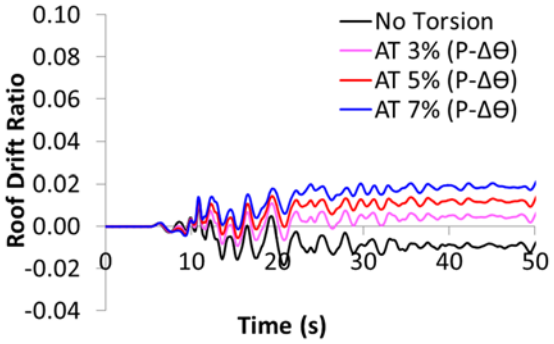

(a) Model A-2 with four leaning columns

(Duzce-Bolu)

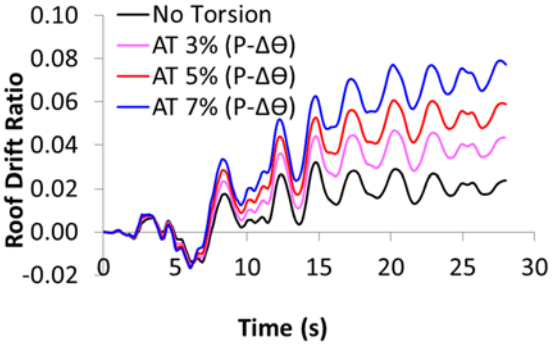

(d) Model A-2 with four leaning columns

(San Fernando-LA)

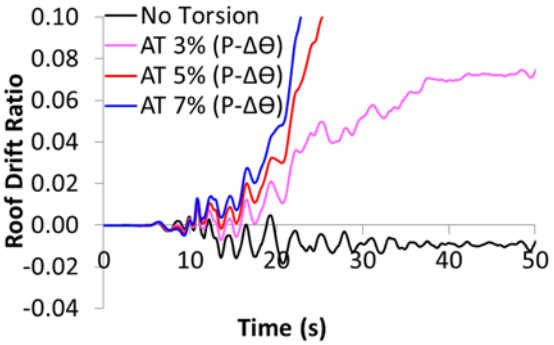

(b) Model A-2

(Duzce-Bolu)

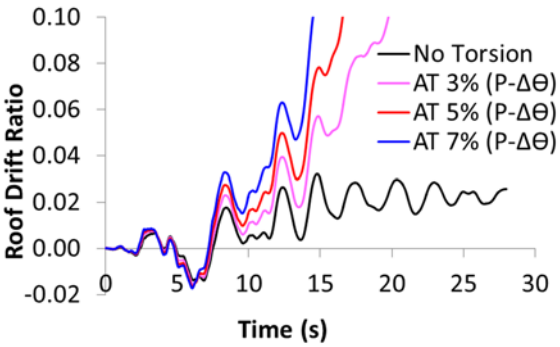

(e) Model A-2

(San Fernando-LA)

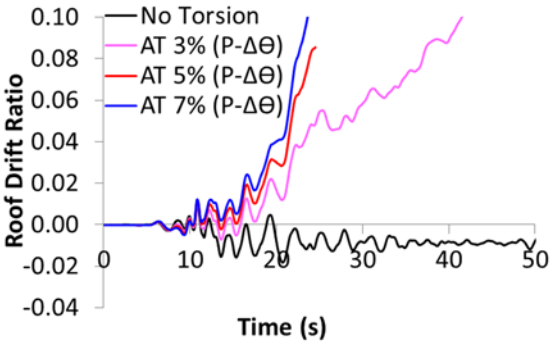

(c) Model A-2 with two leaning columns

(Duzce-Bolu)

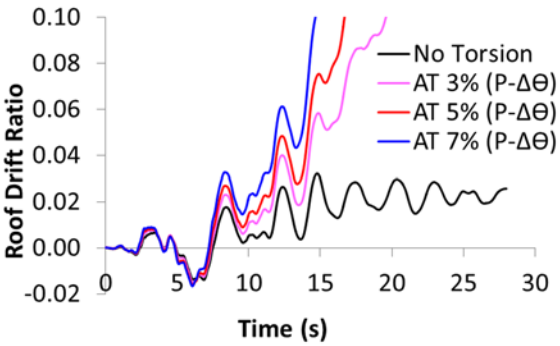

(f) Model A-2 with two leaning columns

(San Fernando-LA)

Figure 17. Nonlinear Dynamic Analyses Comparison

Based on the results presented, it is clear that for the extremely irregular system A-2 that the results are extremely sensitive to the approach used to model geometric nonlinearity. It is believed that the issue with the use of four leaning columns is the location of the columns as it is expected that the gravity load on the columns was appropriately modeled. Torsional resistance, whether based on elastic stiffness or geometric stiffness, is related to the square of the distance of a column from the center of rotation, and thus placing the leaning columns at the center of the quadrants significantly underestimated the P-Theta effect. On the other hand, using two leaning columns placed at the radius of gyration represented P-Delta and P-Theta effects adequately, although there were some differences relative to case where all of the gravity columns were modeled. This difference is likely due to the fact that the geometric stiffness remains constant when two leaning columns are used, but varies spatially when the columns are modeled explicitly.

Table 8. Collapses under Dynamic Loading Comparison

Bidirectional (P-Δθ)	**Accidental Torsion**			
	0%	**3%**	**5%**	**7%**
Model A-2 (with 4 leaning columns)	1	2	2	2
Model A-2 (gravity columns modeled)	1	6	7	8
Model A-2 (with 2 leaning columns)	2	7	7	8

4.9. Summary, Conclusions and Recommendations

It is clear from the analyses reported in this paper that accidental torsion has an important influence on the computed seismic response of structures predicted by nonlinear static analysis and nonlinear dynamic analysis. Additionally, the detrimental effect of accidental torsion is severely impacted by bidirectional loading, and by the P-Theta effect. The influence of accidental torsion increases with the degree of initial torsional irregularity. However, it is important to note

that even moderately irregular systems, such as System B with a TIF of approximately 1.3, were severely impacted by accidental torsion in both nonlinear static and nonlinear dynamic analysis. In the case of regular systems such as System C, collapse performance might not be as affected by accidental torsion, but inter-story drifts at the building's corners might increase up to 60% with accidental torsion.

Based on these results it appears that the exclusion of accidental torsion induced by mass eccentricities as low as 3% of the building width is possibly unconservative for building systems with TIFs lower than about 1.2, is likely unconservative for buildings with TIFs greater than about 1.2, and can be regarded as potentially unsafe for systems with TIFs greater than about 1.4. These observations are based on NRHA with bidirectional loading, and with both P-Delta and P-Theta effects included. Analysis under unidirectional loading often failed to capture potential dynamic instability, even when P-Theta effects were included. Additionally it was found that for all cases, dynamic instability was not captured if P-Theta effects were excluded.

The improvement in performance when he structure was designed including accidental torsion was also investigated. It was found that the models with higher strengths due to accidental torsion requirements in the design stage did not perform as well as expected despite the fact that the performance improved with respect to that of the models without accidental torsion. It is believed the provisions given in ASCE 7 should be more precise about how to increase the strength of the building to fulfill drift and strength requirements when accidental torsion is included. Models with accidental torsion had larger sections in the N-S direction than the models that did not consider accidental torsion in the design. This is why the building response improved when the ground motion was applied in just one direction and when no accidental torsion was included in the analysis. However collapses occurred from a combination of yielding in the lateral resisting

systems in the N-S and the E-W direction. As it was seen from the nonlinear static analysis response, bifurcation occurred when the orthogonal frame started to yield, and this situation caused collapse when nonlinear dynamic analyses were performed. Therefore it could be recommended that if a building has a torsional irregularity in one direction, members of the lateral resisting frame in the orthogonal direction should be increased in size in some percentage of the size increase of the members in the direction with the irregularity.

Among all the guidelines and standards of prestandards cited at the beginning of this paper, some require and mention accidental torsion. However, none of these documents explicitly mentions the importance of including P-Theta effects in nonlinear static or dynamic analysis, nor is the deficiency of using a "leaner column" discussed. This is a serious omission in the reference literature, and must be addressed. Additional analysis is required before detailed recommendations can be made for updated guidelines and code language. However, it appears clear from the analysis reported herein that: (1) NRHA must be carried out in three dimensions under full bidirectional loading, (2) accidental torsion must be included for all systems, (3) both P-Delta and P-Theta effects must be included entirely by modeling all the gravity columns as leaning columns or if the structure is geometrically regular by placing the leaning columns at the radius of gyration

It is possible that exceptions to the requirement of including accidental torsion can be developed, based on three-dimensional nonlinear static analysis with bidirectional loading (including partial loading in the direction orthogonal to the direction of principal loading) and of course, with P-Theta effects included. Moreover, it seems from the literature review described at the beginning of this investigation, that 5% accidental torsion might be excessive, particularly for taller buildings, and that a height-dependent accidental torsion requirement might be appropriate.

4.10. Acknowledgements

The work presented herein was possible through the support of the Pontificia Universidad Catolica de Chile and the National Research Center for Integrated Natural Disaster Management CONICYT/FONDAP/15110017 (Chile). The support also provided by the University of Cuenca is gratefully acknowledged.

4.11. References

[1] NIST, Nonlinear Structural Analysis for Seismic Design (NIST GCR 10-917-5), National Institute of Standards and Technology, Gaithersburg, MD, 2010.

[2] NIST, Applicability of Nonlinear Multiple-Degree-of-Freedom Modeling for Design (NIST GCR 10-917-9), National Institute of Science and Technology, Gaithersburg, MD, 2010.

[3] PEER, Guidelines for Performance Based Design of Tall Buildings, Pacific Earthquake Engineering Research Center, University of California, Berkeley, CA, 2010.

[4] PEER, Modeling and Acceptance Criteria for Seismic Design and Analysis of Tall Buildings (PEER/ATC 72-1). Pacific Earthquake Engineering Research Center, Richmond, CA, 2010.

[5] NIST, Selecting and Scaling Earthquake Ground Motions for Performing Response-History Analysis (NIST GCR 11-917-5), National Institute of Science and Technology, Gaithersburg, MD, 2011.

[6] FEMA, 2015 NEHRP Recommended Provisions for New Buildings and Other Structures (FEMA P-1050), Federal Emergency Management Agency, Washington, D.C, 2015.

[7] ASCE, ASCE 7-10: Minimum Design Loads for Buildings and Other Structures, American Society of Civil Engineers, American Society of Civil Engineers/Structural Engineering Institute, Reston, VA, 2011.

[8] ASCE, Seismic Rehabilitation of Existing Buildings (ASCE/SEI 41-13), American Society of Civil Engineers Reston, Virginia, 2013.

[9] SFBC, Requirements and Guidelines for the Seismic Design of New Tall Buildings Using Non-Prescriptive Design Procedures, 2013 San Francisco Building Code Administrative Bulletin 083, San Francisco, CA, 2013.

[10] LATBSDC, An Alternative Procedure for Seismic Analysis and Design of Tall Buildings Located in The Los Angeles Region, Los Angeles Tall Building Structural Design Council, Los Angeles, CA, 2014.

[11] ASCE, ASCE 7-16: Minimum Design Loads for Buildings and Other Structures, American Society of Civil Engineers, American Society of Civil Engineers/Structural Engineering Institute, Reston, VA, 2017.

[12] N.M. Newmark, Torsion in symmetrical buildings, PROCEEDING OF WORLD CONFERENCE ON EARTHQUAKE ENGINEERING, 1969.

[13] J.C. De la Llera, A.K. Chopra, Accidental torsion in buildings due to stiffness uncertainty, Earthquake engineering & structural dynamics 23(2) (1994) 117-136.

[14] J.C. De la Llera, A.K. Chopra, Accidental torsion in buildings due to base rotational excitation, Earthquake engineering & structural dynamics 23(9) (1994) 1003-1021.

[15] M.R. Ghayamghamian, G.R. Nouri, H. Igel, T. Tobita, The effect of torsional ground motion on structural response: code recommendation for accidental eccentricity, Bulletin of the Seismological Society of America 99(2B) (2009) 1261-1270.

[16] K.G. Stathopoulos, S.A. Anagnostopoulos, Accidental design eccentricity: Is it important for the inelastic response of buildings to strong earthquakes?, Soil Dynamics and Earthquake Engineering 30(9) (2010) 782-797.

[17] D. Basu, S. Giri, Accidental eccentricity in multistory buildings due to torsional ground motion, Bulletin of Earthquake Engineering 13(12) (2015) 3779-3808.

[18] O. Pekau, R. Guimond, Accidental torsion in yielding symmetric structures, Engineering Structures 12(2) (1990) 98-105.

[19] D. Basu, M.C. Constantinou, A.S. Whittaker, An equivalent accidental eccentricity to account for the effects of torsional ground motion on structures, Engineering Structures 69 (2014) 1-11.

[20] M. Ghayamghamian, G. Nouri, On the characteristics of ground motion rotational components using Chiba dense array data, Earthquake engineering & structural dynamics 36(10) (2007) 1407-1429.

[21] D. Basu, A.S. Whittaker, M.C. Constantinou, Characterizing the rotational components of earthquake ground motion, 2012.

[22] D.J. DeBock, A.B. Liel, C.B. Haselton, J.D. Hooper, R.A. Henige, Importance of seismic design accidental torsion requirements for building collapse capacity, Earthquake Engineering & Structural Dynamics 43(6) (2014) 831-850.

[23] FEMA, Quantification of Building Seismic Performance Factors (FEMA P-695), Federal Emergency Management Agency, Washington, D.C, 2009.

[24] F.X. Flores, F.A. Charney, D. Lopez-Garcia, The influence of accidental torsion on the inelastic dynamic response of buildings during earthquakes, XI Congreso Chileno de Sismología e Ingeniería Sísmica, Santiago, Chile, 2015.

[25] ASCE, Seismic Rehabilitation of Existing Buildings (ASCE/SEI 41-06), American Society of Civil Engineers Reston, Virginia, 2006.

[26] M. Mansuri, Torsional effects on the inelastic seismic response of structures, University of Southern California, 2009.

[27] J.A. Jarrett, R.B. Zimmerman, F.A. Charney, A. Jalalian, Response-History Analysis for the Design of New Buildings in the NEHRP Provisions and ASCE/SEI 7 Standard: Part IV-A Study of Assumptions, Earthquake Spectra (2015).

[28] E. Wilson, A. Habibullah, Static and dynamic analysis of multi-story buildings, including P-delta effects, Earthquake Spectra 3(2) (1987) 289-298.

[29] NIST, Evaluation of the FEMA P-695 Methodology for Quantification of Building Seismic Performance Factors (NIST GCR 10-917-8), National Institute of Standards and Technology, Gaithersburg, MD, 2010.

[30] O. Atlayan, F.A. Charney, Hybrid buckling-restrained braced frames, Journal of Constructional Steel Research 96 (2014) 95-105.

[31] AISC, Specification for Structural Steel Buildings, AISC/ANSI 360-05, American Institute of Steel Construction, Chicago, Illinois, 2011.

[32] F. McKenna, G. Fenves, M. Scott, OpenSees: Open system for earthquake engineering simulation, Pacific Earthquake Engineering Center, University of California, Berkeley, CA., http://opensees. berkeley. edu (2006).

APPENDIX A

ACCELERATION DEMANDS ON NONSTRUCTURAL COMPONENTS IN STEEL SPECIAL MOMENT FRAMES

Presented at the XI Congreso Chileno de Sismología e Ingeniería Sísmica ACHISINA 2015 (Santiago, Chile, March 18-20, 2015)

ACCELERATION DEMANDS ON NONSTRUCTURAL COMPONENTS IN STEEL SPECIAL MOMENT FRAMES

F. Flores[1], D. Lopez-Garcia [2], F. Charney [3]

[1] *Ph.D. Candidate, Department of Civil and Environmental Engineering, Virginia Tech, and Department of Structural and Geotechnical Engineering, Pontificia Universidad Catolica de Chile, ffloress@vt.edu*
[2] *Associate Professor, Department of Structural and Geotechnical Engineering, Pontificia Universidad Catolica de Chile, and National Research Center for Integrated Natural Disaster Management CONICYT/FONDAP/15110017, dlg@ing.puc.cl*
[3] *Professor, Department of Civil and Environmental Engineering, Virginia Tech, fcharney@vt.edu*

Abstract

The objective of this study is to analyze in detail floor accelerations in Special Moment Frame (SMF) buildings. For this purpose, floor accelerations in low- and mid-rise SMF building models at which "rigid" and "flexible" nonstructural components are attached are computed in three different manners: using the design provisions of the current US seismic code (ASCE 7-10), performing linear time history analysis, and performing nonlinear time history analysis. The models of the lateral load resisting frames comply with the FEMA P-695 methodology requirements to evaluate the probability of collapse. The gravity frames were also modeled, and several strength levels of their beam-column connections were considered. It was found that the most important modeling feature is the inelastic behavior of the lateral load resisting frames. Elastic assessments of floor accelerations are conservative in most cases, with the only exception of spectral ordinates of floor spectra at periods equal to higher modal periods of the buildings. It was also found that the gravity frames are relevant only if the strength of their beam-column connections is non-negligible. Finally, the acceleration demands on nonstructural components might be quite high, much larger than 1.0 g in some cases, which means that protective measures might be necessary in sensitive or hazardous components.

Keywords: nonstructural components, floor accelerations, floor spectra, peak floor accelerations

1 Introduction

Recent events such as the 1994 Northridge (USA), 1995 Kobe (Japan) and 2010 El Maule (Chile) earthquakes have shown that the majority of buildings performed as expected against collapse. However, there were cases where the building structure did not suffer any structural damage but the nonstructural damage inside the building made it impossible to occupy the facility after the event [1, 2]. In hospitals this represents a major risk against life; moreover the direct and indirect economic losses can be greater than the cost of the structure [3].

Nonstructural Components (NSCs) in buildings are divided into two main categories: those that are sensitive to story drifts and those that are sensitive to accelerations [4]. Acceleration sensitive NSCs, the topic of this investigation, include parapets, suspended ceilings, ducts, boilers, chiller tanks, etc. [5] and they can be also classified as “rigid” or “flexible” depending on their natural period of vibration. The acceleration-sensitive NSCs receive the forces that arise from the motion of the structure to which they are anchored or attached, from now on denoted as the “supporting structure”. The methods usually used to estimate the accelerations that affect rigid and flexible NSCs are the Peak Floor Acceleration (PFA) method and the Floor Response Spectrum (FRS) method respectively. The PFA method quantifies the maximum total acceleration at each floor during an earthquake, and the FRS approach computes the elastic response spectrum of a selected floor using as input the total acceleration response of the same floor. The FRS method can be applied when the interaction between the NSC and the supporting structure is not significant, i.e., when the response of the structure is essentially the same regardless of whether the NSC is present or not. In general, the interaction between the NSC and the supporting structure is not significant when the mass of the NSC is less than approximately 1.0 percent the mass of the supporting structure [6]. If the NSC mass is larger, dynamic interaction will occur between NSCs and the supporting structure, and the FRS method might in some cases produce overly conservative results [7].

Research has been performed to understand the acceleration demands on NSCs. Most of the investigations were executed considering the supporting structure to behave elastically [3, 8, 9]. However, several authors have studied the effect of the building inelastic behavior on the accelerations that are imposed on NSCs. The general trend is that inelastic deformations in the supporting structure reduce the acceleration demands with respect to the demands based on the elastic response of the supporting structure. However, in some cases, particularly for short-period NSCs (say, NSC period less than 0.5 sec), demands based on inelastic structural response might actually be greater. Some of these studies were performed using simple SDOF structures [4, 10], and others studied the effect of plasticity in MDOF structures [11-17].

Currently, nonlinear dynamic analysis is performed using models that present different levels of detail depending on the required outcome. For example, the FEMA P-695 methodology [18] requires very detailed nonlinear models that are able to capture collapse of structures when they are subjected to ground motions scaled to different levels of intensity. In the case of acceleration demands on NSCs, the mathematical models that have been studied so far usually do not have the level of detail as required by other analyses such as that required by FEMA P-695. For instance, Sewell et al. [12] studied a 5-story lumped-mass shear beam structure, where inelastic deformations occurred only at the springs representing the story force-deformation relationship. Rodriguez et al. [15] investigated the floor accelerations of 3-, 6- and 12-story buildings with cantilever walls. The inelastic deformations in the walls occurred only at the bottom of the first story. Medina et al. [11] studied floor accelerations of stiff and flexible one-bay frames of 3, 6, 9 and 18 stories. The one-bay frames used in the study were designed to satisfy the strong-column weak-beam requirement. Therefore,

inelastic deformations were allowed to occur only at the beam ends and at the bottom of the first story columns. Chaudhuri and Villaverde [16] studied the effect of inelastic structure response on the seismic demands on NSCs. In the investigation, 4-, 8-, 12- and 16-story flexible and stiff moment steel frames were analyzed. The frames were modeled using fiber sections with a bilinear material with post-yield stiffness equal to 3% of the initial stiffness. More recently, Wieser et al. [17] studied floor accelerations using three dimensional models. A total of four buildings were analyzed. The numerical models of the buildings used elastic beam-column elements for the gravity system and fiber sections for the lateral force resisting system. The material assigned to the fiber sections is a nonlinear steel material with 2% post-yield stiffness ratio.

These studies demonstrate the analytical sophistication of research that has been performed to characterize the floor accelerations when MDOF structures are subjected to ground motions and behave inelastically. However, it can be seen that the models that have been used did not have all the details that a complete nonlinear mathematical model could include. Fiber models can capture plastification well but since strength degradation is not included, the buildings cannot collapse under larger ground motion intensities. Additionally, models with the capability of plastification only at the beam ends and at the bottom of the first story columns cannot present story mechanisms because plastic hinges in the columns are not allowed to occur.

The main purpose of this study is to contribute to a more detailed and more realistic understanding of floor accelerations by quantifying the accelerations that rigid and flexible NSCs are subjected to during an earthquake in three different manners: using what is recommended by the current US code (ASCE 7-10), performing linear time history analysis, and performing nonlinear time history analysis. It is important to point out is that very detailed nonlinear models are used in order to perform the nonlinear dynamic analysis. This is why the structures chosen to be investigated are the Special Steel Moment Frames (SMFs) analyzed by Zareian et al. [19] for the ATC 76-1 project [20]. These models have the amount of detail required to evaluate their collapse performance using the FEMA P-695 methodology. At the moment, this methodology can be considered the most stringent in terms of requirements of nonlinear mathematical models. In order to define even further the importance of the level of detail of the model, the gravity system is also considered in this investigation. In a recent study [21], it was found that the gravity system has a significant influence on the collapse performance of the same SMFs considered in this investigation. Finally, this study also intends to obtain an accurate quantitative assessment of the level of acceleration demands that can be realistically expected in NSCs anchored to multi-story SMFs located in areas where the level of seismic activity is high, such as the western United States, Japan, and Chile.

2 Methodology

The numerical models of the SMFs to be used in linear and nonlinear time history analysis were created using OpenSees [22]. The first step was to verify the accuracy of the nonlinear models by performing a FEMA P-695 analysis and by comparing the results with the ones presented by Zareian et al. in the ATC 76-1 project. As specified by the FEMA P-695 methodology, the strength and stiffness of the gravity system was not included in the analysis performed by Zareian et al. In this study, however, once the models without the gravity system were verified, the gravity system was explicitly modeled in order to evaluate its possible influence on floor accelerations. The gravity system is modeled using partially-restrained (PR) connections that have different strength levels, and the gravity columns were modeled using fiber sections with a bilinear material with 10% kinematic hardening.

Once the models were validated and the gravity system incorporated, the structures were subjected to the 44 Far-Field ground motions as specified by the FEMA P-695 methodology. The level of intensity to which the ground motions are scaled is the Design Earthquake (from now on denoted simply as DE). This criterion was adopted because the acceleration demands on NSCs indicated in ASCE 7-05 [23] and in ASCE 7-10 [24] are consistent with the DE.

3 Overview of Buildings Analyzed

As already mentioned, the buildings analyzed were taken from the ATC 76-1 project. Complete information about the design and the nonlinear models can be found in the referenced document [20]. However, a summary of the main information is provided herein. The study performed by Zareian et al. considered buildings of 1, 2, 4, 8, 12 and 20 stories. They were designed following the ASCE 7-05 [23] requirements with the exception that the deflection amplification factor C_d was taken equal to the response modification factor, R, as specified in FEMA P-695. The gravity system was not included in the analysis as the P-695 procedure specifies.

Two different analysis methods were used to design the buildings: the Equivalent Lateral Force (ELF) method and the Modal Response Spectrum Analysis (RSA) method. All the SMFs were designed using reduced beam section connections (RBS) for a seismic design category D_{max} (S_S = 1.5 g, S_1 = 0.6 g), for a typical gravity load, and considering Site Class D.

This investigation analyzes a subset of the buildings from the ATC 76-1 project. These are the 2-, 4- and 8-Story models designed using the RSA method. The base of the columns of the buildings were fixed for the 4- and 8-Story models, and pinned for the 2-Story model. The nomenclature that identifies these structures in ATC 76-1 is 2RSA (2 story), 3RSA (4 story) and 4RSA (8 story).

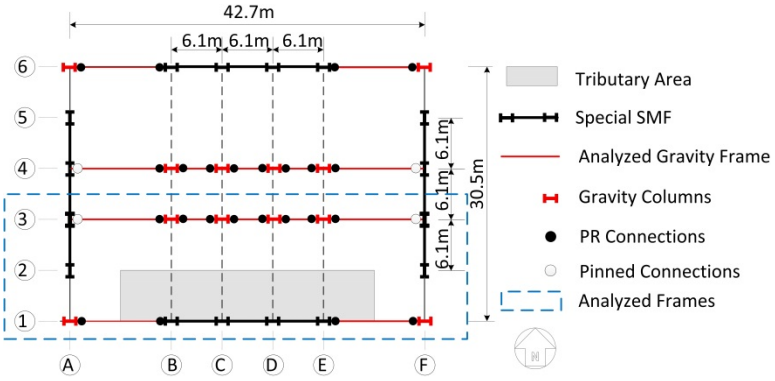

Fig. 1 - Typical Building Plan View

Fig. 1 shows the plan view for all the buildings. The bay width (center line dimensions) between columns of each SMF is 6.1 m (20 ft). The height of the first story is 4.6 m (15 ft) to the top of the steel beam, and the height of all other stories is 4.0 m (13 ft). The design dead load (D) is 4.31 kN/m^2 (90 psf) uniformly distributed over each floor, and the cladding load is applied as a perimeter load of 1.2 kN/m^2 (25 psf). The unreduced design live load (L) is 2.4 kN/m^2 (50 psf) on all floors and 0.96 kN/m^2 (20 psf) on the roof. These loads were considered in the analysis in a combination of 1.0 D + 0.25 L. Fig. 1 illustrates the configuration of the gravity system only in the direction to be analyzed (East-West). The gravity connections are considered to be PR connections. The lateral strength of the SMF columns oriented on the weak axis (A3, F3) is not considered because the sole influence of the gravity columns is intended to be evaluated.

4 Modeling approach

The numerical two-dimensional models idealized to perform the nonlinear analysis were created using OpenSees. Material and geometric nonlinearities were included in every model. In the case where the gravity system was not included, P-Delta effects were considered using a leaning column with no flexural stiffness placed parallel to the SMF. The load applied to this column represents half of the total load from the gravity system that was not tributary to the SMF columns. For the cases where the gravity system was included, a leaning column was not required. The approach applied to model the frames was to use elastic elements and to lump the nonlinear material behavior into plastic hinges located at the ends of the members. The components of the SMF with nonlinear behavior are: panel zones, plastic hinges located at the RBSs of the beam and plastic hinges at the column ends.

For a more complete description of the inelastic behavior of each component the reader is referred to the ATC 76-1 report. The hysteretic behavior of the RBSs in the beams is modeled using a rotational spring. Using OpenSees, the behavior was characterized by the material called "Bilin". The constitutive law of this material is based on the modified Ibarra-Krawlinkler deterioration model [25], and its parameters are described by Lignos and Krawinkler [26]. Panel zones are modeled using a rectangular region composed of eight very stiff elastic beam-column elements and one nonlinear rotational spring to represent shear distortions in the panel zone [27]. These deformations are due to shear yielding and column flange flexure yielding and are represented by a tri-linear backbone curve assigned to the rotational spring.

The phenomenological component used to characterize the nonlinear behavior of the SMF columns is the same as the one used for the beams. This approach was taken because at the time the analysis was performed OpenSees did not have a component with a hysteretic behavior that includes the axial force – bending moment (P-M) interaction. To account for the reduced bending strength of the columns due to the axial force, a representative axial force was computed. Even though the axial force changes during a dynamic analysis, this representative axial force is computed before the analysis and the bending strength is reduced accordingly. It was obtained by performing a nonlinear static pushover analysis and it was considered to be equal to $P_{grav} + 0.5\ P_{E,max}$, where P_{grav} is the gravity load that the column is subjected to and $P_{E,max}$ is the maximum load that the column receives during the pushover analysis. The pushover analysis is performed until a reduction of 20% in the base shear, V_{max}, is reached. With the axial load determined, the reduced bending strength is computed using the AISC P-M interaction equation [28] and subsequently used in the models. The additional components modeled in the case where the gravity system was included are: PR connections and gravity columns modeled using fiber sections. The complete frame, with all the nonlinear components, and the gravity system placed in parallel is shown in Fig. 2.

In order to account for any inelastic deformation that could occur in the gravity columns, they were modeled using force-based fiber elements with a bilinear material with strain hardening equal to 10% of the initial stiffness. The benefit of using fiber sections is that the axial-moment interaction is taken into account. However, because strength degradation is not included, the capability of the model to represent collapse is limited. This is why plastic hinges at columns of the SMFs were modeled using a phenomenological approach.

The flexural strength of the gravity connections was considered to be a percentage of the plastic moment strength (M_p) of the beam. Different strength levels were studied with the purpose of establishing possible influence on floor accelerations. The percentages assigned to the PR connections were 0%, 35%, 50%, and 70%. The 0% represents the influence purely of the gravity columns, and the 35% is the minimum strength required by the connections to avoid yielding under gravity loads.

Although probably too large, the 50% and 70% are considered in order to acquire an extended possible range of behavior. Even though the cyclic behavior of the PR connections is complicated to characterize, it was considered that a simple model, such as the one given by ASCE 41-13 [29], would be accurate enough to the purpose of this study. One of the parameters given by this model is the rotation at which the PR connections yield (0.005 radians). Therefore, the stiffness of the PR connections is different for each strength level. More information regarding the modeling of the PR connections can be found in Flores et. al [21].

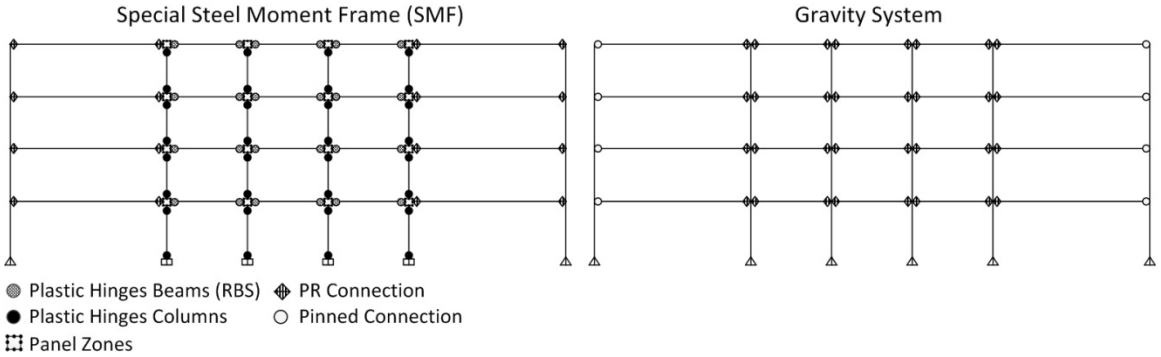

Fig. 2 - Elements of the models that include the gravity system

For the linear and nonlinear dynamic response history analysis, a Rayleigh damping of 2.5% is assigned to the first modal period T_1 and to period $T = 0.2\ T_1$ in all cases. As proposed by Zareian and Medina [30], stiffness proportional damping is assigned to elements that remain elastic, and mass proportional damping is assigned to nodes or elements where mass is lumped.

5 Rigid Nonstructural Components

In this section of the study, the accelerations rigid NSCs are subjected to are computed for the 2-, 4- and 8-Story buildings. As already mentioned, three methods are used to compute them: using the specifications given by the current US code (ASCE 7-10), performing linear time history analysis, and performing nonlinear time history analysis.

5.1. ASCE 7-10 Accelerations on Rigid NSCs

Design accelerations on rigid NSCs are given implicitly by the general formula to compute the horizontal seismic design force for NSCs. The horizontal seismic design force F_p indicated in both ASCE 7-05 [23] and ASCE 7-10 [24] for acceleration-sensitive NSCs is given by:

$$F_p = \frac{0.4 a_p S_{DS} W_p}{\frac{R_p}{I_p}} \left(1 + 2\frac{z}{H}\right) \leq 1.6 S_{DS} I_p W_p \qquad F_p \geq 0.3 S_{DS} I_p W_p \tag{1}$$

where a_p is the component amplification factor (a_p equal to 1.0 and 2.5 for rigid and flexible NSCs respectively), R_p and I_p are the component response modification and importance factor, respectively, W_p is the weight of the component, S_{DS} is the DE short period spectral acceleration and z/H is the relative height ratio of the floor at which component is anchored. One of the topics of interest in this study is the variation of the peak floor acceleration (PFA) along the height of the building. Implicit in Eq. (1) (a_p = 1 for rigid NSCs) is a linear height-wise variation of the PFA from a value equal to the PGA (= 0.4 S_{DS}) at the ground level (i.e., z/H = 0) to a value equal to 3 times the PGA at the roof level (i.e., z/H = 1.0). It can be seen that ASCE 7 does not consider whether the supporting structure behaves

elastically or inelastically, does not differentiate among the different types of lateral resisting systems, and does not take into the account the number of stories or floor levels.

5.2. Peak Floor Accelerations

The Peak Floor Acceleration (PFA) is the maximum total acceleration measured at a given floor, and is equal to the acceleration demand on a rigid NSC located at that floor. This method is used for the linear and nonlinear time history analyses and the results are shown next. The following nomenclature is adopted for identification of results: nStory + sGS, where n is the number of stories and s is the percentage of full strength assigned to the PR connections (if sGS is not included, the model does not include the gravity system, and instead includes a leaning column to account for P-Delta effects).

Fig. 3 (a) and (b) display median PFAs (normalized by the PGA) of the elastic and inelastic 2-Story models, respectively. Fig. 3 also includes PFAs computed using ASCE 7-10. It can be seen that accelerations on rigid NSCs are significantly overestimated by the code. Moreover, PFAs computed using the inelastic models turned out to be significantly lower than those computed using the elastic models. On the other hand, it can also be seen from Fig. 3 that the influence of the gravity system on floor accelerations in the inelastic models is not very significant but in general the accelerations increased a similar amount regardless the strength level of the PR connections.

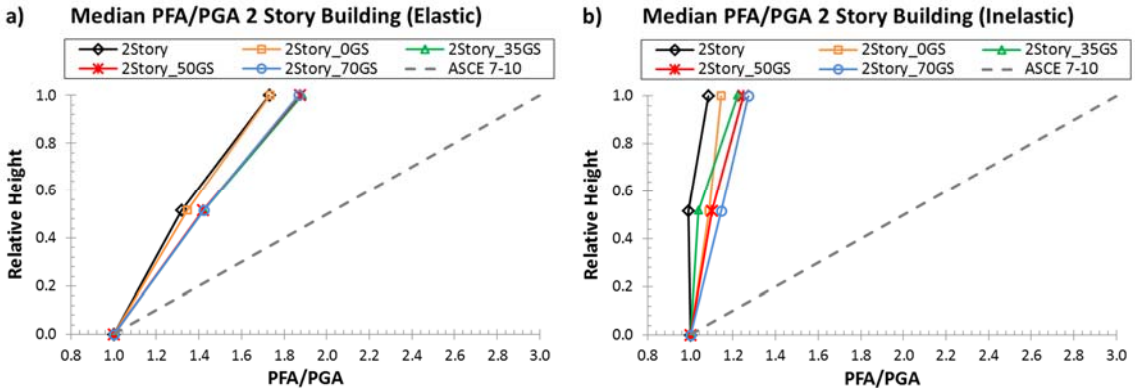

Fig. 3 - Normalized Peak Floor Acceleration (PFA/PGA): 2-Story Model

Fig. 4 (a) and (b) present PFAs of the 4-Story models. The differences between accelerations in the elastic and inelastic models are now even more important than those observed in the previous case. Again, the influence of the gravity system in the inelastic models is not very significant. The exception is the roof level, where the presence of the gravity system increases the PFA, particularly when the strength of the PR connections is not zero. The influence of the exact strength level, however, is virtually irrelevant.

Fig. 5 a) and b) display PFAs of the 8-Story models. Again, the inelastic acceleration demands are significantly lower than the elastic demands, and the influence of the gravity system is even less than that observed in the 2-Story model.

Interestingly, it is found that in the inelastic models the PFAs are roughly equal to (usually less than, occasionally greater than) the PGA at almost all floor levels of the three buildings. Therefore, DE acceleration demands on rigid NSCs can in general be expected to be roughly equal to the PGA, which in turn means that the design accelerations indicated in ASCE 7 for rigid NSCs are very conservative, at

least for the scenario considered in this study (the supporting structure is a SMF, and is located in an area of high seismic activity).

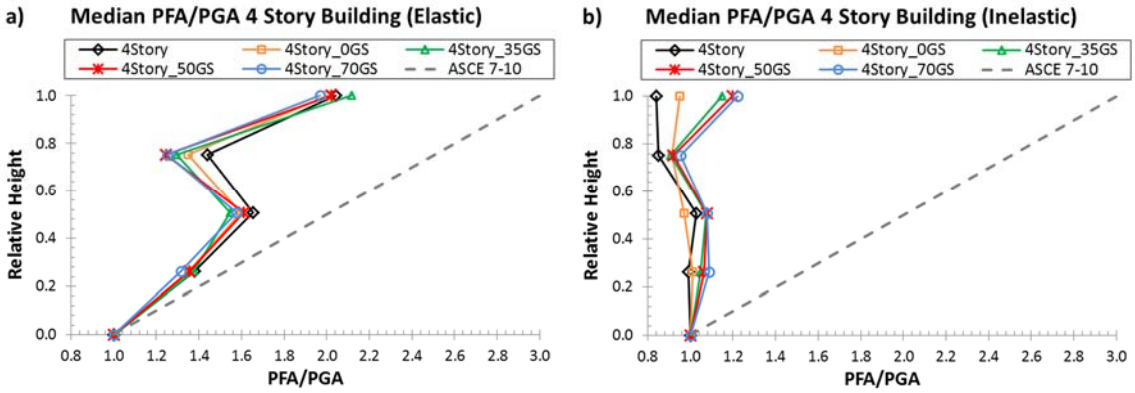

Fig. 4 - Normalized Peak Floor Acceleration (PFA/PGA): 4-Story Model

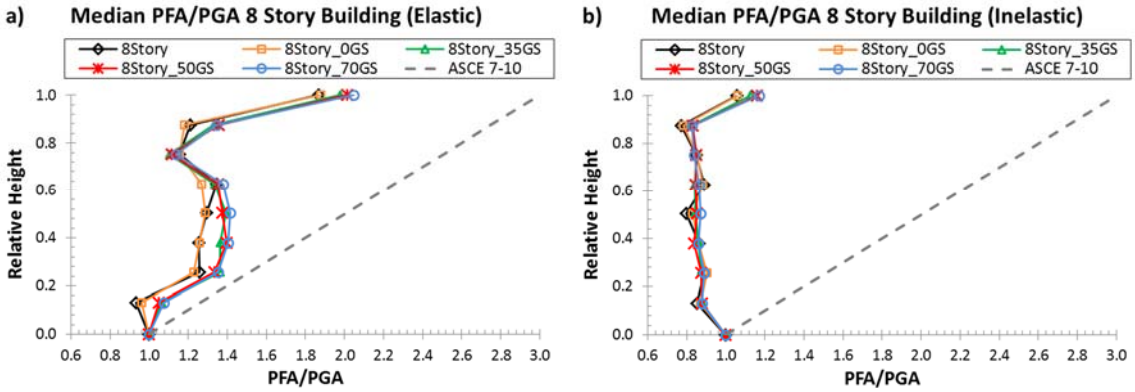

Fig. 5 - Normalized Peak Floor Acceleration (PFA/PGA): 8-Story Model

6 Flexible Nonstructural Components

In this section of the study, the accelerations that flexible NSCs are subjected to are computed for the 2-, 4- and 8-story buildings. Again, three methods are used to compute them: using the specifications given in the current US code (ASCE 7-10), performing linear time history analysis, and performing nonlinear time history analysis.

6.1. ASCE 7-10 Accelerations on Flexible NSCs

It was already stated that the design acceleration demand on rigid NSCs indicated in ASCE 7 depends neither on the type of lateral resisting system nor on the number of stories or floor levels. Notably, Eq. (1) also indicates that the ASCE 7 design acceleration demands on flexible NSCs located at a given relative height of the supporting structure are also independent of the characteristics of the supporting structure. For instance, Eq. (1) indicates that the acceleration demand on flexible NSCs that behave elastically (i.e., R_p = 1) and are located at the roof level (i.e., relative height z/H = 1) is equal to 3.0 x 2.5 = 7.5 times the PGA (a_p = 2.5 for flexible NSCs), regardless of the characteristics of the supporting structure. Recalling that the building models considered in this study were designed for a PGA = 0.4 g (DE level), ASCE 7 indicates that the design acceleration demand on elastic, flexible NSCs located at the roof level is equal to 0.4 g x 7.5 = 3.0 g, regardless of the number of stories (i.e., same value for the 2-, 4- and 8-Story models).

6.2. Floor Response Spectra

The Floor Response Spectra (FRS) indicate the acceleration demands on flexible NSCs. As mentioned before, FRS are obtained by computing the acceleration response spectrum of the total acceleration response history at the floor of interest. Since the response spectrum is computed in the usual, "standard" way, FRS indicate the acceleration demand on NSCs that behave elastically. Recalling Eq. (1), the ASCE 7 approach indicates that the horizontal seismic design force F_p for NSCs is obtained considering that the demand is reduced by the component response modification factor R_p, implying that NSCs are allowed to develop inelastic deformations. However, the factor R_p is in general different for each type of NSC, and is not considered in this study (in other words, this study evaluates floor accelerations, not the design seismic force F_p). All FRS shown in this paper are median spectra of the set of FRS corresponding to each ground motion, and were obtained considering a damping ratio equal to 2%, typical of most NSCs.

Fig. 6 (a) and (b) show the FRS corresponding to the second (roof) level of the 2-Story model. It can be observed that the spectral shape is essentially the same regardless of whether the supporting structure behaves elastically or inelastically: FRS are characterized by large spectral ordinates at the modal periods of the structure. In order to help appreciate this observation, the modal periods of the model that does not include the gravity system are indicated by the vertical dashed lines. However, the amplitude of the spectral ordinates in the vicinity of the first modal period are much less when the structure behaves inelastically than when the structure behaves in a linearly elastic manner. In the extreme case, the spectral ordinate of the elastic model is roughly equal to 8.0 g (no gravity system) and 9.0 g (gravity system with non-zero strength of the PR connections) at first mode resonance, but the spectral ordinate of the inelastic models is not greater than 5.0 g. It can also be observed that the presence of the gravity system is relevant only when the PR connections have some strength. In such a case, the first modal period decreases (the structure becomes stiffer when the PR connections do have some strength), and spectral ordinates are somewhat different in the vicinity of the first modal period. Finally, the exact strength level of the PR connections does not have an influence on the FRS. Regarding the accelerations computed using ASCE7-10, it can be seen that they are conservative except at first mode resonance, in which case they underestimate the expected demand.

Fig. 7 (a) and (b) show the FRS corresponding to the fourth (roof) level of the 4-Story model. Again, the spectral shape is essentially the same regardless of whether the supporting structure behaves elastically or inelastically. In this case, however, the amplitude of the spectral ordinates is much less when the structure behaves inelastically not only in the vicinity of the first modal period but also in the vicinity of the second modal period. Once more, it can also be observed that the presence of the gravity system is relevant only when the PR connections have some strength. In this case, however, spectral ordinates are somewhat different not only in the vicinity of the first modal period but also in the vicinity of the second modal period. Again, the exact strength level of the PR connections does not have an influence on the FRS. When compared to the FRS computed using the inelastic models, the accelerations quantified using the code provisions are again conservative except in the vicinity of the second modal period. However, when compared to the FRS computed using the elastic models, the ASCE 7 design accelerations underestimate the expected demands in the vicinity of all modal periods.

Fig. 8 (a) and (b) show the FRS corresponding to the eighth (roof) level of the 8-Story model. As before, the spectral shape is essentially the same regardless of whether the supporting structure behaves elastically or inelastically. In this case, however, the amplitude of the spectral ordinates are much less when the structure behaves inelastically in the vicinity of the third modal period as well. Again, it can also be observed that the presence of the gravity system is relevant only when the PR

connections have some strength. In this case, however, spectral ordinates are not different in the vicinity of the first modal period (inelastic models) but they are somewhat different in the vicinity of the second and third modal periods.

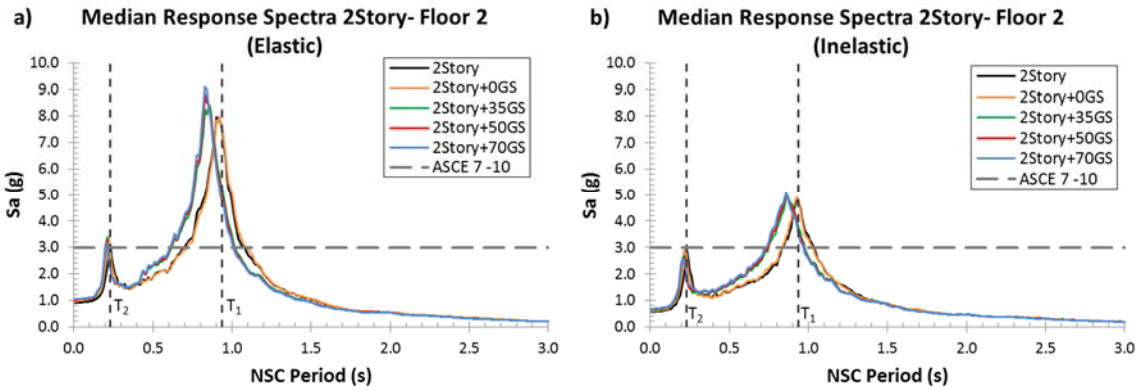

Fig. 6 - FRS at the 2nd (roof) level of the 2-Story Models

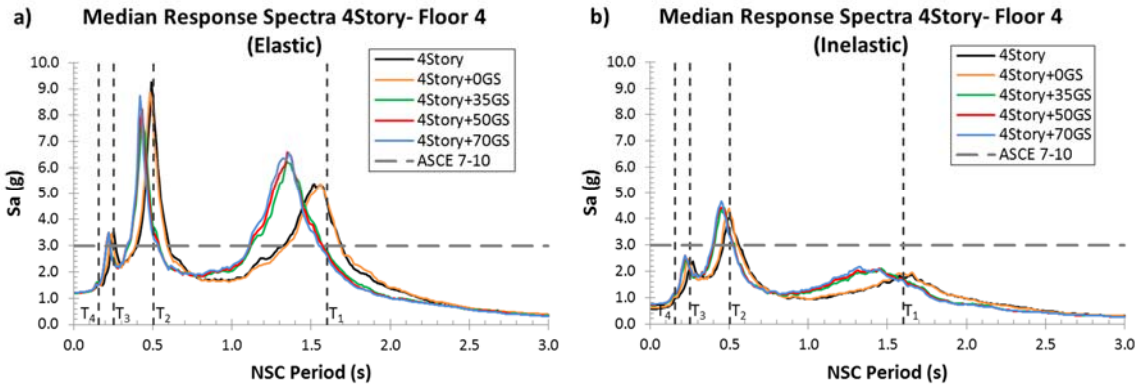

Fig. 7 - FRS at the 4th (roof) level of the 4-Story Models

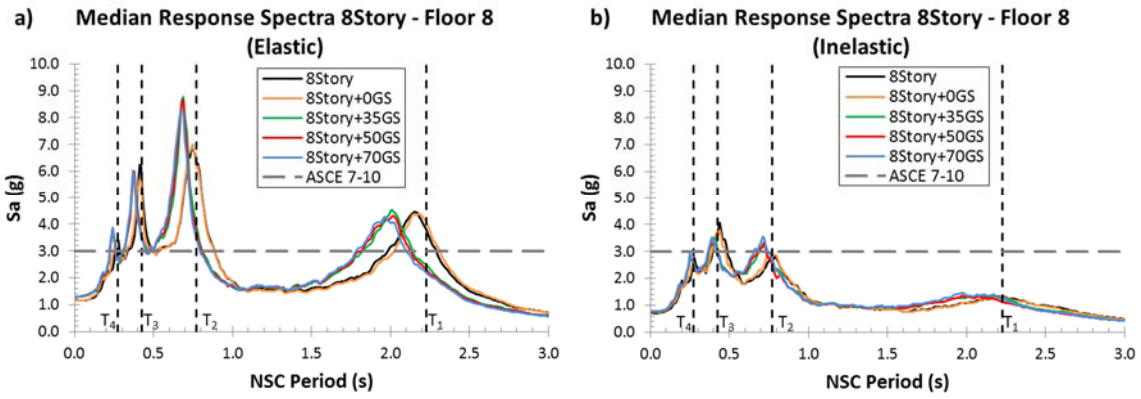

Fig. 8 - FRS at the 8th (roof) level of the 8-Story Models

The exact strength level of the PR connections, as seen before, does not have an influence on the FRS. The accelerations computed using the ASCE 7 -10 provisions are close to the ones quantified using the FRS method (inelastic models) when at periods ranging from the second modal period to the fourth modal period. Otherwise, design accelerations given by ASCE 7 are conservative.

Keeping in mind that the period of flexible NSCs is in most cases less than 0.5 s, Fig. 6 (b), Fig. 7(b) and Fig. 8 (b) (structure behaving inelastically, the realistic scenario) indicate that the ASCE 7 design

demand is exceeded in the 4- and 8-Story models in the extreme case of higher mode resonance, and is conservative otherwise. Of course, such EXTREME demands (up to 4.5 g) are very high, which is why protective measures such as floor isolation systems are a topic of current research.

7 Conclusions

In this study, floor accelerations in Special Steel Moment Frames (SMFs) were investigated considering different modeling options, from a simple linear elastic model of the lateral force resisting system to a sophisticated nonlinear model complying with the requirements of FEMA P-695. Particular attention was paid to the gravity system, which has been shown to significantly influence the collapse performance of SMFs [21]. The building models were subjected to the FEMA P-695 set of far-field ground motions scaled to the DE response spectrum the buildings were designed for, which is representative of seismic demands in areas of high seismic activity in the western United States and in countries such as Japan and Chile. From the analysis of results obtained by time history analysis, the conclusions of this investigation are:

- The most relevant modeling issue is the inelastic behavior of the structure. Although nonlinear time history analysis is still challenging, it leads to levels of accuracy that more than compensate for its drawbacks.
- The acceleration demands on rigid NSCs (inelastic building models) are roughly equal to the PGA, regardless of the floor level at which the NSC is attached. Therefore, in areas of high seismic activity, where DE PGA values are roughly equal to 0.4 g – 0.6 g, the acceleration demands on rigid NSCs are not expected to be as large as those indicated by the ASCE 7 approach, especially at the topmost floor levels.
- The acceleration demands on flexible NSCs indicated by the ASCE 7 approach are conservative except at higher mode resonance, i.e., when the period of the NSC is very close to one of the higher modal periods of the supporting structure.

8 Acknowledgements

The work presented herein was possible through the support of the Pontificia Universidad Catolica de Chile and the National Research Center for Integrated Natural Disaster Management CONICYT/FONDAP/15110017.

9 References

[1] B. Reitherman, T. Sabol, R. Bachman, D. Bellet, R. Bogen, D. Cheu, P. Coleman, J. Denney, M. Durkin, C. Fitch, Nonstructural damage, Earthquake Spectra, 11 (1995) 453-514.

[2] E. Miranda, G. Mosqueda, R. Retamales, G. Pekcan, Performance of nonstructural components during the 27 February 2010 Chile earthquake, Earthquake Spectra, 28 (2012) S453-S471.

[3] E. Miranda, S. Taghavi, Approximate floor acceleration demands in multistory buildings. I: Formulation, Journal of structural engineering, 131 (2005) 203-211.

[4] J. Lin, S.A. Mahin, Seismic response of light subsystems on inelastic structures, Journal of Structural Engineering, 111 (1985) 400-417.

[5] S. Taghavi, E. Miranda, Response assessment of nonstructural building elements, Report No. PEER 2003/05. Dept. of Civil and Environmental Engineering, Stanford University, Stanford, CA. Pacific Earthquake Engineering Research Center, Richmond, CA, 2003.

[6] A. Singh, A.H.S. Ang, Stochastic prediction of maximum seismic response of light secondary systems, Nuclear Engineering and Design, 29 (1974) 218-230.

[7] R. Villaverde, Seismic design of secondary structures: state of the art, Journal of structural engineering, 123 (1997) 1011-1019.

[8] B. Kehoe, M. Hachem, Procedures for estimating floor accelerations, in: Proc., ATC-29-2 Seminar on Seismic Design, Performance, and Retrofit of Nonstructural Components in Critical Facilities, Applied Technology Council, Redwood City, Calif, 2003.

[9] M. Singh, L. Moreschi, L. Suarez, E. Matheu, Seismic design forces. I: Rigid nonstructural components, Journal of structural engineering, 132 (2006) 1524-1532.

[10] I. Politopoulos, C. Feau, Some aspects of floor spectra of 1DOF nonlinear primary structures, Earthquake engineering & structural dynamics, 36 (2007) 975-993.

[11] R.A. Medina, R. Sankaranarayanan, K.M. Kingston, Floor response spectra for light components mounted on regular moment-resisting frame structures, Engineering structures, 28 (2006) 1927-1940.

[12] R. Sewell, C. Cornell, G. Toro, R. McGuire, R. Kassawara, A. Singh, J. Stepp, Factors influencing equipment response in linear and nonlinear structures, in: Transactions of the 9th international conference on structural mechanics in reactor technology. Vol. K2, 1987.

[13] R. Sankaranarayanan, R.A. Medina, Acceleration response modification factors for nonstructural components attached to inelastic moment-resisting frame structures, Earthquake Engineering & Structural Dynamics, 36 (2007) 2189-2210.

[14] I. Politopoulos, Floor spectra of MDOF nonlinear structures, Journal of Earthquake Engineering, 14 (2010) 726-742.

[15] M. Rodriguez, J. Restrepo, A. Carr, Earthquake-induced floor horizontal accelerations in buildings, Earthquake engineering & structural dynamics, 31 (2002) 693-718.

[16] S.R. Chaudhuri, R. Villaverde, Effect of building nonlinearity on seismic response of nonstructural components: a parametric study, Journal of structural engineering, 134 (2008) 661-670.

[17] J. Wieser, G. Pekcan, A.E. Zaghi, A. Itani, M. Maragakis, Floor accelerations in yielding special moment resisting frame structures, Earthquake Spectra, 29 (2013) 987-1002.

[18] FEMA, Quantification of Building Seismic Performance Factors, FEMA P-695, Washington, D.C., 2009.

[19] F. Zareian, D. Lignos, H. Krawinkler, Evaluation of seismic collapse performance of steel special moment resisting frames using FEMA P695 (ATC-63) methodology, in: Proceedings of Structures Congress ASCE, Orlando, FL, 2010, pp. 12-14.

[20] NIST, Evaluation of the FEMA P-695 Methodology for Quantification of Building Seismic Performance Factors, GCR 10-917-8, (2010).

[21] F.X. Flores, F.A. Charney, D. Lopez-Garcia, Influence of the Gravity Framing System on the Collapse Performance of Special Steel Moment Frames, Journal of Constructional Steel Research, 101 (2014), 351-362.

[22] S. Mazzoni, F. McKenna, M.H. Scott, G.L. Fenves, OpenSees command language manual, Pacific Earthquake Engineering Research (PEER) Center, (2006).

[23] ASCE, Minimum Design Loads for Buildings and Other Structures, ASCE Standard ASCE/SEI 7-05, in, American Society of Civil Engineers, Reston, VA, 2005.

[24] ASCE, Minimum Design Loads for Buildings and Other Structures, ASCE Standard ASCE/SEI 7-10, in, American Society of Civil Engineers, Reston, VA, 2010.

[25] L.F. Ibarra, R.A. Medina, H. Krawinkler, Hysteretic models that incorporate strength and stiffness deterioration, Earthquake engineering & structural dynamics, 34 (2005) 1489-1511.

[26] D.G. Lignos, H. Krawinkler, Deterioration modeling of steel components in support of collapse prediction of steel moment frames under earthquake loading, Journal of Structural Engineering, 137 (2010) 1291-1302.

[27] F.A. Charney, J. Marshall, A Comparison of the Krawinkler and Scissors Models for Including Beam-Column Joint Deformations in the Analysis of Moment-Resisting Steel Frames, Engineering journal., 43 (2006) 31.

[28] AISC, Specification for Structural Steel Buildings, ANSI/AISC 360-05, American Institute of Steel Construction., Chicago, IL, (2005).

[29] ASCE, Seismic Rehabilitation of Existing Buildings, ASCE Standard ASCE/SEI 41-13, American Society of Civil Engineers, Reston, Va., 2013.

[30] F. Zareian, R.A. Medina, A practical method for proper modeling of structural damping in inelastic plane structural systems, Computers & structures, 88 (2010) 45-53.

APPENDIX B

THE INFLUENCE OF ACCIDENTAL TORSION

ON THE INELASTIC DYNAMIC RESPONSE OF BUILDINGS

DURING EARTHQUAKES

Presented at the XI Congreso Chileno de Sismología e Ingeniería Sísmica ACHISINA

2015 (Santiago, Chile, March 18-20, 2015)

THE INFLUENCE OF ACCIDENTAL TORSION ON THE INELASTIC DYNAMIC RESPONSE OF BUILDINGS DURING EARTHQUAKES

F. Flores[(1)], F. Charney[(2)], D. Lopez-Garcia[(3),(5)], J. C. de la Llera[(4),(5)]

[(1)] *Ph.D. Candidate, Department of Civil and Environmental Engineering, Virginia Tech, and Department of Structural and Geotechnical Engineering, Pontificia Universidad Catolica de Chile, ffloress@vt.edu*
[(2)] *Professor, Department of Civil and Environmental Engineering, Virginia Tech, fcharney@vt.edu*
[(3)] *Associate Professor, Department of Structural and Geotechnical Engineering, Pontificia Universidad Catolica de Chile, and National Research Center for Integrated Natural Disaster Management CONICYT/FONDAP/15110017, dlg@ing.puc.cl*
[(4)] *Professor, Department of Structural and Geotechnical Engineering, Pontificia Universidad Catolica de Chile, jcllera@ing.puc.cl*
[(5)] *National Research Center for Integrated Natural Disaster Management CONICYT/FONDAP/15110017*

Abstract

Nonlinear dynamic analysis is becoming an accepted procedure to assess the performance of building structures during earthquakes. Several documents have emerged to provide guidance in terms of mathematical modeling, ground motion selection and scaling, and acceptability of results. While there are some significant differences in these documents, one feature in common is that explicit inclusion of accidental torsion in the nonlinear dynamic response history analysis is generally not required. In the few instances where accidental torsion is required, exceptions are provided that makes the application of accidental torsion necessary only under extreme conditions, or, allowance is made to assess the influence of accidental torsion in an ad-hoc manner, such as by use of a separate linear analysis procedure. Analyses presented in this paper shows conclusively that accidental torsion may be neglected in the analysis of torsionally regular buildings, but should be included in the analysis of all torsionally irregular buildings. Failure to include accidental torsion in torsionally irregular buildings may indicate stable response instead of dynamic instability, or may significantly under-predict deformations and thereby falsely indicate that deformation-based acceptance criteria have been met. Additionally, it is shown that geometric nonlinearities related to global torsional response must be included in the analysis.

Keywords: Nonlinear Analysis, Accidental Torsion, Geometric Nonlinearities, Codes and Standards

1 Introduction

Nonlinear dynamic response history (NLRH) analysis is becoming an accepted procedure to assess the performance of building structures during earthquakes. In support of this trend, several documents [1-5] have emerged to provide guidance in terms of mathematical modeling, ground motion selection and scaling, and specification/evaluation of acceptance criteria. Additionally, several standards (or prestandards) [6-11] provide specific requirements for performing such analysis.

A review of these documents has indicated various areas of agreement and disagreement. One of the most striking areas of disagreement is related to methodologies required to capture accurate three-dimensional response, and more specifically, whether or not accidental torsion is required.

In regards to accidental torsion, there are two issues. First, there is the question as to whether accidental torsion is needed in the (generally linear elastic) analysis used to design the structure that will be later analyzed using the NLRH procedure. Second, there is the issue of whether or not accidental torsion must be included in the nonlinear response history analysis itself. Related to the second issue is the specific manner in which the decision to omit or include accidental torsion in the NLRH analysis is made, and how the accidental torsion is included in the analysis after it has been determined that it is necessary.

The issue of accidental torsion in seismic design and analysis was, until recently, a resolved issue. Where linear elastic analysis procedures are used, most building codes require accidental torsion to be included, either by applying equivalent lateral forces at some eccentricity in static analysis, or by shifting the center of mass in dynamic analysis. However, a debate has arisen as to whether accidental torsion is in-fact needed in the design of all buildings. In this regard, DeBock et al. [12] have shown, using the FEMA P-695 Methodology [13], that accidental torsion is not warranted in the design of structures in low to moderate seismic hazard areas, but is needed for structures in high seismic hazard areas. This observation, which is based on collapse criteria alone, will likely lead to a relaxation of the accidental torsion requirements in future editions of ASCE 7.

Whether or not accidental torsion should be included in NLRH analysis was extensively debated by members of the task committee charged with developing a fully revised set of requirements for NLRH analysis for Chapter 16 of ASCE 7-16. This chapter, which was not finalized at the time of writing this paper, is included in a preliminary form in the 2015 NEHRP Provisions [11]. Ultimately, the guidelines for NLRH analysis that were approved for the Provisions do require the inclusion of accidental torsion in the elastic analysis-based design phase, but not in the subsequent NLRH analysis that is used to evaluate the computer response against predefined acceptance criteria. The decision not to include accidental torsion in the NLRH analysis was based primarily on practical considerations, as it was thought that requiring as many as four additional analyses (for four different mass offset locations per ground motion, with a minimum of 11 ground motions required) was onerous. It is noted, however, that the commentary for the 2015 Provisions suggests that the influence of uncertainties in the location of center of mass and/or in the strength and stiffness of structural components be evaluated for torsionally sensitive systems.

The decision not to include accidental torsion in the NLHR analysis used to assess performance is contrary to recommendations made in analyses by Mansuri [14] and Jarrett et al. [15]. Even though the building systems analyzed by Mansuri were not particularly torsionally sensitive, it was noted that increases in response due to accidental torsion was significant, and was more significant for taller systems relative to shorter systems. Mansuri also noted that inelastic torsional response was

generally greater than elastic torsional response, and that P-Delta effects had a very significant influence on behavior. In Jarett et al. [15] it was found that shifting the location of center of mass had a more significant effect on torsional response of buildings than imposing uncertainty in stiffness and strength of structural components. Based on the analysis it was recommended that accidental torsion be included in NLRH analysis, but that exceptions could be developed on the basis of preliminary nonlinear static pushover analysis.

In the new work presented in this paper, the need to include accidental torsion in NLRH analysis is further investigated through the evaluation of the response of a 9-story steel building with Buckling Restrained Braces (BRB) used to resist lateral loads. Three versions of the building are considered, wherein the only difference is the plan location of individual braced frames. The variation in plan location produces different levels of torsional irregularity, from moderate to extreme.

The analysis agrees in principle with Mansuri [14] and Jarrett et al. [15] in the basic finding that accidental torsion is an important consideration in NLRH analysis. Supplementary to this finding two important side issues emerged. These are related to the specific methodology used to incorporate P-Delta effects, and the need to include both components of horizontal ground motion when assessing the importance of accidental torsion. The issues related to including both components of motion are discussed later in the paper. However, the issue related to P-Delta effects requires some preliminary theoretical discussion, and this is provided next.

2 Modeling of Second Order Effects in 3-D Structural Analysis

Most analysts recognize the importance of including second-order effects in NLRH analysis. These effects cause amplification of lateral displacements (the P-Delta effect) as well as amplification of system torsional rotation (the P-Theta effect). Habibullah and Wilson [16] provide a thorough discussion of such effects, and provide approximate methods for incorporating them in analysis of building systems with idealized rigid diaphragms.

If both the gravity system and the lateral system are physically modeled in 3-D analysis, both the P-Delta and the P-Theta effects are automatically captured when element stiffness formulations include geometric stiffness. Such models with spatially distributed columns may be used for both rigid and semi-rigid diaphragm idealizations. If the gravity columns are not included in the model, the destabilizing gravity loads tributary to these columns must be accounted for, and this is often done using "leaner columns" which, in essence, lump all of the P-Delta effects into one element with zero elastic stiffness and negative geometric stiffness. Where geometric stiffness is not included in the elements of the lateral system, the leaner column can be used to represent the destabilizing gravity load for the full system. It is very important to note, however, that leaner columns do not capture P-Theta effects, and this omission can lead to underestimates of torsional response, and for torsionally irregular systems may fail to recognize cases where torsion induces structural collapse.

This paper specifically investigates the role that P-Theta effects play in assessing the torsional response of buildings. This is done by performing analysis with and without P-Theta effects, and comparing the computed response. Additionally, both the lateral and torsional stability ratios are computed and presented for each system. The lateral stability ratios, Q_{Δ}, are determined by performing a static linear-material analysis for the structure under lateral loads, without accidental torsion, with and without P-Delta effects, and computing the following quantity at each story level:

$$Q_\Delta = 1 - \frac{\Delta_o}{\Delta_f} \quad (1)$$

where Δ_o is the story drift computed without P-Delta and Δ_f is the story drift including P-Delta.

The torsional stability ratios, Q_θ, are determined by running a static linear-material analysis for the structure loaded with accidental torsion only, with and without P-Theta effects, and computing the following quantity at each story level:

$$Q_\theta = 1 - \frac{\theta_o}{\theta_f} \quad (2)$$

where θ_o is the difference in torsional rotations at the top and bottom of the story without P-Theta and θ_f is the same quantity computed for analysis that includes P-Theta.

Lateral deflection and torsional rotation amplifiers, λ_Δ and λ_θ, respectively, are determined as follows:

$$\lambda_\Delta = \frac{1}{1 - Q_\Delta} \quad (3)$$

$$\lambda_\theta = \frac{1}{1 - Q_\theta} \quad (4)$$

3 Description of System Analyzed

The system analyzed, illustrated in Figure 1, is nine stories tall, with a rectangular plan consisting of two 30-ft bays on one direction, and eight 30-ft bays in the other direction. The system was adapted from a similar square-plan building described in the ATC 76 project [17], and analyzed in detail by Atlayan [18].

The lateral load resisting system consists of four bays of buckling restrained braced (BRB) frames, with two bays in each direction. The sizes of the elements of the BRB systems are shown in Figure 1. The yielding core in the BRBs use ASTM A992 steel with a nominal yield strength of 50 ksi. Three variations of this system are investigated, wherein the *only difference* between the systems is the placement of the BRBs that resist load in the N-S direction. All systems have BRBs on gridlines A and C to resist loads in the E-W direction. For system A, BRBs for N-S loads are positioned only along gridlines 4 and 6 as shown in Figure 1. System B has N-S BRBs only on gridlines 3 and 7, and system C has N-S BRBs only on gridlines 2 and 8. Based on ASCE 7-10 definitions, System A has a Type-1b (extreme) torsional irregularity, System B has a Type 1a torsional irregularity, and system is not torsionally irregular.

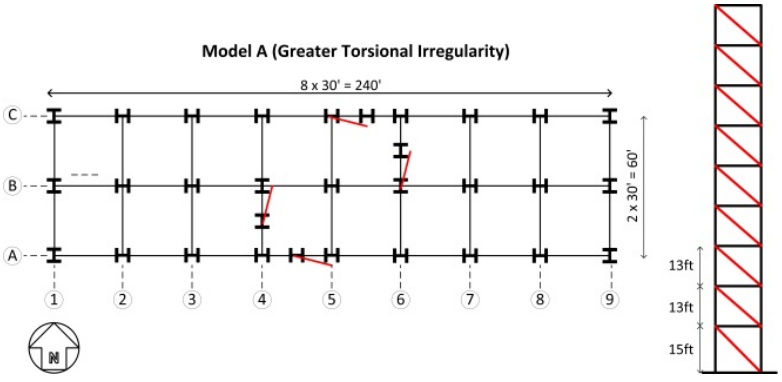

BRB Section Sizes

Level / Story	Brace Area (in^2)	Beams	Columns
Roof	-	W21x62	-
9	9.0	W24x76	W14x370
8	9.0	W24x76	W14x370
7	10.0	W24x76	W14x370
6	10.0	W27x94	W14x398
5	11.0	W27x94	W14x398
4	11.0	W27x94	W14x455
3	11.0	W27x94	W14x455
2	12.0	W27x94	W14x500
Ground	12.0	-	W14x500

Figure 1. Structural System Analyzed (Model A)

The gravity system consists of a metal deck and concrete floor slab supported by an assembly of steel beams and columns. The total seismic weight of the system, W, is 14490 kips, which represents a weight density of 8.6 pounds per cubic foot. The design floor load was 100 psf dead and 50 psf. Seismic design was based on ASCE 7-05 [19] and the 2005 AISC Seismic Specification [20]. Design level spectral accelerations S_{DS} and S_{D1} are 1.0g and 0.6g, respectively.

4 Mathematical Model

Each system was analyzed in three dimensions using OpenSees [21]. Floor diaphragms were assumed rigid in-plane and flexible out of plane. The gravity system was included in the analysis, but did not contribute to the lateral strength and stiffness. P-Delta effects were included using two different approaches, each incorporating the P-Delta transformation within OpenSees. The first of these used a "leaning column" at the center of the building, wherein the P load on the column represented the entire gravity load of the system. In the second approach the story P loads were distributed by tributary area to each of the individual columns. The influence of the different P-Delta modeling approaches on the computed response is discussed in detail later in this paper. In the remainder the first approach is referred to as P-Δ, and the second is as P-$\Delta\theta$. The symbol θ in the second case indicates that torsional P-delta effects are included.

Material nonlinearities were included in the beams, columns, and braces of the BRB systems. The analytical approach used to model the BRB system is discussed in detail in Atlayan [18].

In the dynamic analyses the effect of accidental torsion was introduced by modifying the diaphragm mass distribution such that the desired mass eccentricity was achieved.

5 Torsional Properties of Systems

The lateral and rotational stability ratios were computed for each story of the building (Eqs. 1 and 2), and the maximum values along the height computed for Systems A, B, and C are reported in Table 1. Also provided are the corresponding amplification factors (Eqs. 3 and 4).

Table 1. Stability and Amplification Factors

System	Q_Δ	λ_Δ	Q_θ	λ_θ
A	0.060	1.064	0.274	1.377
B	0.060	1.064	0.107	1.120
C	0.060	1.064	0.049	1.052

The lateral stability ratios for all systems is the same, at 0.060. Note that ASCE7-10 [7] requires that P-Delta analysis be included only where the maximum lateral stability ratio is greater than 0.10. ASCE 7 does not require P-Theta evaluations of any kind. As noted from Table 1, however, the torsional stability ratio for System A is very significant at 0.274, indicating an increase in static plan-wise torsional rotations by a factor of 1.377 due to P-Theta effects alone. The torsional stability ratio and amplification factor for Systems B and C are somewhat less, but still significant for System B.

Another indicator of the likelihood of torsional response is the torsional irregularity factor (TIF) which is equal to the maximum ratio, over all stories, of the building edge drift to the building center drift when an equivalent lateral load is applied at a 5% eccentricity. In ASCE 7 this factor is used to determine if a torsional irregularity occurs. If the TIF is greater than 1.2 and less than 1.4 the building

is torsionally irregular, and if the ratio is greater than or equal to 1.4 the system is extremely irregular. The TIFs computed for Systems A, B, and C with different approaches for including geometric nonlinearity are shown in Table 2. It is interesting to note that the P-Δ model reports slightly lower TIFs than those obtained when no geometric nonlinearity is used. For the system with torsional irregularities, TIFs obtained using the P-$\Delta\theta$ model increase, particularly so for Model A with the extreme torsional irregularity.

Table 2. Torsional Irregularity Factors

System	No P-Δ or P-Θ	P-Δ	P-$\Delta\theta$	Irregularity?
A	1.83	1.80	2.02	Extreme
B	1.32	1.31	1.34	Irregular
C	1.16	1.15	1.15	None

As a final check of the torsional sensitivity of the buildings the first three periods of vibration were computed with and without accidental torsion, and using both the P-Δ and the P-$\Delta\theta$ methods. The results of the analysis are presented in Tables 3a, 3b, and 3c for Systems A, B, and C, respectively. From the left part Table 3a, for System A without a mass offset, it may be seen that the first mode is torsional, with a period of 4.116 s when geometric nonlinearity is not included. The first mode period does not increase when the P-Δ model is used, but increases significantly to 4.797 s when the P-$\Delta\theta$ model is used. For the same system the P-Δ model influences the lateral modes, but not the torsional mode. It is noted that the torsion mode for System A is significantly larger that the lateral modes, an indicator of extreme torsional flexibility. The comparison between the left and right halves of Table 3a indicates the influence of including a 5% mass eccentricity in the system. As may be seen there is a slight increase in the torsional period for each of the geometric nonlinearity assumptions.

The trends of the results for Model B, shown in Table 3b, are similar to that for System A, except that the torsional period is only marginally larger than the lateral period. This, however, is still indicative of a torsionally flexible system. For System C, it is seen in Table 3c that the first two modes are lateral, and torsion dominates the third mode response. The influence of geometric nonlinearity is similar to that for Systems A and B in the lateral directions, and is only marginal on the torsional mode.

Table 3a. Modal Properties for Model A

Mode	Model Analyzed with No Accidental Torsion				Model Analyzed with 5% Accidental Torsion			
	No P-Δ or P-$\Delta\theta$	P-Δ	P-$\Delta\theta$	Mode Type	No P-Δ or P-$\Delta\theta$	P-Δ	P-$\Delta\theta$	Mode Type
1	4.116	4.116	4.797	Torsion	4.201	4.204	4.887	Torsion
2	2.476	2.558	2.559	Lateral	2.476	2.558	2.559	Lateral
3	2.473	2.554	2.555	Lateral	2.424	2.503	2.511	Lateral

Table 3b. Modal Properties for Model B

Mode	Model Analyzed with No Accidental Torsion				Model Analyzed with 5% Accidental Torsion			
	No P-Δ or P-$\Delta\theta$	P-Δ	P-$\Delta\theta$	Mode Type	No P-Δ or P-$\Delta\theta$	P-Δ	P-$\Delta\theta$	Mode Type
1	2.622	2.622	2.769	Torsion	2.783	2.814	2.922	Torsion
2	2.476	2.558	2.559	Lateral	2.476	2.558	2.559	Lateral
3	2.473	2.554	2.555	Lateral	2.331	2.382	2.424	Lateral

Table 3c. Modal Properties for Model C

Mode	Model Analyzed with No Accidental Torsion				Model Analyzed with 5% Accidental Torsion			
	No P-Δ or	P-Δ	P-$\Delta\theta$	Mode	No P-Δ or	P-Δ	P-$\Delta\theta$	Mode

	P-Δθ			Type	P-Δθ			Type
1	2.457	2.558	2.558	Lateral	2.513	2.591	2.596	Lateral
2	2.473	2.554	2.554	Lateral	2.476	2.558	2.559	Lateral
3	1.866	1.866	1.914	Torsion	1.837	1.841	1.885	Torsion

6 Nonlinear Static Pushover Analysis

Prior to preforming NLRH analysis on the systems, a series of nonlinear static pushover analyses were performed. All pushover analyses were performed under displacement control with a first-mode lateral load distribution. Gravity load consisting of 1.05 times the dead load plus 0.25 times the live load was applied prior to lateral loading.

In these analyses three basic parameters were varied:

a) The magnitude of accidental eccentricity as a percentage of the length perpendicular to the direction of load

b) Whether or not P-Theta effects were included

c) Whether or not lateral loads were applied simultaneously in the orthogonal direction

In the first series of analyses the lateral load was applied in the N-S direction only, at some eccentricity from the center of mass. Both P-Delta and P-Theta effects were included. The results are shown for System A in Figure 2a. Here it may be seen that accidental eccentricities of 2, 3, and 4% had a nominal impact on performance, but increasing the eccentricity from 4% to 5% had a tremendous influence on the shape of the pushover curve. As shown in Figure 2b, the sudden change in pushover response does not occur when P-Theta effects are ignored, even when the lateral loads are applied at a 10% eccentricity.

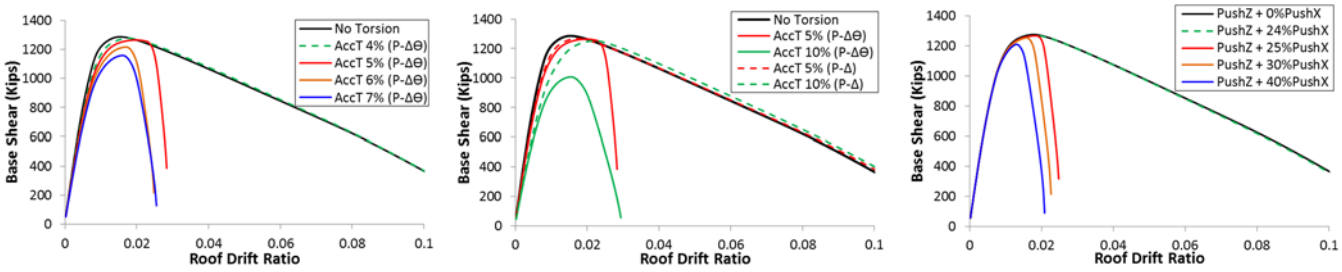

a) Unidirectional loading with Various Eccentricity (with P-Theta)

b) Unidirectional loading (with and without P-Theta)

c) Bidirectional loading with 4% Eccentricty (With P-Theta)

Figure 2. Pushover curves for System A under unidirectional loading

Figure 2c illustrates the influence of bidirectional loading on the extremely irregular System A, when the N-S loading eccentricity is 4% of the building width, P-Theta effects are included, and orthogonal (E-W) loading is applied at the center of mass at some percentage of the full load. As may be seen, a bifurcation in behavior occurs when the orthogonal load reaches 25% of the full value. This percentage varies depending on the the amount of accidental torsion in the building. For instance, for a 3% eccentricity the orthogonal load that causes the bifurcation is equal to 40% of the full value.

The behavior of System B, which is moderately torsionally irregular, is similar to that of System A. This is illustrated in the pushover curves of Figure 3. Figure 3a shows the pushover response with unidirectional loading at various levels of eccentricity, with P-Theta effects included. As may be seen, the bifurcation in response does not occur until the eccentricity reaches 7% for the model without orthogonal load. Again, the sudden change in pushover response does not occur when P-Theta effects are ignored, even when the lateral loads are applied at a 10% eccentricity (in Figure 3b). On

the other hand, when orthogonal load effects are included for a system with 5% accidental eccentricity, Figure 4c, the system's behavior changes suddenly when the orthogonal load reaches 29% of the full load.

On the basis of the pushover responses alone it seems that P-Theta effects are essential, and that evaluation of system behavior should include orthogonal loading effects. This is the case even for System B for which is only moderately irregular (IF=1.33). Based on these results alone it could be inferred that accidental torsion should be included in analysis, P-Theta effects must be included, and some level of orthogonal loading must be applied.

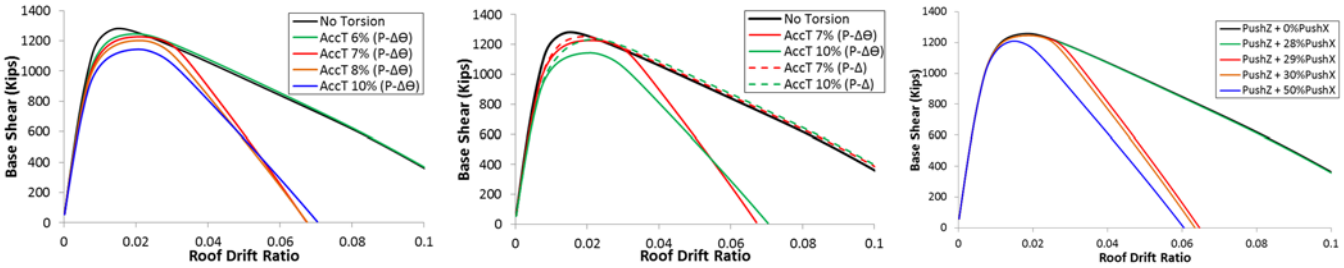

a) Unidirectional loading with Various Eccentricity (with P-Theta)

b) Unidirectional loading (with and without P-Theta)

c) Bidirectional loading with 6% Eccentricty (With P-Theta)

Figure 3. Pushover curves for System B under uniaxial and biaxial loading

Figure 4 illustrates the pushover response for System C. For this torsionally regular system NS lateral loading at a 5% eccentricity has only a marginal influence on behavior when the system is loaded in one direction only (Figure 4a). However, a significant change in behavior occurs when an E-W loading of 50% of the full value is applied together with 100% of the eccentric N-S load (Figure 4c). The bifurcation is for this system is not as clear as it was for the more torsional susceptible systems but it can be seen that occurs when the eccentricity is equal to 10%. Figure 4b shows the influence of including P-Theta, which is the same as already seen for the other systems, the sudden change in the pushover curves does not occur, even for large eccentricities.

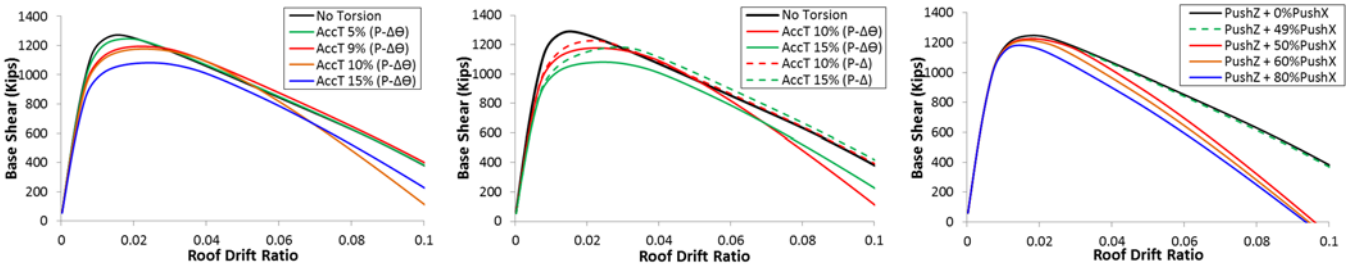

a) Unidirectional loading with Various Eccentricity (with P-Theta)

b) Unidirectional loading (with and without P-Theta)

c) Bidirectional loading with 5% Eccentricty (With P-Theta)

Figure 4. Pushover curves for System C under uniaxial and biaxial loading

The important findings related to pushover analysis are that (1) including P-Theta effects is essential, (2) pushover response can change suddenly when accidental eccentricities are marginally increased, and (3) orthogonal loading has a strong influence on pushover response.

Among these findings, the sudden change or bifurcation that occurs when the accidental eccentricity increases needs to be addressed. In order to explain the reason behind this behavior the sequence of yielding when the pushover analysis is performed is analyzed. Figure 5 displays the system B sequence of yielding for a pushover analysis with an eccentricity equal to 6% and 7%. The color lines drawn next to BRBs frames are correlated directly to the points drawn in the pushover curves and they represent the different states of the structure. The number (N) placed next to the colored lines are the number

of BRBs that are yielding at that specific point in the pushover analysis. By comparing the state of the system at the red dot and rhombus in Figure 5, the bifurcation occurrence is explained. It can be seen that for a 6% eccentricity just of the orthogonal BRB frames is yielding while for 7% eccentricity both orthogonal BRB frames are yielding. Therefore, the sudden degradation of the system capacity is due to yielding of the frames in the orthogonal direction. This outcome was also seen by De La LLera and Chopra in their investigation [22].

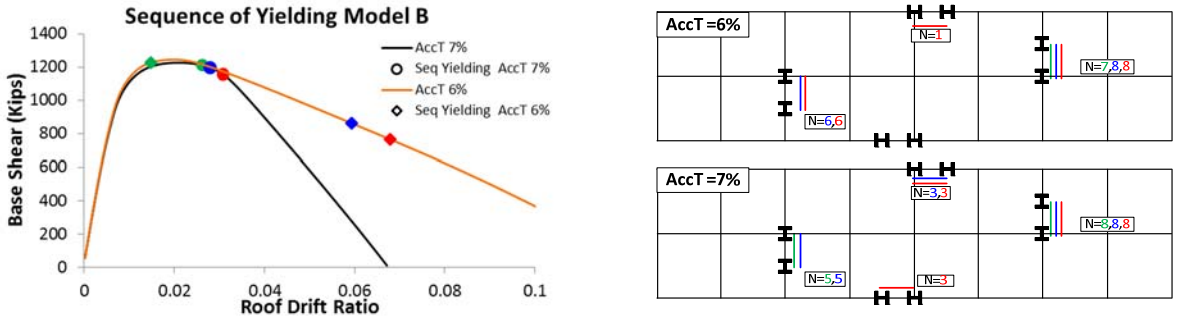

Figure 5. Pushover Sequence of Yielding (Model B)

7 Nonlinear Dynamic Analysis

NLRH analysis was carried out for each model using 11 ground acceleration recordings, representing 11 actual earthquake events selected from the P-695 Far-field record set. The event horizontal component with the largest peak ground acceleration was selected for use for N-S direction shaking, and each was amplitude scaled for consistency with MCE_R level shaking. Where ground motions were applied simultaneously in the orthogonal direction the orthogonal component was applied at full values, with scaling consistent to that used for the N-S direction. For each analysis the system was first subjected to gravity load, followed by ground shaking. As with the pushover analysis the parameters varied included the amount of accidental eccentricity, inclusion or non-inclusion of P-Theta effects, and presence of orthogonal load (included or not included).

Figure 6a shows the response history of roof corner drift ratio for System A under unidirectional shaking under the Kocaeli-Duzce ground motion. Analysis included P-Theta effects, but not orthogonal loading. As may be observed, drifts at the corner of the roof were significantly increased when accidental torsion was included, and peak drifts almost doubled when the accidental torsion eccentricity was increased from 0% to 5%. In Figure 6b the response under bidirectional loading is shown. It is important to emphasize again that accidental eccentricity was included for loading only in the N-S direction, and that P-Theta effects are included. The corner deflections with 5% eccentricity are more than twice the values with no accidental eccentricity, and the response is trending towards dynamic instability when the N-S loading eccentricity exceeds 5%.

Figure 6c shows the response history of roof drift of System A with 5% accidental torsion and full orthogonal loading, with and without P-Theta effects. The response for the system with no accidental torsion is shown for reference. As may be seen, the influence of P-Theta is dramatic. Clearly, analysis without P-Theta effects included may significantly underestimate response, and may indicate stable response where collapses would occur if P-Theta is included.

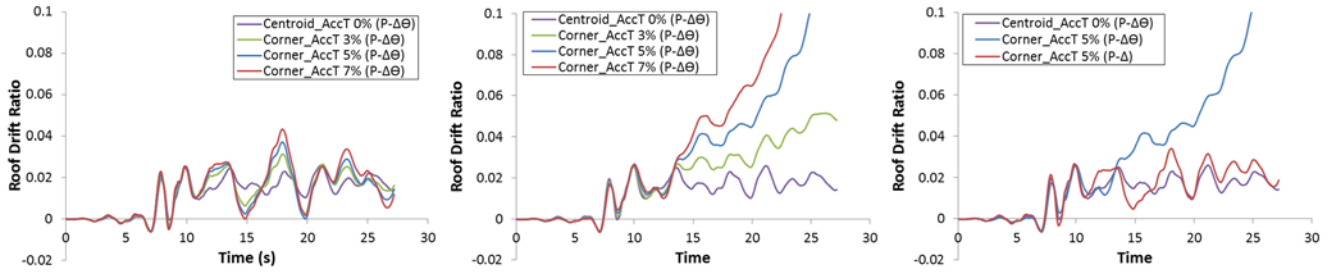

(a) Unidirectional loading (with P-Theta) (b) Bidirectional loading (with P-Theta) (c) Bidirectional loading (w & w/o P-Theta)

Figure 6. Response histories of roof drift for System A

Response History traces for System B under the Landers earthquake with P-Theta effects included is presented in Figure 7. In part (a) of the figure the response under unidirectional loading is shown with various mass eccentricities, and it is seen that the influence of accidental torsion is not significant. When bidirectional loading is applied the increase response is very significant even when the mass eccentricity is only 5%.

Due to space limitations the dynamic response of System C is not presented here, however it is noted that the inclusion of 5% accidental torsion produced a marginal increase in corner drift, and that the including P-Theta effects did not have a significant impact on the computed response.

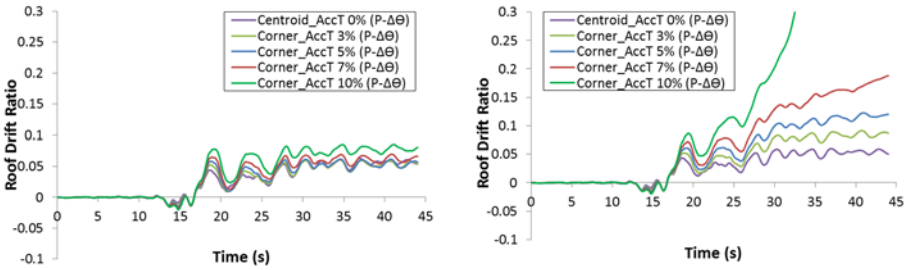

(a) Unidirectional loading (with P-Theta) (b) Bidirectional loading (with P-Theta)

Figure 7. Response histories of roof drift for System B

Table 4 provides a summary of the collapse NLRH analysis statistics for all system analyzed. For system A, which has an extreme torsional irregularity, only one collapse occurred under unidirectional shaking, including P-Theta, and this did not happen until the accidental eccentricity reached 7%. When bidirectional loading is applied, including P-Theta, eight of the eleven ground motions caused collapsed when the eccentricity is was only 3%, and this increased to 9 of eleven motions when analysis was run with 5 and seven percent accidental eccentricity. It is very important to point out that no collapses occurred when P-Theta effects were excluded from the analysis, even though a leaning column was used to model P-Delta effects.

For System B, which is torsionally irregular but not extremely irregular, one collapse occured when the accidental eccentricity was only 3%, and P-Theta effects were included. This collapse was not captured when P-Theta effects were ignored. No collapses occurred for System C, which is torsionally regular.

Table 4. Collapses Under Dynamic Loading

System	Unidirection Including P-Theta			Bidirection Including P-Theta			Bidirection P-Delta Only		
	3%	5%	7%	3%	5%	7%	3%	5%	7%
A	0	0	**1**	**8**	**9**	**9**	0	0	0
B	0	0	0	**1**	**1**	**1**	0	0	0
C	0	0	0	0	0	0	0	0	0

From these results, it is clear the importance of including both ground motions and P-theta effects. In fact, all the collapses occurred because of yielding in the orthogonal frames. A sequence of yielding analysis was performed to corroborate this statement but due to space limitations the results are not included herein.

8 Summary, Conclusions and Recommendations

It is clear from the limited analyses reported in this paper that accidental torsion has an important influence on the computed seismic response of structures predicted by nonlinear static analysis and nonlinear dynamic analysis. Additionally, the detrimental effect of accidental torsion is severely impacted by bidirectional loading, and by the P-Theta effect.

The influence of accidental torsion increases with the degree of initial torsional irregularity. However, it is important to note that even moderately irregular systems, such as model B with an TIF of approximately 1.3, was severely impacted by accidental torsion in both nonlinear static and nonlinear dynamic analysis.

Based on these results it appears that the exclusion of accidental torsion induced by mass eccentricities as low as 3% of the building width is unconservative for building systems with TIFs greater than about 1.2, and can be regarded as potentially unsafe for systems with TIFs greater than about 1.4. These observations are based on NLRH analysis with bidirectional loading, and with both P-Delta and P-Theta effects included. Analysis under unidirectional loading often failed to capture potential dynamic instability, even when P-Theta effects were included. In all cases analysis under bidirectional loading, with accidental eccentricities less than or equal to 7%, the analyses failed to capture dynamic instability when P-Theta effects were excluded. It is recommended, therefore, that the current practice, which excludes accidental torsion in NLRH analysis, be thoroughly reassessed. Among all the guidelines [1-4] and standards or prestandards [6-10] reviewed, the only guidelines that required the exclusion of accidental were those provided by the Los Angeles Tall Building Council [9], and in this case the inclusion of accidental torsion is required only where the TIF is greater than approximately 1.5. Among prestandards and standards reviewed, only ASCE 41-13 [10] requires the inclusion of accidental torsion in NLRHA. However, this standard (as well as [9]) provides an exclusion wherein accidental torsion need not be included directly in the NLRH analyses if, instead, the effects of accidental torsion are evaluated by use of "Amplification Factors". Unfortunately, the standard does not provide details regarding methods for computing the factors (which are presumably based on linear analysis).

None of the guidelines or prestandards/standards reviewed explicitly mentions the importance of including P-Theta effects in nonlinear static or dynamic analysis, nor is the deficiency of using a "leaner column" discussed. This is a serious omission in the reference literature, and must be addressed.

Additional analysis is required before detailed recommendations can be made for updated guidelines and code language. However, it appears clear from the analysis reporter herein that: (1) NLRH analysis must be carried out in three dimensions under full bidirectional loading; (2) accidental torsion must be included for all systems with torsional irregularity factors greater than 1.2; and (3) both P-Delta and P-Theta effects must be included. It is possible that exceptions to the requirement of including accidental torsion can be developed, based on three-dimensional nonlinear static pushover analysis with bidirectional loading (including partial loading in the direction orthogonal to the

direction of principal loading) and of course, with P-Theta effects included. A similar, but less detailed recommendation was made in Jarrett et al. [15].

9 Acknowledgements

The work presented herein was possible through the support of the Pontificia Universidad Catolica de Chile and the National Research Center for Integrated Natural Disaster Management CONICYT/FONDAP/15110017.

10 References

[1] PEER (2010), *Guidelines for Performance Based Design of Tall Buildings*, Pacific Earthquake Engineering Research Center, University of California, Berkeley, CA.

[2] NIST (2010), Nonlinear Structural Analysis for Seismic Design (NIST GCR 10-917-5), National Institute of Standards and Technology, Gaithersburg, MD,

[3] NIST (2010), *Applicability of Nonlinear Multiple-Degree-of-Freedom Modeling for Design* (NIST GCR 10-917-9), National Institute of Science and Technology, Gaithersburg, MD.

[4] PEER (2010), *Modeling and Acceptance Criteria for Seismic Design and Analysis of Tall Buildings (PEER/ATC 72-1)*. Pacific Earthquake Engineering Research Center, Richmond, CA.

[5] NIST (2011), *Selecting and Scaling Earthquake Ground Motions for Performing Response-History Analysis (NIST GCR 11-917-5)*, National Institute of Science and Technology, Gaithersburg, MD.

[6] FEMA (2009), *2009 NEHRP Recommended Seismic Provisions for New Buildings and Other Structures (FEMA P-750)*, Federal Emergency Management Agency, Washington, D.C.

[7] ASCE (2011), *ASCE 7-10: Minimum Design Loads for Buildings and Other Structures*, American Society of Civil Engineers, Reston, VA.

[8] SFBC (2013), *Requirements and Guidelines for the Seismic Design of New Tall Buildings Using Non-Prescriptive Design Procedures*, 2013 San Francisco Building Code Administrative Bulletin 083, San Francisco, CA.

[9] LATBSDC (2014), *An Alternative Procedure for Seismic Analysis and Design of Tall Buildings Located in The Los Angeles Region*, Los Angeles Tall Building Structural Design Council, Los Angeles, CA.

[10] ASCE (2014), *ASCE 41-13: Seismic Evaluation and Retrofit of Existing Buildings*, American Society of Civil Engineers, Reston, VA.

[11] FEMA (2015), *2015 NEHRP Recommended Provisions for New Buildings and Other Structures (FEMA P-1050)*, Federal Emergency Management Agency, Washington, DC.

[12] DeBock, D.J., Liel, A., Haselton, C., Hoope, J., and Henige, R. (2014), "Importance of Seismic Design Accidental Torsion Requirements for Building Collapse Capacity", *Earthquake Engineering and Structural Dynamics,* 43:831-850.

[13] FEMA (2009). *Quantification of Building Seismic Performance Factors (FEMA P-695),* Federal Emergency Management Agency, Washington D.C.

[14] Mansuri, M. (2009), *Torsional Effects in the Inelastic Response of Structures*, Ph.D. Dissertation, Department of Civil Engineering, University of Southern California, Los Angeles, CA.

[15] Jarrett, J., Zimmerman, R., and Charney, F. (2014), *Accidental Torsion in Nonlinear Response History Analysis*, Proceedings of the 10th National Conference in Earthquake Engineering, Earthquake Engineering Research Institute, Richmond, CA.

[16] Habibullah, A., and Wilson, E. (1987), "Static and Dynamic Analysis of Multi-Story Buildings, Including P-Delta Effects", *Earthquake Spectra*, Vol. 2, No 3, pp 289-298.

[17] Atlayan, O. (2013), Hybrid Steel Frames, Ph.D. Dissertation, Department of Civil and Environmental Engineering, Virginia Tech, Blacksburg, VA.

[18] NIST (2010), *Evaluation of the FEMA P-695 Methodology for Quantification of Building Seismic Performance Factors (NIST GCR 10-917-8)*, National Institute of Standards and Technology, Gaithersburg, MD.

[19] ASCE (2005), *Minimum Design Loads for Buildings and Other Structures (ASCE 7-10)*, American Society of Civil Engineers,

Reston, VA.

[20] AISC (2005), *Specification for Structural Steel Buildings (ANSI/AISC 360-05)*, American Institute of Steel Construction, Chicago, IL.

[21] PEER (2007), *OpenSees: Open system for earthquake engineering simulation*, Pacific Earthquake Engineering Research Center, Richmond, CA.

[22] J.C.D.l. Llera, A.K. Chopra, Inelastic behavior of asymmetric multistory buildings, Journal of Structural Engineering, 122 (1996) 597-606.

APPENDIX C

P-DELTA EFFECTS IN THE TORSIONAL RESPONSE OF STRUCTURES

Presented at the 16th World Conference on Earthquake Engineering (Santiago, Chile, January 9-13, 2017)

16th World Conference on Earthquake Engineering, 16WCEE 2017
Santiago Chile, January 9th to 13th 2017
Paper N° 1076
Registration Code: S-K1464726362

P-DELTA EFFECTS IN THE TORSIONAL RESPONSE OF STRUCTURES

F. Flores[1], F. Charney[2], D. Lopez-Garcia[3],[4]

[1] *Ph.D. Candidate, Department of Civil and Environmental Engineering, Virginia Tech, and Department of Structural and Geotechnical Engineering, Pontificia Universidad Catolica de Chile, ffloress@vt.edu*
[2] *Professor, Department of Civil and Environmental Engineering, Virginia Tech, fcharney@vt.edu*
[3] *Associate Professor, Department of Structural & Geotechnical Engineering, Pontificia Universidad Catolica de Chile, dlg@ing.puc.cl*
[4] *Researcher, National Research Center for Integrated Natural Disaster Management CONICYT/FONDAP/15110017, dlg@ing.puc.cl*

Abstract

Nonlinear dynamic analysis is an accepted procedure to assess the performance of building structures during earthquakes. Several documents have emerged to provide guidance in terms of mathematical modeling, ground motion selection and scaling, and acceptability of results. Due to computational advances, one of the newer requirements provided by these standards is to perform a three dimensional analysis and to include P-Delta effects. Unfortunately, the same provisions do not provide details on methods for incorporating P-Delta effects into the mathematical model, and as a result important response characteristics, including the potential for global torsional collapse may be overlooked. The issue at hand is the potential for not including or improperly modeling the P-Theta effect, which is an amplification of rotations about the vertical axis due to gravity loads. In this paper, the P-Theta effect is investigated for a torsionally irregular nine-story buckling restrained braced frame system. Three methods for incorporating the P-Delta and P-Theta effects are illustrated. The first method, which uses a single leaning column at the building's center of mass, properly includes P-Delta effects but does not capture P-Theta effects. The second method uses four leaning columns, each located at the centroid of a quadrant of the buildings. This method captures P-Delta effects and P-Theta effects, although the influence of P-Theta effects is underestimated. Finally, each column of the structure, including gravity columns, is explicitly modeled, and geometric stiffness is assigned to the column based on its tributary gravity load. This method is deemed the most accurate, and captures detrimental behavior, including collapses, that the other methods miss.

Keywords: Nonlinear Analysis, Accidental Torsion, Geometric Nonlinearities, Codes and Standards

1. Introduction

Nonlinear dynamic response history (NLRH) analysis is becoming an accepted procedure to assess the performance of building structures during earthquakes. In support of this trend, several documents [1-5] have emerged to provide guidance in terms of mathematical modeling, ground motion selection and scaling, and specification/evaluation of acceptance criteria. Additionally, several standards (or prestandards) [6-11] provide specific requirements for performing such analysis. A review of these documents has indicated various areas of agreement and disagreement. One of the most striking areas of disagreement is related to methodologies required to capture accurate three-dimensional response, and more specifically, whether or not accidental torsion is required. However, ASCE 7-16 [12] explicitly requires the three-dimensional modeling, and for torsionally irregular systems, incorporation of accidental torsion when NLRH is performed.

The inclusion of accidental torsion for torsionally irregular systems in ASCE 7-16 was in part based on research performed by DeBock et al. [13] where using the FEMA P-695 Methodology [14], it was found that accidental torsion is not warranted in the design of torsionally regular structures in low to moderate seismic hazard areas, but is needed for torsionally irregular structures in high seismic hazard areas. Another study that had an important influence on the decision of including accidental torsion in NLRH analysis was presented by Flores et al. [15]. This investigation showed that accidental torsion significantly increased global displacements at the edges of the building, and can strongly influence dynamic instability, especially when the structure is torsionally irregular. An important factor in both studies was the treatment of P-Delta effects, and particularly the P-Theta effect which is the amplification of global torsional rotation about the vertical axis due to destabilizing gravity load effects.

In the new research presented in this paper, the influence of three-dimensional P-Delta effects in NLRH analysis is investigated through the evaluation of the response of a 9-story steel building with Buckling Restrained Braces (BRB) used to resist lateral loads. The building was designed considering accidental torsion requirements given by ASCE7-10 [7]. The structure is regular in plan and height and has an extreme torsional irregularity. Three mathematical models of the building were developed, wherein the only difference is the method used to incorporate P-Delta effects. The influence of P-Delta modeling on the building's torsional response is illustrated by performing nonlinear static pushover and nonlinear dynamic analyses. Accidental torsion was induced in all analysis, either by applying the lateral loads at an eccentricity (pushover) or by shifting the location of the center of mass (dynamic).

2. Second Order Effects in 3-D Structural Analysis

Most analysts recognize the importance of including second-order effects. These effects cause amplification of lateral displacements (the P-Delta effect) as well as amplification of system torsional rotation (referred to herein as the *P-Theta effect*, where Theta is the global rotation about the vertical axis). Wilson and Habibullah [16] provide a thorough discussion of such effects, and present approximate methods for incorporating them in analysis of building systems with idealized rigid diaphragms.

If both the gravity system and the lateral system are physically modeled in 3-D analysis, both the P-Delta and the P-Theta effects are automatically captured when element stiffness formulations include geometric stiffness. Such models with spatially distributed columns may be used for both rigid and semi-rigid diaphragm idealizations. If the gravity columns are not included in the model, the destabilizing gravity loads tributary to these columns must be accounted for, and this is often done using a "leaner column" which, in essence, lumps some or all of the P-Delta effects into one element with zero elastic stiffness and negative geometric stiffness. It is very important to note, however, that use of a single leaner column at the center of mass will not capture P-Theta effects at all, and the use of a few leaner columns at inappropriate locations may not capture P-Theta effects entirely. In both cases the result is that important torsional response will be underestimated. Where the system is initially torsionally irregular the misuse of leaner columns may fail to recognize cases where torsion induces structural collapse.

This paper specifically investigates the role that P-Theta effects play in assessing the torsional response of buildings. This is done by performing analysis with and without P-Theta effects, and comparing the computed

response. Additionally, both the lateral and torsional stability coefficients are computed and presented for each system. The lateral stability coefficients, Q_Δ, are determined by performing a static linear-material analysis for the structure under gravity and lateral loads, without accidental torsion, with and without P-Delta effects, and computing the following quantity at each story level:

$$Q_\Delta = 1 - \frac{\Delta_0}{\Delta_f} \tag{1}$$

where Δ_0 is the story drift computed without P-Delta and Δ_f is the story drift including P-Delta. The torsional stability ratios, Q_θ, are determined by running a static linear-material analysis for the structure loaded with gravity load and accidental story torques, with and without P-Theta effects, and computing the following quantity at each story level:

$$Q_\theta = 1 - \frac{\theta_0}{\theta_f} \tag{2}$$

where θ_0 is the difference in torsional rotations at the top and bottom of the story without P-Theta and θ_f is the same quantity computed for analysis that includes P-Theta. Lateral deflection and torsional rotation amplifiers, λ_Δ and λ_θ, respectively, are determined as follows:

$$\lambda_\Delta = \frac{1}{1 - Q_\Delta} \tag{3}$$

$$\lambda_\theta = \frac{1}{1 - Q_\theta} \tag{4}$$

3. Building Description

The system analyzed, illustrated in Figure 1, is nine stories tall, with a rectangular plan consisting of two 30-ft bays on one direction, and eight 30-ft bays in the other direction. The system was adapted from a similar square-plan building described in the ATC 76 project [17], and analyzed for the purpose of assessing torsional performance in Flores et al. [15]. For the study reported herein the design was revised because in the ATC 76 project the displacement amplification factor (C_d) was taken equal to the response modification factor (R=8). In the current design, C_d was taken equal to the value given by ASCE7-10 [7] which is 5. This difference had an important influence in the design of the buckling restrained braced (BRB) frames because it changed from a structure design controlled by drift to one controlled by strength.

The lateral load resisting system consists of four bays BRB frames, with two bays in each direction (Figure 1). The yielding core in the BRBs use ASTM A992 steel with nominal yield strength of 50 ksi. Three variations of this system are investigated, wherein the *only difference* between the systems is the placement of the leaning columns to capture P-Delta effects. All systems have BRBs on gridlines A and C to resist loads in the E-W direction and for N-S loads the BRBs are positioned only along gridlines 4 and 6 as shown in Figure 1. Based on ASCE 7-10 definitions, the system has a Type-1b (extreme) torsional irregularity. The building was designed considering the effects of accidental torsion during the design stage. Following what is specified by ASCE7-10, loads were applied with accidental eccentricity equal to 5% the building's width and interstory drifts were checked at the corners. This system from now will be called Model A-2 (this is one of several models investigated in a broader study that will be discussed in a future paper). The member sections of the building are shown in Table 1. The difference of the member sections between the BRBs in the N-S and E-W direction is due to the influence of accidental torsion in the N-S direction.

The gravity system consists of a metal deck and concrete floor slab supported by an assembly of steel beams and columns. The total seismic weight of the system, W, is 14490 kips, which represents a weight density of 8.6 pounds per cubic foot. The design floor load was 100 psf dead and 50 psf live. Seismic design was based on ASCE 7-10 and the 2005 AISC Seismic Specification [18]. Design level spectral accelerations S_{DS} and S_{D1} are

1.0g and 0.6g, respectively. These are the Seismic Design Category D_{max} spectral accelerations in FEMA P-695 [14] .

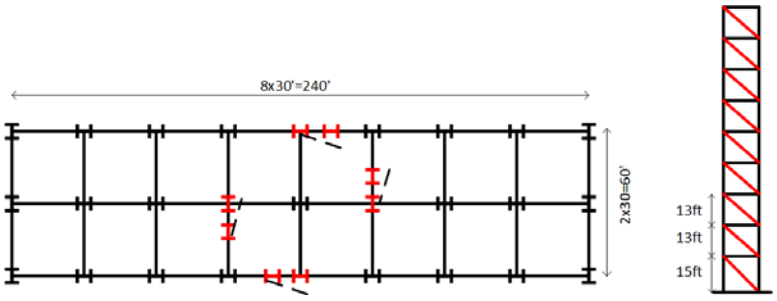

Figure 1 Structural System Analyzed (Model A-2)

Table 1 Model A-2 Member Sections

Model A-2						
Level	North-South			East-West		
	Column	Beam	BRB (in^2)	Column	Beam	BRB (in^2)
Roof	W14x370	W21x62	9	W14x120	W21x62	7
Level 8	W14x370	W24x76	9	W14x120	W24x76	7
Level 7	W14x370	W24x76	10	W14x120	W24x76	8
Level 6	W14x398	W24x76	10	W14x193	W24x76	8
Level 5	W14x398	W27x94	11	W14x193	W24x84	9
Level 4	W14x455	W27x94	11	W14x311	W24x84	9
Level 3	W14x455	W27x94	11	W14x311	W24x84	9
Level 2	W14x500	W27x94	12	W14x342	W24x84	10
Level 1	W14x500	W27x94	12	W14x342	W24x84	10

4. Mathematical Model

Each system was analyzed in three dimensions using OpenSees [19]. Floor diaphragms were assumed rigid in-plane and flexible out of plane. The gravity system was included in the analysis, but did not contribute to the lateral strength and stiffness. P-Delta effects were included using three different approaches, each incorporating the P-Delta transformation within OpenSees. The first, as illustrated in Figure 2a, used a "leaning column" at the center of the building, wherein the P load on the column represented the entire gravity load of the system. This method includes only the translational P-Delta effect, and in the remainder of this paper it is referred to as P-Δ. The second approach was the same as the one taken by DeBock et al. [13] in their study about accidental torsion. The method incorporates, as displayed in Figure 2b, four “leaning columns” placed at the centroid of each building quadrant, wherein the P load on the column represented 25% of the gravity load of the system. This method includes translational P-Delta effects and, as demonstrated later, partially includes the rotational P-Theta effects. Thus from now on in this study, this approach is referred as P-Δθp where the symbol θp in the second case indicates that torsional P-Delta effects are included partially in addition to P-Δ. The third approach distributes the story P loads using the tributary area to each of the individual columns. In this method the torsional and P-Theta and translational P-Delta are incorporated entirely, so for the remainder of this study this approach is referred as P-Δθ. The influence of the different P-Delta modeling approaches on the computed response is the main topic of investigation of this paper.

Material nonlinearities were included in the beams, columns, and braces of the BRB systems. Beams and columns were modeled using displacement control fiber elements and the BRBs were modeled using a phenomenological model. The analytical approach used to model the BRB system is discussed in detail in the study by Atlayan [20]. In the dynamic analyses the effect of accidental torsion was introduced by modifying the diaphragm mass distribution such that the desired mass eccentricity was achieved. Inherent damping was

modeled as Rayleigh damping by setting the critical damping ratio to 2% at the fundamental and fifth modes of the structure.

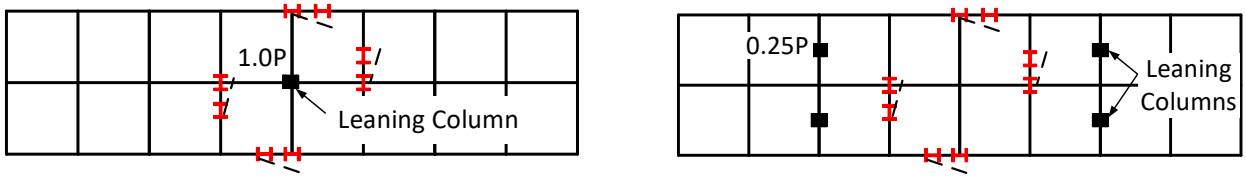

Figure 2 Modeling P-Delta effects a) Model with P-Δ effects b) Model with P-Δθp effects

5. Torsional Properties of Systems

The lateral and rotational stability coefficients were computed for each story of the building (Eqs. 1 and 2), and the maximum values along the height computed for Model A-2 are reported in Table 2. Also provided are the corresponding amplification factors (Eqs. 3 and 4).

Table 2 Stability Coefficients and Amplification Factors

System	Q_Δ	λ_Δ	$Q_{\theta p}$	$\lambda_{\theta p}$	Q_θ	λ_θ
A-2	0.032	1.033	0.152	1.179	0.258	1.347

The lateral stability coefficient for system A-2 is 0.032. Note that ASCE 7-05 and newer versions of this standard require that P-Delta analysis be included only where the maximum lateral stability ratio is greater than 0.10. Thus, in this case the building would not require P-Delta to be included. Moreover, ASCE 7 does not require P-Theta evaluations of any kind. However, as noted from Table 2 the torsional stability coefficient is greater than 0.10 for both cases: when rotational P-Theta is included partially and when it is included completely. The torsional stability for the latter case is very significant at 0.258 indicating an increase in static plan-wise torsional rotations by a factor of 1.347 due to P-Theta effects alone. With a lateral stability coefficient this high (larger than 0.25), ASCE7 would require the design to be modified. Note also that there is a 14% increment when the two methods used to incorporate P-Theta effects are compared.

Another indicator of the likelihood of torsional response is the torsional irregularity factor (TIF) which is equal to the maximum ratio, over all stories, of the building edge inter-story drift to the building center inter-story drift when an equivalent lateral load is applied at a 5% eccentricity. In ASCE 7 this factor is used to determine if a torsional irregularity occurs. If the TIF is greater than 1.2 and less than 1.4 the building is torsionally irregular, and if the ratio is greater than or equal to 1.4 the system is extremely irregular. The TIFs computed for Model A-2 with different approaches for including geometric nonlinearity are shown in Table 3. It is interesting to note that the P-Δ model reports slightly lower TIFs than those obtained when no geometric nonlinearity is used. However the TIFs increase progressively when P-Δθp and P-Δθ are included respectively.

Table 3 Torsional Irregular Factors

Model	No P-Δ or P-θ	P-Δ	P-Δθp	P-Δθ	Irregularity?
A-2	1.93	1.90	2.02	2.12	Extreme

As a final check of the torsional sensitivity of the buildings, the first three periods of vibration were computed with and without an accidental eccentricity, and using all the P-Δ the P-Δθp and the P-Δθ methods. The accidental eccentricity was induced by moving the mass a certain percentage with respect to the centroid of the building. The results of the analysis are presented in Table 4.

Table 4 Periods of Vibration Model A-2 (seconds)

Model	Mode	Model analyzed with No Accidental Torsion					Model analyzed with 5% Accidental Torsion				
		No P-Δ or P-θ	P-Δ	P-Δθp	P-Δθ	Mode type	No P-Δ or P-θ	P-Δ	P-Δθp	P-Δθ	Mode type
A-2	1	4.538	4.559	4.869	5.177	Torsion	4.623	4.586	4.623	5.267	Torsion
	2	2.928	3.068	3.068	3.068	Lateral	2.928	3.068	2.928	3.068	Lateral
	3	2.501	2.586	2.586	2.586	Lateral	2.456	2.537	2.456	2.543	Lateral

From Table 4, when no accidental torsion is included, it can be seen that the first mode is torsional, with a period of 4.538 s when geometric nonlinearity is not included. The first mode period barely increases when the P-Δ model is used (4.559 s), but increases to 4.869 s and 5.177 s when the P-Δθp and P-Δθ models are used, respectively. It is clear from the results that the P-Δ model influences the lateral modes, but not the torsional modes. It is noted also that the torsion mode for System A-2 is significantly larger than the lateral modes, an indicator of extreme torsional flexibility. By comparing the periods of vibration between the models that includes and does not include a mass eccentricity of 5% it may be seen there is a slight increase in the torsional period for each of the geometric nonlinearity assumptions when accidental torsion is incorporated.

6. Nonlinear Static Pushover Analyses

Prior to performing NLRH analysis on the systems, a series of nonlinear static pushover analyses were performed to evaluate the influence of modeling P-Delta effects. All pushover analyses were analyzed using displacement control with a first-mode lateral load distribution. The displacements were measured at the roof at the centroid of the building. The pushover is an analysis that takes to building to failure so it would not matter if it is measured at the centroid or the building's corner. However for the dynamic analysis was measured at the corner. Gravity load consisting of 1.05 times the dead load plus 0.25 times the live load and was applied prior to lateral loading. In these analyses two basic parameters were varied: a) the magnitude of accidental eccentricity as a percentage of the length perpendicular to the direction of load, and b) whether or not lateral loads were applied simultaneously in the orthogonal directions considering one of the loads (E-W direction) to be a percentage of the other load (N-S direction). The results of the pushover analyses for each of the cases are shown in the following subsections.

6.1 Including P-Delta Effects (P-Δ)

The model analyzed in this section is the one that includes only translational P-Δ effects. In order to evaluate these effects on the torsional response in the first series of analyses the lateral load was applied in the N-S direction only, at some eccentricity to the right from the center of mass. The results of these analyses are shown in Figure 3a. This figure also includes the pushover curve when the P-Δ is not considered in the analyses to demonstrate its importance. From the pushover curves it can be seen that induced torsion in the building causes early yielding but the post yield stiffness remains the same for all the values of accidental torsion. Figure 3b illustrates the influence of bidirectional loading on the extremely irregular System A-2, when the N-S loading eccentricity is 3% of the building width, and orthogonal (E-W) loading is applied at the center of mass at some percentage of the full load. The orthogonal load in the E-W direction is applied as a percentage of the full load applied in the N-S direction. This fraction of the load is going to be called from now on Orthogonal Load Factor (OLF) and it is considered to give an idea of how vulnerable the building is when is subjected to both ground motion components. The results shown in Figure 3b display the effect of having loads applied in both orthogonal directions and it is clear that for this model, which includes only translational P-Δ effects, there is no change in the pushover curve. Even for an OLF equal to 60%, the results are the same.

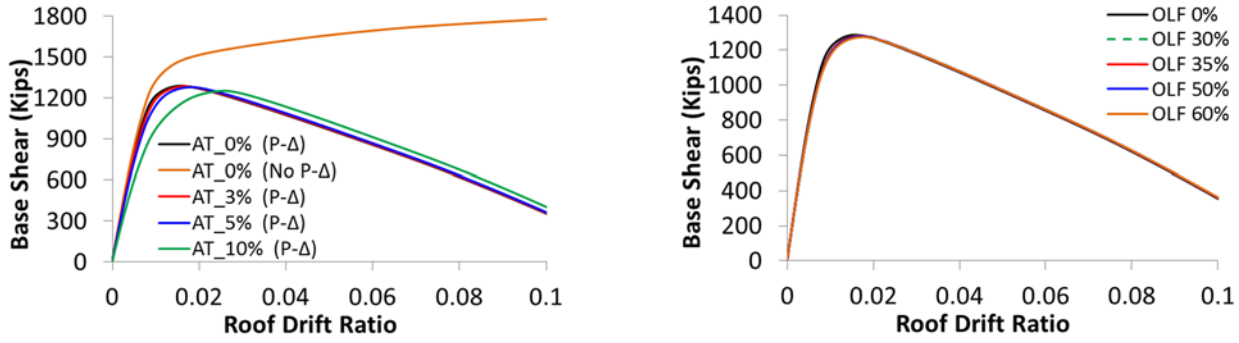

a) Unidirectional loading with Various Eccentricity

b) Bidirectional loading with 3% Eccentricity

Figure 3 Pushover Curves Including P-Δ effects

6.2 Including P-Delta effects and partial P-Theta effects

The second model to be analyzed using a nonlinear static approach is the one that includes translational and partially includes the torsional P-Delta effects (P-Δθp). The same methodology described in the previous sections was followed to load the building and induce a torsional response. The results of the loads applied in one and both directions are shown in Figure 4 a) and b). Figure 4a presents the results of applying the load unidirectionally in N-S direction with different accidental torsions. The pushover curves obtained up to an accidental torsion equal to 7% are the same as the ones shown in the previous case. However, after this point, larger amounts of accidental torsion produce a sudden change (bifurcation) where the strength of the system degrades rapidly. The results for the second analysis are shown in Figure 4b where it can be seen that unlike the results obtained for the previous case, the bifurcation of the pushover curves occurs at an OLF equal to 45%. An explanation for the sudden strength degradation is provided in Section 7 of this paper.

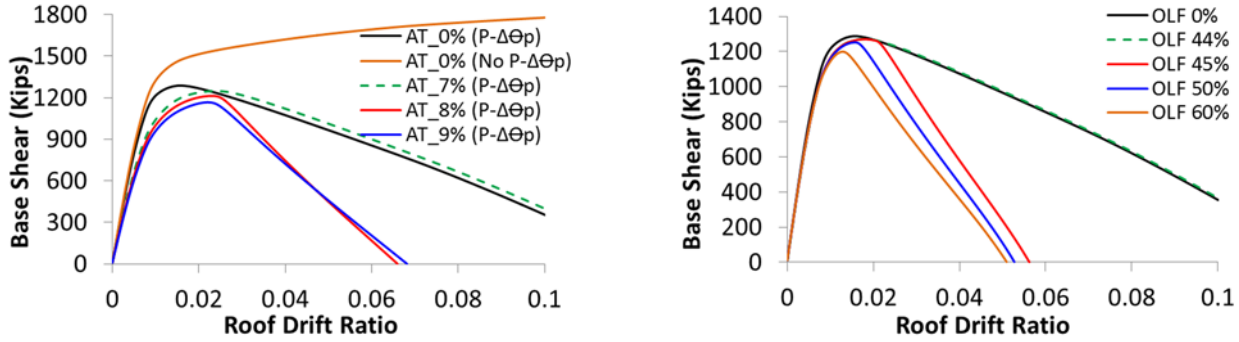

a) Unidirectional loading with Various Eccentricity

b) Bidirectional loading with 3% Eccentricity

Figure 4 Pushover Curves Including P-Δθp effects

6.3 Including P-Delta and P-Theta effects

The third case to be analyzed is the one that includes translational and rotational P-Delta effects (P-Δθ). From the previous results it is clear now that the methodology used to model P-Delta effects have a significant influence on the torsional response of a building. The influence of including all the gravity columns to incorporate P-Delta effects is seen in Figure 5. For the analysis in one direction, the bifurcation of the pushover curves occurs only at 4% of accidental torsion (Figure 5a). On the other hand, the OLF required to cause the sudden strength reduction when both orthogonal loads are applied simultaneously is equal to 23%. An OLF this low could mean that the building‘s dynamic response is susceptible when both ground motions are applied simultaneously.

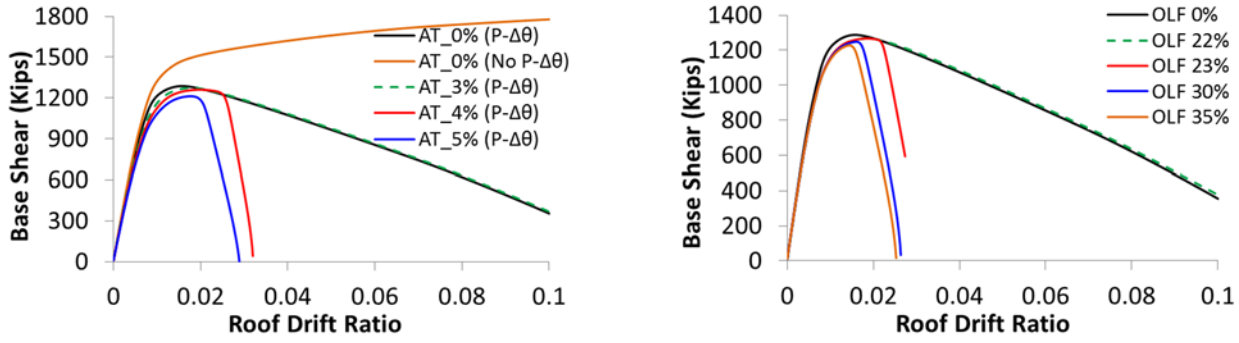

a) Unidirectional loading with Various Eccentricity

b) Bidirectional loading with 3% Eccentricity

Figure 5 Pushover Curves Including P-Δθ effects

The results presented for all three cases demonstrated the importance of modeling P-Delta effects on the torsional response of a structure. Modeling with one leaning column is clearly erroneous and modeling with just four leaning columns fails to capture significant structural deficiencies.

7. P-Theta Effects on Nonlinear Static Pushover Analyses

The previous sections showed a sudden change in the strength of the building when a certain amount of eccentricity was used to induce a torsional response to the building. In order to explain the reason for this behavior the sequence of yielding when the pushover analysis is performed is analyzed. Figure 6 displays the Model A-2 sequence of yielding for a unidirectional pushover analysis with an eccentricity equal to 3% and 4%. These accidental eccentricities are the limit point where the bifurcation of the pushover curve occurs. The colored lines drawn next to the BRB frames are correlated directly to the points drawn in the pushover curves and they represent the different states of the structure. The number (N) placed next to the colored lines represents the number of BRBs that are yielding at that specific point in the pushover analysis.

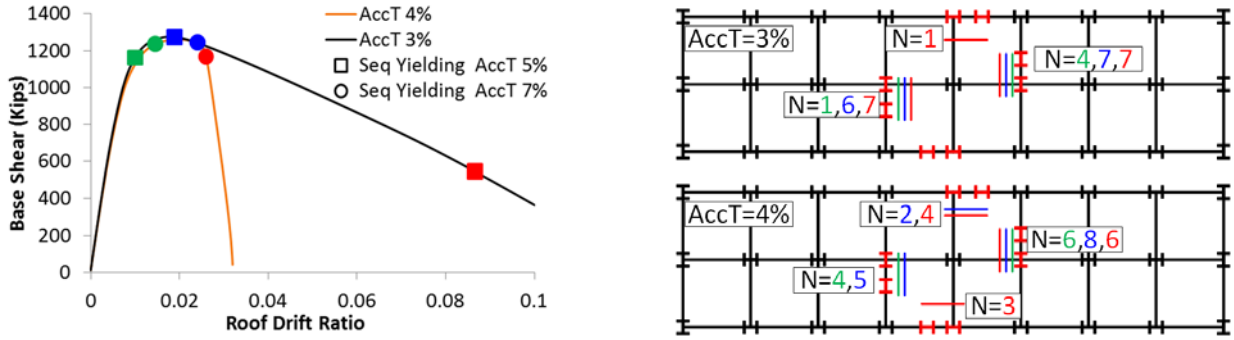

Figure 6 Sequence of Yielding Model A-2 including P-Δθ effects

By comparing the state of the system at the red dot and square in Figure 6, the bifurcation occurrence is explained. It can be seen that for a 3% eccentricity just one of the orthogonal BRB frames (E-W direction) is yielding while for 4% eccentricity, both orthogonal BRB frames are yielding. Therefore, the sudden degradation of the system capacity is due to yielding of the frames in the orthogonal direction. This outcome was also seen by De la Llera and Chopra [21] in their investigation.

8. Nonlinear Dynamic Analyses

While nonlinear static pushover analysis clearly illustrated the importance of adequately model P-Delta effects and P-Theta, NLRH provide additional insight into the performance of the system. This section shows the results of the NLRH analysis were each model was subjected to 11 ground acceleration recordings, representing 11 actual earthquake events selected from the P-695 Far-field record set listed in Table 5. The number of ground motions to be used in this investigation is the minimum required by ASCE7-16 when NLRH is to be performed.

Table 5 Input Ground Motions

Earthquake		PGA (N-S)	PGA (E-W)	Earthquake		PGA (N-S)	PGA (E-W)
1	Cape Mendocino-Rio Dell	0.45g	0.32g	7	Manjil-Abbar	0.41g	0.39g
2	Duzce-Bolu	0.52g	0.46g	8	Northridge-BH	0.34g	0.27g
3	Hector-Hector	0.37g	0.29g	9	Northridge-CC	0.40g	0.34g
4	Kobe-Nishi Akashi	0.52g	0.52g	10	San Fernando-LA	0.44g	0.37g
5	Kocaeli-Duzce	0.25g	0.22g	11	Superstition Hills-Poe	0.52g	0.35g
6	Landers-Yermo	0.24g	0.15g				

The horizontal component with the largest peak ground acceleration was selected for use for N-S direction shaking, and each component was amplitude scaled for consistency with MCE_R level shaking at the lateral period of vibration in the N-S and E-W direction. For each analysis the system was first subjected to gravity load, followed by ground shaking and the drifts were the largest measured at the corners of the building. As with the pushover analysis the parameter varied for the analyses was the amount of accidental eccentricity. The results shown in the following subsection are for the structures subjected to both components of ground motions simultaneously. Due to page limit restrictions the results of the structures subjected to only one ground motion component are not shown in this paper. However, the influence of subjecting the structure to both components is significant, as demonstrated in Flores et al. [15].

8.1 Including P-Delta Effects

NLRH analysis was performed on each of the models with different approaches of including P-Delta effects. In order to evaluate the effects of P-Delta on the torsional response, an accidental torsion was introduced to the model by moving the center of mass a certain eccentricity while maintaining a constant total mass. The eccentricities at which the structures were subjected to were 3%, 5% and 7%. The roof drift time history for Model A-2 with translational P-Δ effects subjected to Duzce-Bolu and Landers-Yermo are shown in Figure 7 a) and b) respectively. It can be seen that in both cases the influence of the torsional response is minimum. Thus if only P-Δ effects are included it would not matter if accidental torsion is taken into consideration.

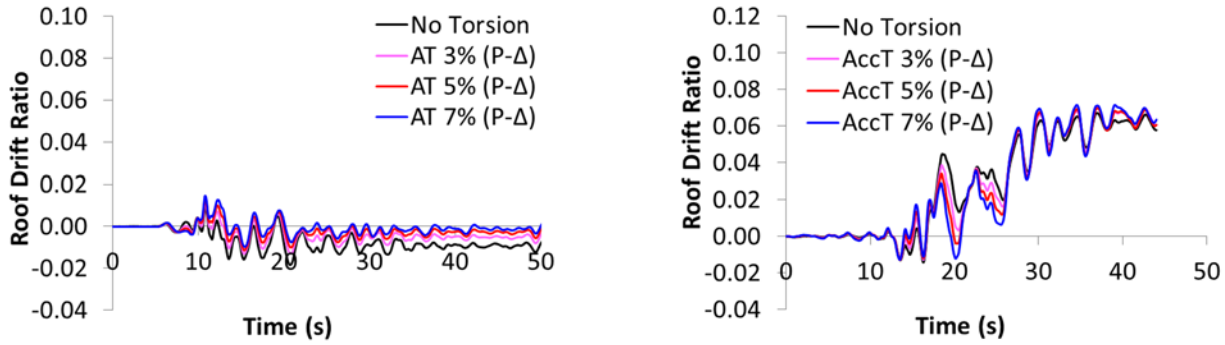

a) Bidirectional loading Duzce-Bolu

b) Bidirectional loading Landers-Yermo

Figure 7 Total Drift Time History Response Model A-2 including P-Δ effects

8.2 Including P-Delta effects and partially P-Theta effects

The building analyzed to incorporate P-Δθp effects was subjected to the same ground motions as the first case. The results of these analyses are shown in Figure 8 a) and b). Figure 8 a) illustrates the effects of accidental torsion when the structure is subjected to the Duzce-Bolu earthquake. It can be seen that in this case the torsional effects worsen the response because P-θ effects are included. A similar response occurred when the building was subjected to the Landers-Yermo ground motion. For the latter case, an accidental torsion of 7% is causing according to FEMA 350 [22] collapse because it has a drift of 10%.

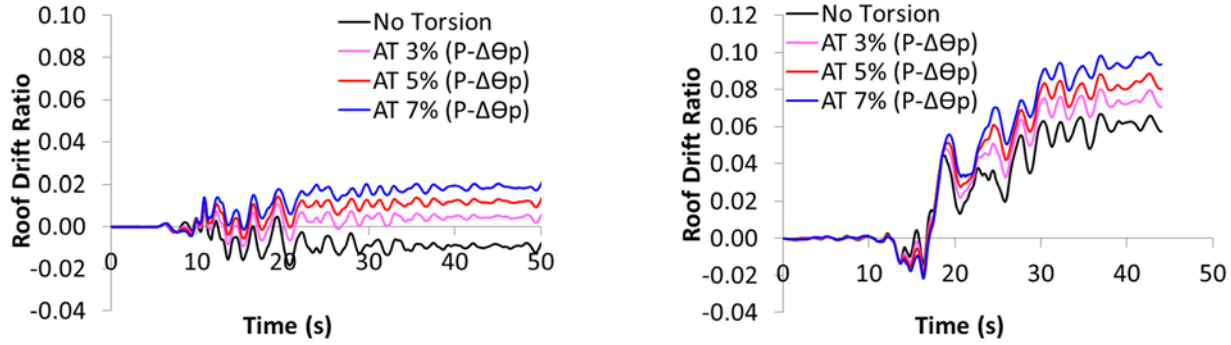

a) Bidirectional loading Duzce-Bolu

b) Bidirectional loading Landers-Yermo

Figure 8 Total Drift Time History Response Model A-2 including P-Δθp effects

8.3 Including P-Delta and P-Theta effects

From the previous two cases it was seen that torsional effects worsen the building's response when P-θ effects are being considered even if it is just partially. Where P-Delta and P-Theta effects are fully represented by modeling the geometric stiffness of all columns, the building was subjected to the same ground motions and the results for Duzce-Bolu and Landers-Yermo are shown in Figure 9 a) and b). Unlike the other two approaches, for this case the Duzce-Bolu ground motion is causing dynamic instability when accidental torsion is included. The same is occurring for Landers-Yermo where for all accidental eccentricities the building is collapsing.

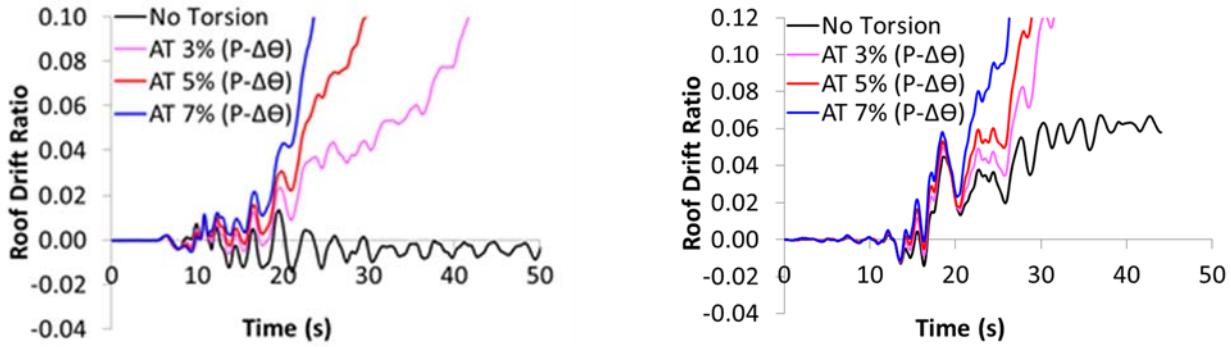

a) Bidirectional loading Duzce-Bolu

b) Bidirectional loading Landers-Yermo

Figure 9 Total Drift Time History Response Model A-2 including P-Δθ effects

The results obtained from the NLRH demonstrated once more the fundamental importance of modeling P-Theta effects adequately when the torsional response is to be evaluated. The effects of accidental torsion went from no effect whatsoever when only P-Δ effects are included to collapse of the structure when P-Δθ effects were incorporated adequately. The results were improved when P-Δθp was included in the model, but important response characteristic were underestimated. These results followed the same trend for all the 11 ground motions that were analyzed and this is shown in Table 6 with a summary of the collapses occurred for all the cases. Table 6 presents all the collapses that occurred for each of the approaches used to incorporate P-Δ and P-θ effects. The lack of the model to predict any collapses is a serious shortcoming of using a single leaning column at the center of the building. Using four leaning columns at the middle of the four building quadrants is an improvement, but P-θ effects are incorporated just partially. For this case only 1 collapse occurred for all the accidental eccentricities. Using four leaning columns might be sufficient but more research is required to define the exact location and gravity load for the columns. Finally it can be seen that if P-θ effects are incorporated adequately the number of collapses is equal to 6 for an accidental torsion equal to 5%. It is important to point out that 5% is the accidental torsion usually given by codes and that the number of collapses allowed by ASCE7-16 is one among the 11 ground motions analyzed. Therefore failing to include correctly these effects significantly overestimates the building response.

Table 6 Summary of Collapses under Dynamic Loading

	Model A-2			
Accidental Torsion	**0%**	**3%**	**5%**	**7%**
Bidirectional (P-Δ)	0	0	0	0
Bidirectional (P-Δθp)	0	1	1	1
Bidirectional (P-Δθ)	0	5	6	7

9. Conclusions

This study focused on the consequences of including P-Delta and P-Theta effects in analysis of the torsional response of structures. Three approaches for including such effects were considered. The first approach used only one leaning column at the centroid of the building, including only translational P-Δ effects. The second approach was the same as used in the study by DeBock et al., where only four leaning columns were placed at the centroid of each of the building's quadrant. This approach incorporates completely translational P-Δ effects but just partially the rotational P-θ effects. The third and last approach used all the gravity columns as leaning columns to incorporate completely translational P-Δ and rotational P-θ effects. The results obtained from using the three approaches when nonlinear static and dynamic analyses were performed are significantly different. In the case of the pushover analyses, a bifurcation point appeared when P-θ effects are incorporated, even when only partially included. This bifurcation point, where a sudden strength degradation occurred, was a result of the orthogonal frames yielding. This behavior was not seen at all for the first approach, it occurred for an accidental torsion equal to 8% for the second approach and an accidental torsion equal to 4% for the last method. The bifurcation seen on the pushover curves had a detrimental effect on the NLRH analysis. The incorporation of P-Δθ effects into the analyses caused the collapse of the structure for several cases. This was not seen at all for the first approach and it occurred only once when the P-θ effects were included partially.

After performing all the analyses and observing and analyzing all the results, it can be concluded that inclusion of P-θ effects are essential when a model is analyzed in three dimensions, especially if torsional response is to be evaluated. The approach of using four leaning columns might be viable by placing them in specific locations that capture rotational P-Delta effects adequately. However, it would be difficult to implement this approach for structures that have a complex geometry. Thus, the only rational approach is to use the "Full System Modeling" method wherein each gravity column is explicitly modeled in the correct location with the correct vertical load. Where the column is not part of the lateral load resisting system the stiffness and strength need not be included, although there might be an advantage to include this as shown by the studies by Flores et. al.[23, 24].

10. Acknowledgments

The work presented herein was possible through the support of the Pontificia Universidad Catolica de Chile, Virginia Tech and the University of Cuenca.

11. References

[1] NIST, (2010): Nonlinear Structural Analysis for Seismic Design (*NIST GCR 10-917-5*), National Institute of Standards and Technology, Gaithersburg, MD.

[2] NIST, (2010): Applicability of Nonlinear Multiple-Degree-of-Freedom Modeling for Design (*NIST GCR 10-917-9*), National Institute of Science and Technology, Gaithersburg, MD.

[3] PEER, (2010): Guidelines for Performance Based Design of Tall Buildings, Pacific Earthquake Engineering Research Center, University of California, Berkeley, CA.

[4] PEER, (2010): Modeling and Acceptance Criteria for Seismic Design and Analysis of Tall Buildings (*PEER/ATC 72-1*). Pacific Earthquake Engineering Research Center, Richmond, CA.

[5] NIST, (2011): Selecting and Scaling Earthquake Ground Motions for Performing Response-History Analysis (*NIST GCR 11-917-5*), National Institute of Science and Technology, Gaithersburg, MD.

[6] FEMA, (2009): 2009 NEHRP Recommended Seismic Provisions for New Buildings and Other Structures (*FEMA P-750*), Federal Emergency Management Agency, Washington, D.C.

[7] ASCE, (2011): ASCE 7-10: Minimum Design Loads for Buildings and Other Structures, American Society of Civil Engineers, American Society of Civil Engineers/Structural Engineering Institute, Reston, VA.

[8] ASCE,(2013): Seismic Rehabilitation of Existing Buildings (*ASCE/SEI 41-13*), in, American Society of Civil Engineers Reston, Virginia.

[9] SFBC, (2013): Requirements and Guidelines for the Seismic Design of New Tall Buildings Using Non-Prescriptive Design Procedures, 2013 San Francisco Building Code Administrative Bulletin 083, San Francisco, CA.

[10] LATBSDC, (2014): An Alternative Procedure for Seismic Analysis and Design of Tall Buildings Located in The Los Angeles Region, Los Angeles Tall Building Structural Design Council, Los Angeles, CA.

[11] FEMA, (2015): 2015 NEHRP Recommended Provisions for New Buildings and Other Structures (*FEMA P-1050*), Federal Emergency Management Agency, Washington, D.C.

[12] ASCE, (2017): ASCE 7-16: Minimum Design Loads for Buildings and Other Structures, American Society of Civil Engineers, American Society of Civil Engineers/Structural Engineering Institute, Reston, VA.

[13] D.J. DeBock, A.B. Liel, C.B. Haselton, J.D. Hooper, R.A. Henige, (2014): Importance of seismic design accidental torsion requirements for building collapse capacity, Earthquake Engineering & Structural Dynamics, **43** (6) 831-850.

[14] FEMA, (2009): Quantification of Building Seismic Performance Factors (*FEMA P-695*), Federal Emergency Management Agency, Washington, D.C.

[15] F.X. Flores, F.A. Charney, D. Lopez-Garcia, (2015): The influence of accidental torsion on the inelastic dynamic response of buildings during earthquakes, in: *XI Congreso Chileno de Sismología e Ingeniería Sísmica*, Santiago, Chile.

[16] E. Wilson, A. Habibullah, (1987): Static and dynamic analysis of multi-story buildings, including P-delta effects, *Earthquake Spectra*, **3** (2) 289-298.

[17] NIST, (2010): Evaluation of the FEMA P-695 Methodology for Quantification of Building Seismic Performance Factors (*NIST GCR 10-917-8*), National Institute of Standards and Technology, Gaithersburg, MD.

[18] AISC, (2005): Seismic Provisions for Structural Steel Buildings, *ANSI/AISC 341-05*, American Institute for Steel Construction., Chicago, Ill.

[19] F. McKenna, G. Fenves, M. Scott, (2006): OpenSees: Open system for earthquake engineering simulation, Pacific Earthquake Engineering Center, University of California, Berkeley, CA., http://opensees. berkeley. edu.

[20] O. Atlayan, (2013) Hybrid steel frames.

[21] J.C. De la Llera, A.K. Chopra, (1996): Inelastic behavior of asymmetric multistory buildings, *Journal of Structural Engineering*, **122** (6) 597-606.

[22] FEMA 350, (2000): Recommended seismic design criteria for new steel moment-frame buildings, *FEMA 350 Report.*

[23] F. Flores, F. Charney, D. Lopez-Garcia, (2016): The influence of gravity column continuity on the seismic performance of special steel moment frame structures, *Journal of Constructional Steel Research*, **118** 217-230.

[24] F.X. Flores, F.A. Charney, D. Lopez-Garcia, (2014) Influence of the gravity framing system on the collapse performance of special steel moment frames, *Journal of Constructional Steel Research*, **101** 351-362.

Appendix D: Additional Results "Assessment of Floor Accelerations in Special Steel Moment Frames"

Elastic Floor Response Spectra: 8-Story SMRF

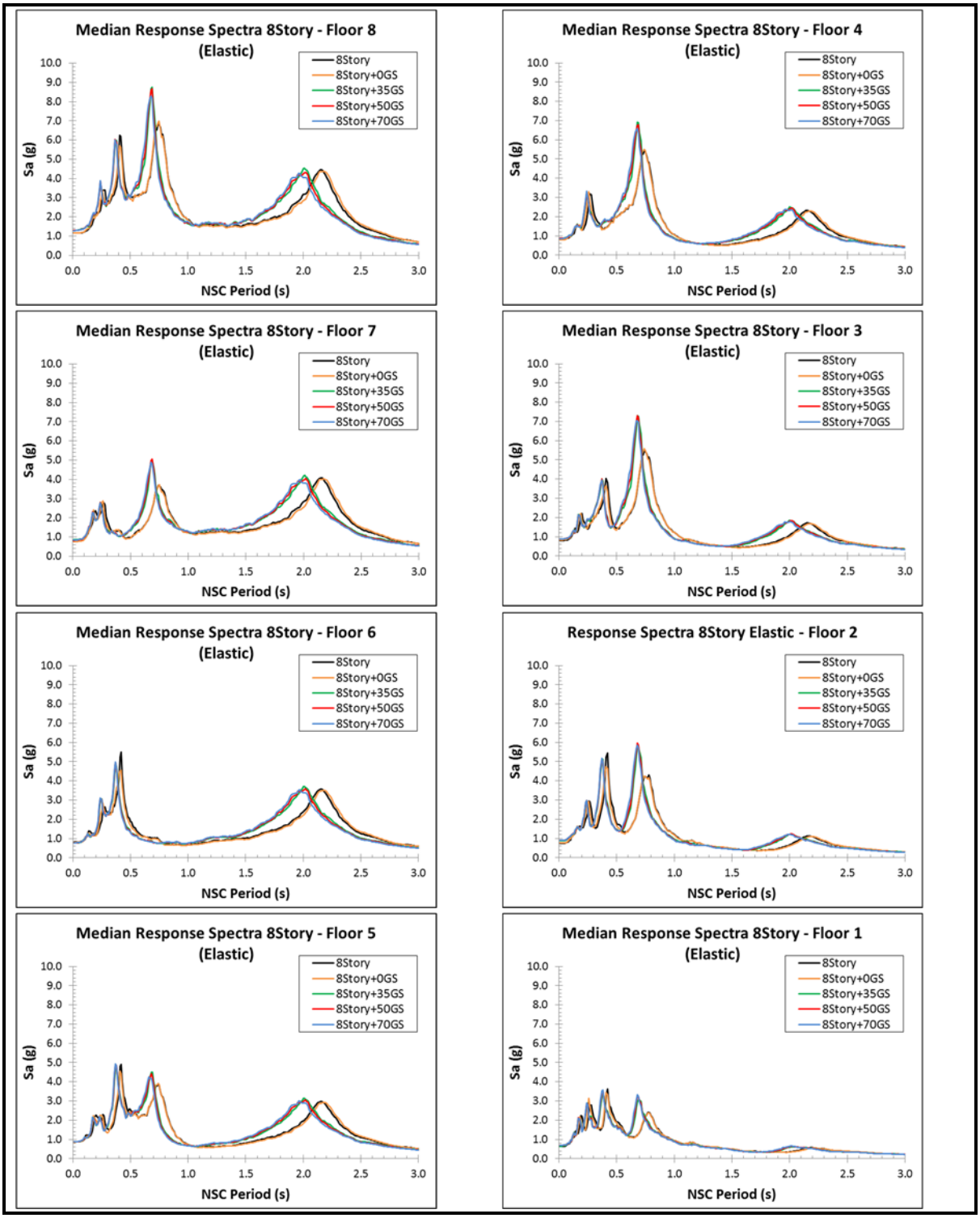

Inelastic Floor Response Spectra: 8-Story SMRF

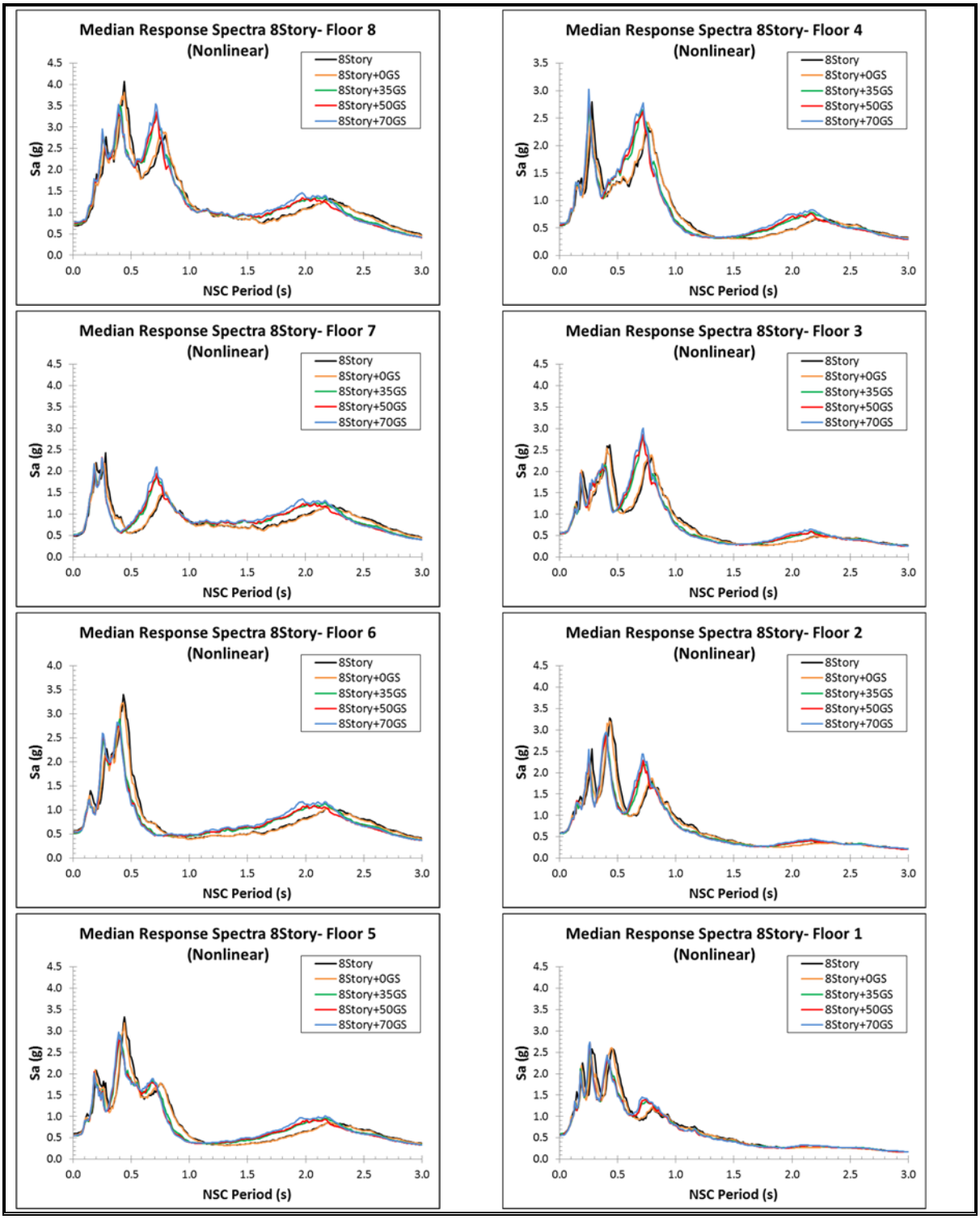

Floor Response Spectra Ratio: 8-Story SMRF

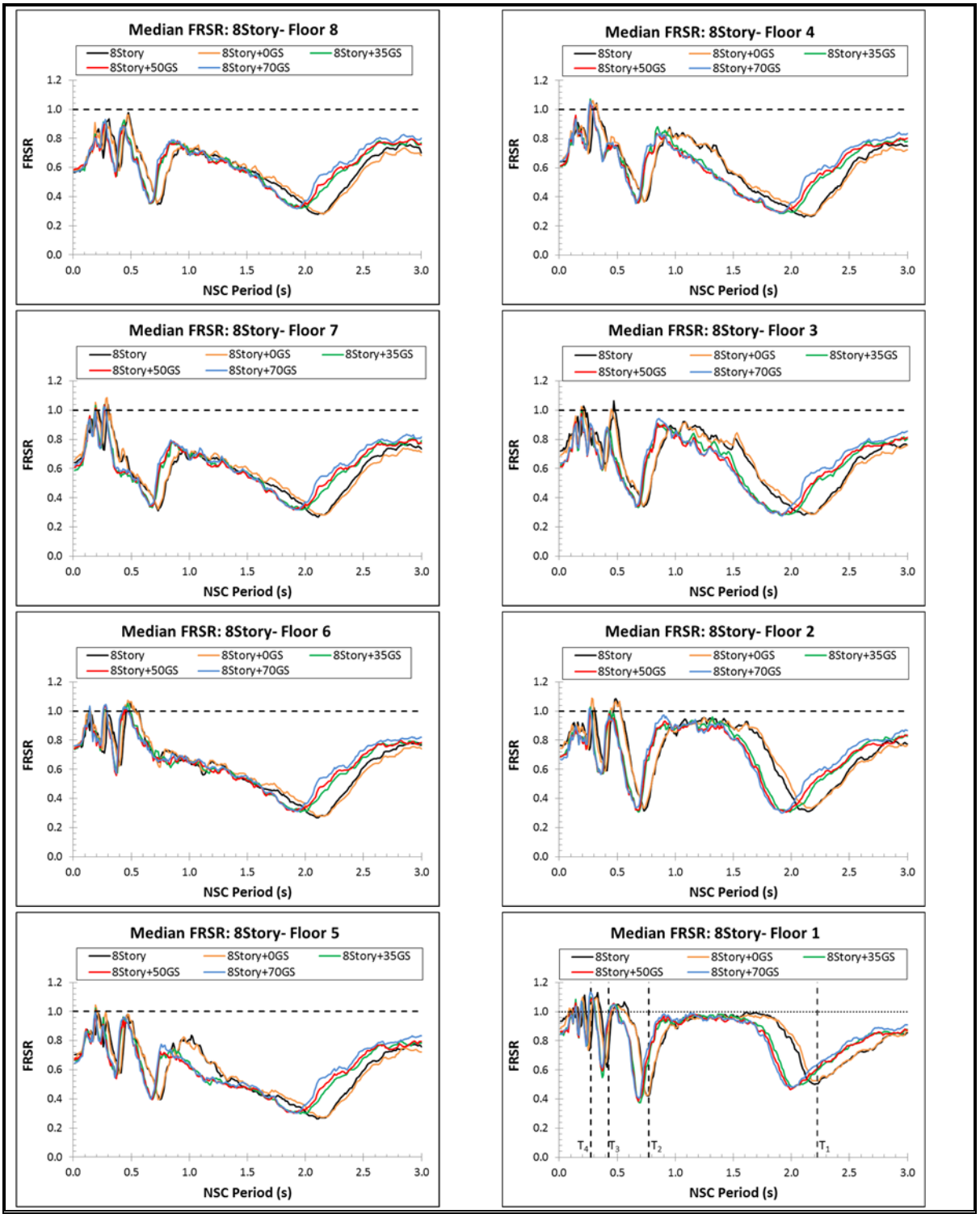

Elastic Floor Response Spectra: 4-Story SMRF

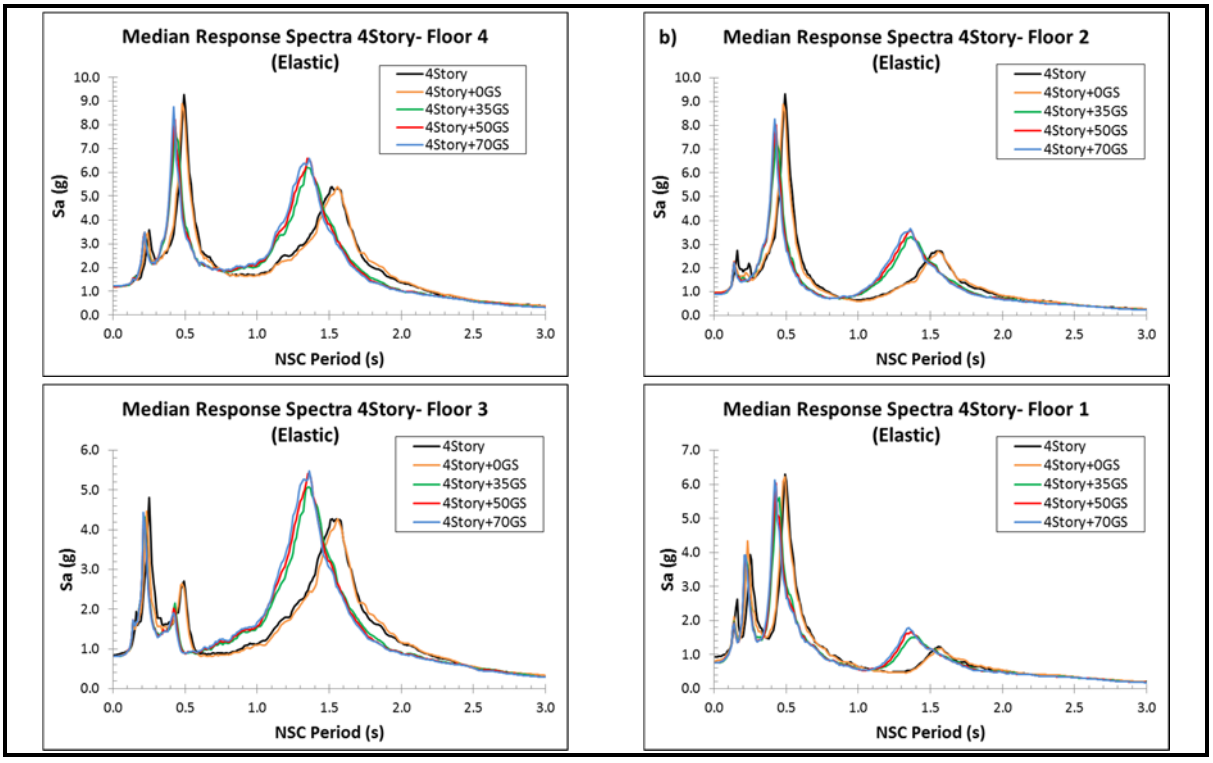

Inelastic Floor Response Spectra: 4-Story SMRF

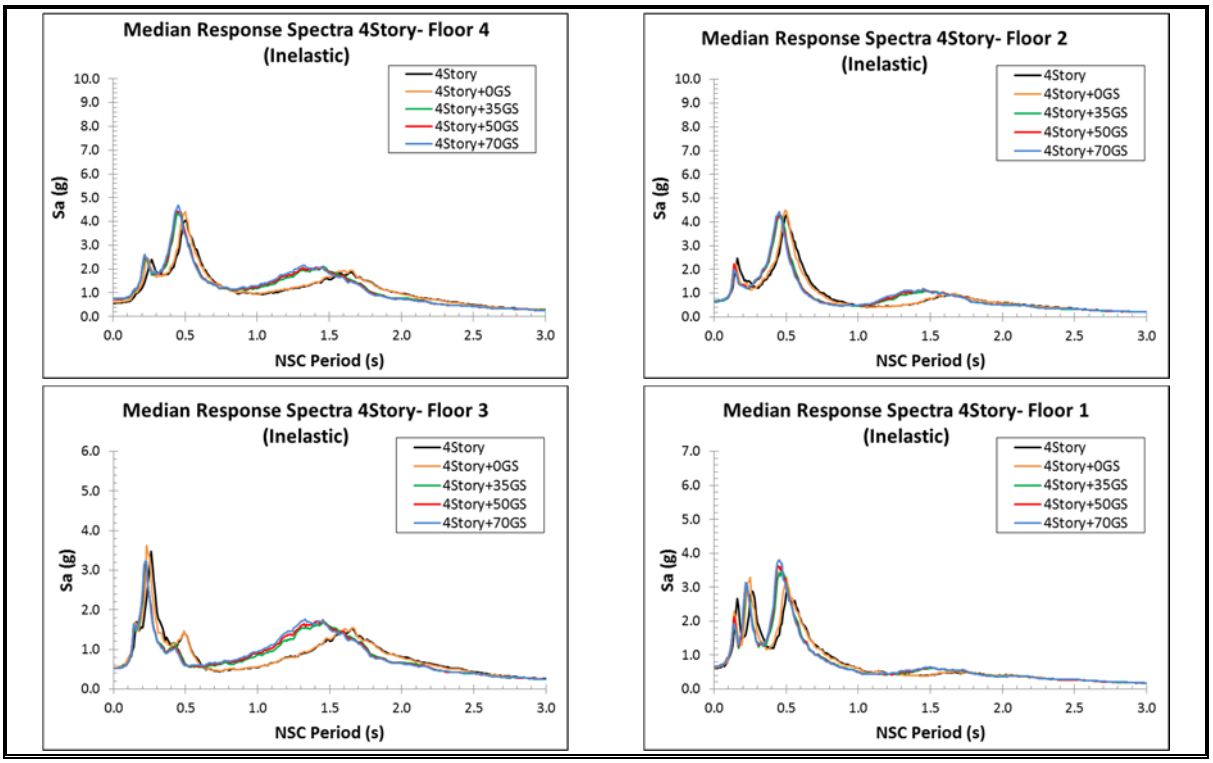

Floor Response Spectra Ratio: 4-Story SMRF

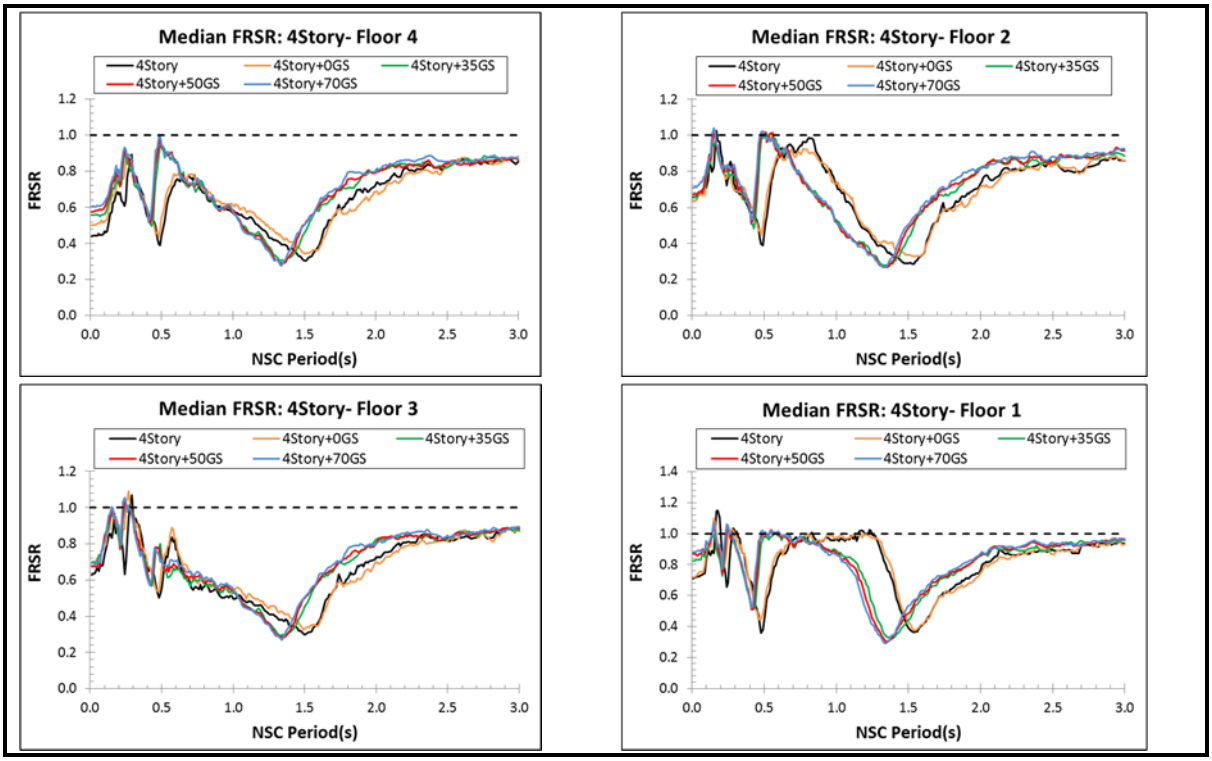

Elastic Floor Response Spectra: 2-Story SMRF

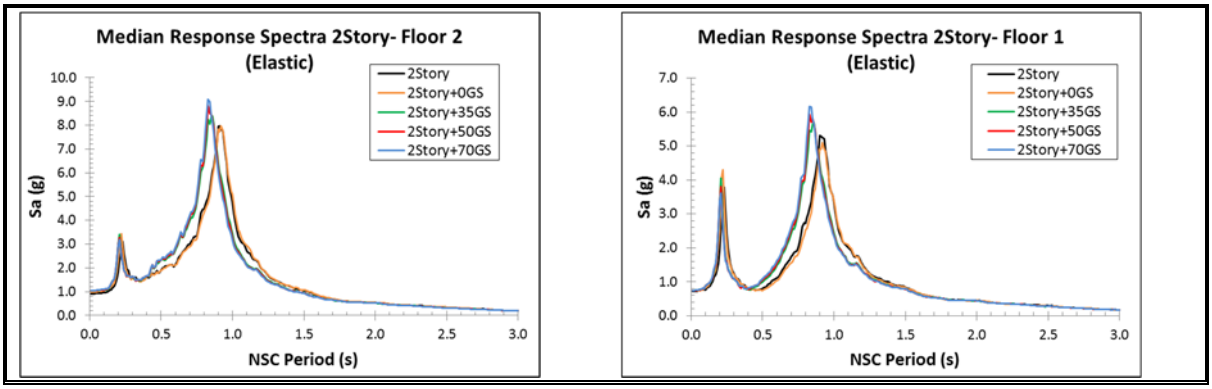

Inelastic Floor Response Spectra: 2-Story SMRF

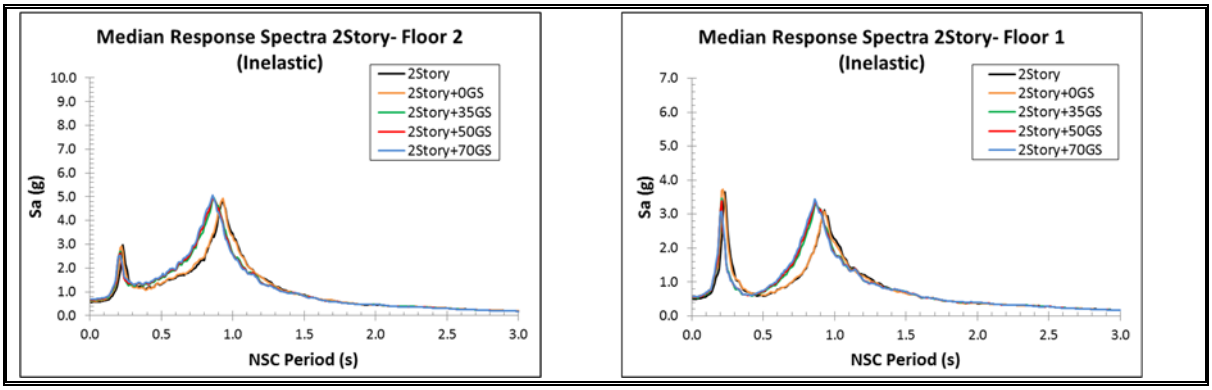

Floor Response Spectra Ratio: 2-Story SMRF

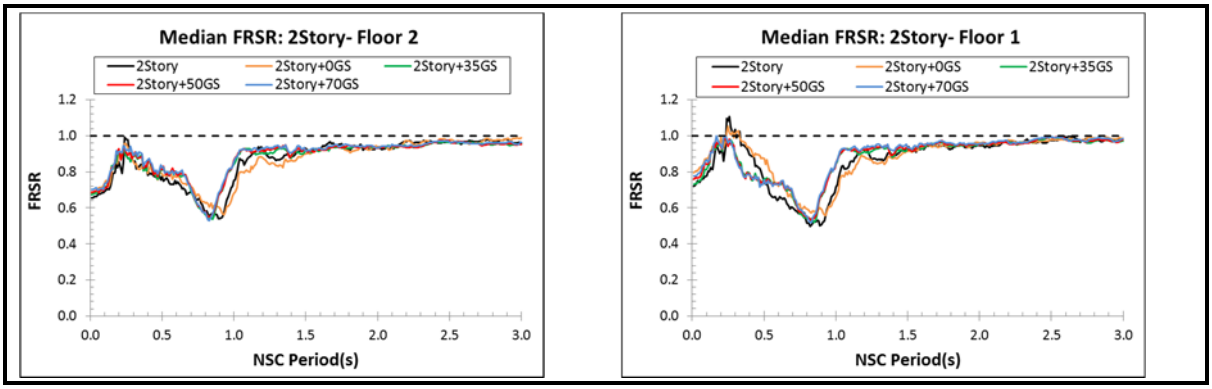

Appendix E: Additional Results "Floor Accelerations in SMRFs Having Different Structural Systems"

Elastic vs Inelastic Floor Response Spectra: 9-Story BRBF

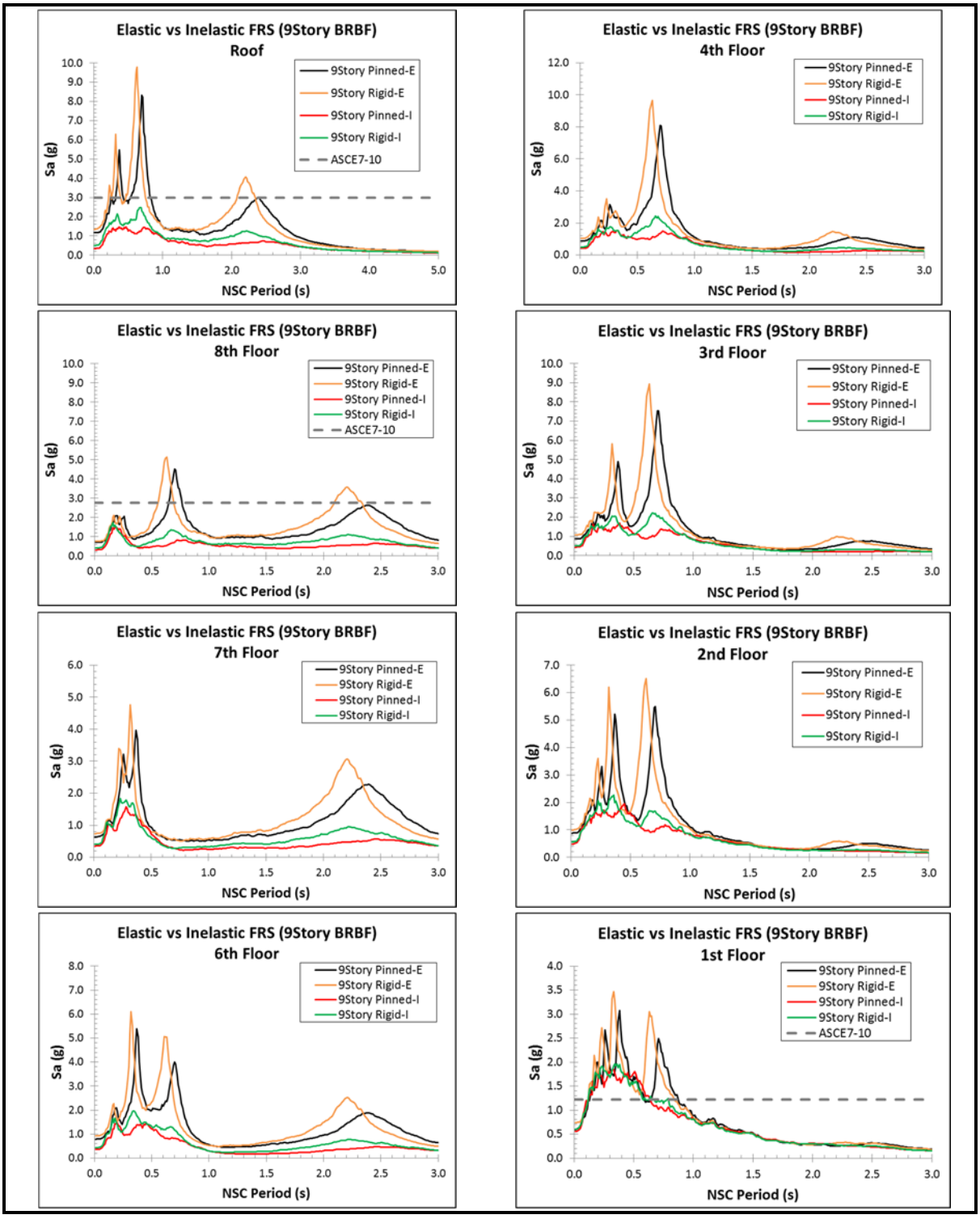

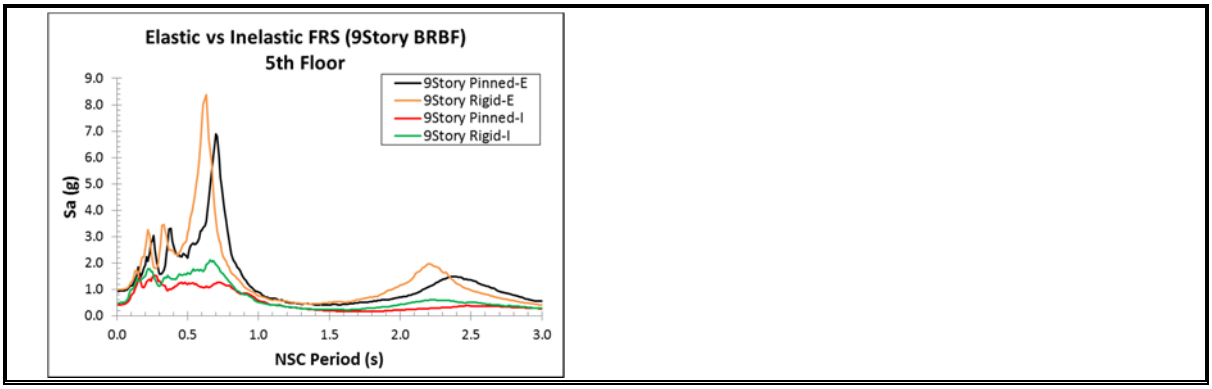

Floor Response Spectra Ratio: 9-Story BRBF

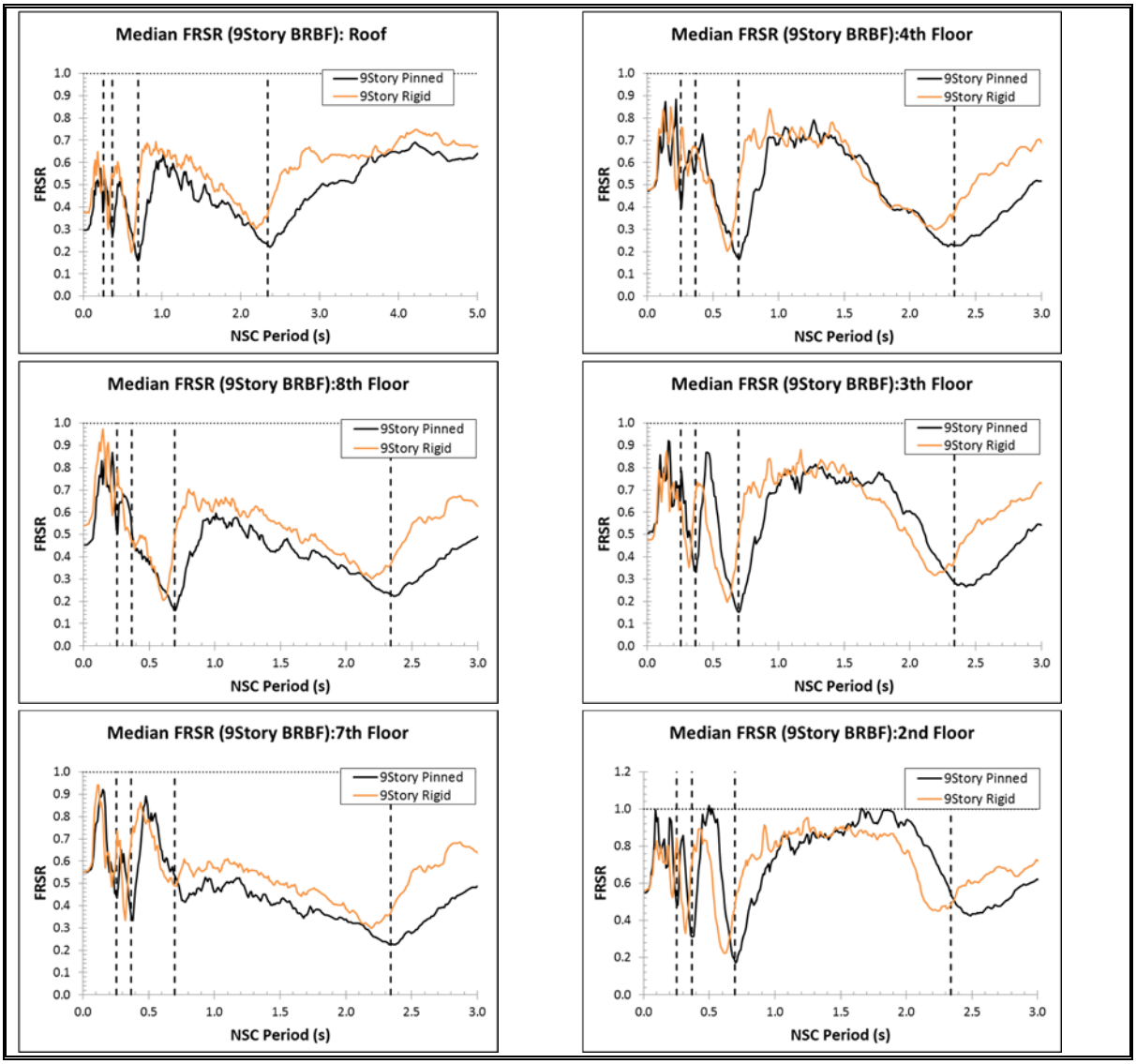

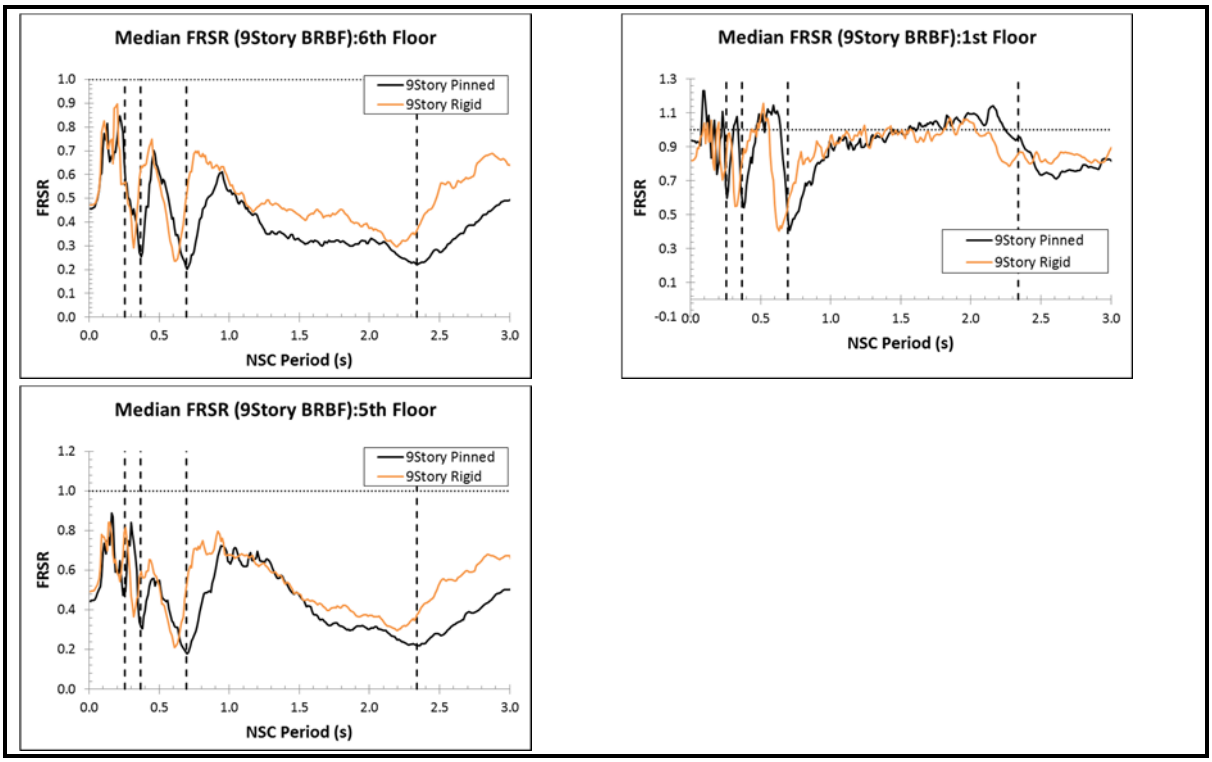
Median FRSR (9Story BRBF):6th Floor
9Story Pinned
9Story Rigid
FRSR
NSC Period (s)
Median FRSR (9Story BRBF):1st Floor
9Story Pinned
9Story Rigid
FRSR
NSC Period (s)
Median FRSR (9Story BRBF):5th Floor
9Story Pinned
9Story Rigid
FRSR
NSC Period (s)

Elastic vs Inelastic Floor Response Spectra: 4-Story BRBF

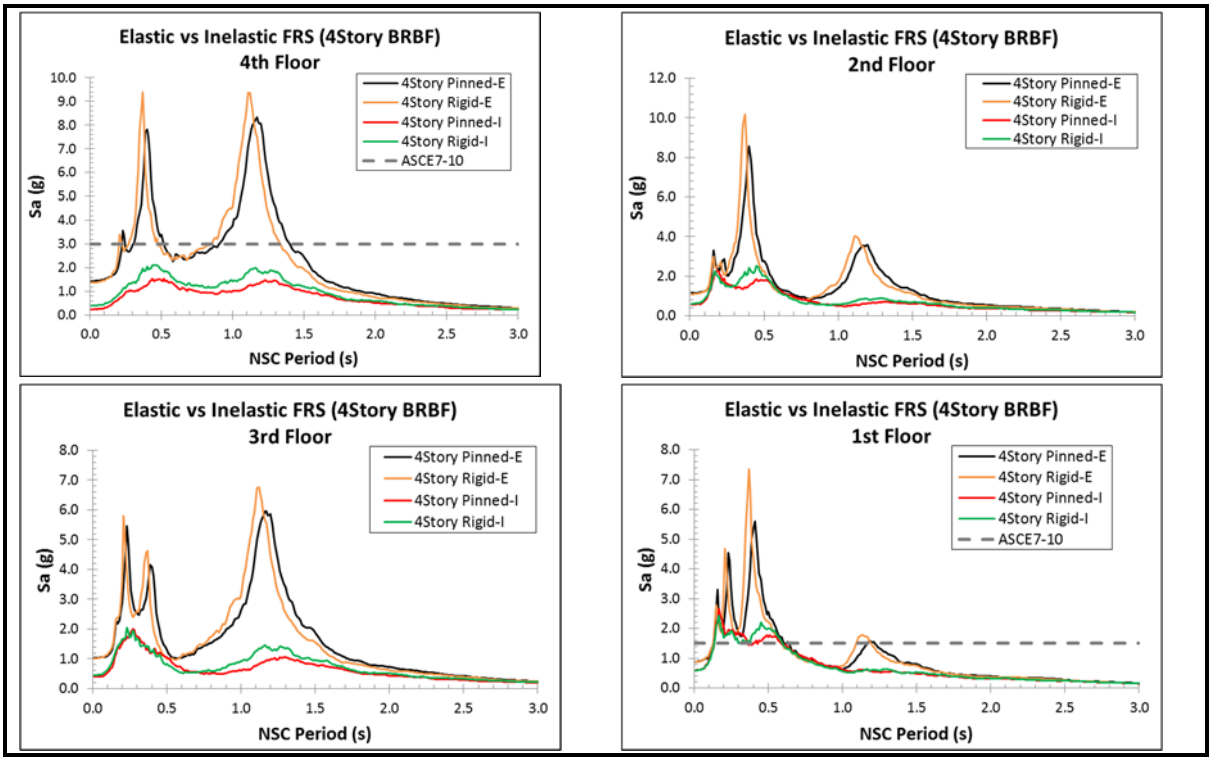

Floor Response Spectra Ratio: 4-Story BRBF

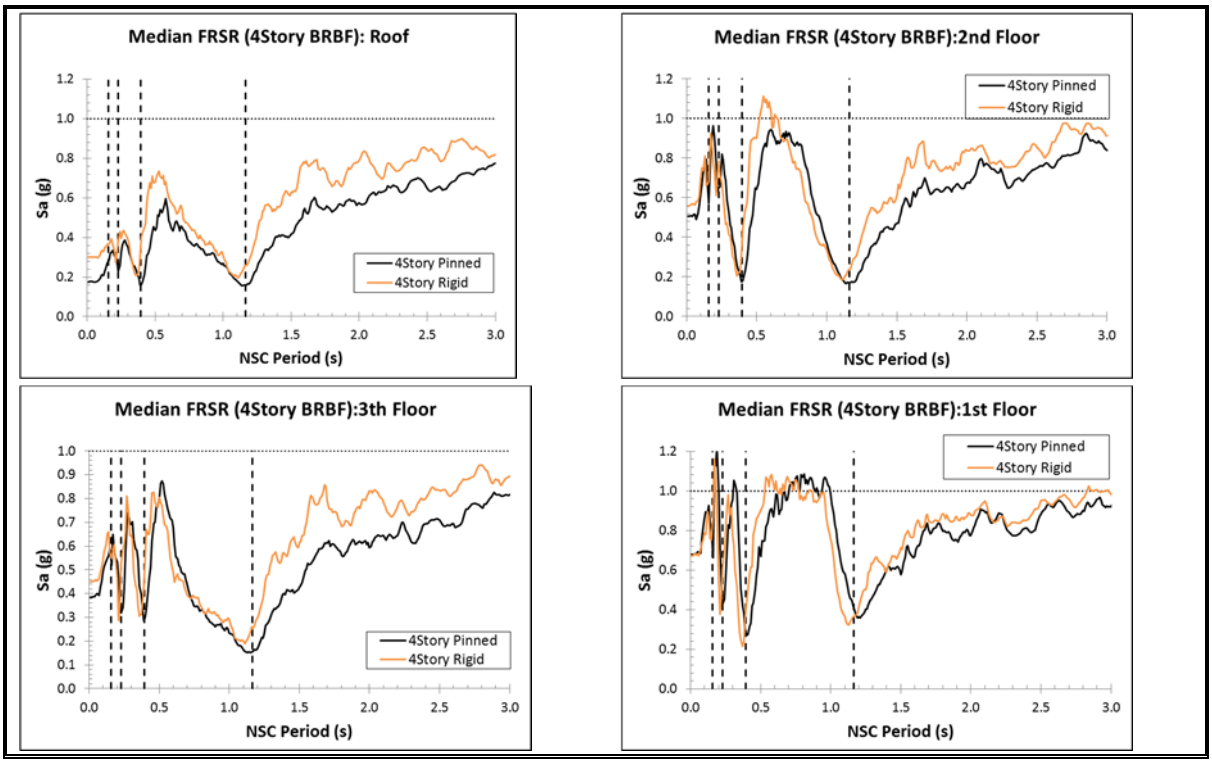

Elastic vs Inelastic Floor Response Spectra: 2-Story BRBF

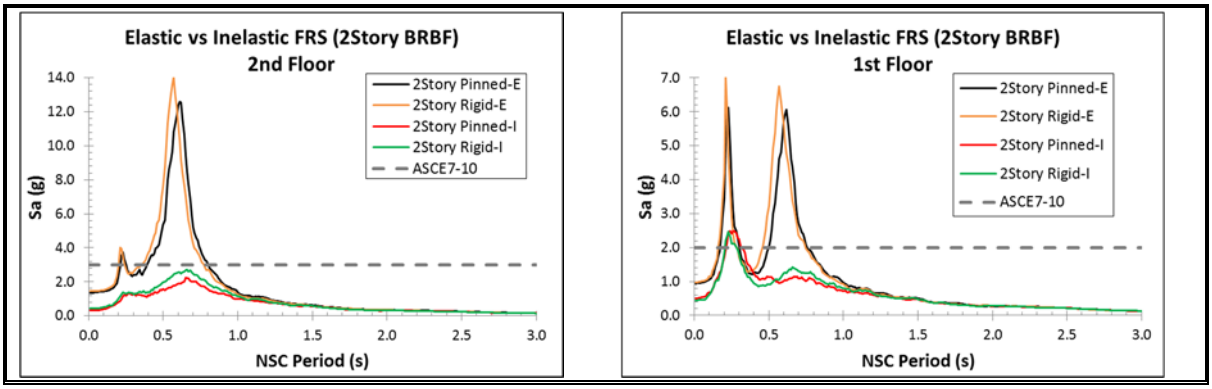

Floor Response Spectra Ratio: 2-Story BRBF

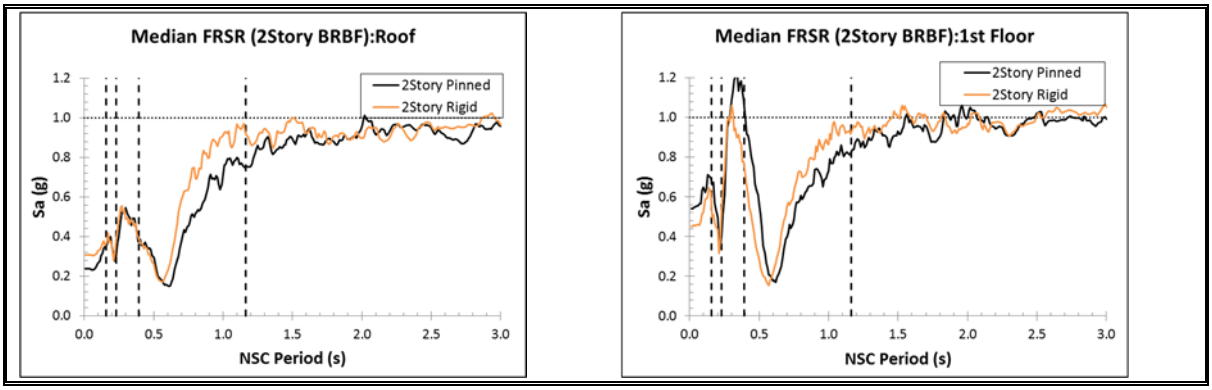

Appendix F: Additional Results "The Influence of Accidental Torsion on the Inelastic Dynamic Response of Buildings during Earthquakes"

Results Including P-Theta Effects

Model A: Unidirectional Loading

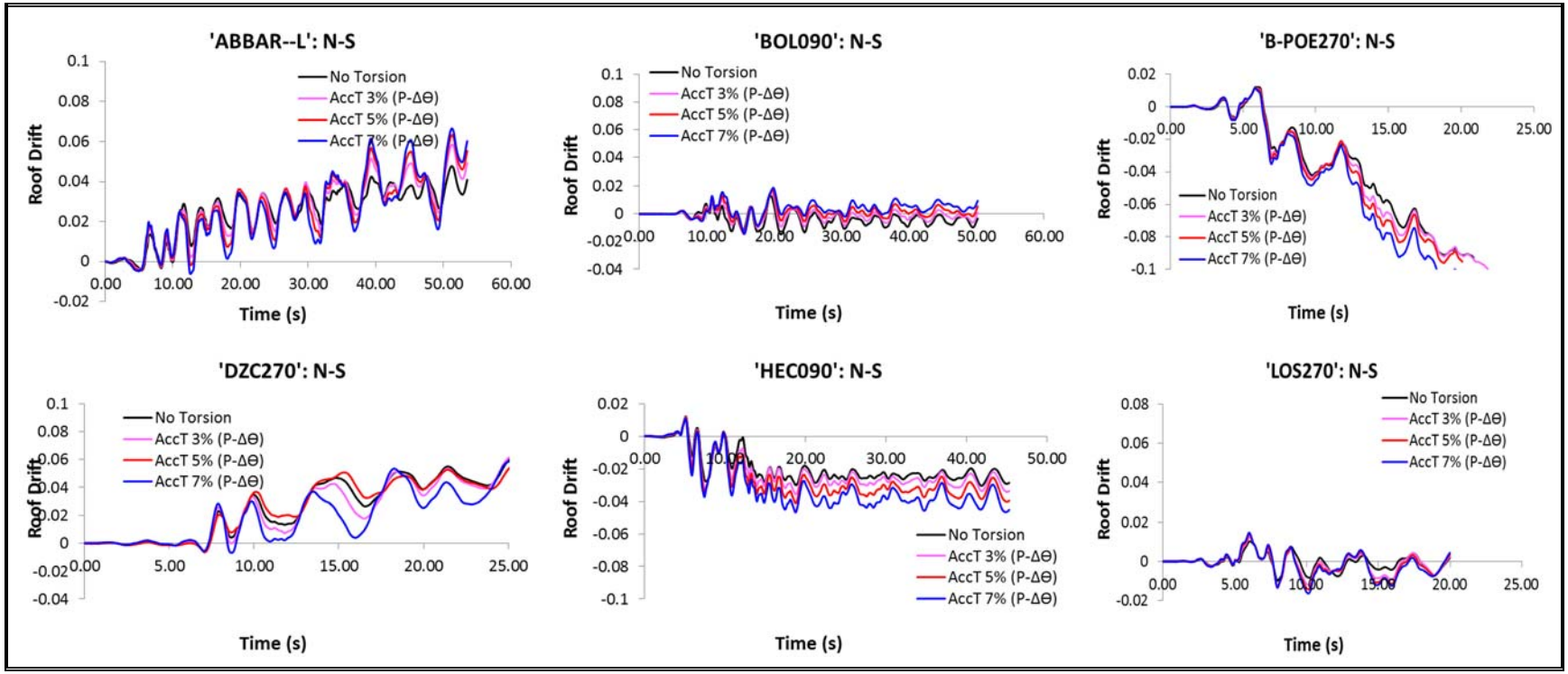

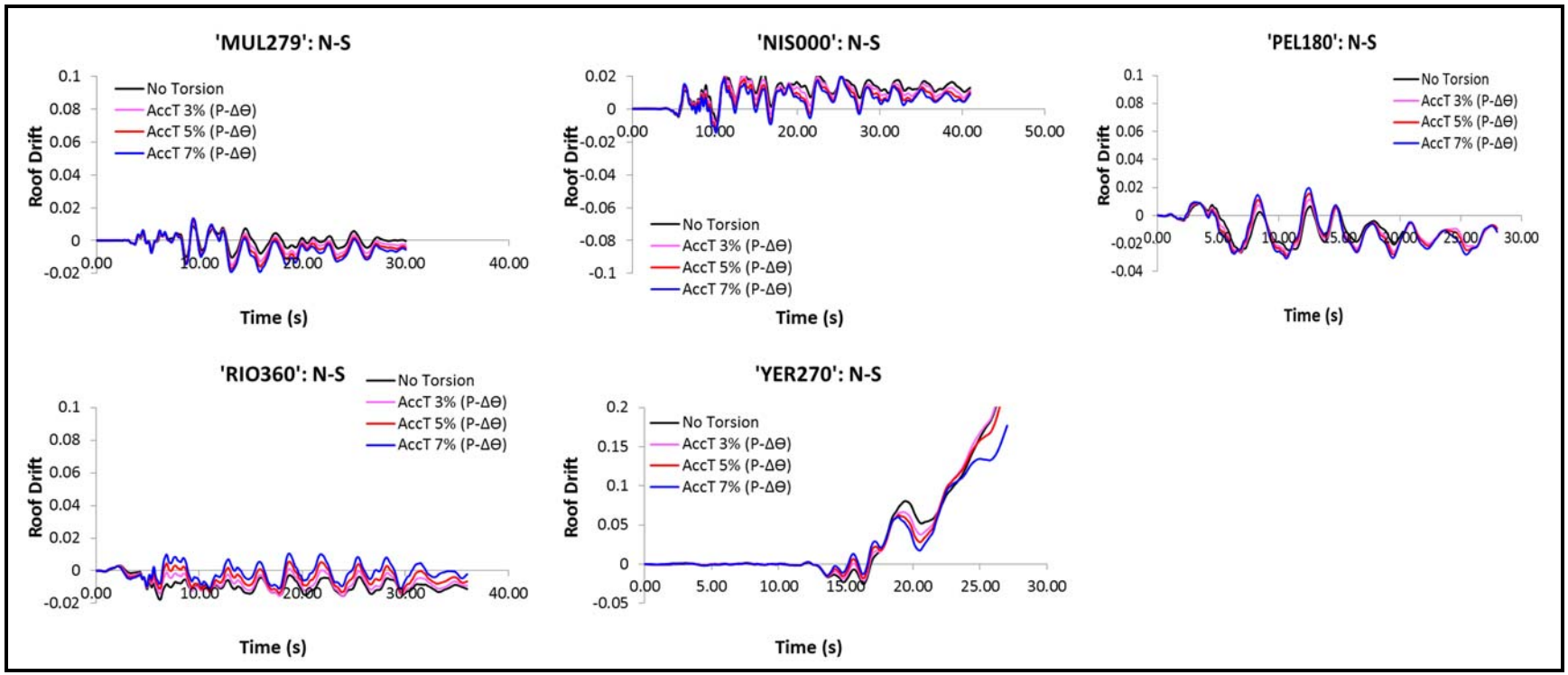
'MUL279': N-S
No Torsion
AccT 3% (P-ΔΘ)
AccT 5% (P-ΔΘ)
AccT 7% (P-ΔΘ)
Roof Drift
Time (s)
'NIS000': N-S
No Torsion
AccT 3% (P-ΔΘ)
AccT 5% (P-ΔΘ)
AccT 7% (P-ΔΘ)
Roof Drift
Time (s)
'PEL180': N-S
No Torsion
AccT 3% (P-ΔΘ)
AccT 5% (P-ΔΘ)
AccT 7% (P-ΔΘ)
Roof Drift
Time (s)
'RIO360': N-S
No Torsion
AccT 3% (P-ΔΘ)
AccT 5% (P-ΔΘ)
AccT 7% (P-ΔΘ)
Roof Drift
Time (s)
'YER270': N-S
No Torsion
AccT 3% (P-ΔΘ)
AccT 5% (P-ΔΘ)
AccT 7% (P-ΔΘ)
Roof Drift
Time (s)

Model A: Bidirectional Loading

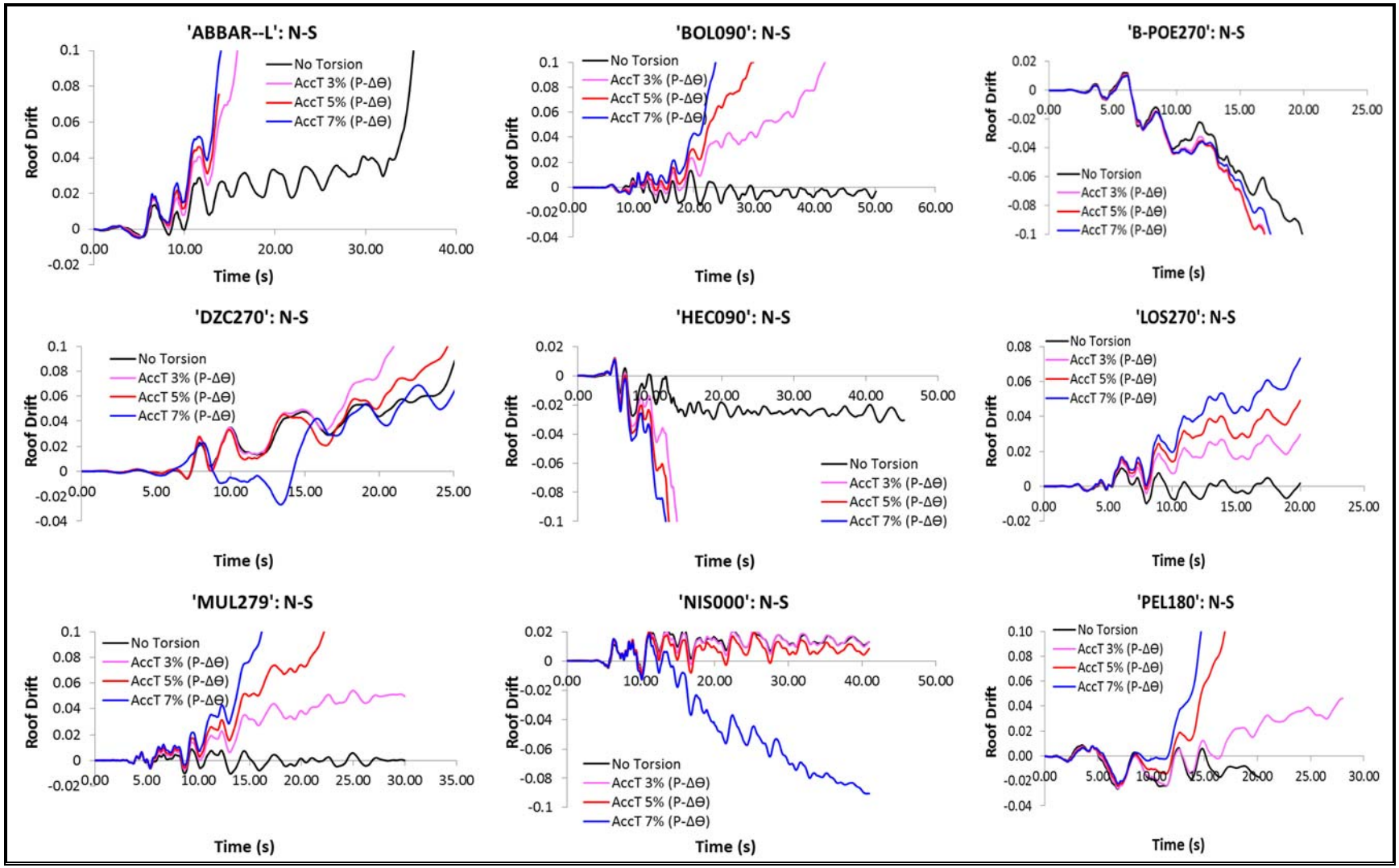

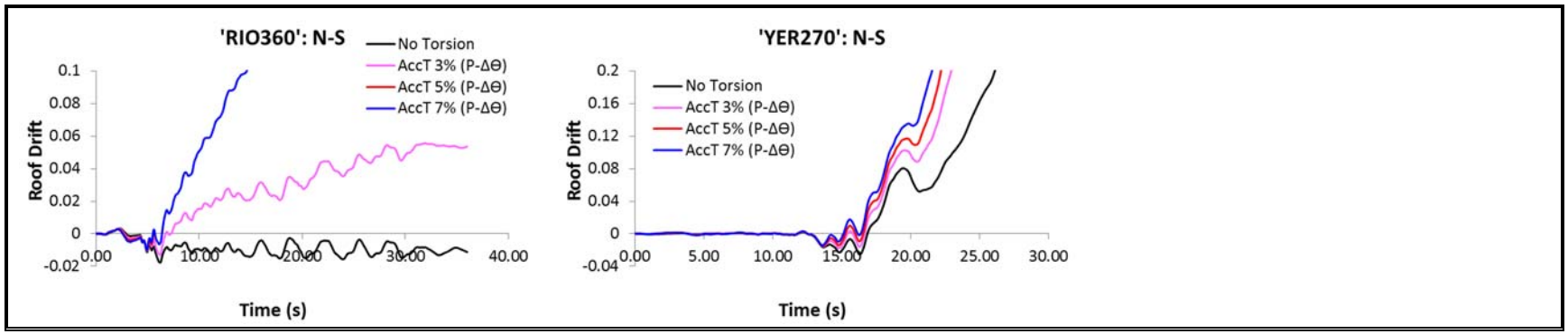
'RIO360': N-S
No Torsion
AccT 3% (P-ΔΘ)
AccT 5% (P-ΔΘ)
AccT 7% (P-ΔΘ)
Roof Drift
0.1
0.08
0.06
0.04
0.02
0
-0.02
0.00
10.00
20.00
30.00
40.00
Time (s)
'YER270': N-S
No Torsion
AccT 3% (P-ΔΘ)
AccT 5% (P-ΔΘ)
AccT 7% (P-ΔΘ)
Roof Drift
0.2
0.16
0.12
0.08
0.04
0
-0.04
0.00
5.00
10.00
15.00
20.00
25.00
30.00
Time (s)

Model A-2: Unidirectional Loading

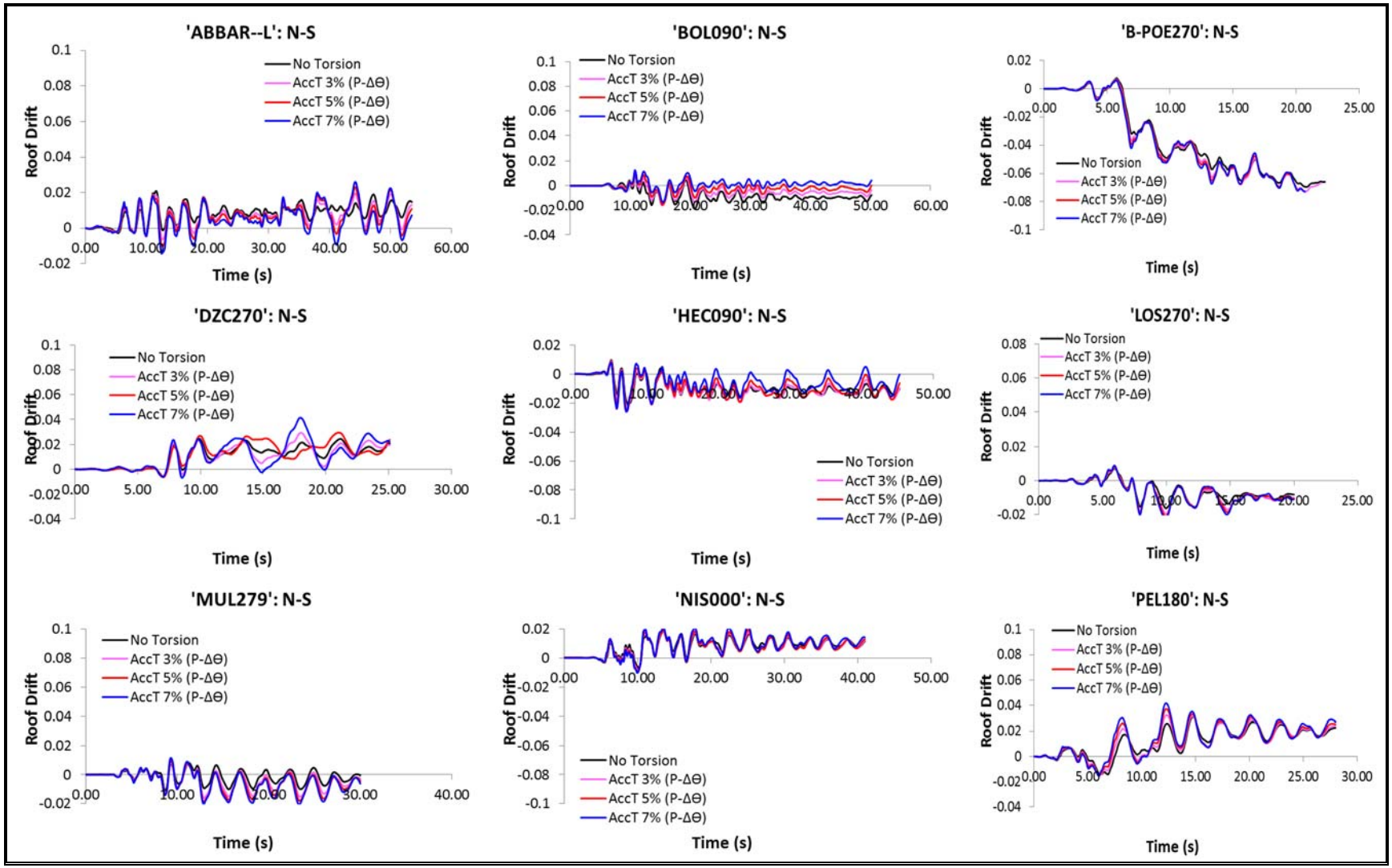

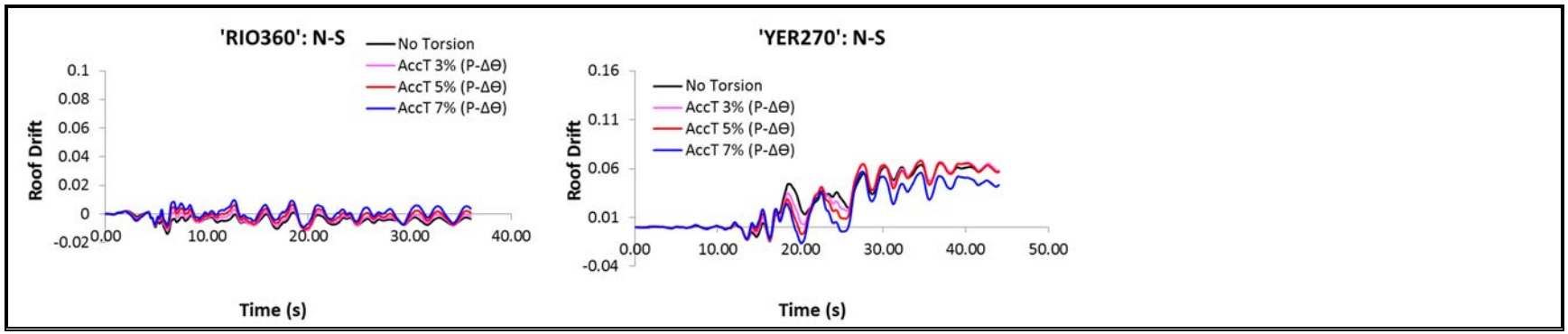
'RIO360': N-S
No Torsion
AccT 3% (P-ΔΘ)
AccT 5% (P-ΔΘ)
AccT 7% (P-ΔΘ)
Roof Drift
0.1
0.08
0.06
0.04
0.02
0
-0.02
0.00
10.00
20.00
30.00
40.00
Time (s)
'YER270': N-S
No Torsion
AccT 3% (P-ΔΘ)
AccT 5% (P-ΔΘ)
AccT 7% (P-ΔΘ)
Roof Drift
0.16
0.11
0.06
0.01
-0.04
0.00
10.00
20.00
30.00
40.00
50.00
Time (s)

Model A-2: 2-Directions

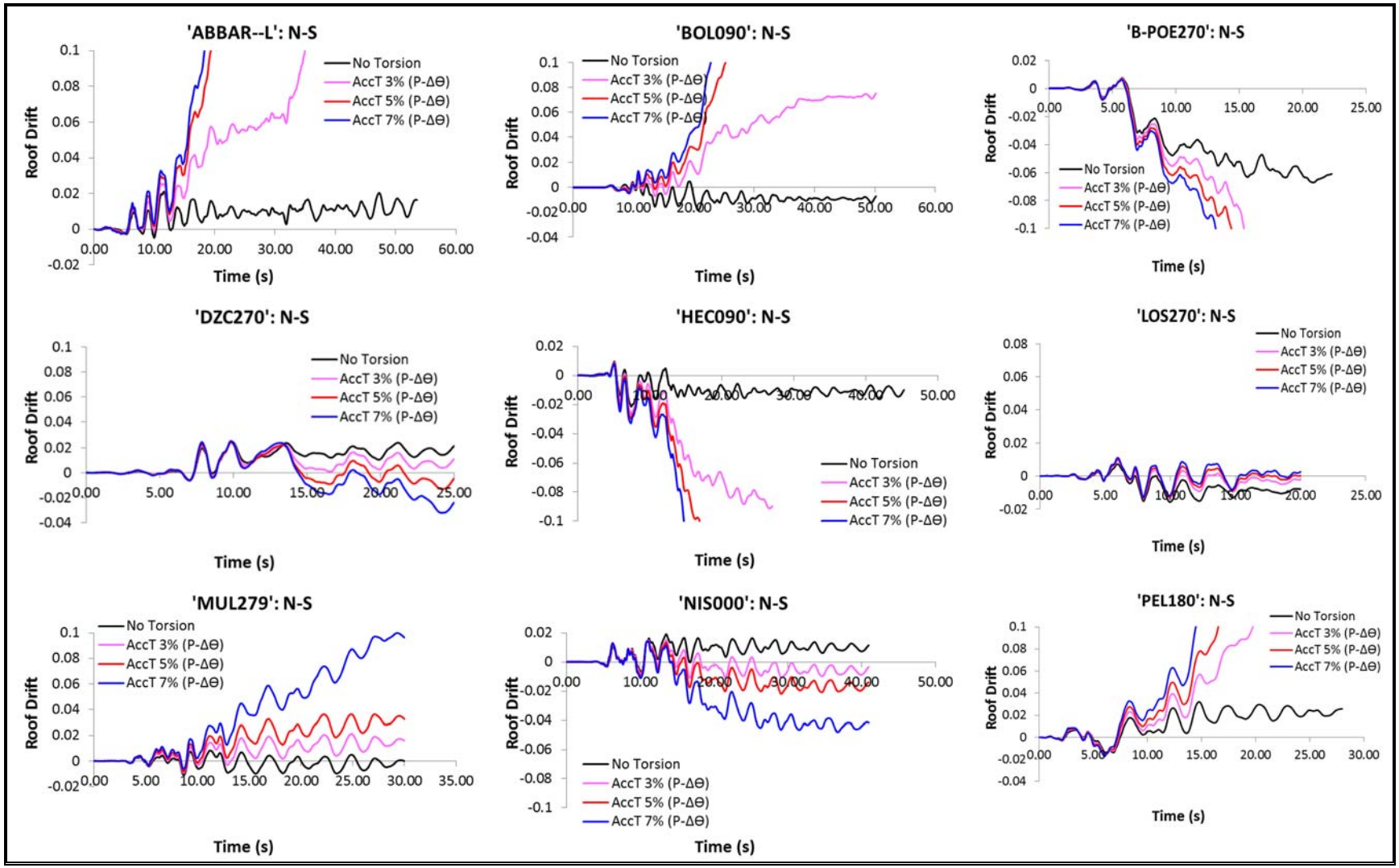

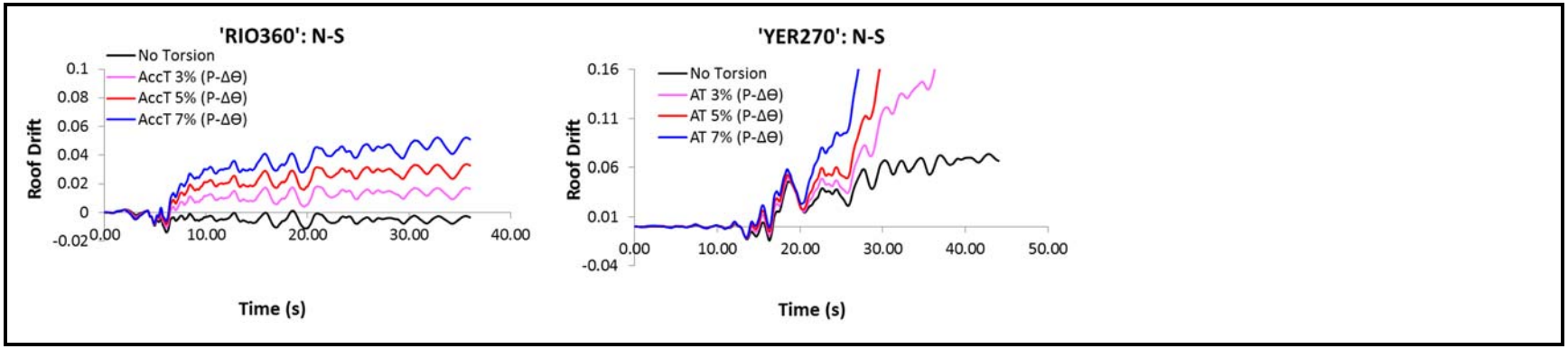
'RIO360': N-S
No Torsion
AccT 3% (P-ΔΘ)
AccT 5% (P-ΔΘ)
AccT 7% (P-ΔΘ)
Roof Drift
0.1
0.08
0.06
0.04
0.02
0
-0.02
0.00
10.00
20.00
30.00
40.00
Time (s)
'YER270': N-S
No Torsion
AT 3% (P-ΔΘ)
AT 5% (P-ΔΘ)
AT 7% (P-ΔΘ)
Roof Drift
0.16
0.11
0.06
0.01
-0.04
0.00
10.00
20.00
30.00
40.00
50.00
Time (s)

Model B: Unidirectional Loading

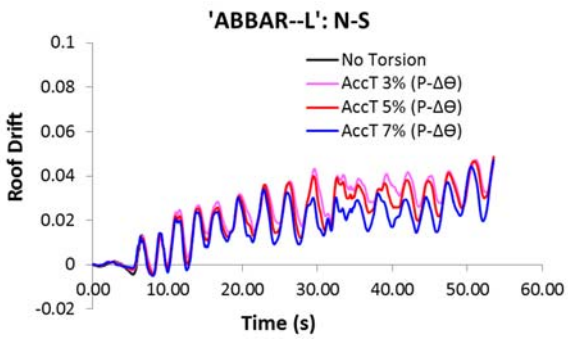

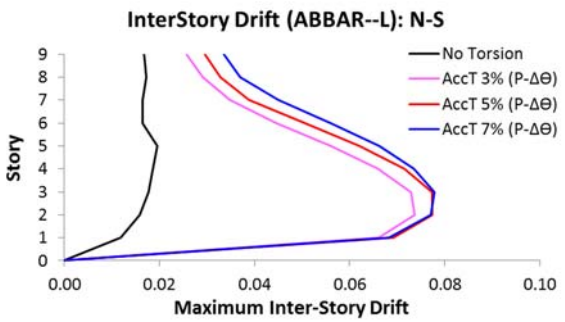

Abbar-L 1Direction without Accidental Torsion did not converge

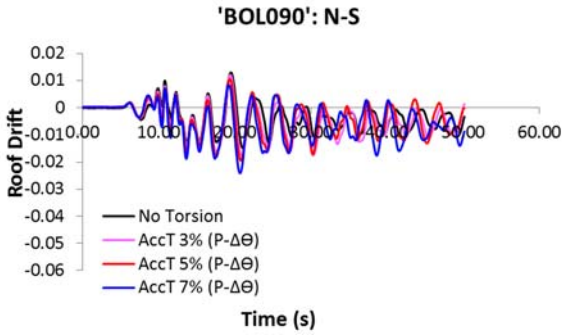

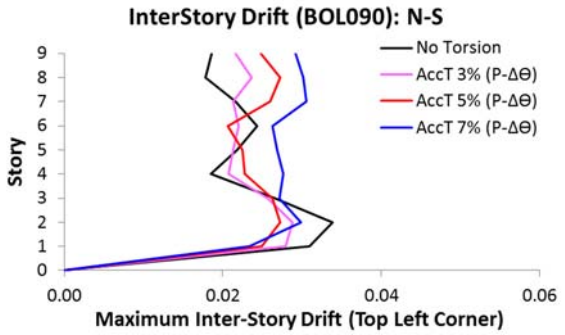

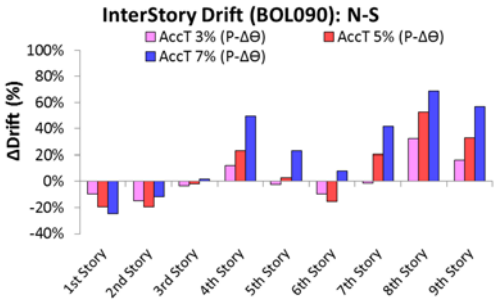

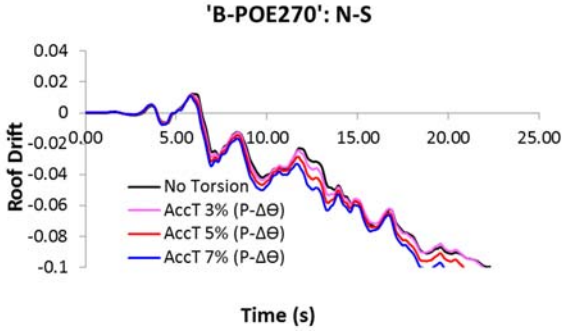

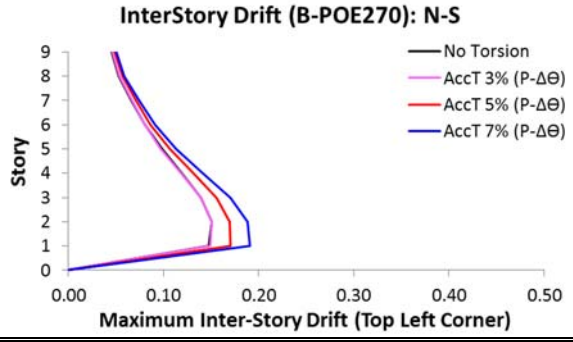

Inter-story drift larger than 0.1= collapse

Inter-story drift larger than 0.1= collapse

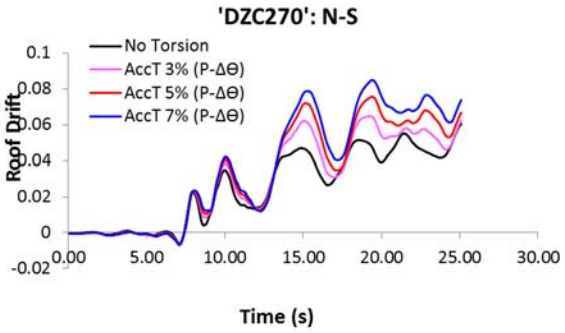

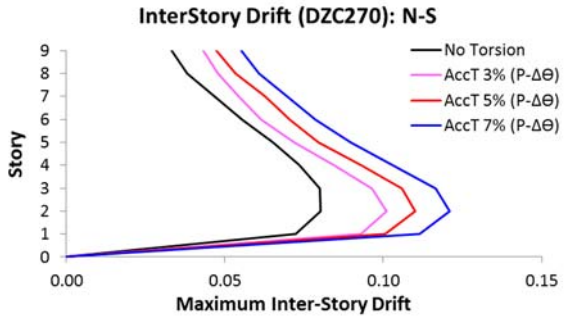

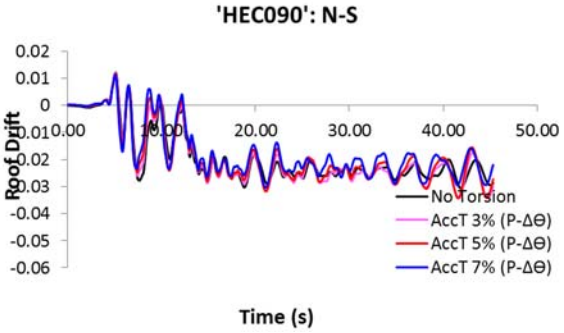

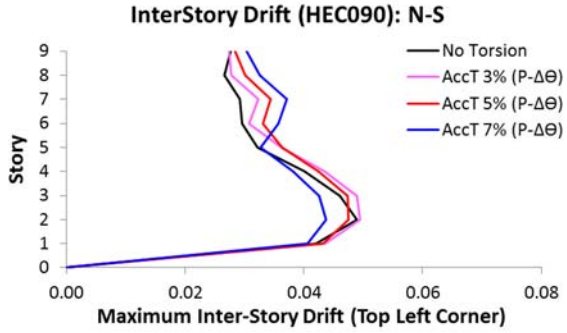

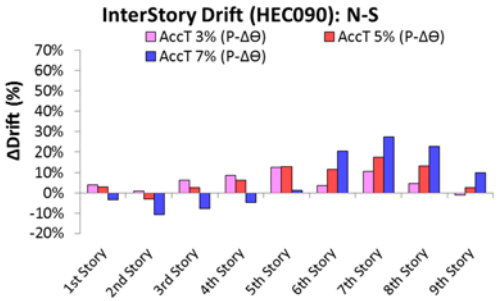

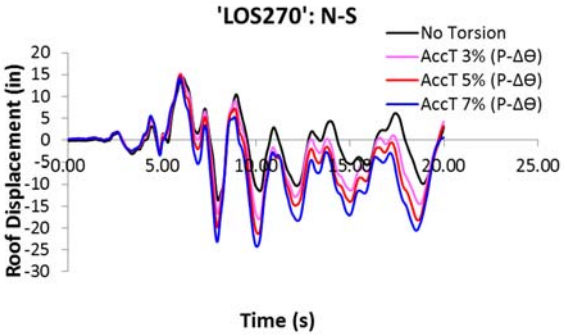

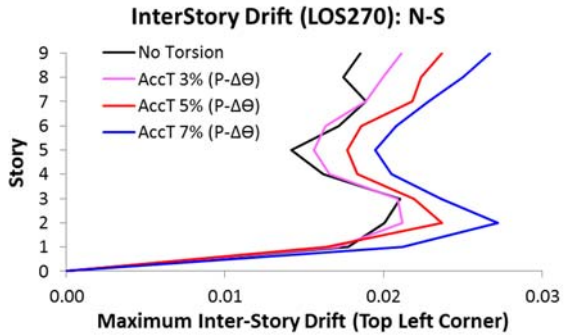

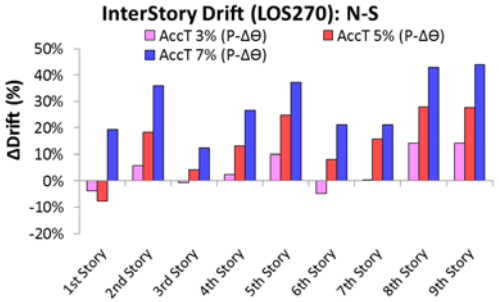

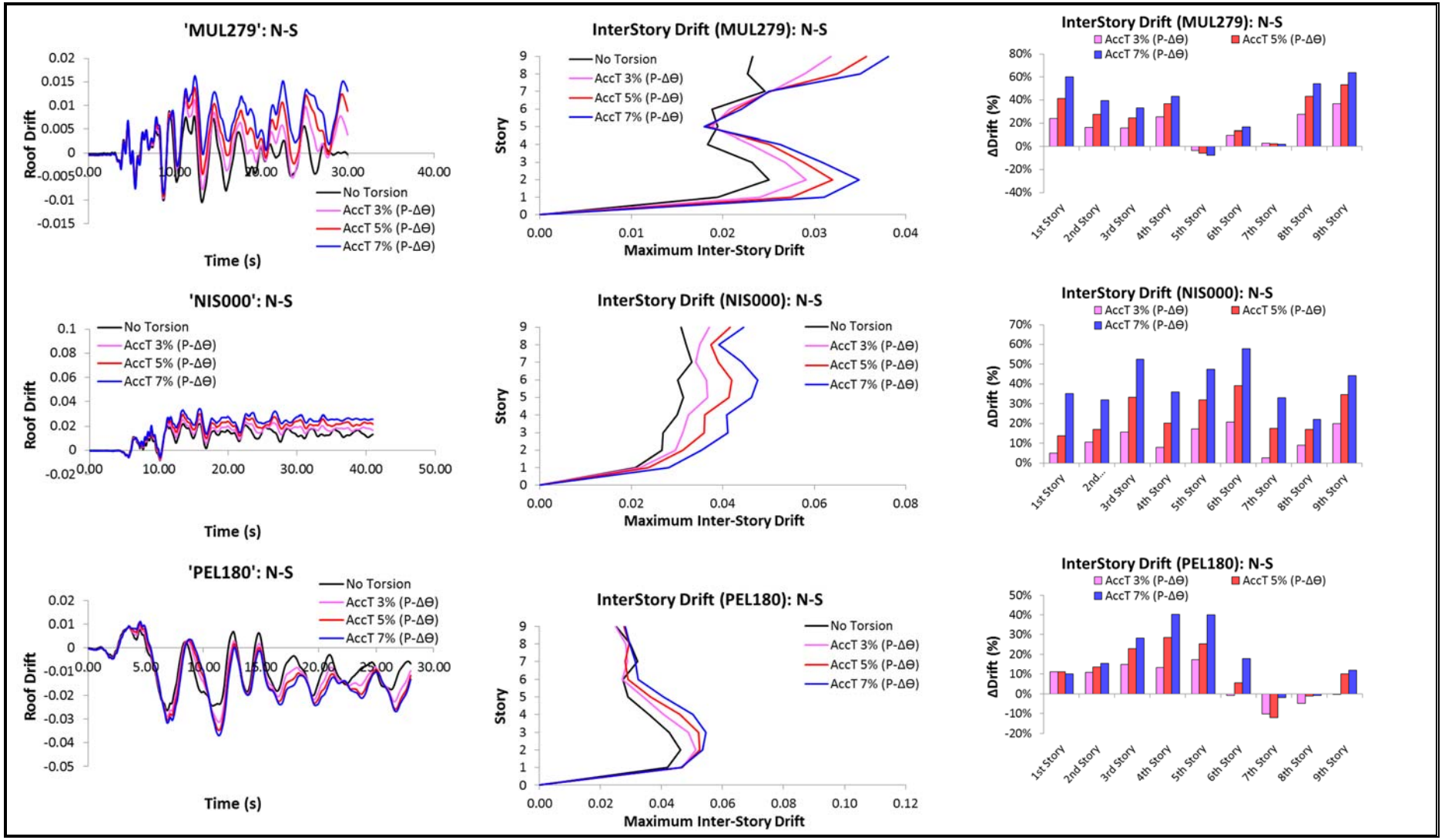
'MUL279': N-S
Roof Drift
Time (s)
No Torsion
AccT 3% (P-ΔΘ)
AccT 5% (P-ΔΘ)
AccT 7% (P-ΔΘ)
InterStory Drift (MUL279): N-S
Story
Maximum Inter-Story Drift
InterStory Drift (MUL279): N-S
ΔDrift (%)
1st Story
2nd Story
3rd Story
4th Story
5th Story
6th Story
7th Story
8th Story
9th Story
'NIS000': N-S
Roof Drift
Time (s)
InterStory Drift (NIS000): N-S
Story
Maximum Inter-Story Drift
InterStory Drift (NIS000): N-S
ΔDrift (%)
'PEL180': N-S
Roof Drift
Time (s)
InterStory Drift (PEL180): N-S
Story
Maximum Inter-Story Drift
InterStory Drift (PEL180): N-S
ΔDrift (%)

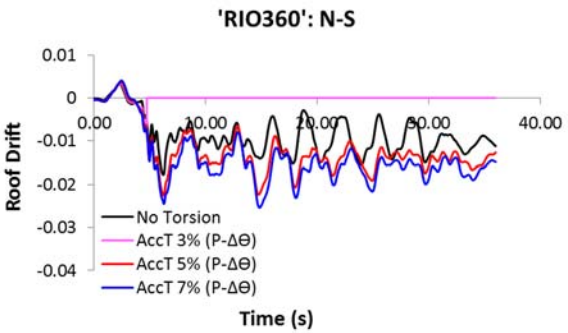

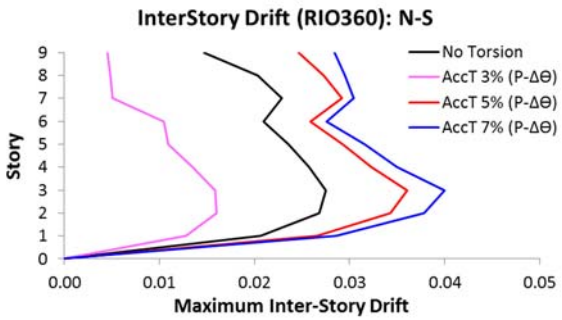

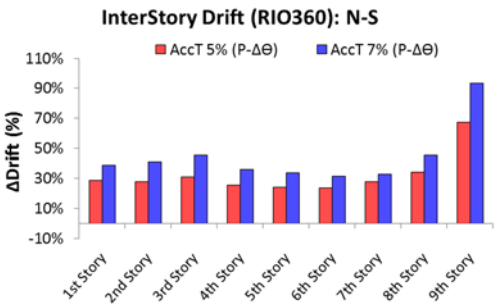

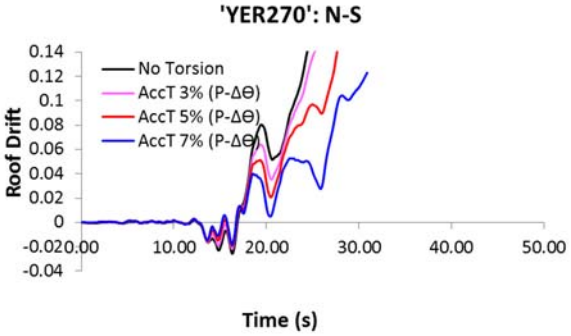

Structure collapsed

Structure collapsed

Model B: Bidirectional Loading

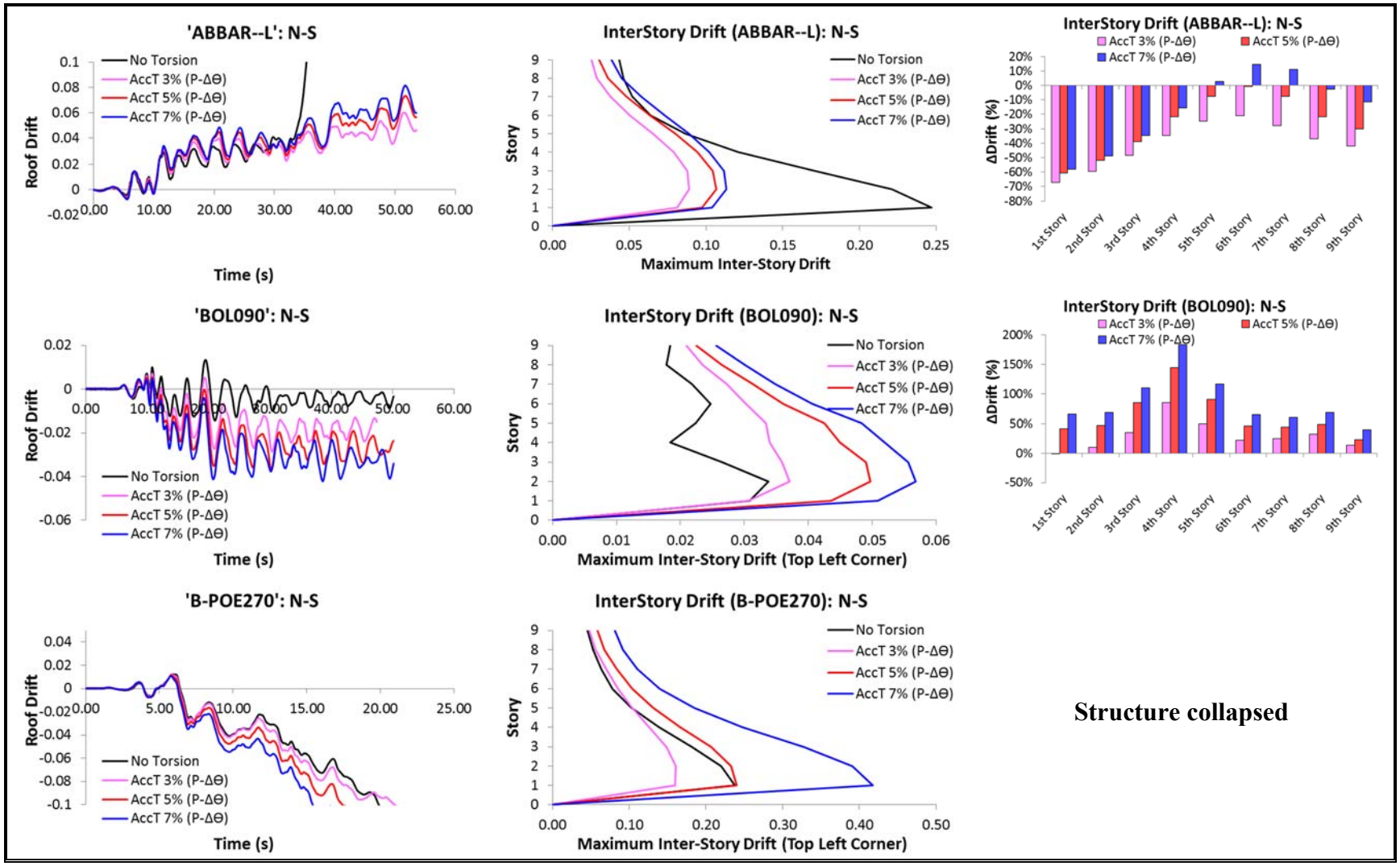

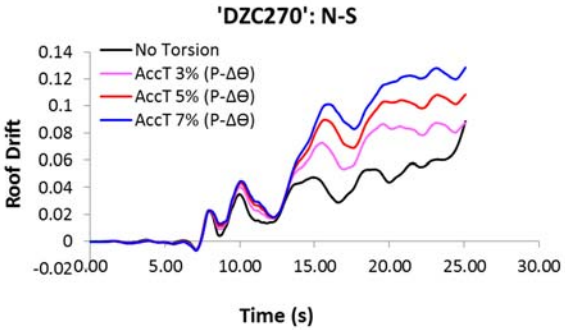

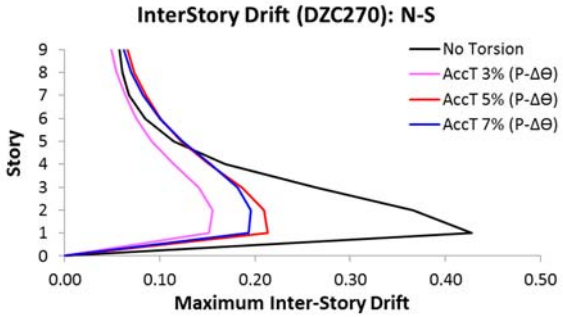

Structure collapsed

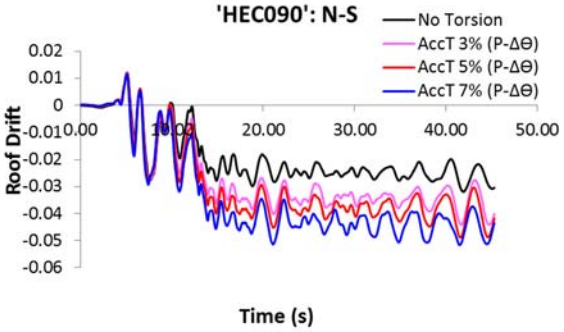

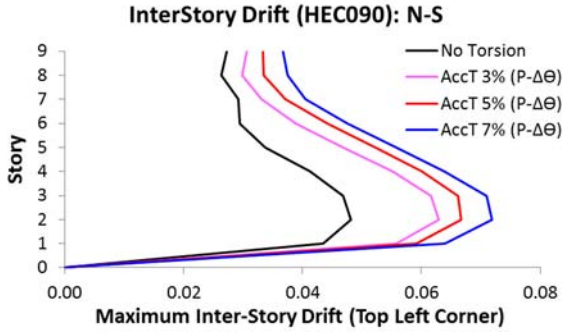

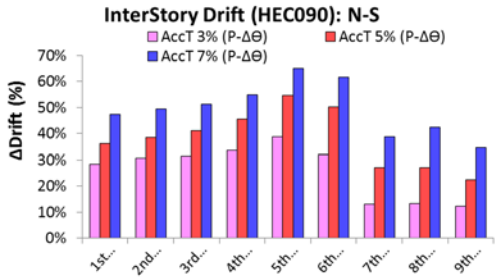

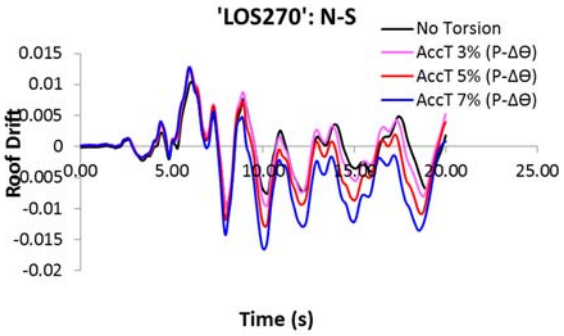

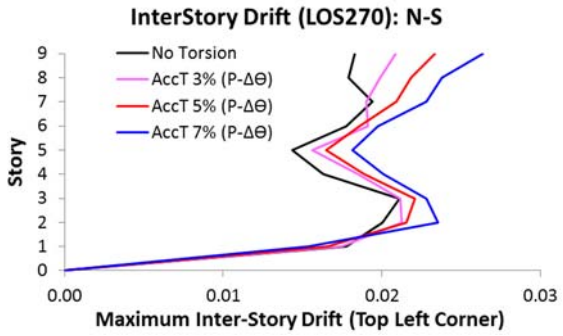

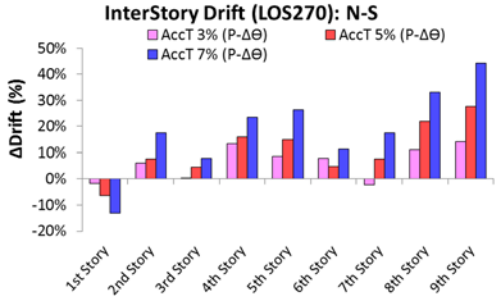

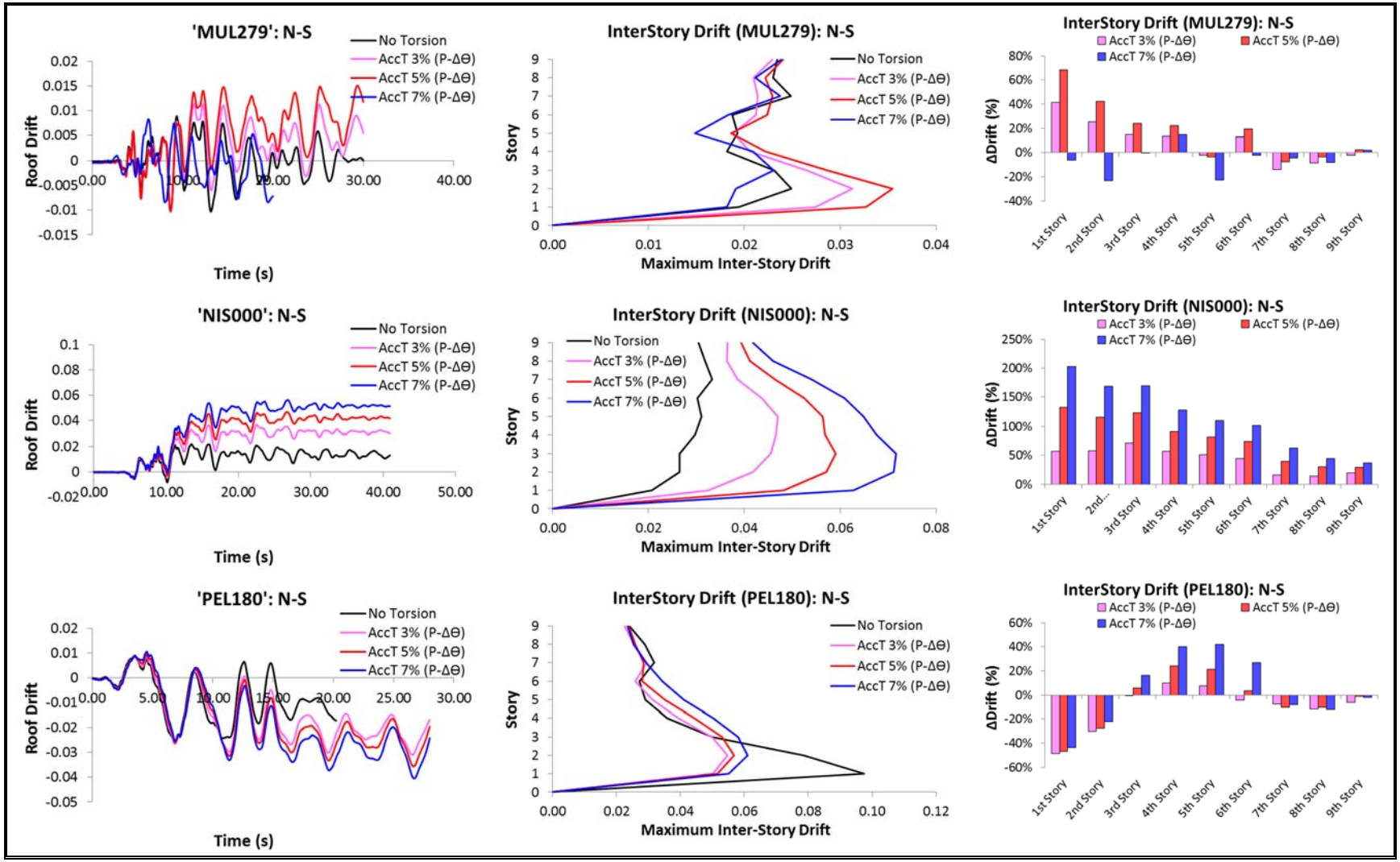
'MUL279': N-S
No Torsion
AccT 3% (P-ΔΘ)
AccT 5% (P-ΔΘ)
AccT 7% (P-ΔΘ)
Roof Drift
Time (s)
InterStory Drift (MUL279): N-S
Story
Maximum Inter-Story Drift
InterStory Drift (MUL279): N-S
ΔDrift (%)
1st Story
2nd Story
3rd Story
4th Story
5th Story
6th Story
7th Story
8th Story
9th Story
'NIS000': N-S
InterStory Drift (NIS000): N-S
'PEL180': N-S
InterStory Drift (PEL180): N-S

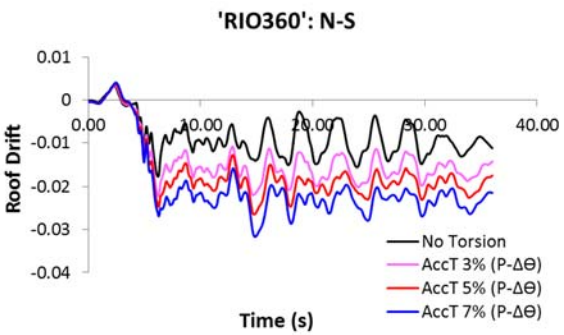

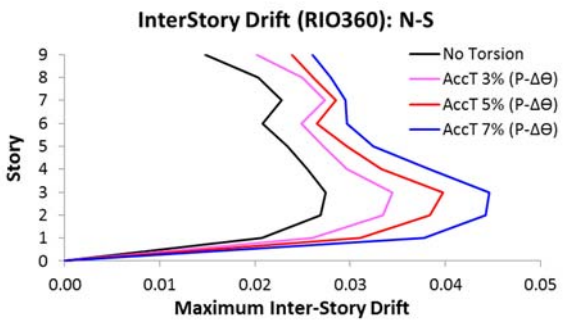

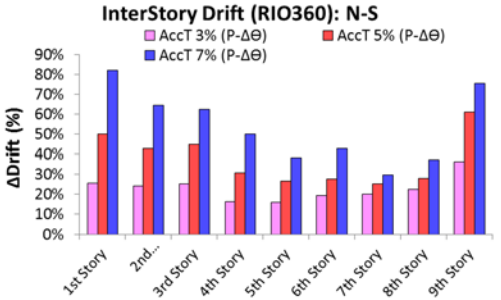

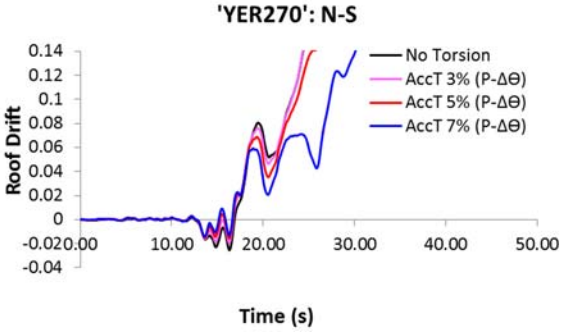

Structure collapsed

Structure collapsed

Model C: Bidirectional Loading

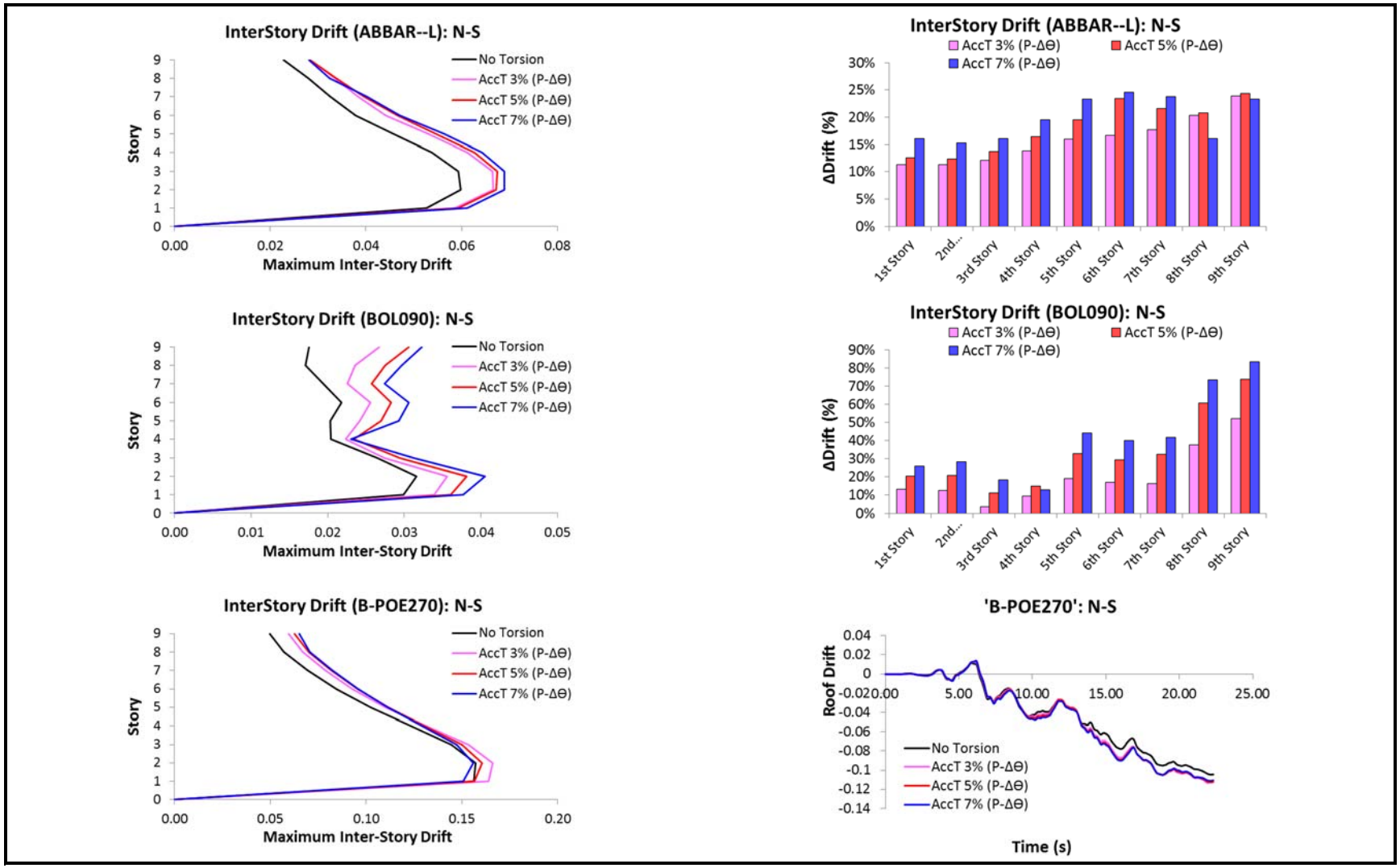

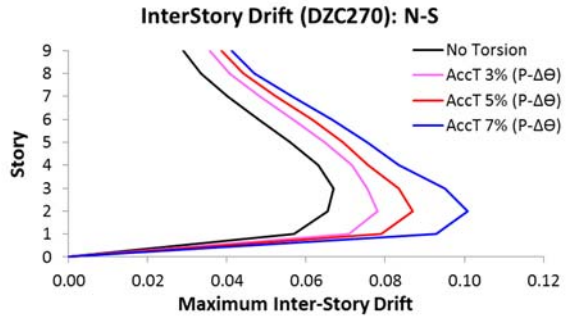
InterStory Drift (DZC270): N-S
No Torsion
AccT 3% (P-ΔΘ)
AccT 5% (P-ΔΘ)
AccT 7% (P-ΔΘ)
Story
Maximum Inter-Story Drift

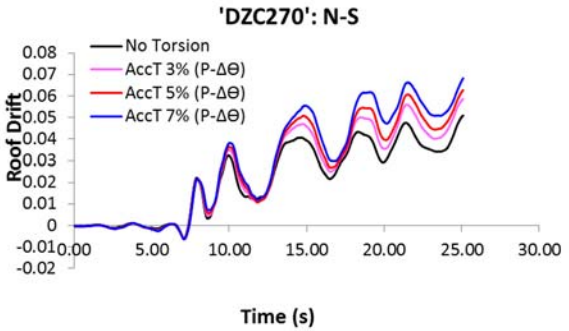
'DZC270': N-S
No Torsion
AccT 3% (P-ΔΘ)
AccT 5% (P-ΔΘ)
AccT 7% (P-ΔΘ)
Roof Drift
Time (s)

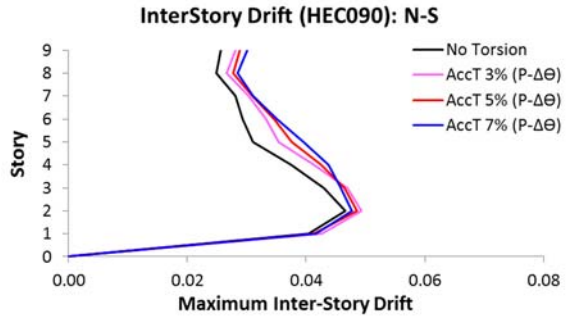
InterStory Drift (HEC090): N-S
No Torsion
AccT 3% (P-ΔΘ)
AccT 5% (P-ΔΘ)
AccT 7% (P-ΔΘ)
Story
Maximum Inter-Story Drift

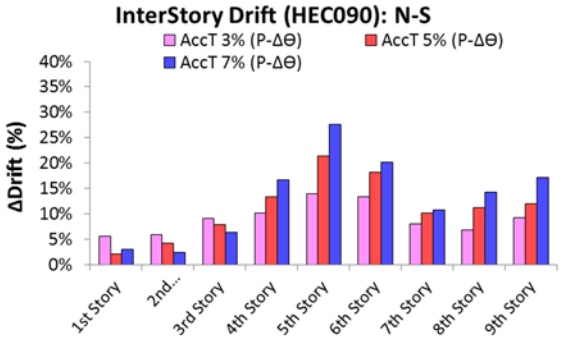
InterStory Drift (HEC090): N-S
AccT 3% (P-ΔΘ)
AccT 5% (P-ΔΘ)
AccT 7% (P-ΔΘ)
ΔDrift (%)
1st Story
2nd...
3rd Story
4th Story
5th Story
6th Story
7th Story
8th Story
9th Story

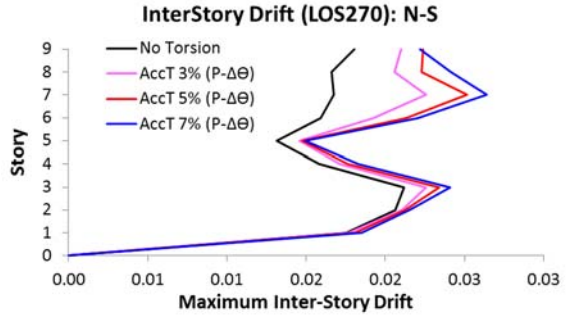
InterStory Drift (LOS270): N-S
No Torsion
AccT 3% (P-ΔΘ)
AccT 5% (P-ΔΘ)
AccT 7% (P-ΔΘ)
Story
Maximum Inter-Story Drift

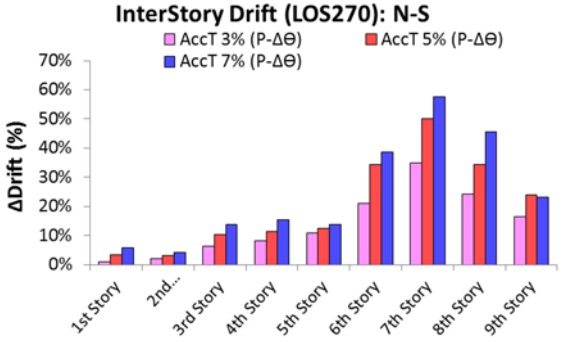
InterStory Drift (LOS270): N-S
AccT 3% (P-ΔΘ)
AccT 5% (P-ΔΘ)
AccT 7% (P-ΔΘ)
ΔDrift (%)
1st Story
2nd...
3rd Story
4th Story
5th Story
6th Story
7th Story
8th Story
9th Story

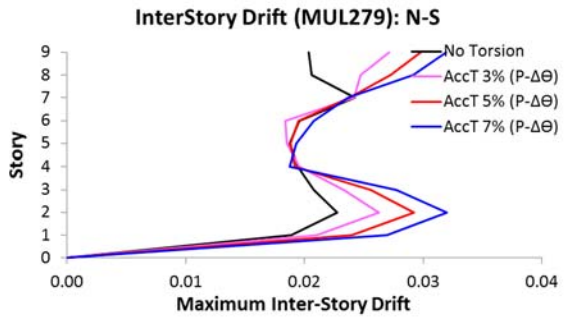
InterStory Drift (MUL279): N-S
No Torsion
AccT 3% (P-ΔΘ)
AccT 5% (P-ΔΘ)
AccT 7% (P-ΔΘ)
Story
Maximum Inter-Story Drift

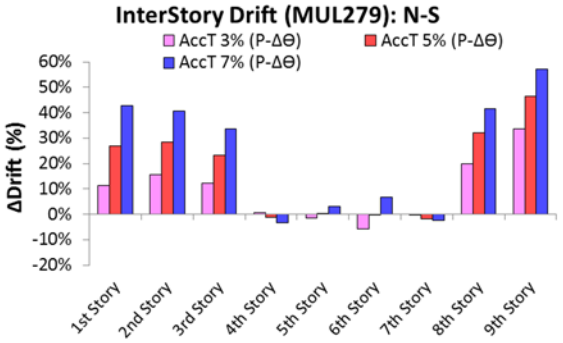
InterStory Drift (MUL279): N-S
AccT 3% (P-ΔΘ)
AccT 5% (P-ΔΘ)
AccT 7% (P-ΔΘ)
ΔDrift (%)
1st Story
2nd Story
3rd Story
4th Story
5th Story
6th Story
7th Story
8th Story
9th Story

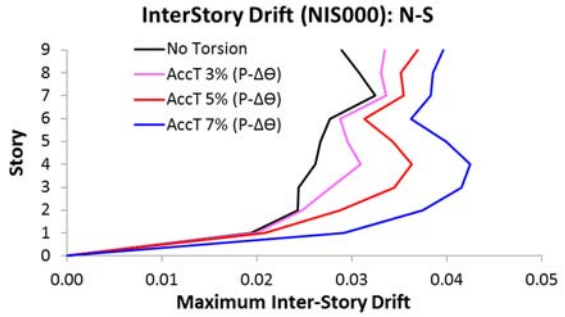
InterStory Drift (NIS000): N-S
No Torsion
AccT 3% (P-ΔΘ)
AccT 5% (P-ΔΘ)
AccT 7% (P-ΔΘ)
Story
Maximum Inter-Story Drift

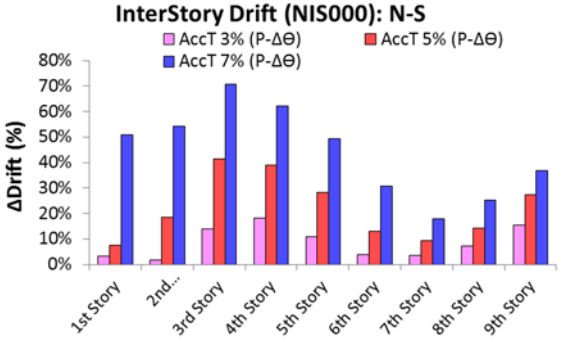
InterStory Drift (NIS000): N-S
AccT 3% (P-ΔΘ)
AccT 5% (P-ΔΘ)
AccT 7% (P-ΔΘ)
ΔDrift (%)
1st Story
2nd...
3rd Story
4th Story
5th Story
6th Story
7th Story
8th Story
9th Story

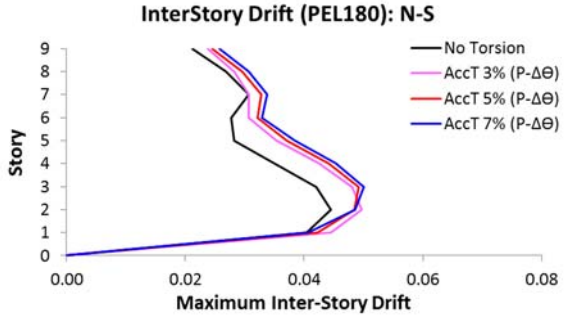
InterStory Drift (PEL180): N-S
No Torsion
AccT 3% (P-ΔΘ)
AccT 5% (P-ΔΘ)
AccT 7% (P-ΔΘ)
Story
Maximum Inter-Story Drift

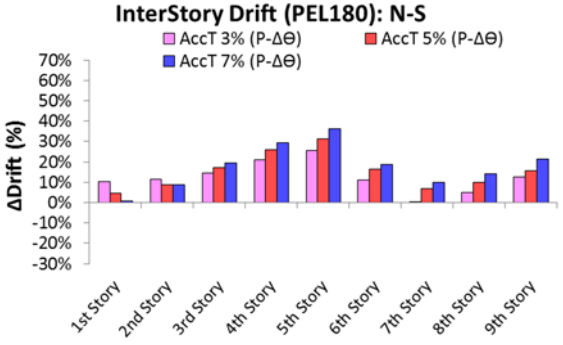
InterStory Drift (PEL180): N-S
AccT 3% (P-ΔΘ)
AccT 5% (P-ΔΘ)
AccT 7% (P-ΔΘ)
ΔDrift (%)
1st Story
2nd Story
3rd Story
4th Story
5th Story
6th Story
7th Story
8th Story
9th Story

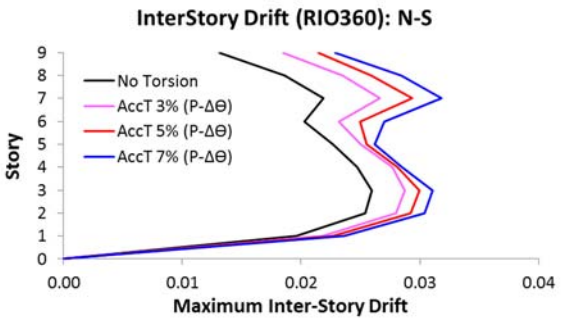
InterStory Drift (RIO360): N-S
Story
Maximum Inter-Story Drift
No Torsion
AccT 3% (P-ΔΘ)
AccT 5% (P-ΔΘ)
AccT 7% (P-ΔΘ)
0
1
2
3
4
5
6
7
8
9
0.00
0.01
0.02
0.03
0.04

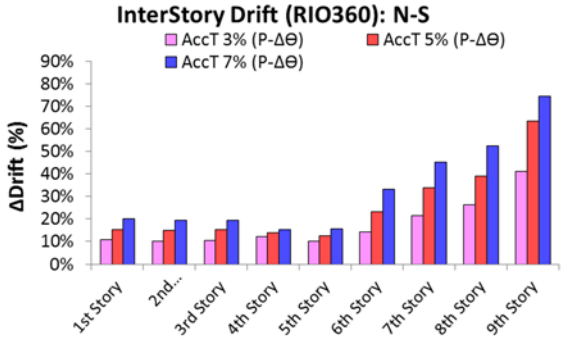
InterStory Drift (RIO360): N-S
AccT 3% (P-ΔΘ)
AccT 5% (P-ΔΘ)
AccT 7% (P-ΔΘ)
ΔDrift (%)
0%
10%
20%
30%
40%
50%
60%
70%
80%
90%
1st Story
2nd...
3rd Story
4th Story
5th Story
6th Story
7th Story
8th Story
9th Story

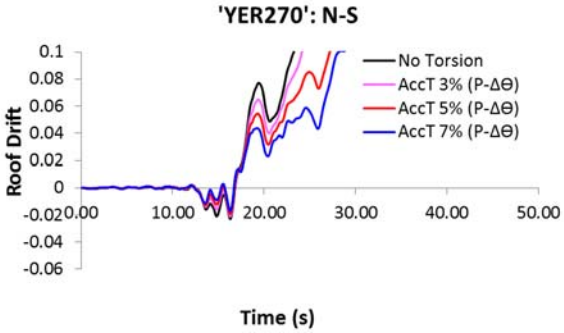
'YER270': N-S
Roof Drift
Time (s)
No Torsion
AccT 3% (P-ΔΘ)
AccT 5% (P-ΔΘ)
AccT 7% (P-ΔΘ)
0.1
0.08
0.06
0.04
0.02
0
-0.02
-0.04
-0.06
0.00
10.00
20.00
30.00
40.00
50.00

Model C-2: Bidirectional Loading

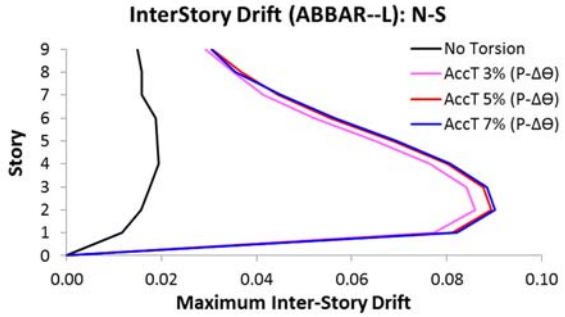

Abbar-L 1Direction without Accidental Torsion did not converge

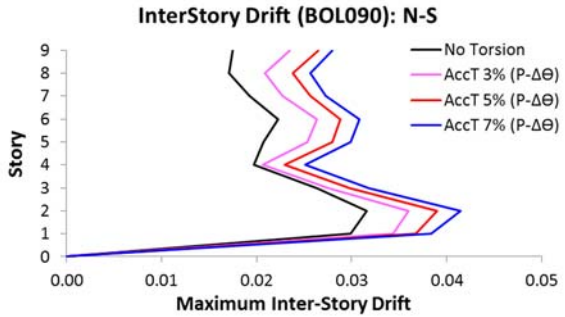

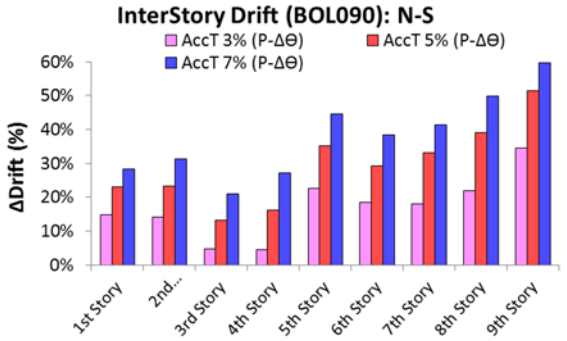

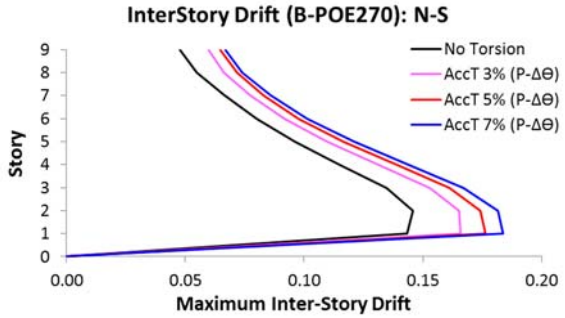

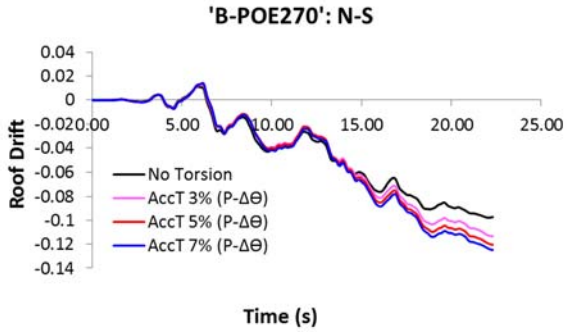

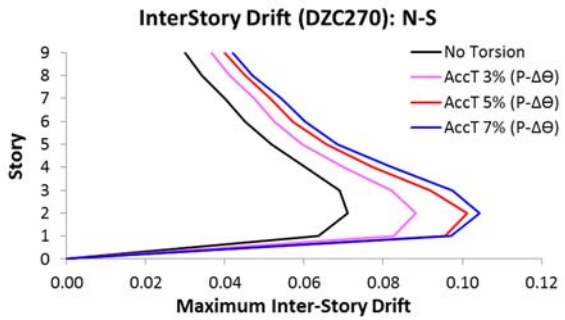
InterStory Drift (DZC270): N-S
No Torsion
AccT 3% (P-ΔΘ)
AccT 5% (P-ΔΘ)
AccT 7% (P-ΔΘ)
Story
Maximum Inter-Story Drift

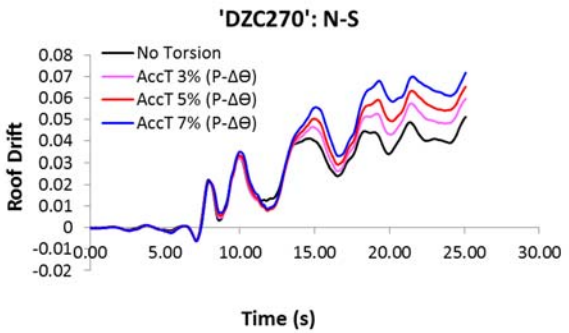
'DZC270': N-S
No Torsion
AccT 3% (P-ΔΘ)
AccT 5% (P-ΔΘ)
AccT 7% (P-ΔΘ)
Roof Drift
Time (s)

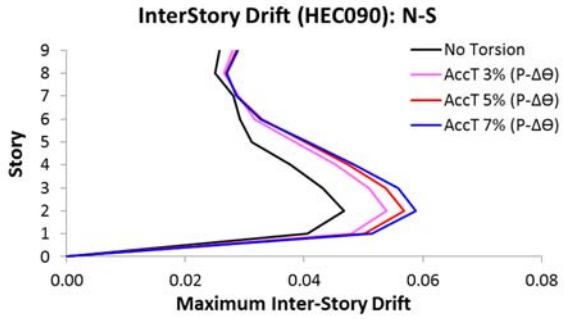
InterStory Drift (HEC090): N-S
No Torsion
AccT 3% (P-ΔΘ)
AccT 5% (P-ΔΘ)
AccT 7% (P-ΔΘ)
Story
Maximum Inter-Story Drift

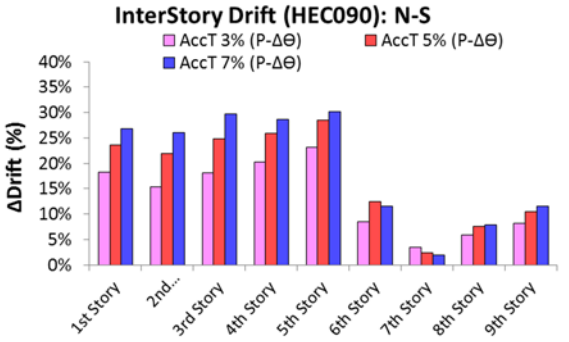
InterStory Drift (HEC090): N-S
AccT 3% (P-ΔΘ)
AccT 5% (P-ΔΘ)
AccT 7% (P-ΔΘ)
ΔDrift (%)
1st Story
2nd...
3rd Story
4th Story
5th Story
6th Story
7th Story
8th Story
9th Story

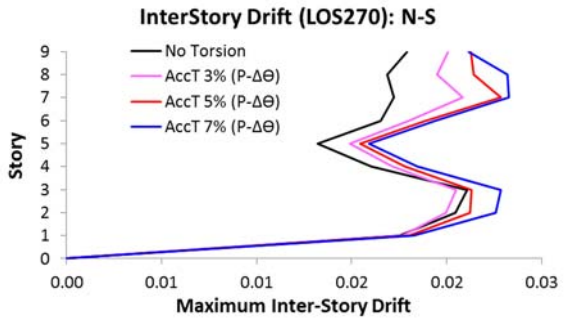
InterStory Drift (LOS270): N-S
No Torsion
AccT 3% (P-ΔΘ)
AccT 5% (P-ΔΘ)
AccT 7% (P-ΔΘ)
Story
Maximum Inter-Story Drift

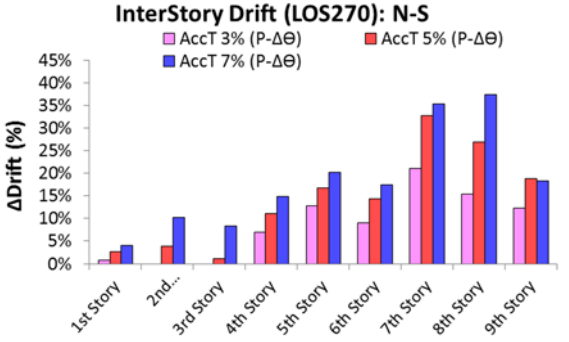
InterStory Drift (LOS270): N-S
AccT 3% (P-ΔΘ)
AccT 5% (P-ΔΘ)
AccT 7% (P-ΔΘ)
ΔDrift (%)
1st Story
2nd...
3rd Story
4th Story
5th Story
6th Story
7th Story
8th Story
9th Story

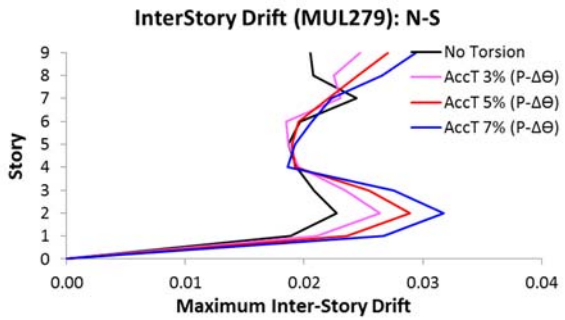
InterStory Drift (MUL279): N-S
No Torsion
AccT 3% (P-ΔΘ)
AccT 5% (P-ΔΘ)
AccT 7% (P-ΔΘ)
Story
Maximum Inter-Story Drift

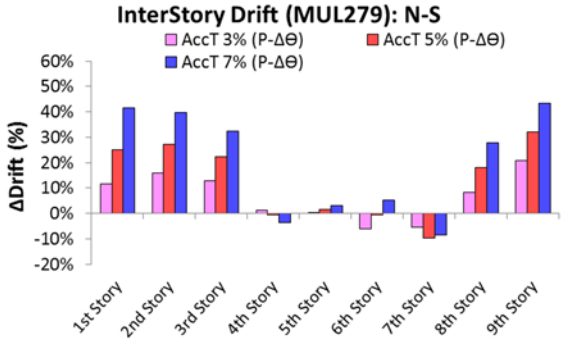
InterStory Drift (MUL279): N-S
AccT 3% (P-ΔΘ)
AccT 5% (P-ΔΘ)
AccT 7% (P-ΔΘ)
ΔDrift (%)
1st Story
2nd Story
3rd Story
4th Story
5th Story
6th Story
7th Story
8th Story
9th Story

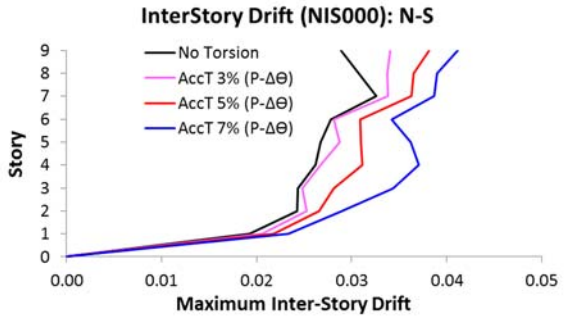
InterStory Drift (NIS000): N-S
No Torsion
AccT 3% (P-ΔΘ)
AccT 5% (P-ΔΘ)
AccT 7% (P-ΔΘ)
Story
Maximum Inter-Story Drift

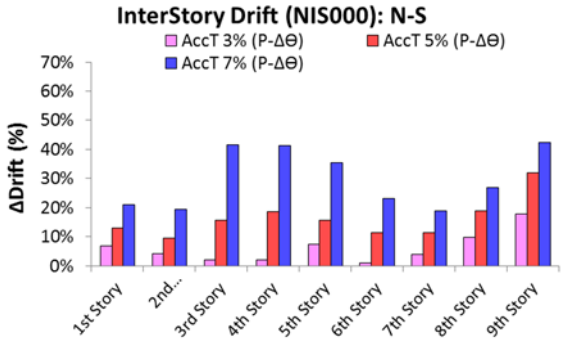
InterStory Drift (NIS000): N-S
AccT 3% (P-ΔΘ)
AccT 5% (P-ΔΘ)
AccT 7% (P-ΔΘ)
ΔDrift (%)
1st Story
2nd...
3rd Story
4th Story
5th Story
6th Story
7th Story
8th Story
9th Story

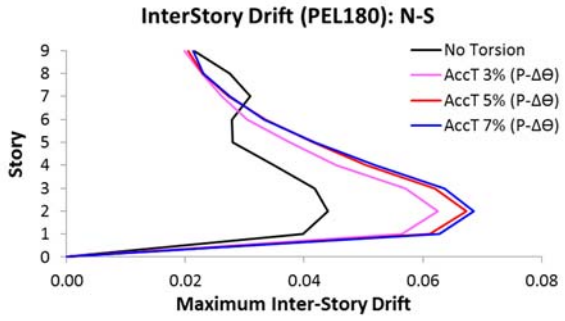
InterStory Drift (PEL180): N-S
No Torsion
AccT 3% (P-ΔΘ)
AccT 5% (P-ΔΘ)
AccT 7% (P-ΔΘ)
Story
Maximum Inter-Story Drift

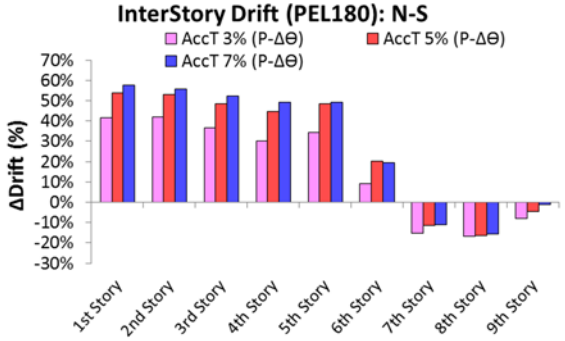
InterStory Drift (PEL180): N-S
AccT 3% (P-ΔΘ)
AccT 5% (P-ΔΘ)
AccT 7% (P-ΔΘ)
ΔDrift (%)
1st Story
2nd Story
3rd Story
4th Story
5th Story
6th Story
7th Story
8th Story
9th Story

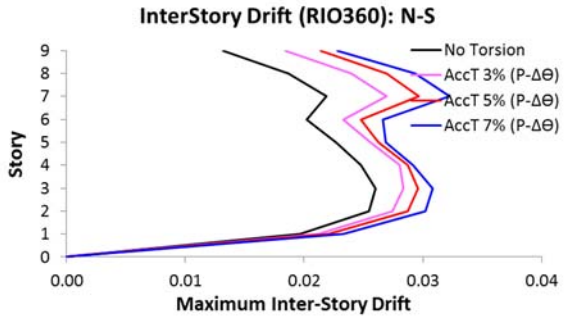
InterStory Drift (RIO360): N-S
No Torsion
AccT 3% (P-Δθ)
AccT 5% (P-Δθ)
AccT 7% (P-Δθ)
Story
Maximum Inter-Story Drift

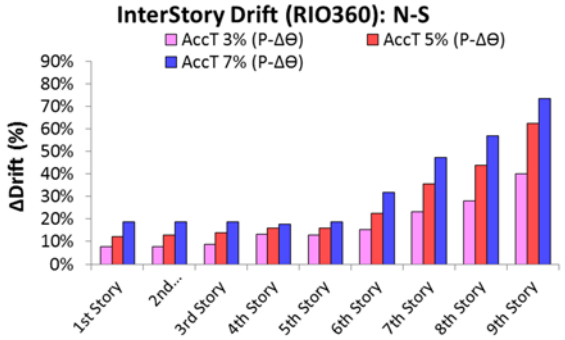
InterStory Drift (RIO360): N-S
AccT 3% (P-Δθ)
AccT 5% (P-Δθ)
AccT 7% (P-Δθ)
ΔDrift (%)
1st Story
2nd...
3rd Story
4th Story
5th Story
6th Story
7th Story
8th Story
9th Story

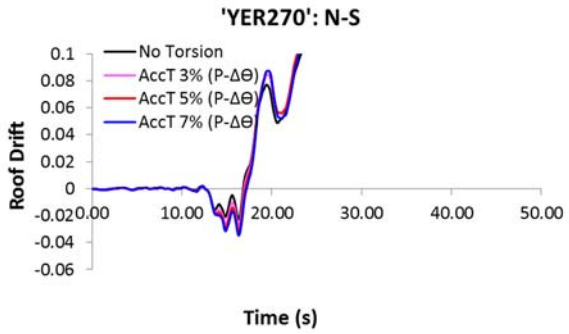
'YER270': N-S
No Torsion
AccT 3% (P-Δθ)
AccT 5% (P-Δθ)
AccT 7% (P-Δθ)
Roof Drift
Time (s)

Results without P-Theta Effects

Model A: Bidirectional Loading

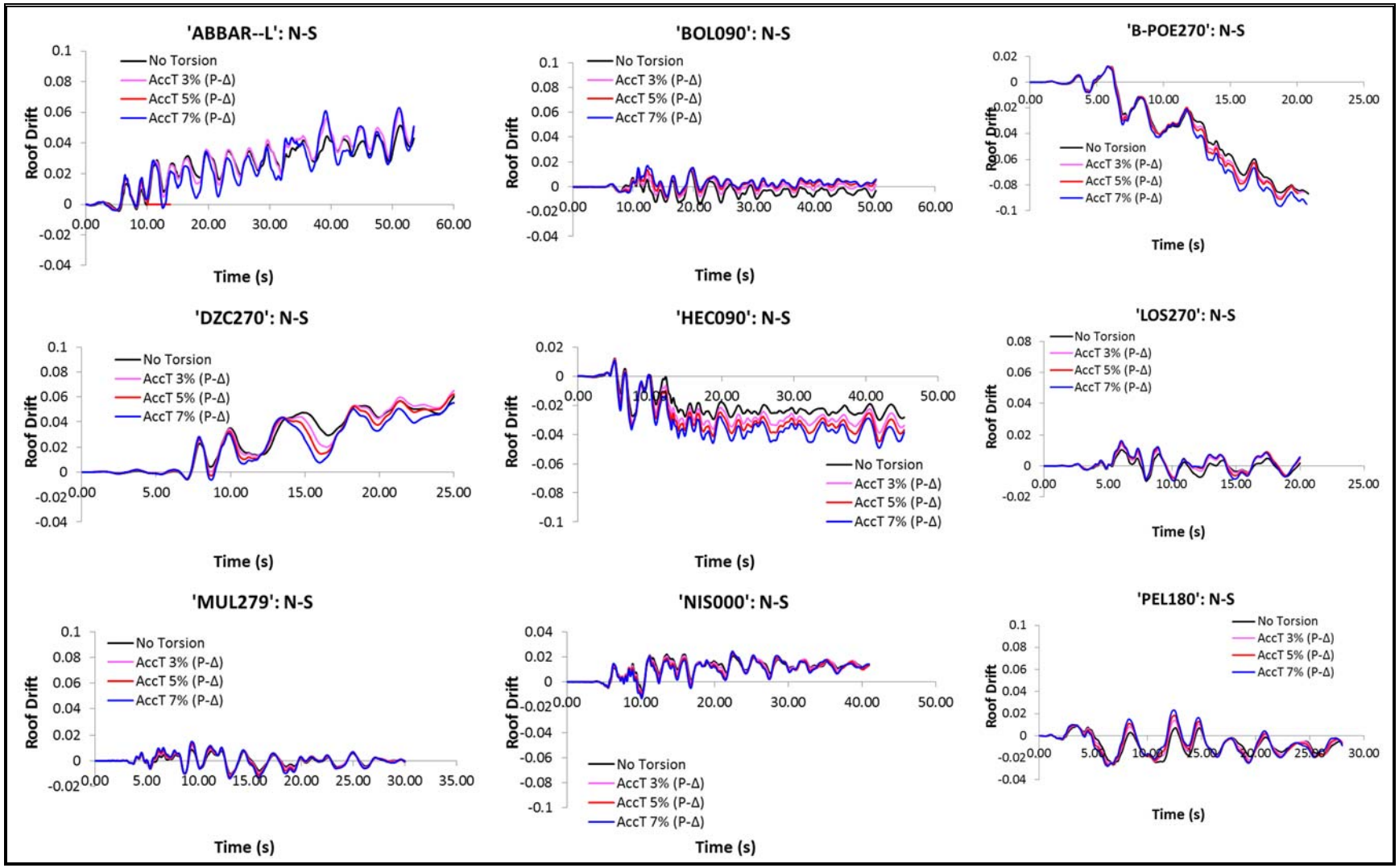

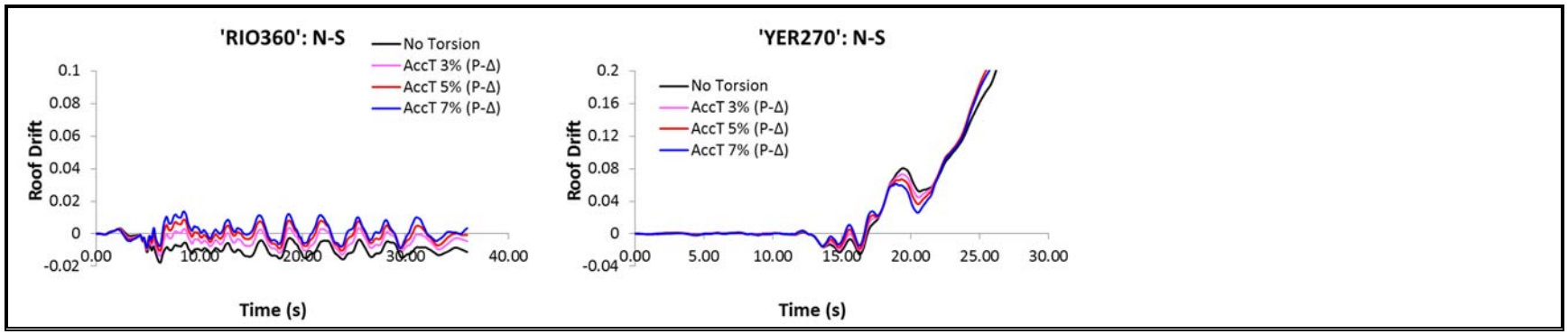
'RIO360': N-S
No Torsion
AccT 3% (P-Δ)
AccT 5% (P-Δ)
AccT 7% (P-Δ)
Roof Drift
0.1
0.08
0.06
0.04
0.02
0
-0.02
0.00
10.00
20.00
30.00
40.00
Time (s)
'YER270': N-S
No Torsion
AccT 3% (P-Δ)
AccT 5% (P-Δ)
AccT 7% (P-Δ)
Roof Drift
0.2
0.16
0.12
0.08
0.04
0
-0.04
0.00
5.00
10.00
15.00
20.00
25.00
30.00
Time (s)

Model A-2: Bidirectional Loading

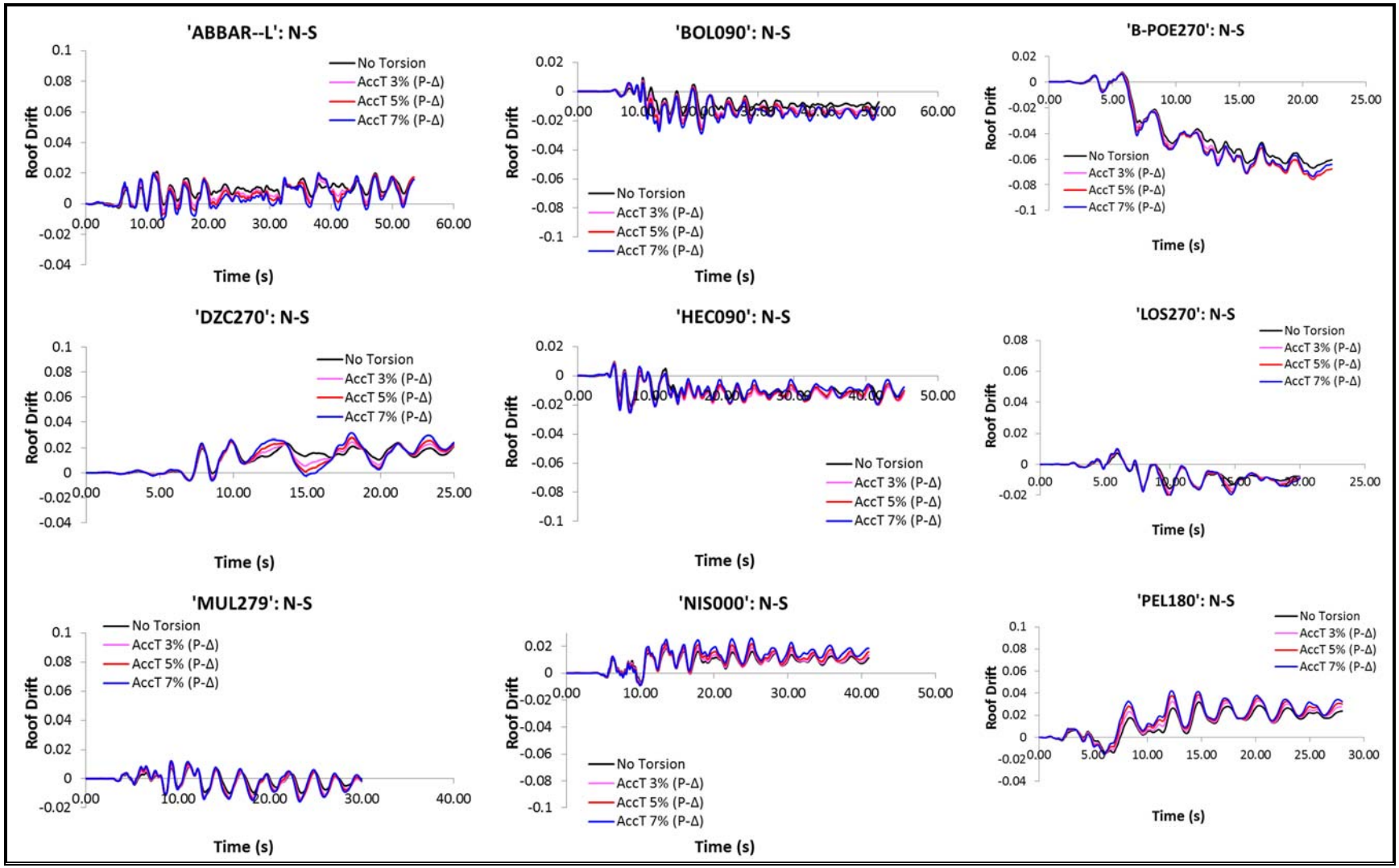

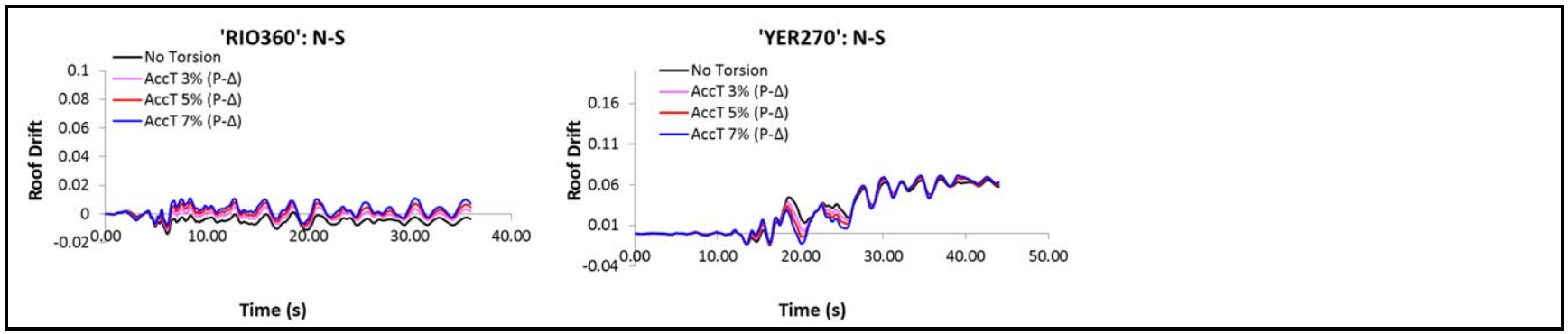
'RIO360': N-S
No Torsion
AccT 3% (P-Δ)
AccT 5% (P-Δ)
AccT 7% (P-Δ)
Roof Drift
0.1
0.08
0.06
0.04
0.02
0
-0.02
0.00
10.00
20.00
30.00
40.00
Time (s)
'YER270': N-S
No Torsion
AccT 3% (P-Δ)
AccT 5% (P-Δ)
AccT 7% (P-Δ)
Roof Drift
0.16
0.11
0.06
0.01
-0.04
0.00
10.00
20.00
30.00
40.00
50.00
Time (s)

Model B: Bidirectional Loading

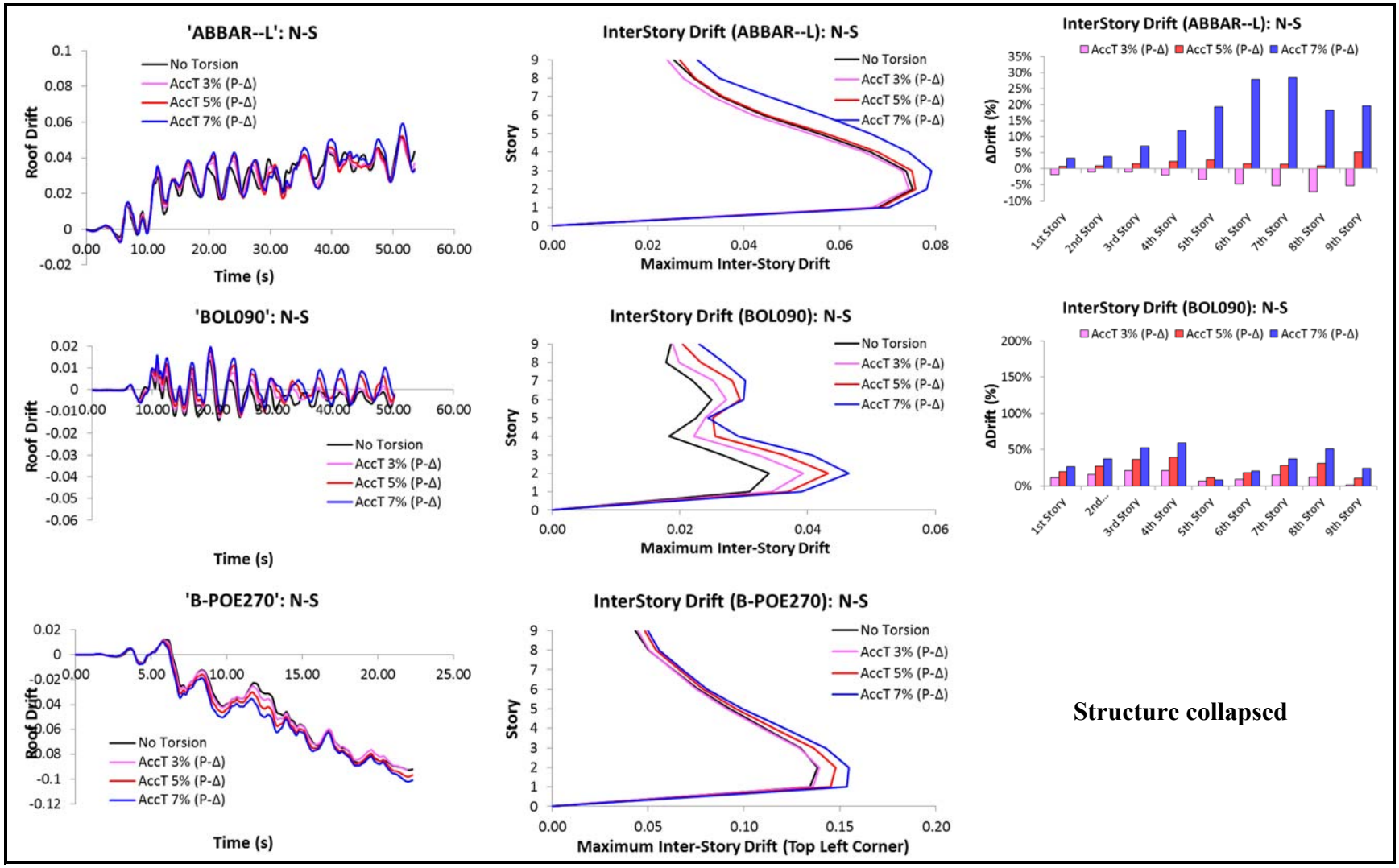

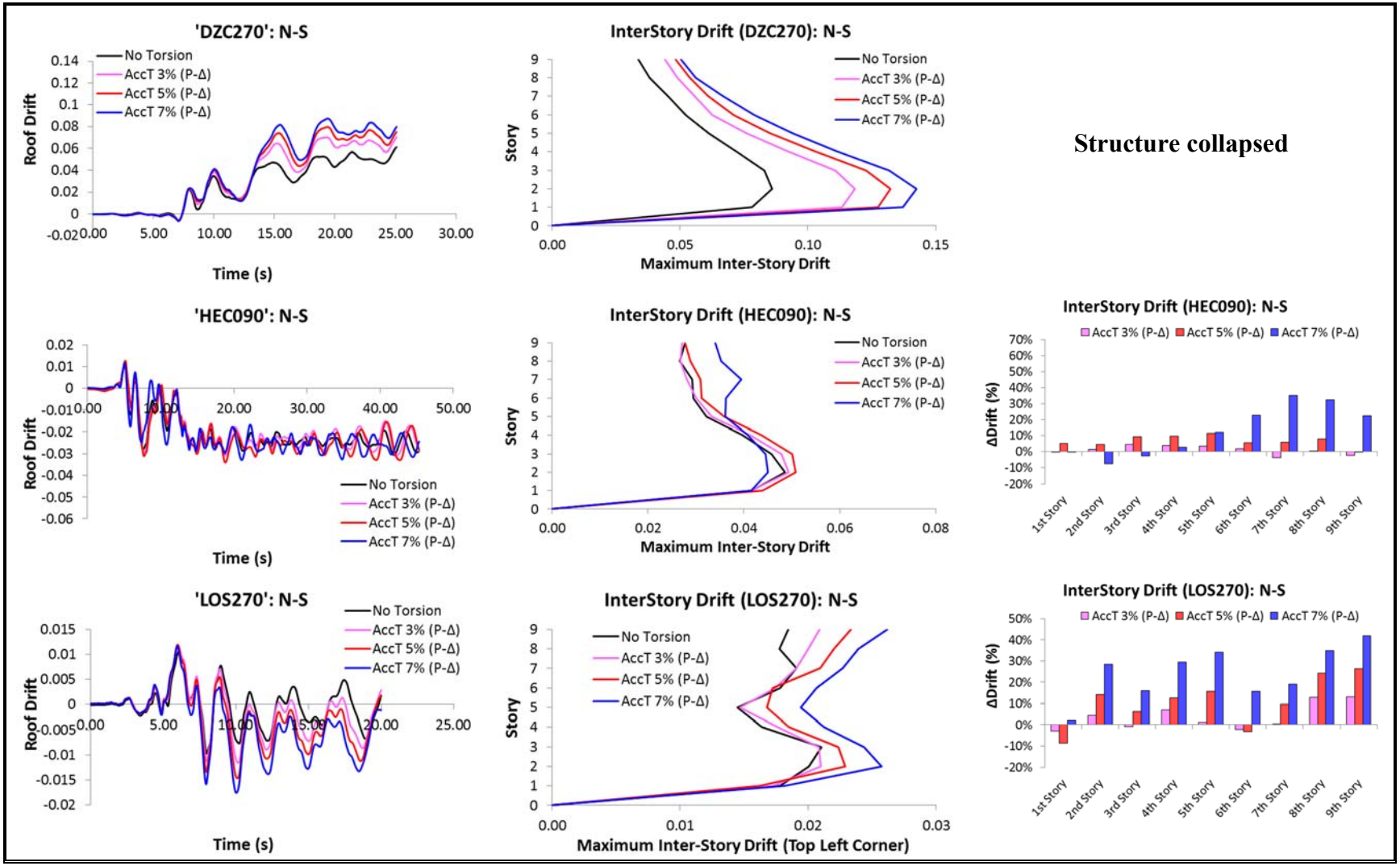
'DZC270': N-S
No Torsion
AccT 3% (P-Δ)
AccT 5% (P-Δ)
AccT 7% (P-Δ)
Roof Drift
Time (s)
InterStory Drift (DZC270): N-S
Story
Maximum Inter-Story Drift
Structure collapsed
'HEC090': N-S
Roof Drift
Time (s)
InterStory Drift (HEC090): N-S
Story
Maximum Inter-Story Drift
InterStory Drift (HEC090): N-S
ΔDrift (%)
1st Story
2nd Story
3rd Story
4th Story
5th Story
6th Story
7th Story
8th Story
9th Story
'LOS270': N-S
Roof Drift
Time (s)
InterStory Drift (LOS270): N-S
Story
Maximum Inter-Story Drift (Top Left Corner)
InterStory Drift (LOS270): N-S
ΔDrift (%)

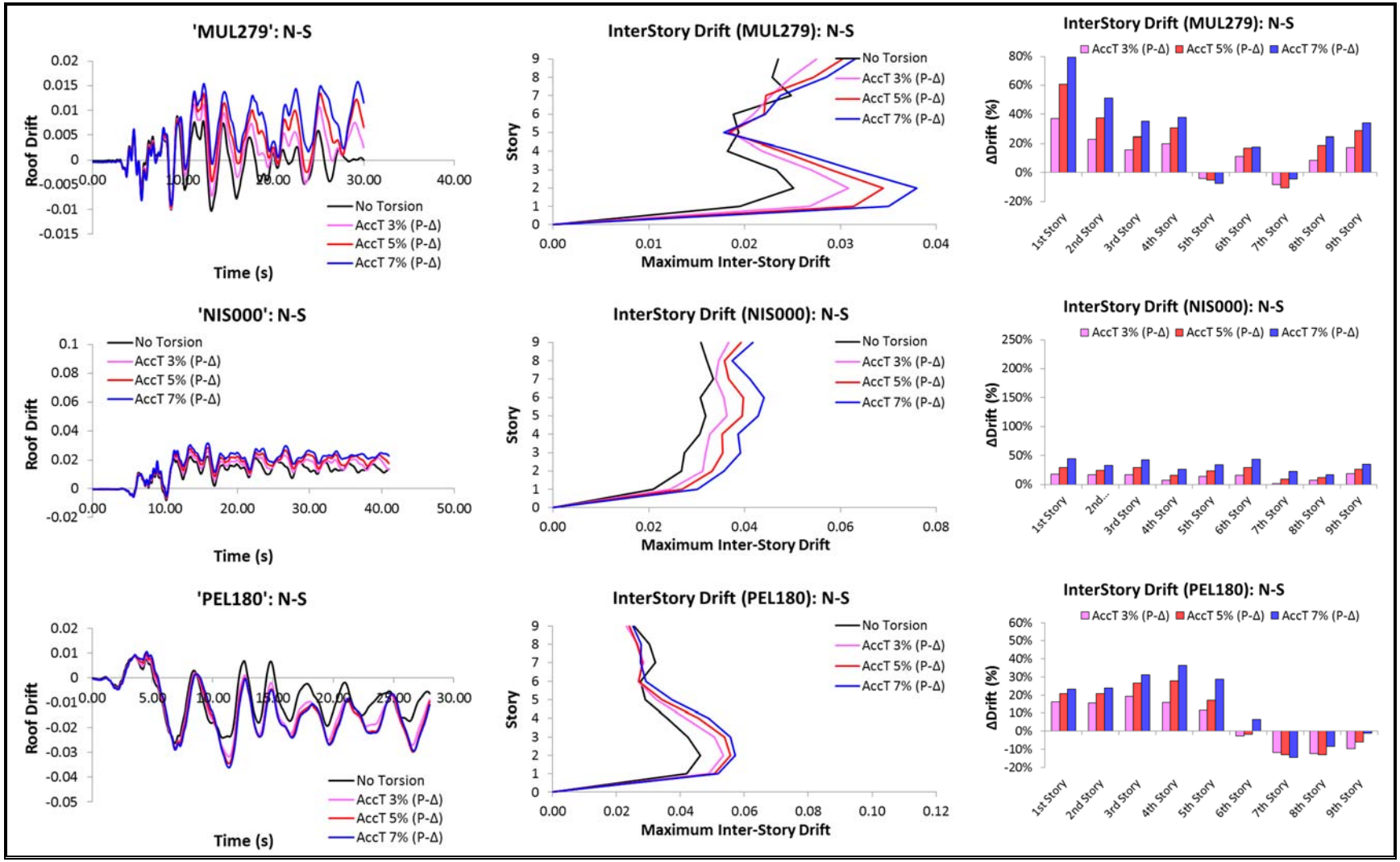
'MUL279': N-S
Roof Drift
Time (s)
No Torsion
AccT 3% (P-Δ)
AccT 5% (P-Δ)
AccT 7% (P-Δ)
InterStory Drift (MUL279): N-S
Story
Maximum Inter-Story Drift
InterStory Drift (MUL279): N-S
ΔDrift (%)
1st Story
2nd Story
3rd Story
4th Story
5th Story
6th Story
7th Story
8th Story
9th Story
'NIS000': N-S
InterStory Drift (NIS000): N-S
'PEL180': N-S
InterStory Drift (PEL180): N-S

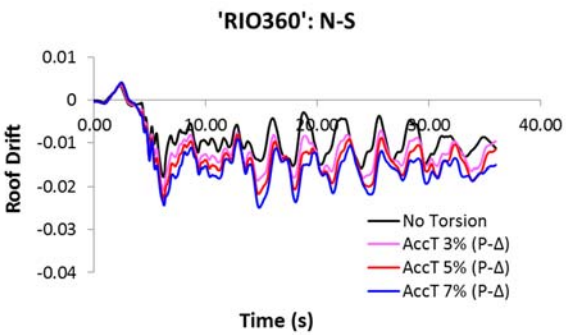

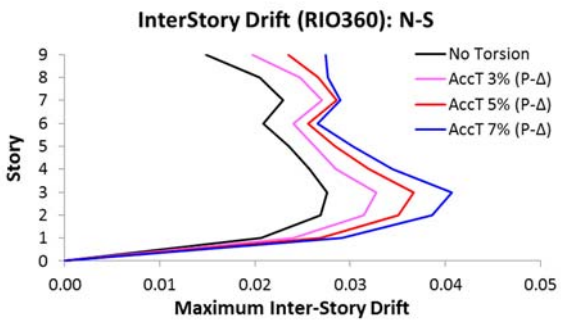

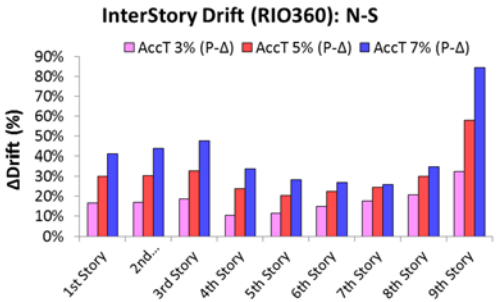

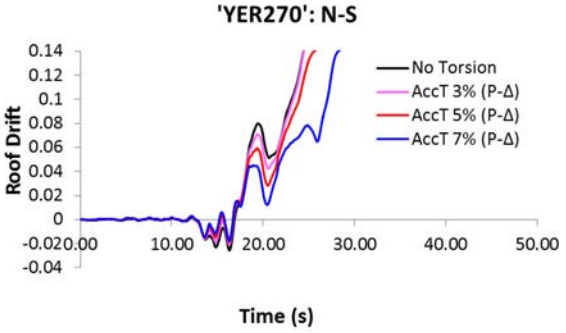

Structure collapsed

Structure collapsed

Model B-2: Bidirectional Loading

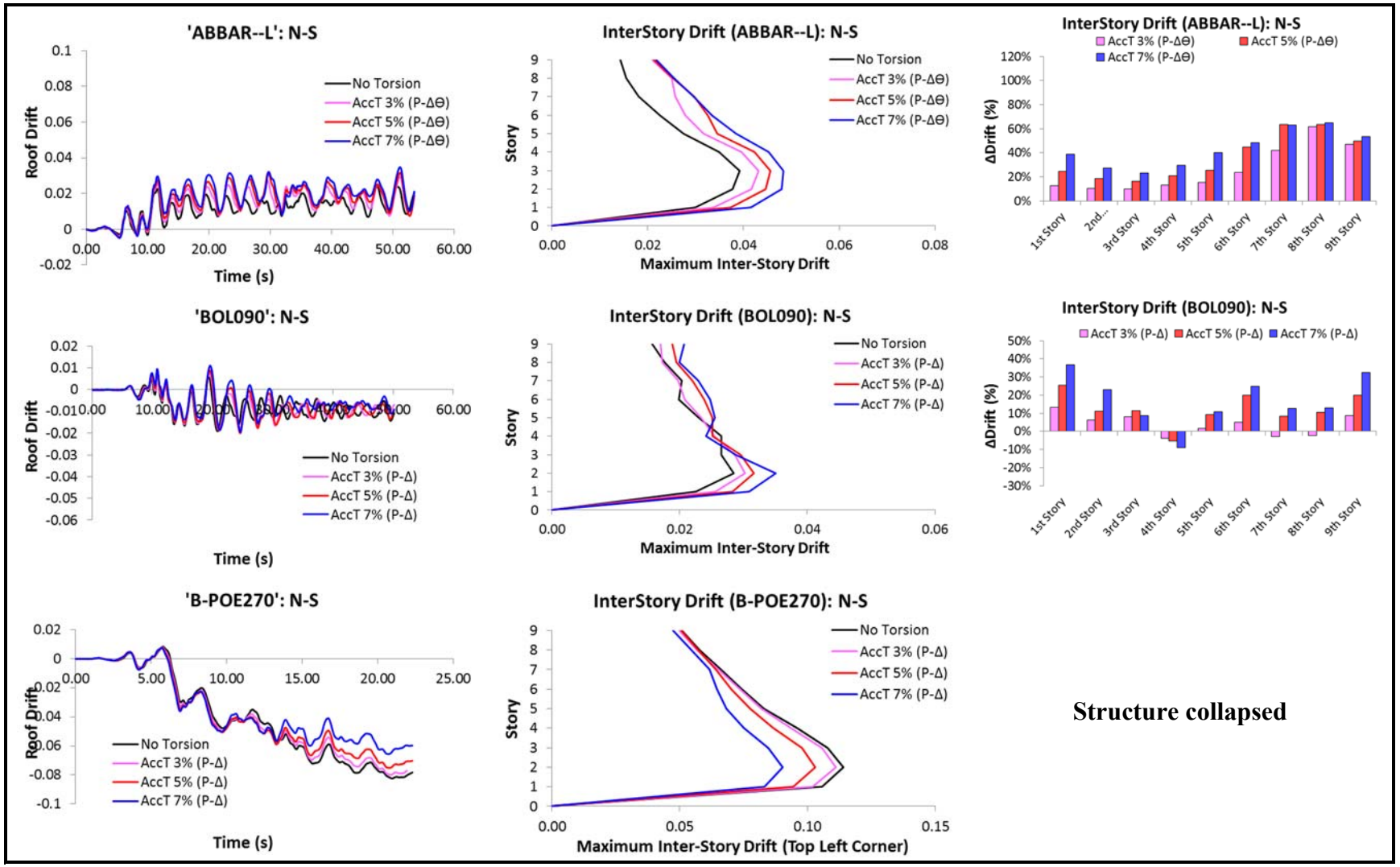

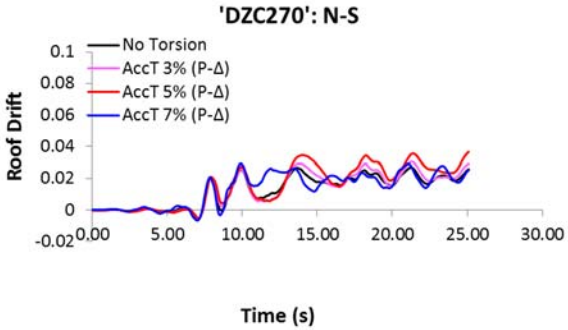

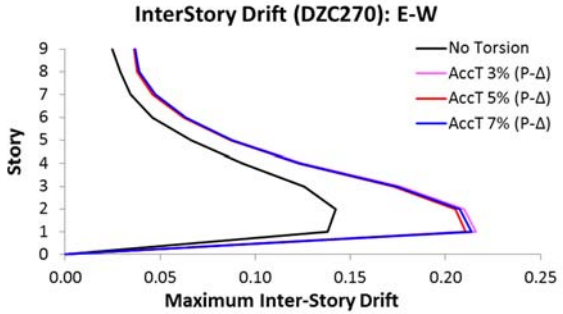

Structure collapsed

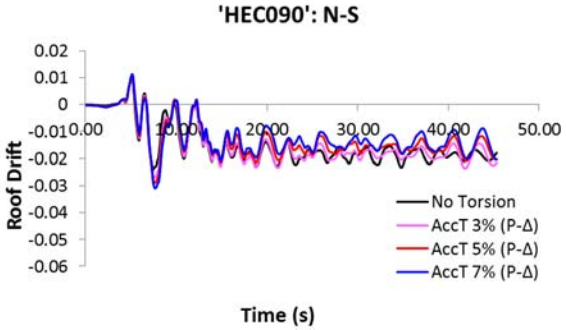

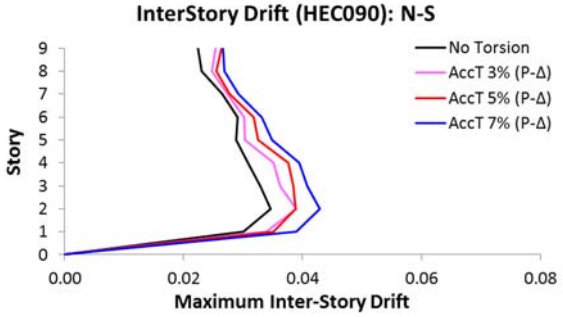

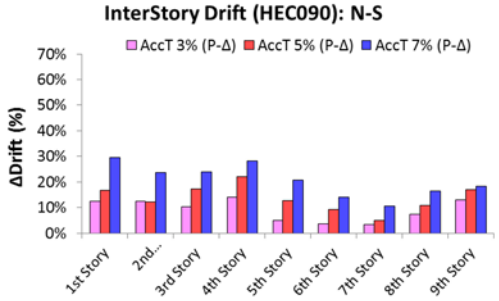

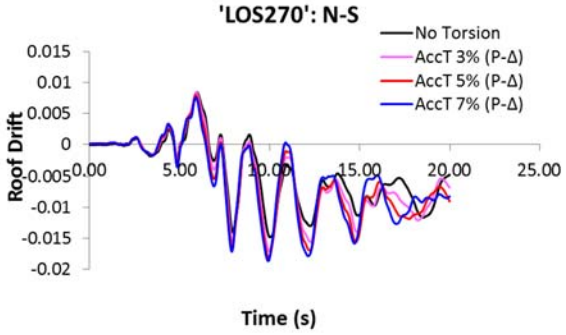

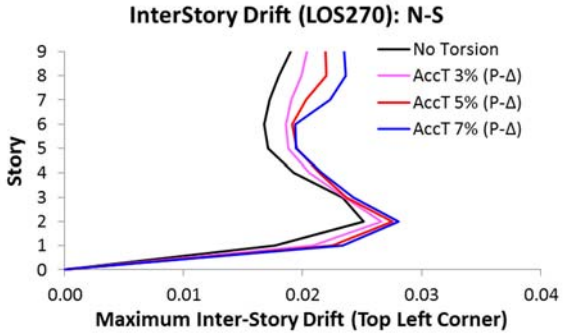

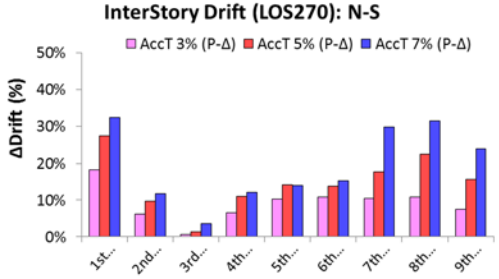

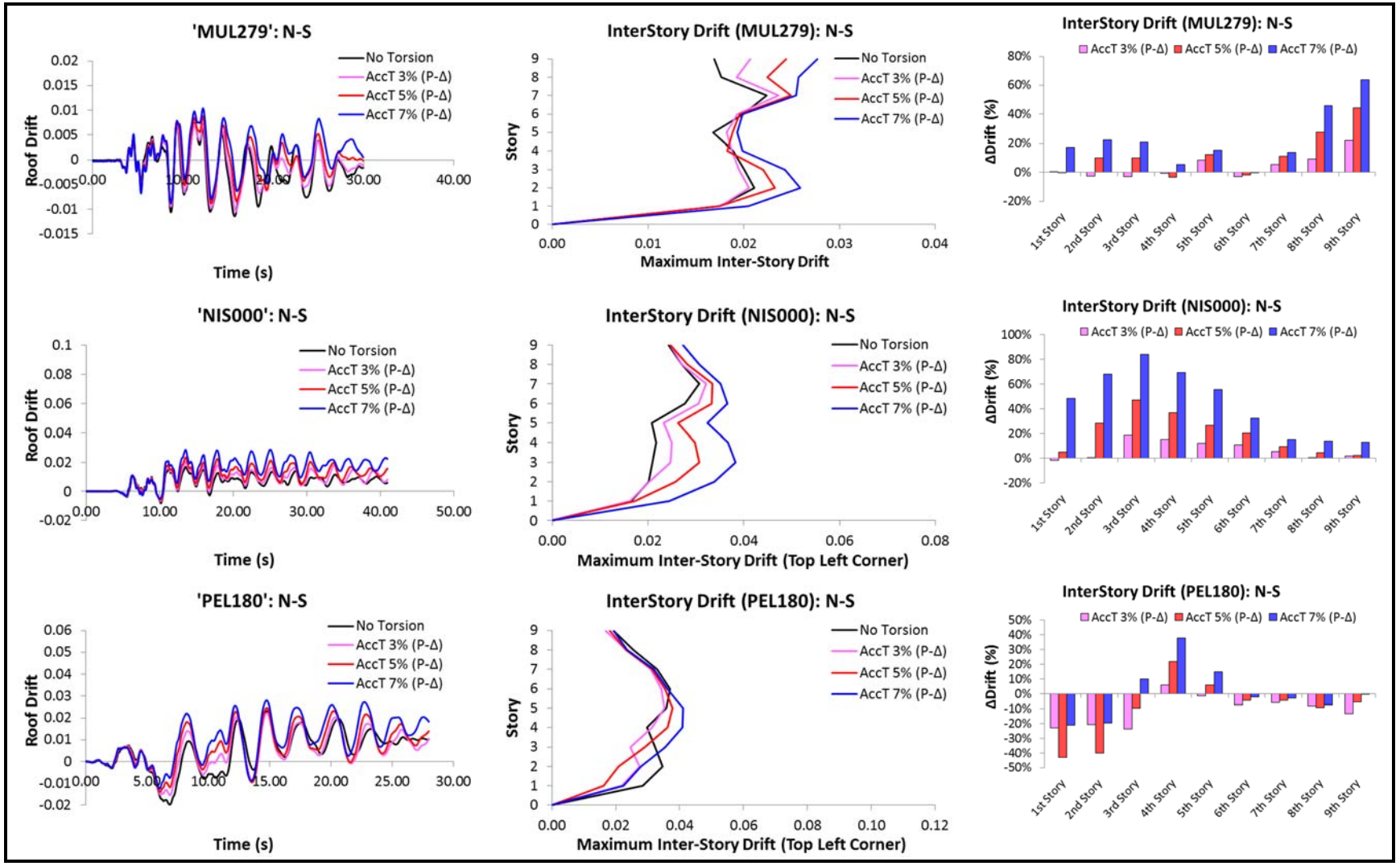
'MUL279': N-S
Roof Drift
Time (s)
No Torsion
AccT 3% (P-Δ)
AccT 5% (P-Δ)
AccT 7% (P-Δ)
InterStory Drift (MUL279): N-S
Story
Maximum Inter-Story Drift
InterStory Drift (MUL279): N-S
ΔDrift (%)
1st Story
2nd Story
3rd Story
4th Story
5th Story
6th Story
7th Story
8th Story
9th Story
'NIS000': N-S
Roof Drift
Time (s)
InterStory Drift (NIS000): N-S
Story
Maximum Inter-Story Drift (Top Left Corner)
InterStory Drift (NIS000): N-S
ΔDrift (%)
'PEL180': N-S
Roof Drift
Time (s)
InterStory Drift (PEL180): N-S
Story
Maximum Inter-Story Drift (Top Left Corner)
InterStory Drift (PEL180): N-S
ΔDrift (%)

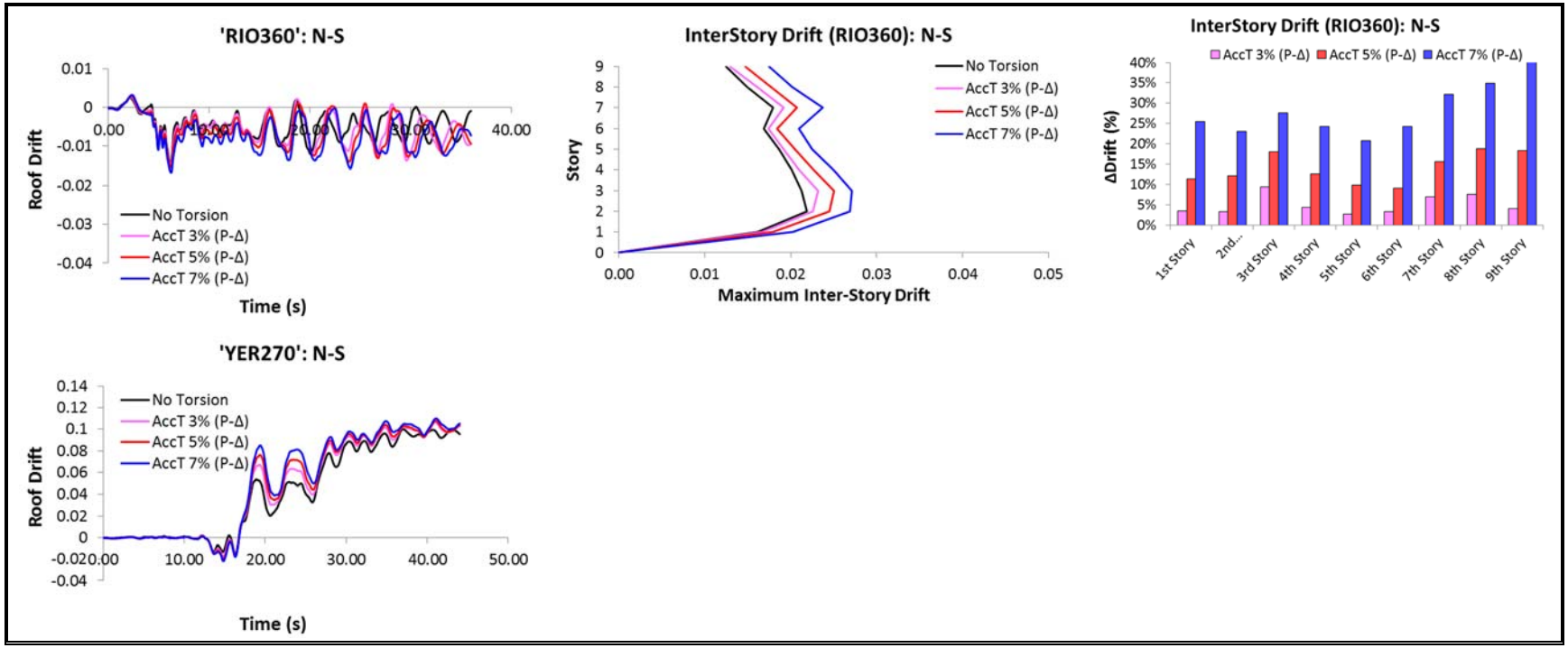
'RIO360': N-S
Roof Drift
Time (s)
No Torsion
AccT 3% (P-Δ)
AccT 5% (P-Δ)
AccT 7% (P-Δ)
InterStory Drift (RIO360): N-S
Story
Maximum Inter-Story Drift
InterStory Drift (RIO360): N-S
ΔDrift (%)
1st Story
2nd...
3rd Story
4th Story
5th Story
6th Story
7th Story
8th Story
9th Story
'YER270': N-S
Roof Drift
Time (s)

Results with Four Leaning Columns located at Each Quadrant's Centroid

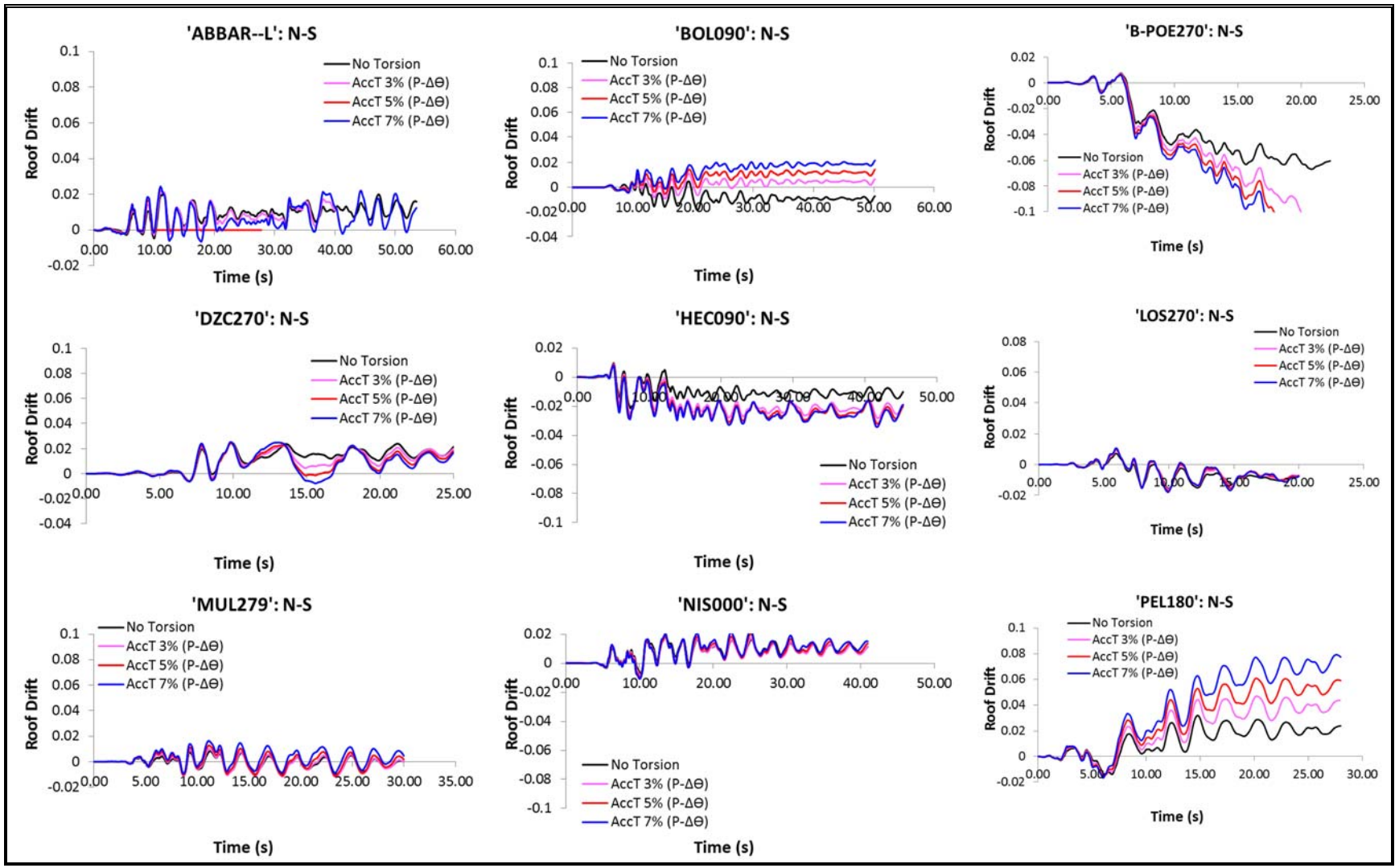

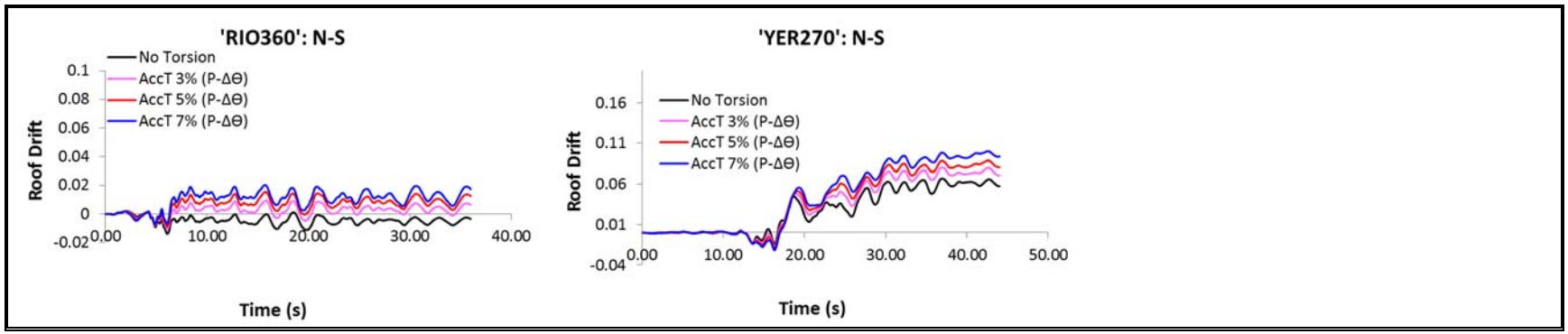
'RIO360': N-S
No Torsion
AccT 3% (P-ΔΘ)
AccT 5% (P-ΔΘ)
AccT 7% (P-ΔΘ)
Roof Drift
0.1
0.08
0.06
0.04
0.02
0
-0.02
0.00
10.00
20.00
30.00
40.00
Time (s)
'YER270': N-S
No Torsion
AccT 3% (P-ΔΘ)
AccT 5% (P-ΔΘ)
AccT 7% (P-ΔΘ)
Roof Drift
0.16
0.11
0.06
0.01
-0.04
0.00
10.00
20.00
30.00
40.00
50.00
Time (s)

Results with 2-Leaning Columns Located at Center of Radius of Gyration

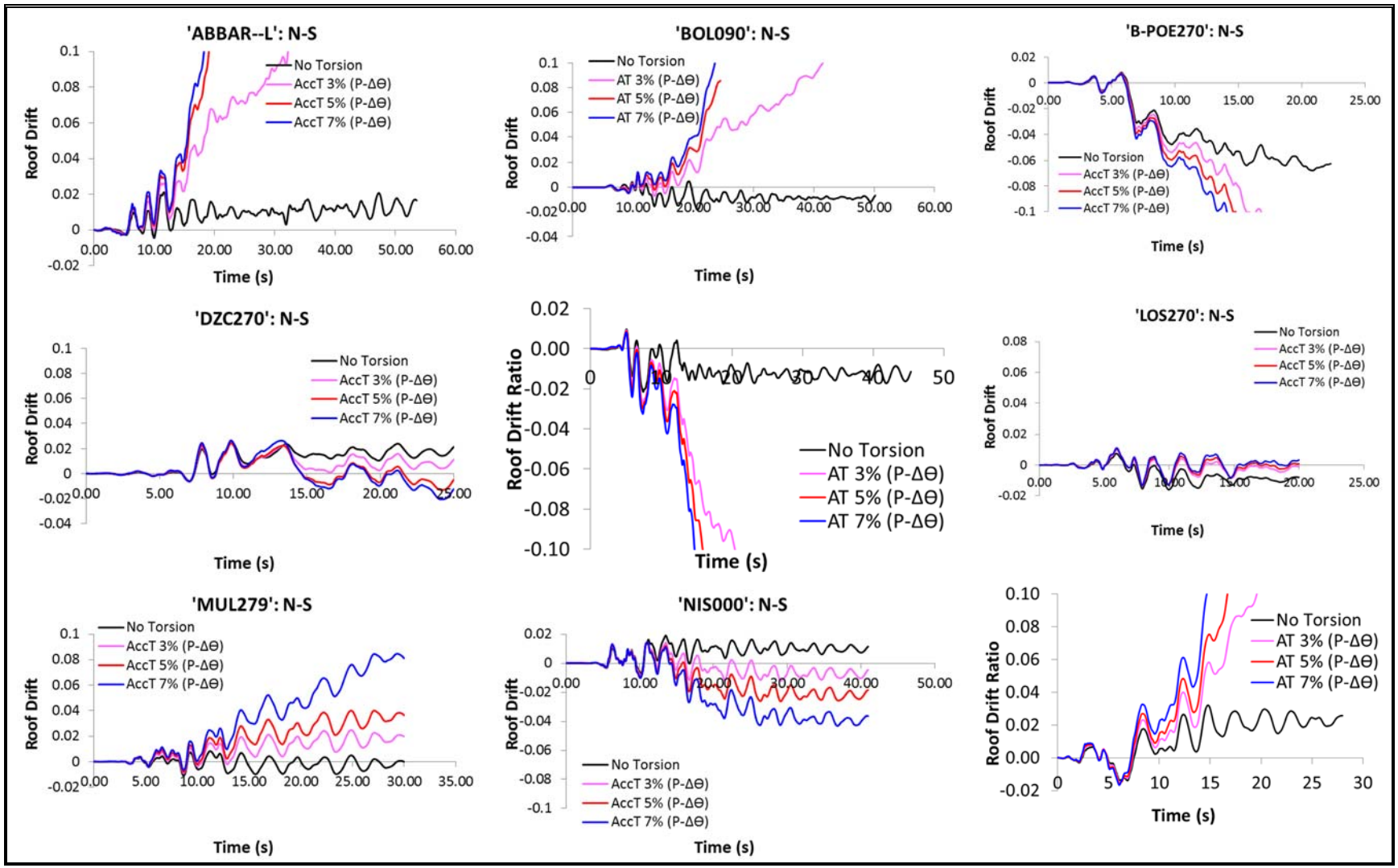

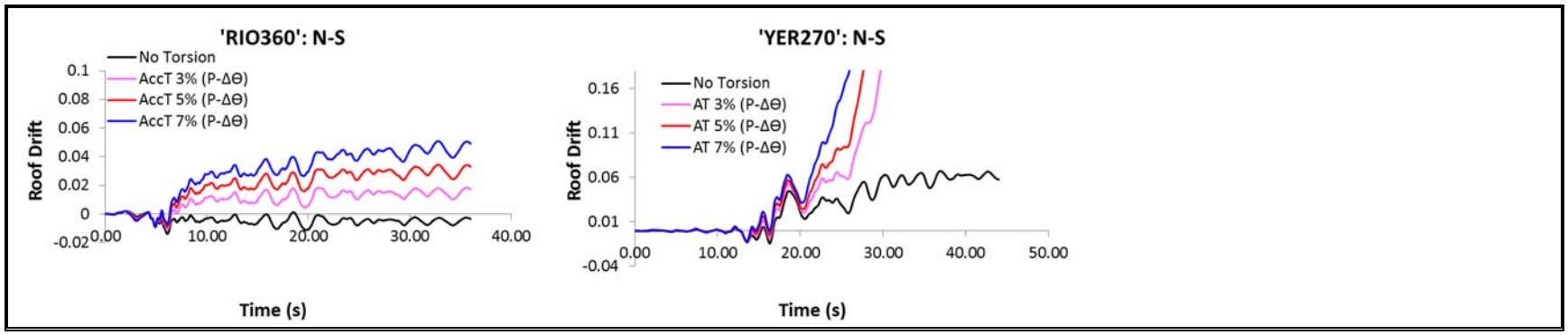
'RIO360': N-S
No Torsion
AccT 3% (P-ΔΘ)
AccT 5% (P-ΔΘ)
AccT 7% (P-ΔΘ)
Roof Drift
0.1
0.08
0.06
0.04
0.02
0
-0.02
0.00
10.00
20.00
30.00
40.00
Time (s)
'YER270': N-S
No Torsion
AT 3% (P-ΔΘ)
AT 5% (P-ΔΘ)
AT 7% (P-ΔΘ)
Roof Drift
0.16
0.11
0.06
0.01
-0.04
0.00
10.00
20.00
30.00
40.00
50.00
Time (s)